# - The absorption of xanthohumol in *in vitro* and *in vivo* studies and the investigation of the biological activity of structurally related chalcones -

**Dissertation**
**zur Erlangung des Doktorgrades der Naturwissenschaften**
**(Dr. rer. nat.)**
**der Fakultät für Chemie und Pharmazie**
**der Universität Regensburg**

vorgelegt von
Magdalena Motyl
aus Tuttlingen

2012

Diese Arbeit entstand in der Zeit von Januar 2009 bis Dezember 2011 am Lehrstuhl für Pharmazeutische Biologie der Universität Regensburg.

Die Arbeit wurde von Prof. Dr. Jörg Heilmann angeleitet.

**Promotionsgesuch eingereicht am:** 14.09.2012

**Datum der mündlichen Prüfung:** 26.10.2012

**Prüfungsausschuss:** Prof. Dr. Sigurd Elz
Prof. Dr. Jörg Heilmann
Prof. Dr. Claus Hellerbrand
Prof. Dr. Joachim Wegener

Für meinen Ehemann Matthias

An dieser Stelle möchte ich mich bei allen bedanken, die maßgeblich zum Gelingen dieser Arbeit beigetragen haben:

Prof. Dr. Jörg Heilmann möchte ich ganz herzlich für die Vergabe der interessanten Fragestellung meiner Promotionsarbeit, die wertvollen Diskussionen und Ratschläge sowie die hervorragende langjährige Unterstützung danken.

Prof. Dr. Claus Hellerbrand möchte ich für die sehr nette Kooperation und die Möglichkeit in seinem Fachbereich Versuche durchführen zu dürfen danken.

Dr. Manfred Gehring und der Firma NATECO möchte ich herzlich für die wissenschaftliche Unterstützung sowie für die Bereitstellung des Xanthohumols danken.

Dr. Guido Jürgenliemk danke ich für die Unterstützung bei praktischen und theoretischen Fragestellungen und für die sehr nette Atmosphäre im Praktikum danken.

Dr. Birgit Kraus möchte ich für die wissenschaftliche Begleitung dieser Arbeit und die zahlreichen Hilfestellungen in der Fluoreszenzmikroskopie und Zellkulturarbeiten sowie für die Durchsicht der Arbeit danken. Dr. Horst Wolff danke ich für die fluoreszenzmikroskopischen Messungen und die damit verbundene Auswertungen.

Dr. Christoph Dorn danke ich für die Organisation und die Durchführung der Tierversuche am Universitätsklinikum Regensburg. Dr. Thomas Weiß danke ich für die Bereitstellung der primären Hepatozyten.

Ich möchte mich bei allen meinen Arbeitskollegen für das sehr nette und offene Klima bedanken. Mein Dank gilt ganz besonders Dr. Sarah Sutor und Dr. Susann Haase für die fachlichen Diskussionen und die gemeinsame Zeit. Bei Gabriele Brunner möchte ich mich für ihre Unterstützung bei der Aufreinigung der Xanthohumol Matrix, der Unterstützung im Labor und die gemeinsamen Gespräche bedanken. Ganz besonders möchte ich mich bei Dr. Anne Freischmidt, Katharina Zenger und Rosmarie Scherübl für die fachlichen Diskussionen, die praktischen Unterstützungen und die gemeinsamen heiteren Abende bedanken.

Meinen Wahlpflichtstudenten Sarah Stecher, Janina Staffel, Andreas Locker, Nikola Plenagel und Alexander Bonmann danke ich für die sehr nette und erfolgreiche Zusammenarbeit.

Der zentralen Analytik der Universität Regensburg danke ich für Ihre Unterstützung in fachlichen Fragestellungen sowie den NMR und MS Messungen. Petr Jirásek möchte ich für die Synthese der hydrierten Chalcone, Rosmarie Scherübl für die Untersuchung der eingesetzten Substanzen mittels HPTLC Analyse und Katharina Zenger für die Unterstützung bei den fluoreszenzmikroskopischen Messungen sowie Auswertungen danken. Herrn Keith Buckley danke ich für die schnelle und zuverlässige Korrekturlesung dieser Arbeit.

Mein herzlicher Dank gilt meiner ganzen Familie und meinen Freunden. Ganz besonders möchte ich mich bei meinen Eltern für die immer währende Unterstützung, Zuversicht und die gemeinsamen humorvollen Abende bedanken. Meinen Schwiegereltern danke ich ganz herzlich für Ihre Unterstützung, das harmonische Miteinander und die hervorragenden Kuchen. Meinen Großmüttern Ursula und Doris danke ich ganz herzlich für die herzlichen Telefonate.
Meiner Freundin und Trauzeugin Nicole Herhoffer möchte ich danken für die ausgiebigen fachlichen und persönlichen Gespräche und für Ihre Freundschaft.

Zu guter Letzt möchte ich all denjenigen danken, die nicht namentlich erwähnt wurden und zu dieser Arbeit beigetragen haben.

**1 GENERAL INTRODUCTION ..... 1**

**1.1. Xanthohumol ..... 6**

1.1.1. Anti-infective activity ..... 7

1.1.1.1 Anti-bacterial activity ..... 7

1.1.1.2 Anti-fungal activity ..... 8

1.1.1.3 Anti-viral activity ..... 9

1.1.1.4 Anti-protozal activity ..... 10

1.1.2. Anti-obesity activity ..... 11

1.1.3. Anti-osteoporosis activity ..... 14

1.1.4. Influence of XN on phase I and phase II enzymes ..... 16

1.1.5. (Anti)-oxidative effect ..... 18

1.1.6. Anti-inflammatory effect ..... 22

1.1.7. Pro-apoptotic mechanism ..... 26

1.1.8. Estrogen modulating activity ..... 29

1.1.9. Anti-angiogenesis, -metastasis and –invasive properties ..... 30

**1.2 Safety studies ..... 32**

**1.3 Bioavailability, metabolism and cell uptake ..... 33**

**1.2. Aims ..... 36**

**2 PITFALLS IN CELL CULTURE WORK WITH XANTHOHUMOL [1)] ..... 38**

**2.1 Abstract ..... 38**

**2.2 Introduction ..... 38**

**2.3 Material and Methods ..... 39**

**2.4 Investigation, results and discussion ..... 41**

**2.5 Acknowledgments ..... 45**

**3 CHARACTERIZATION OF MINOR HOP COMPOUNDS, XN METABOLITES AND RELATED COMPOUNDS ..... 46**

**3.1 Abstract ..... 46**

**3.2 Introduction ..... 46**
3.2.1 Minor hop compounds, XN metabolites and related compounds ..... 47
3.2.2 Biological effects of XN metabolites ..... 49

**3.3 Aims of the study ..... 54**

**3.4 Material ..... 54**
3.4.1 Chemicals ..... 54
3.4.2 Cell lines and culture materials ..... 55

**3.5 Methods ..... 56**
3.5.1 Purity analysis ..... 56
3.5.2 Comparison of lipophilicity by high performance thin layer chromatography (HPTLC) ..... 56
3.5.3 Hydrogenation and NMR analysis ..... 57
3.5.4 FCS heat inactivation ..... 57
3.5.5 Cell cultivation and harvesting ..... 57
3.5.6 Cell counting ..... 58
3.5.7 Dilution of test compounds ..... 58
3.5.8 Viability assay ..... 59
3.5.9 Proliferation assay ..... 61
3.5.10 Nitric oxide assay (Griess assay) ..... 62
3.5.11 iNOS protein expression ..... 64
3.5.12 Statistical analysis and calculations ..... 65

**3.6 Results ..... 65**
3.6.1 Purity degree, lipophilicity and structure determination ..... 65
3.6.2 Effect on the cell viability and proliferation ..... 67
3.6.3 Nitric oxide assay ..... 72
3.6.4 iNOS protein expression ..... 73

**3.7 Discussion ..... 74**
3.7.1 Effect on the cell viability and proliferation ..... 74
3.7.2 Nitric oxide assay and iNOS protein expression ..... 77

**3.8 Summary ..... 79**

**4 *IN VITRO* UPTAKE OF XANTHOHUMOL IN HEPATIC AND COLORECTAL CANCER CELL LINES AND PRIMARY HEPATOCYTES [2)] ..... 81**

**4.1 Abstract ..... 81**

**4.2 Introduction ..... 81**

**4.3 Aim ..... 83**

**4.4 Material ..... 83**

4.4.1 Chemicals ..... 83

4.4.2 Cell lines and culture materials ..... 83

**4.5 Methods ..... 84**

4.5.1 FCS heat inactivation ..... 84

4.5.2 Cell cultivation and harvesting ..... 84

4.5.3 Measurement of XN uptake ..... 85

4.5.4 Quantification of XN ..... 85

4.5.5 Determination of protein content per cell ..... 86

4.5.6 Determination of the cell volumes ..... 86

4.5.7 Calculation and statistical analysis ..... 86

**4.6 Results ..... 87**

**4.7 Discussion ..... 89**

**4.8 Summary ..... 90**

**5 INFLUENCE OF DOSE AND PHENOLIC CONGENERS ON ABSORPTION AND DISTRIBUTION OF THE HOP CHALCONE XANTHOHUMOL AFTER ORAL APPLICATION IN MICE [3)] ..... 91**

**5.1 Abstract ..... 91**

**5.2 Introduction ..... 91**

**5.3 Aim ..... 93**

**5.4 Material and Methods ..... 94**

5.4.1 Chemicals ..... 94

5.4.2 Animals, animal treatment and sample asservation ..... 94

5.4.3 Sample preparation ..... 95

5.4.4 Analytical methods ..... 95

5.4.5 Statistical analysis ..... 96

**5.5 Results and Discussion ..... 96**

**5.6 Summary ..... 105**

**5.7 Appendix ..... 106**

**6 DISCUSSION ..... 108**

**7 SUMMARY ..... 115**

**8 REFERENCES ..... 117**

**9 APPENDIX ..... 154**

**9.1 Abbreviation ..... 154**

**9.2 NMR spectra of hydrogenated chalcones ..... 159**

**9.3 List of publications ..... 162**

**9.4 Curriculum Vitae ..... 163**

**9.5 Eidesstattliche Erklärung ..... 164**

# 1 General introduction

Chalcones belong to the large group of polyphenolic compounds. They are precursors of flavanones, which exhibit an open C ring, a phloroglucinol A ring and a phenylpropanoid B ring (Figure 1-1).

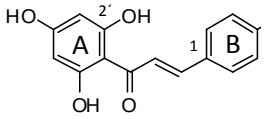


**Figure 1-1: Chalcone skeleton with substituted A-Ring.**

Chalcones biosynthetically derived from phenylpropanoic acids such as 4-coumaroyl-CoA which are synthesized via the shikimate pathway (Figure 1-2).

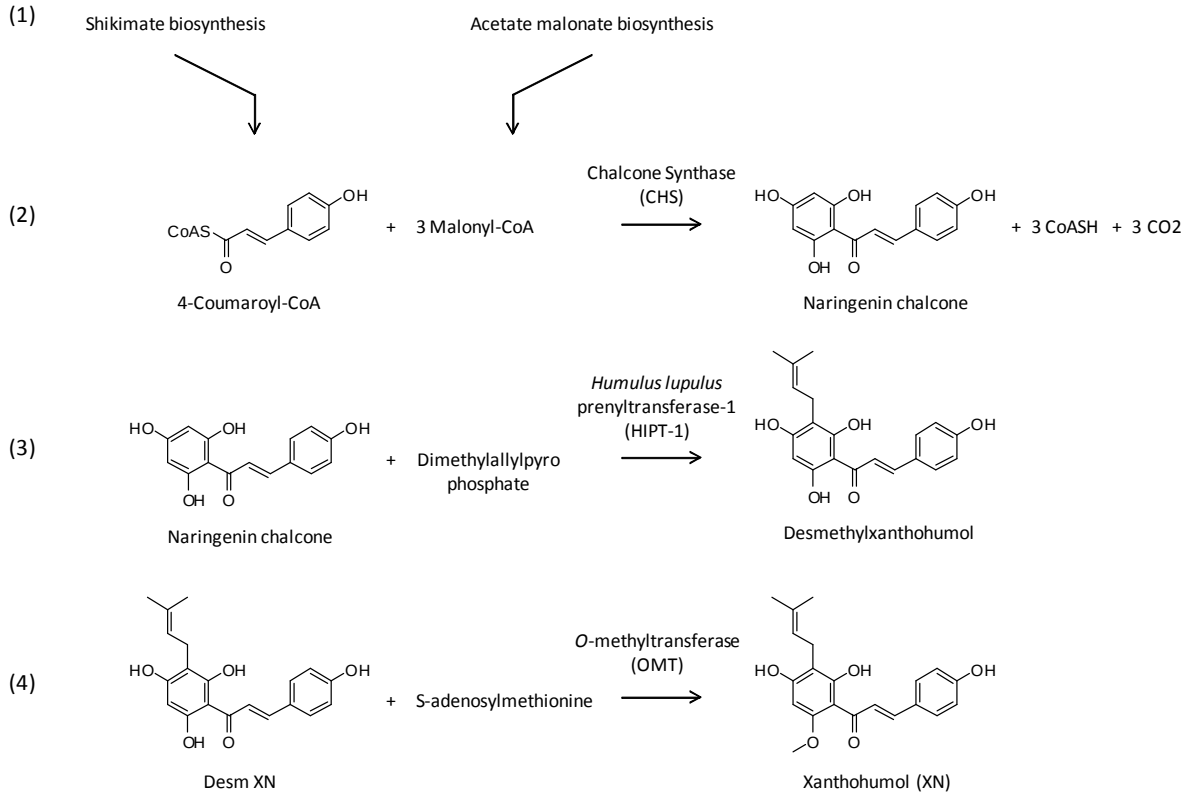


**Figure 1-2: Biosynthesis of the chalcone xanthohumol (XN) (adaped from [1]).**

The phloroglucinol A ring is built from malonyl-CoA units via the acetate malonate pathway. 3 Malonyl CoA units are added at the carbonyl function of the activated phenylpropanoic acids via the elimination of 3 carbon dioxide molecules and 3 CoASH.

The chalcone biosynthesis in plants is catalyzed by the chalcone synthase (CHS) [2–4]. There are many different chalcones which are synthesized in plants such as kuraridin, xanthohumol (XN), isosalipurposide and isoliquiritin. In addition, there are a variety of synthetic chalcones.

The synthesis of chalcones is correlated with bioassay testing, which leads to a fast development of potent synthetic compounds [5–7]. However it is out of the scope of this work to summarize the biological and pharmacological activity of synthetic chalcones. In the following, the focus lays on the activity of natural chalcones in general and XN in particular.

The difference in the structure of natural chalcones is processed mainly after the chalcone synthesis. The prenylated hop chalcone XN, for instance, is first prenylated by the *Humulus lupulus* prenyltransferase-1 (HlPT-1) [8] and then *O*-methylated by an *O*-methyltransferase (OMT) [1] (see Figure 1-2). The chalcones can be further isomerized into flavanoids. Chalcone flavanone isomerase catalyzes the isomerization from the chalcone to the correspondent flavanone. This isomerization can happen also under non enzymatic conditions such as fermentation of beverages [9]. Chalcones are found in vegetables (e.g. tomatoes [10]), fruits (e.g. *Citrus kinokuni* [11]), beverages (e.g. beer [12]), various medicinal plants (e.g. *Glycyrriza glabra* [13]) and spices (e.g. *Carthamos tinctorius* [14,15]). They show remarkable pharmacological activity in a wide range of assays such as anti-bacterial or anti-fungal. Moreover the initiation promotion and progression of cancer is effected by different chalcones, too.

Microorganisms live for example on the dermis and in the intestine of humans. They maintain a human's defense against harmful microorganisms and produce beneficial vitamins. Beside the beneficial effects, there are microorganisms which can lead to harmful diseases. Methicillin-resistant *Staphylococcus aureus* (MRSA) accounts for about 170 000 new infections and 5 000 deaths per year in Europe [16]. An emerging risk is the widespread infection not only with health care associated methicillin-resistant *Staphylococcus aureus* (HA-MRSA), but also with community associated methicillin-resistant *Staphylococcus aureus* (CA-MRSA). Understandably, many investigations are being performed to find effective antibiotics also in the group of plant secondary metabolites. Kuraridin isolated from the Chinese herb *Sophora flavescens* AIT. showed an anti-bacterial effect on MRSA. The minimum inhibitory concentration (MIC) of kuraridin, saphorflavanone G and antibiotics on several MRSA strains were investigated. In addition to the investigation of MIC, the cytotoxic effect of kuraridin on human peripheral mononuclear cells was determined. Kuraridin inhibited the growth of MRSA strain ATCC 25923 at a MIC of 8 µg/ml in comparison to oxacillin at 0.13 µg/ml. The growth of MRSA strain 11998 was inhibited at a MIC of 16 µg/ml kuraridin and by ciprofloxacin at a MIC of 16 µg/ml. Interestingly, kuraridin showed no cytotoxic effect on human peripheral mononuclear cells up to a concentration of 64 µg/ml

[17]. Licochalcone A, a chalcone from *Glycyrrhiza glabra* L., showed a MIC of 16 µg/ml against a further MRSA strain. Hatano and co-workers [18] discussed an interaction of the prenyl chain with the cell membrane of bacteria as a possible mechanistic explanation for the observed activity [18]. However, the anti-bacterial effect of chalcones is not restricted to MRSA strains. Also, *Micrococcus luteus*, *Staphylococcus epidermis, Bacillus subtilis* [19] and further strains [20–23] were inhibited by chalcones. Not only antiviral [24,25], but also anti-plasmodial effects [25,26] were observed during the pharmacological investigation of chalcones. The anti-plasmodial effect was observed only for a few natural chalcones such as licochalcone A [27] and uvaretin [28]. Thus, new anti-plasmodial chalcones were mainly developed through synthesis [27]. Licochalcone A also showed an inhibitory effect on *Leishmania major* and *Leishmania donovani* [29]. In addition, chalcones such as geranyl substituted chalcones from *Artocarpus nobilis* THW. [30], aurentacin A from *Myrica serrata* LAM. [31], isobavachalcone from *Maclura tinctoria* (L.) D.DON EX STEUD. [32] and licochalcone A [33] showed anti-fungal activity. However, chalcones were also active against cancer and inflammation.

Cancer can occur in several places in the organism. It is an independent up regulation of cell growth from the neighbor cells and invasion as well as the spread into other compartments/tissues of the organism. There are more than 100 types of cancer with different characteristics. The molecular mechanisms differ between the cancer types [34]. Beside the different cancer characteristics the stages of carcinogenesis can be classified equally. First a cell must mutate to turn up its growth independently from its environment (initiation). Without an intervention the cell may proliferates further (promotion). After the promotion malignant cells can leave the side of origin and metastasize into other tissues (progression). These stages are possible points of attack. For example the inhibition of growth might inhibit the promotion of cancer. With this cancer stage subsumption, potent anticancer substances can be classified. Understandably, the initiation, promotion and progression are stages of cancer that are not separated from each other. For example the apoptotic action of compounds during the promotion stage might also be beneficial in the progression of cancer. The cancer stage model is quite simple and today a complex and multi process of carcinogenesis is discussed [35]. Nevertheless, for the effect classification of compounds, the initiation, promotion and progression cancer stage model is used in the literature (e. g. [36]) and in this thesis.

“Chemoprevention is the use of pharmacologic or natural agents that inhibit the development of invasive cancer either by blocking the DNA damage that initiates carcinogenesis or by arresting or reversing the progression of premalignant cells in which such damage has already occurred” [37]. In the initiation stage chemoprevention is often attributed to

anti-oxidative and anti-inflammatory properties, and the ability to induce phase II and inhibit phase I enzymes [36,38,39]. Therefore, anti-oxidative and anti-inflammatory effects of chalcones were studied in different bioassays. Some chalcones were able to spread chemopreventive effects such as panduratin A [40], isoliquiritigenin [41] and xanthohumol (XN) [36].

Usually inflammation is a temporary physiological reaction, but in some cases inflammation remains and leads to a chronic disease. Chronic inflammation is correlated with higher risk to initiate cancer [34] and is therefore correlated with the initiation cancer stage for example. Several common chalcones were screened concerning their ability to inhibit inflammation such as licochalcone A, butein and hydroxysafflor yellow A (HYSA). The investigated chalcones were able to influence and inhibit inflammation through different mechanism such as inhibition of NF-κB [42] but also had anti-oxidative activity. Liquiritigenin, for instance, showed moderate activity against LDL peroxidation [13] whereat butein showed remarkable effect as scavenger of reactive oxygen species (ROS) [43].

The other main ability of chemopreventive compounds is to induce phase II and to inhibit phase I enzymes of the biotransformation. During the biotransformation, enzymes convert lipophilic compounds into more hydrophilic ones. In doing so, phase I enzymes activate the compound and phase II transfer hydrophilic groups. Chalcones were found to be more potent phase II inducers than phase I inhibitors. CYP3A4 was inhibited by isoliquiritigenin at an $IC_{50}$ value of 29 µM ($IC_{50}$ values without a standard deviation (SD)) [44] and the mRNA level of CYP1A1 was decreased by phloretin in combination with an CYP1A1 inducer in the human colorectal cell line (Caco-2) at 100 µM [45]. However, Kinghorn et al. [46] reviewed its collaboration work on chemopreventive natural compounds. Several chalcones induced the phase II enzyme NAD(P)H:quinone reductase (QR) such as flavokawain B (concentration to double induction (CD) of QR = 1.7 µg/ml, mouse Hepa 1c1c7) [47] and isoliquiritigenin (CD of QR = 0.7 µg/ml, mouse Hepa 1c1c7) [48], (CD of QR = 2 µM, mouse Hepa 1c1c7) [49]. Further phase II enzymes such as the heme oxygenase-1 (HO-1) and the glutathione S-transferase (GST) were also affected by different chalcones. After 24 h treatment with 25 µM butein the mRNA level of GST in rat primary hepatocytes increased to 211% and the enzyme activity by 27%, for instance [50]. After 12 h 10 µM isoliquiritigenin induced the HO-1 mRNA as well as HO-1 protein levels in RAW 264.7 macrophages [51].

After cancer is initiated, the growth and proliferation of cancer can be affected. This concerns the induction of cell death in cancer cells and the inhibition of the inflammatory process in the environment of cancer. Depending on the types of cancer, the inhibition of inflammation can inhibit cancer and is thus a point of attack. Chalcones are potent anti-inflammatory drugs as mentioned before and are additionally able to induce cell death in cancer cells, like alpinetin chalcone [52], phloretin [53] and isoliquiritigenin [54]. There are different cell death

mechanism such as necrosis, apoptosis and autophagy. The mechanism of cell death induction by chalcones was investigated in different assays. Chalcones such as butein, licochalcone A [55], phloretin [56] and uvaretin [57] induced cell death in cancer cell lines via apoptosis. Isoliquiritigenin triggered adenoid cystic carcinoma cells into death through apoptosis and autophagy [58]. Furthermore, the activity to inhibit cancer growth *in vivo* was also studied for some chalcones, like isobavachalcone. Isobavachalcone inhibited the skin carcinogenesis induced by 7,12-dimethylbenz[*a*]anthracene and promoted via 12-*O*-tetradecanoylphorbol-13-acetate in mice [59].

The difference between a benign and malignant cancer is the ability to metastasize, invade and induce angiogenesis [34]. Therefore, the inhibition of this ability is a target in order to affect cancer. Isoliquiritingenin, for instance, showed anti-angiogenetic [60] and anti-metastatic ability [61] as well as butein [62,63] and licochalcone A [64,65].

Apart from the anti-infective and anti-cancer effects of chalcones, other beneficial effects were observed such as the influence of phlorizin, kuraridin, iso- and bavachalcone on the carbohydrate metabolism [66–69], the effect on osteoporosis of licochalcone A and isoliquiritin [70,71] and the influence of butein, licochalcone and kuraridin on hyperpigmentation [72,73]. Furthermore, isoliquiritin spread effects, in the estrogen metabolism and is judged as a phytoestrogen. In addition to these effects the ability to protect cells was determined, too. HSYA protected pheochromocytoma cells against apoptosis induced by oxygen and glucose deprivation in a dose dependent manner [74] and spread neuroprotective effects *in vivo* and *in vitro* [75].

Chalcones influenced positively the aforementioned abilities which were mostly determined in *in vitro* bioassays. In order to spread the activity also *in vivo*, the required concentration has to be reached. Therefore, bioavailability and metabolism studies were conducted to determine the behavior of HSYA [76,77], isoliquiritigenin [41] and butein [78], for instance. The absorption after oral intake of HYSA was determined in rats and humans and showed after ingestion of 100 mg/kg in rats and 100 mg HSYA in humans serum levels of 8.27 ± 0.38 µM HSYA [76] and 0.13 ± 0.01 µM HSYA [77] respectively after 1 h. The observed discrepancy concerning the values is due to species related aspects and different amounts of ingestion. However, the serum levels of HSYA in rats reaches the impressive concentration of 8.27 ± 0.38 µM and might therefore be suitable to spread the determined *in vitro* effects.

Chalcones showed a wide range of biological and pharmacological abilities such as anti-infective, anti-oxidative and anti-cancer. Thus the activity of XN, a prenylated chalcone of hops [79], was also investigated in different bioassays (1.1 Xanthohumol). XN spread activity in a variety of *in vitro* assays and is a compound with multifunctional abilities.

Therefore, the effects of XN were investigated in a variety of *in vivo* models to determine the activity, absorption and the metabolism.

## 1.1. Xanthohumol

XN is accumulated in female inflorescences of *Humulus lupulus* L. (Cannabinaceae) and was isolated by different research groups [79,80]. 2005 Jung and co-workers identified *Sophora flavescens* as second plant source of XN [81]. XN as the most abundant prenylated chalcone in the resin of leaf glands of hops account for 80-90% of the chalcones, and is accompanied by desmethylxanthohumol (2-3%), xanthohumol C (2-4%), xanthohumol B (3-5%) and isoxanthohumol (<1-2%) [12] as well as one further secondary metabolite named xanthogalenol [82]. Xanthogalenol was found in American (*Humulus lupulus* var. *cordifolius*) and Japanese hop cultivars, but was absent in European and southwest American plants. This pointed to at least two separate lineages [82]. In humans nutrition prenylated chalcones could be found as an ingredient of beer. XN content differ in bearer as well as in the beer sorts, because of spontaneous decomposition or environmental impact. The XN concentration was determined in different hop products such as pellets, ethanolic and $CO_2$ extracts [83] and beer sorts [84]. The ethanolic extracts contained 3.75 ± 0.05 g XN/100 g and were the richest in XN. In comparison 0.62 ± 0.01 g XN/100 g was found in pellets and 0.089 ± 0.001 g XN/100 g in the $CO_2$ extracts. Imported lager contained 0.002 mg/l equivalent to 0.01 µM XN (isoxanthohumol 0.04 mg/l) and American porter 0.69 mg/l equivalent to 1.95 µM XN (isoxanthohumol 1.33 mg/l) [84]. However, at least 95% of XN is lost during the brewing process [85]. There are four main reasons for the loss of XN. First, XN is converted to isoxanthohumol during the wort production. Second, the hydrophobic properties of XN lead to an inefficient extraction from hops, third the adsorption to malt proteins and extraction with the filtered trub [9] and at least the water solubility is low.
Wunderlich et al. [85] achieved a much higher finale XN concentration of up to 10 mg/l in dark beer, by changing the brewing process in few ways. They used XN enriched hop cones, added the hop cones 5 min before the end of word boiling and used intensively roasted malt.

Since 1997 XN has been tested in a variety of assays and has been described in 120 published articles (pubmed since 1997 - search properties “xanthohumol”). XN was found to be a chalcone with a broad spectrum of pharmacological effects. Examples include anti-infective, anti-obesity, anti-osteoporotic, anti-oxidative, chemopreventive, anti-inflammatoric effects as well as pro-apoptotic effects in cancer cell lines and tumor cells. XN is able to inhibit cancer initiation, promotion and progression by blocking of metastasis,

invasion and angiogenesis. Furthermore XN was found to have beneficial effects on normal cells (1.2 Safety studies).

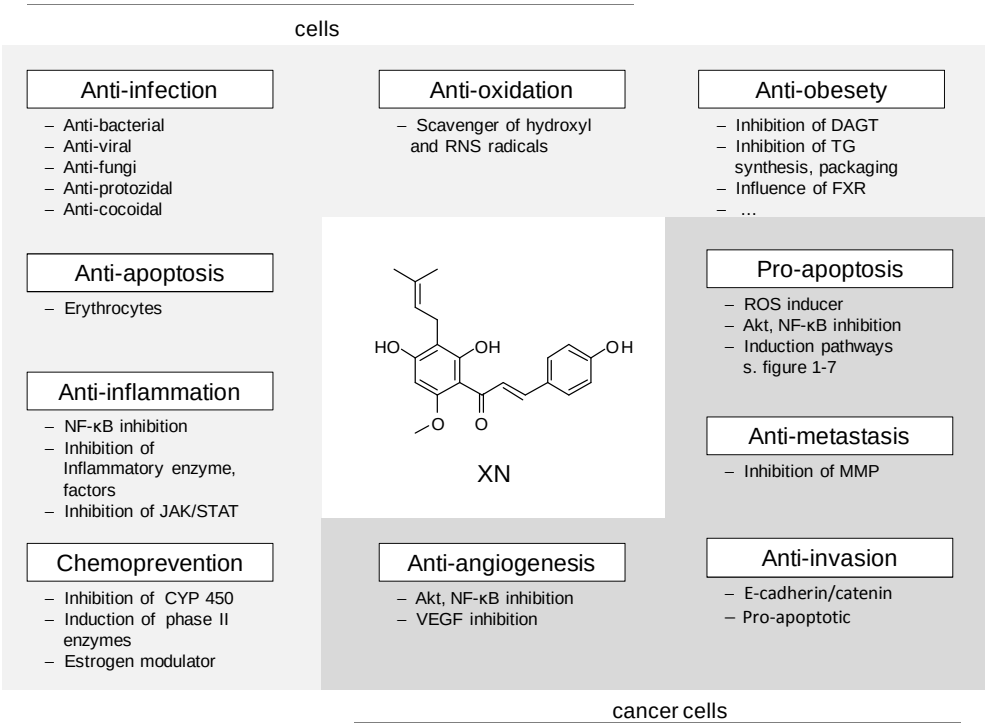


**Figure 1-3: Summary of XN effects and mechanism (*in vitro*) on cells and cancer cells. XN lead to a wide range of abilities as it is displayed. The effects are grouped and the roughly outlined mechanism is listed beyond. The groups cannot be seen as bordered and might overlap. For the sake of clarity the groups were divided and overlapping effects were not noted in each group.**

XN has anti-infective activity such as anti-bacterial, anti-viral, anti-plasmodial, anti-protozoal and anti-coccidial against different microorganisms.

## 1.1.1. Anti-infective activity

### 1.1.1.1 Anti-bacterial activity

Anti-infective activity is a well established investigation and a benefit in the development of diverse application e.g. mouthwash or in teas for treatment of a sore throat. XN was studied in several anti-infective assays and exhibited inhibition on the growth especially of gram positive bacteria. Different studies were conducted to detect the MIC, to investigate if XN spread a low MIC and could be used for the treatment of e.g. dental caries [86] and acne vulgaris [87]. Bhattacharya et al. [86] determined the MIC of XN for *Streptococcus mutans*, which are the main initiators of dental caries. XN (MIC of 12.5 µg/ml

(35.3 µM)) inhibited the growth of *S. mutans* and exhibited a stronger antibacterial activity than thymol (MIC of 150 µg/ml (999 µM)) at pH 7.5. Additionally, XN was found to have anti-bacterial activity against *Streptococcus salivarius* and *Streptococcus sanguis* [86] too. *Staphylococcus aureus* is one of the normal substituents of our bacterial flora present in the nasal passages and perineum [88]. Usually *S. aureus* causes no infection in humans with an intact immune system, but in abnormal terms, it can induce harmless skin disease as well as critical diseases such as pneumonia. XN was tested concerning its effects on *S. aureus* and showed MIC of 6.25 µg/ml (17.6 µM) [89].

In a further study, XN was tested concerning the growth inhibition of MRSA and their virulent factor staphyloxanthin [90]. The results indicated an inhibition of MRSA staphyloxanthin by XN, but no effects on their growth. Staphyloxanthin, a carotenoid pigment, is a virulent factor that exhibits anti-oxidative properties. Staphyloxanthin reacts with reactive oxygen species from the immune system and renders them harmless [91]. XN might be therefore indicated as co-treatment because it reacts with staphyloxanthin and this might lead to a more effective action of the immune system.

XN was also tested for the treatment of acne vulgaris. Acne vulgaris is a dermatological disease and has four main pathological factors: Follicular hyperkeratosis, increased sebum production, *Propionibacterium acnes* colonization and inflammation. Each pathological factor can be treated with different therapeutics [92,93]. XN as a known anti-bacterial agent, was tested concerning its effect on the acne vulgaris strains *Propionibacterium acnes*, *Staphylococcus epidermis*, *Staphylococcus aureus*, *Kocuria rhizophila* and *Staphlycoccus pyogenes* [87]. XN showed anti-bacterial activity against these strains and thus might find application in the treatment of acne vulgaris in the future.

#### 1.1.1.2 Anti-fungal activity

Anti-infective activity also includes anti-fungal activity. XN was examined in anti-fungal assays, but has shown low effectiveness so far. E.g. Mizobuchi et al. [89] investigated the pathogenicity of five fungi during stimulation with XN. Two fungi that were investigated usually induce dermatosis: *Trichophyton mentagrophytes* and *Trichophyton rubrum*. In addition *Candida albicans* that usually causes candidosis, *Fusarium oxysporum* a plant pathogenous that causes fusariosi and *Mucor rouxianus* were investigated. *T. mentagrophytes* and *T. rubrum* were both inhibited with a MIC of 8.83 µM XN. *M. rouxianus* was inhibited with a MIC of 141.08 µM XN. No inhibitory effect was observed during the incubation of *C. albicans* and *F. oxysporum* with XN.

Srinivasan et al. investigated the inhibitory effect of XN and other hop components on mold fungi [94]. XN showed only anti-fungal activity against *Rhizopus nigricans*, a producer of

bread mold [95]. Unfortunately the results within the tables 9 and 10 are not included in the paper and are replaced by the $IC_{50}$ values of anti-plasmodial results. Furthermore, they measured an effect by *R. nigricans* and *Penicillium roqueforti* in the disc diffusion test at 200 µg/disc. Srinivasan et al. [94] described the disc diffusion assay as a screening method for potential anti-fungal compounds, but the outcome of the assay is not valuable enough for effective determination of an inhibitory concentration.

#### 1.1.1.3 Anti-viral activity

The anti-viral potency of XN was determined against several RNA and DNA viruses [96]. XN was found to inhibit bovine viral diarrhea virus (BVDV) at $IC_{50}$ values of 4.80 ± 3.95 µM, herpes simplex-1 (HSV-1) at $IC_{50}$ values of 7.05 ± 1.58 µM, herpes simplex-2 (HSV-2) at $IC_{50}$ values of 7.62 ± 4.80 µM and cytomegalovirus (CMV) at $IC_{50}$ values of 1.5 ± 0.35 µM. The therapeutic dose of a compound also called therapeutic index (TI) is calculated by division of the toxic concentration and the inhibitory concentration. The RNA virus BVDV reached an IT of 4.2 and the DNA viruses HSV-1 of 3.7, the HSV-2 of 6.3 and CMV of 2.6. In comparison with the inhibition of the four viruses before, XN were more potent than IXN. But IXN showed activity in the RNA rhino virus at $IC_{50}$ values of 18.62 ± 9.31 µM (XN not reached). Comparing the studies of Buckwold´s et al. [96] and Wang et al. [97] the results differ concerning the activity at the HIV-1 RNA virus. Wang et al. [97] described an activity of XN at the HIV-1 virus. In contrast to this result, Buckwold et al. [96] report no effects using an extract enriched with 8.4% (w/w) XN. Pure XN was not tested. Wang et al. [97] showed that XN inhibited the HIV-1 induced cytopathic effect at $EC_{50}$ 0.82 µg/ml (2.00 µM). The production of viral p24 antigen at $EC_{50}$ 1.28 µg/ml (3.21 µM) and the reverse transcriptase at $EC_{50}$ 0.50 µg/ml (1.22 µM) in C8166 lymphocytes, were described to be inhibited too. They also found an inhibition of the HIV-1 replication at $EC_{50}$ of 20.74 µg/ml (50.55 µM) and a TI of 10.8 in peripheral blood mononuclear cells (without a SD). However, XN exhibited no effect on recombinant HIV-1 reverse transcriptase and the HIV-1 entry, thus a possible inhibition of enzymes concerning the after transcription period was discussed [97].

As already mentioned, XN showed inhibitory activity also at the BVDV. In a study conducted by Zhang et al. [98] this activity was determined in a surrogate model for the hepatitis C virus (HCV) on the basis of primary calf testis cells. The activity of XN was compared to ribavirin and interferon-α. Ribavirin a nucleoside analogous and interferon (IFN)-α (pegylated) are used in combination or on its own in the therapy of chronically courses of the HCV [99]. XN was found to inhibit the replication of the BVDV and the cytopathic effect [96]. CT cells were incubated with BVDV at 1000 tissue culture inhibition dose of 50% ($TCID_{50}$) and 100 $TCID_{50}$. The determined $EC_{50}$ of XN was 3.24 ± 0.02 mg/l (9.14 ± 0.06 µM at 1000 $TCID_{50}$) and

2.77 ± 0.19 mg/l (7.82 ± 0.54 µM at 100 $TCID_{50}$) with a TI of 7.72 and 9.03, respectively. An inhibition of E2 expression and the viral RNA levels were described too. However even higher concentrations of XN could not eliminate the viral RNA completely. The effectiveness of XN was better compared to ribavirin but worse compared to IFN-α [98]. In a second study of the same group, a possible synergistic effect of XN and IFN-α was assayed. The combination of both showed a significant ($p < 0.001$) better inhibitory effect than either substance on its own [100]. The life cycle of the HCV is dependent on the lipid metabolism. XN interacts with different enzymes within the lipid metabolism (1.1.2 Anti-obesity activity) such as DGAT and MTP. Zhang et al. [98] explained a possible inhibitory mechanism of HCV via DGAT and MTP inhibition by XN.

#### 1.1.1.4 Anti-protozal activity

Protozoa are grouped in the termini of eukaryota [95]. The group of protozoa exhibits a cell nucleus and some are able to move. Some protozoa are known as pathogens for human and animals. They can induce different diseases such as leishmaniosis, amoebiasis, malaria and toxoplasmosis [99]. *Plasmodium falciparum*, one of three inducers of malaria, is responsible for estimated 665.000 malaria deaths in 2012 [101]. *Plasmodium falciparum* is passed through a bite of the Anopheles mosquito. Different malaria treatments are available, that affect the life cycle of *P. falciparum*, e.g. with chloroquine. Chloroquine inhibits the haem polymerase, an enzyme that induces the polymerization of haemin in the digest vacuole of *P. falciparum.* For quite some time, physicians and researchers have been confronted with the chloroquine resistance. The chloroquine resistance is attributed to the mutation of *P. falciparum* chloroquine resistant transporter (PfCRP), which is located in the digest vacuole membrane [102] and significantly reduces the chloroquine concentration.

Three groups tested the ability of XN to inhibit *P. falciparum* of chloroquine-sensitive (CS) and chloroquine-resistant (CR) strains. In the study of Herath et al. [103] two fungi were used to produce four XN metabolites. In the next step they investigated the anti-plasmodial and cytotoxic effects of XN and the produced metabolites. Both strains were fragile to XN, at an $IC_{50}$ value of 9.31 µM (CS) and at 2.82 µM (CR) ($IC_{50}$ values without SD)) which were determined by a lactate dehydrogenase assay (LDH). Notably XN has a stronger ability to inhibit the CR than the CS strain [103].

In a second study, Frölich et al. [26] investigated the inhibitory activity of XN, 6 different XN metabolites and chloroquine on *P. falciparum*. The [$^3$H]hypoxanthine assay was used to determine the $IC_{50}$ values. An $IC_{50}$ value of 8.2 ± 0.3 µM (CS) and an $IC_{50}$ of 24.0 ± 0.8 µM (CR) were determined for XN. The $IC_{50}$ values determined for chloroquine were 0.015 ± 0.002 µM (CS) and $IC_{50}$ 0.14 ± 0.012 µM (CR) respectively. Among the test

compounds XN was the most potent inhibitor of the CS strain in this study. Dihydroxanthohumol C (see Figure 3-1) was the most potent inhibitor of the CR strain. The authors proposed that the anti-malarial activity of chalcones is based on binding haemin. The ability to bind haemin was evaluated in a GSH-haemin interaction assay. XN bound to approximately 60% haemin, chloroquine up to 80% and dihydroxanthohumol C to less than 5% compared to the drug free control [26].

In a third study, the inhibition of CS and CR plasmodium strains by a combination of XN and $CO_2$ was investigated [94]. Unfortunately the plasmodium strain number is not mentioned and the reference of the used method for the determination of IC values is incorrect. However, a 61% inhibition of the CS plasmodium strain by XN was achieved at a XN concentration of 5.64 µM (3% $CO_2$). In a further experiment they changed the $CO_2$ concentration and investigated both the CS and the CR strain. The study revealed an inhibition of 47% (3% $CO_2$) and 61% (5% $CO_2$) for the CS strain, and 40% (5% $CO_2$) for the CR strain. In the second part of this study the ability to cause death of different protozoa was determined in a time dependent manner. The protozoa investigated were *Paramecium candatum* also known as slipper animalcules and *Chaos sp.* that belongs to the amoebae. XN exhibited activity against both protozoa [94].

Summing up, XN exhibits inhibitory activity against gram positive bacteria, some fungi strains and viruses. Furthermore XN exhibits inhibitory effects against *P. falciparum*, which cause malaria. XN was also tested concerning its activity against the initiation, promotion and progression of cancer as well as the activity against obesity.

### 1.1.2. Anti-obesity activity

Hyperlipidemia and –glucosemia are indicators for insulin resistance, which is often a consequence of obesity. Diabetes mellitus II, the metabolic syndrome, and atherosclerosis are rising problems worldwide [104]. In this context, XN´s influence on the carbohydrate metabolism was investigated by different research groups. Tabata et al. [105] investigated the ability of XN to inhibit the enzyme diacylglycerol acyltransferase (DGAT). DGAT catalyzes the last step within the triacylglycerol synthesis. XN showed an inhibitory effect in a rat liver microsomal radioactive assay at a concentration of 50.3 µM ($IC_{50}$ values without a SD) [105].

XN´s effect on the uptake of [$^{14}$C]-oleic acid, the synthesis and amount of triacylglycerides, the synthesis of cholesterol esters, the accumulation of lipid droplets, the cell proliferation and the cell motility was investigated under normoxia (21% $O_2$) and hypoxia (1% $O_2$) by Goto et al. [106]. An increase in the synthesis of triacylglycerides, cholesterol esters and the accumulation of lipid droplets was observed under hypoxic conditions. The incubation with

XN (3 µM) under hypoxia decreased the aggregation of lipid droplets, the proliferation and the cell motility. The inhibitory effect of XN was solely observed under hypoxic conditions and was attributed to an inhibitory effect on enzymes necessary for the lipogenesis of triaclyglycerides. The synthesis and accumulation of neutral lipids such as triglyceride was attributed to the protection of pH decrease within the cancer cells and the survival. The decrease of pH is induced by the metabolism of glucose to lactic acid under hypoxic conditions [106].

Because of the lipophilic character of triglycerides and the amphiphilic character of phospholipids, cholesterols and cholesterol esters cannot be transported in the blood stream on their own. They are packed in so-called lipoproteins. Lipoproteins are separated in two segments, a shell and a core. The shell is composed of phospholipids, apoproteins and cholesterol. It separates the lipophilic core from the hydrophilic blood and has an amphiphilic character. The ratio between triglycerides, cholesterol esters, proteins and phospholipids depend on the lipoprotein species. For the assembling of lipoproteins with apoprotein B the chaperon microsomal triglyceride transfer protein (MTP) is indispensible. MTP consist of three active domains. The first is involved in the transfer of triglycerides from the microsomal lumen into the lumen of the endoplasmatic reticulum (ER). The second is associating to the membrane of the ER and the third binds to apoprotein B [107].

The effect of XN on the secretion of apoprotein B, the synthesis and secretion of triglyceride, the activity of MTP and DGAT in HepG2 was described by Casaschi et al. [108]. At a concentration of 15 µM, XN decreased the synthesis and segregation of triglycerides in the presence or absence of oleic acid. This effect was attributed to an inhibition of DGAT. In addition to the lowered triglyceride synthesis, the accumulation of triglycerides was inhibited to 37% in the cytosol and 64% in the microsomal lumen. A diminished availability of triglycerides may lead to an inhibition of the lipoprotein assembling. Besides the influence of XN on the triglyceride levels a decreased apoprotein B secretion at a concentration of 5, 10 and 15 µM XN was detected. Again the observed effects were detected whether or not oleic acid was added. The apoprotein B secretion e.g. at a concentration of 15 µM XN was lowered to 43 ± 2% (- oleic acid) and 31 ± 2% (+ oleic acid). The authors discussed that apoprotein B might be depleted through proteasomes, because the highest recovery of apoprotein B was found for the control cells. Further results showed an inhibition of the MTP activity of 30 ± 1% (- oleic acid) at a concentration of 25 µM XN and 30 ± 4% (+ oleic acid) at a concentration of 15 µM XN [108].

In another study the ability of XN to interact with the farneosid X receptor (FXR) was investigated in a transient transfection assay using HepG2 cells transfected with the human bile salt export pump (BSEP). Additionally the influence of XN on the FXR in KK-$A^y$ mice was investigated. In HepG2 cells XN induced the activity of luciferase and pointed to an agonistic

effect on FXR [109]. FXR is a bile acid receptor and down-regulates the activity of cholesterol-7-hydroxylase (CYP7A1). CYP7A1 converts cholesterol into bile acids via the small heterodimer partner (SHP) [110]. FXR were shown to exhibit important function for the bile acid and lipid homeostasis [111]. The effect of XN on KK-$A^y$ mice suffering from diabetes mellitus, hyperinsulinemia, hyperglycemia and hyperlipidemia was investigated by Nozawa et al. [109]. The KK-$A^y$ mice showed lower water intake, reduced white adipose tissue, reduced plasma glucose levels and reduced TG levels. In addition an increase of the adiponectin concentration was observed. Adiponectin is excreted in adipocytes and leads to a higher uptake of insulin, β-oxidation in skeletal muscle and adipose tissue, and an inhibition of glucose excretion from hepatic cells [112]. The reduction of the TG and glucose concentrations was attributed to an increased adiponectin production after XN feeding of KK-$A^y$ mice. In order to verify if XN acts through the FXR *in vivo*, the liver of the KK-$A^y$ mice were analyzed. In doing so the expression levels of the downstream proteins of the FXR were determined by real-time PCR. The obtained results from the liver did not confirm the results obtained *in vitro* in the transient transfection assay transfected with the human BSEP in HepG2 cells. Compared to the control group, the mRNA concentrations of the liver proteins BSEP and SHP were reduced. The amount of mRNA of the CYP7A1 was significantly increased and thus implicated that XN may act as an antagonist on FXR. As described above FXR is a bile acid receptor and down-regulates the activity of CYP7A1. The mRNA levels of Sterol regulatory element binding protein (SREBP) 1c were reduced during the stimulation with XN [109]. The transcription factor SREBR-1c is involved in the lipid metabolism of fatty acids and cholesterol. Furthermore it is downregulated in obese humans and is than upregulated after weight loss [113]. Interestingly, no effect on the cholesterol concentration in the liver could be observed [109].

In order to investigate the influence of XN on the live death cycle and the level of adipogenetic factors such as peroxisome proliferator-activated receptor γ (PPARγ), CCAAT/enhancer binding protein α (C/EBPα), adipocyte lipid binding protein (aP2) of 3T3-L1 mouse embryo fibroblasts, the cells were stimulated with XN concentrations. [114]. The performed western blot showed that all aforementioned proteins were diminished. These proteins are involved in the differentiation of adipocytes [115]. In addition to an inhibitory effect of XN on the proteins of the adipogenesis, the inhibition of the DGAT 1 could be confirmed [114].

In a second study, the effect of XN with and without the lignane honokiol of *Magnolia officinalis* REHD. et WILS on apoptosis of 3T3-L1 mouse embryo fibroblasts was determined [116]. Obesity is associated with diabetes mellitus II, the metabolic syndrome, and atherosclerosis, which are diseases with increasing death causes worldwide [104]. Obesity is defined as a body mass index of 30 kg/m$^2$ or higher [117] combined with an

increase in adipocytes number and storage volume of triglycerides [118]. One therapy strategy of obesity might be the induction of apoptosis in adipocytes to limit the fat storage [118]. The inhibition of the cell viability by the induction of apoptosis, which was described in the study of Yang et al. 2007 [114] could not been confirmed at XN concentrations up to 50 µM in the second study of Yang et al. 2008 [116]. Further experiments with higher XN concentrations were not conducted. However the stimulation with XN in combination with honokiol resulted in an increased apoptosis and decreased cell viability of 3T3-L1 mouse embryo fibroblasts [116].

Mendes et al. [119] investigated the influence of XN on the differentiation of preadipocytes to adipocytes. In doing so the effect of XN on the time dependent inhibition of the lipid content, the apoptosis, the Ki-67 levels (proliferation marker [120]) and the nuclear factor kappa light chain enhancer of activated B-cells (NF-κB) was determined in preadipocytes and adipocytes [119]. XN did not influence the lipid content in differentiated adipocytes. However XN decreased the lipid content in adipocytes if the preadipocytes were incubated with XN. XN significantly increased the amount of apoptotic cells in adipocytes compared to the preadipocyte. In addition, XN led to a decrease of the Ki-67 expression in preadipocytes. In contrast to Zhang et al. [118] Mendes et al. [119] discussed the decrease of adipocytes number contrary. The XN induced decrease of adipocytes number may lead in adipocyte hypertrophy. Adipocyte hypertrophy is correlated with insulin resistance, lower adiponectin levels and may lead to lysis of the cells. The latter can lead to infiltration of macrophages and inflammation. In addition to the performed experiments the level of the inflammatoric transcriptional factor NF-κB was determined in the preadipocytes and adipocytes. Increased NF-κB levels were found in preadipocytes. No effect on the NF-κB level could be observed in adipocytes [119].

Summing up, XN was shown to affect the carbohydrate metabolism as well as the expression and activity of DGAT in variety of model systems. XN led to a lower lipid accumulation and a lower apoprotein B secretion. In addition, XN was shown to induce apoptosis in adipocyte cell culture systems.

### 1.1.3. Anti-osteoporosis activity

During the menopause and the post menopause the estrogen level decreases. Decreased estrogen levels can lead to a variety of pathophysiological effects such as cardiovascular diseases, osteoporosis and furthermore non-critical unpleasant climacteric compliance. In order to overcome the estrogen deficiency, a hormone replacement therapy was introduced. At first a combination of estrogen or estrogen in combination with gestagen was and is the therapy of choice [99]. However, an increased risk for mamma carcinoma was observed for

the ingestion with estrogen and cardiovascular diseases was correlated with the intake of estrogen in combination with gestagen [99]. Additionally, women also use herbal drugs in order to relieve the detrimental and painful effects associated with the decreased estrogen levels. Extracts of *Cimicifuga racemosa* (L.) NUTT. [121], *Glycine max* (L.) MERR. [122] and *Humulus lupulus* L. (literature see below) were found to be promising therapy options. Several of their secondary metabolites can be assigned to the group of selective estrogen receptor modulators (SERMs). SERMs induce agonistic and antagonistic effects at α and β estrogen receptors. Thereby SERMs might positively influence bone homeostasis without negatively affecting endometric proliferation. The effects of SERMs depend on the affinity of the ligand at its receptor and the structure of the formed ligand-receptor complex binding to the estrogen response element [99].

8-Prenylnaringenin (8-PN) is the most abundant phytoestrogen in *H. lupulus*. XN and IXN showed no or less activity compared to estrogen [123]. However IXN was found to be a proestrogen, because it is converted to 8-PN by the gut microflora and CYP 450. XN was found to be spontaneously converted to IXN (1.3 Bioavailability, metabolism). However, XN showed noteworthy effects in the prevention of osteoporosis. Osteoporosis is correlated with a degradation of bone mass and a change in the bone architecture. These pathophysiological conditions can lead to nontraumatic fractures of the vertebral bodies and the femoral neck. Already in 1997, Tobe and co-workers [124] described the inhibition of bone resorption by XN and humulone in the pit formation assay. Effenberger and co-workers [125] investigated the affinity of XN and related metabolites to bind to α and β estrogen receptors. In addition, the influence of XN on the expression of down-stream proteins such as alkaline phosphatase, which is a bone formation marker, and IL-6 was investigated. In human osteosarcoma cells U-2 OS, transfected with the α and β estrogen receptor, the expression and activity of alkaline phosphatase was increased by XN. The expression of IL-6 was decreased (U-2 OS ER α and β; U-2 OS ER α) [125].

The performed estrogen receptor affinity studies showed that XN (ER α: 1.94; ER β: 0.73) exhibit a three orders of magnitude lesser affinity to the estrogen receptor than 8-PN (ER α: $1.53 \times 10^{-3}$; ER β: $1.88 \times 10^{-3}$). XN, 8-PN, 6-PN and IXN affected the expression of proteins such as alkaline phosphatase and IL-6 in a dose dependent manner. For example 8-PN exhibited the highest activity to induce alkaline phosphatase mRNA expression (in U-2 OS ER α cells) at a concentration of 0.1 (approximately 7.6 densitometry of the bands of RT-PCR without SD) and 1.0 µg/ml XN (approximately 11.2 without SD). At a concentration of 10 µg/ml the activity of XN to induce the alkaline phosphatase mRNA expression decreased (approximately 3.8 without SD). Thus Effenberger and co-workers [125] suggested a review of the suitable doses of herbal drugs.

In another study the effects of XN on osteoporosis related factors were investigated in a mesenchymal stem cell line [126]. Osteoblast markers, alkaline phosphatase, bone morphogenic protein 2, collagen type 1α, bone sialoprotein and osteocalcin were up-regulated after stimulation with XN. The osteoblast differentiation, the expression of Runt-related transcription factor 2 (RUNX2) and the transcriptional activity were increased via the p38 MAPK and the ERK pathway. RUNX2 is an essential transcription factor for the differentiation and the proper function of osteoblasts [127].
Summing up, XN is a potent osteoblast stimulus and might relieve the detrimental and painful effects associated with decreased estrogen levels during and after the menopause.

### 1.1.4. Influence of XN on phase I and phase II enzymes

The chemopreventive effects of substances are correlated with the ability to inhibit phase I and to induce phase II enzymes (see Chapter 1). Chemopreventive substances might inhibit the production of genotoxic substances such as heterocyclic aromatic amine e.g. 2-amino-3-methylimidazol[4,5-f]quinoline (IQ), benzo(a)pyrene (BaP), 2-amino-1-methyl-6-phenylimidazol[4,5-*b*]pyridine (PhIP), 2-amino-3,8-dimethylimidazol[4,5-*f*]quinoxaline (MelQx). IQ is activated in a two step reaction by the CYP1A/CYP1A2/N-acetyltransferase and sulfotransferase. During this reaction active genotoxic esters are formed [128].
The effect of XN on inhibition of genotoxicity was determined in different assays. Miranda et al. [129] investigated the ability of XN to inhibit the mutagenic effect of IQ using the Ames Salmonella assay. In addition, the ability of XN to inhibit the binding of IQ to DNA and proteins was determined in a radioactive assay. XN showed a significant inhibition at 10 µM in both assays [129].
In another study the cell based Comet assay (in HepG2) yielded comparable results. XN showed significant inhibition of IQ and BaP induced genotoxicity at 0.01 µM. XN itself showed no genotoxicity up to concentrations of 10 µM [130].
Viegas et al. [131] investigated the ability of XN to inhibit the genotoxicity of MelQx and PhlP. During co-incubation with MelQx and PhlP, XN showed protective effects at concentrations between 0.01-1 µM. DNA strand breaks were induced during the incubation with PhlP and XN at 10 µM. The authors discussed an additional prooxidative effect of PhlP and XN at higher XN concentrations [131].
The effect of XN to inhibit the genotoxicity of IQ was also tested *in vivo.* The foci (preneoplastic alteration) and the DNA damage of colon and liver were investigated in F344 rats. XN inhibited genotoxic effects induced by IQ in both tissues [132].
HAA´s are metabolized in the organism to genotoxic intermediates through P450 enzymes (see above). Thus the ability of XN to affect phase I and phase II enzymes was discussed.

Phase I enzymes are responsible for the activation of drugs and thus permit a conjugation e.g. with glucuronic acid by phase II enzymes. Usually the conjugation enhances the hydrophilicity of compounds, thereby allowing the fast renal excretion of toxic metabolites [99]. Various studies were conducted in order to investigate the effect of XN on the phase I and phase II metabolism [36,131,133,134,135]. Henderson et al [133] investigated the effect of XN on the CYP 450 in microsomes of insect cells. XN inhibited the catalytic activity of CYP1A1 and CYP1B1. A moderate inhibitory effect was observed for CYP1A2. The activity of CYP2E1 and CYP3A4 was only poorly inhibited by XN [133]. An inhibitory effect of XN on the CYP1A was also detected in a cell-based assay in H4IIE rat hepatoma cells [36].

XN also induced the NAD(P)H:quinone reductase (QR) in murine hepatoma cell Hepa 1c1c7 [36,134,135].

In an *in vitro* study Viegas et al. [131] determined the mRNA levels of phase I (CYP1A1, CYP1A2, NAT2, SULT1A1) and phase II (UGT1A1 and GSTA1) enzymes in HepG2 cells. The co-treatment with MelQx and XN led to dose dependent up-regulation of mRNA levels of all enzymes except of CYP1A2. The co-incubation with PhIP and XN led to an up-regulation of CYP1A2 and a down-regulation of GSTA1 [131]. Ferk et al. [132] did not observe differences in the activity of phase I and phase II enzymes in the liver of F344 rats after co-treatment with XN and QC [132]. However, it should be considered that *in vitro* results can hardly be compared to *in vivo* results.

The mechanism of the QR induction by XN was investigated in several assays by different research groups [36,134,135,136,137]. It was found that XN is a monofunctional inducer of the QR. XN did not affect the induction of phase I enzymes [36,135]. In brief, Gerhäuser et al. [36] transfected Hepa 1c1c7 cells with plasmids that carry selective elements of the QR or/and phase I enzymes. The incubation of the transfected cells with XN showed an induction solely of the QR element. In another study conducted by Miranda et al. [135], the ability of XN to act as a monofunctional or bifunctional inducer was investigated in aryl hydrocarbon (Ah) receptor deficient Hepa 1c1c7 cells. XN induced the expression of the QR in the Ah receptor deficient cells. Thus it could be concluded that XN acts as a monofunctional inducer of the QR [135]. The expression of the QR in Ah receptor deficient cell lines is induced by the antioxidant response element (ARE). The transcription factor nuclear factor-erythroid 2 (NF-E2)-related factor 2 (Nrf 2) is bound to Kelch-such as ECH-associated protein 1 (Keap 1) in the cytosol. After an electrophilic reaction of thiol groups of Keap 1 and/or the phosphorylation of Nrf 2, Nrf 2 is released to the nucleus. Nrf 2 binds to ARE with the small Maf and regulates the transcription of proteins such as the glutathione synthetase (GS), HO 1, SOD, QR and UDP-glucuronosyltransferase (UGT) [138] (Figure 1-4). The Nrf 2-Keap 1 pathway is activated if cells are exposed to chemicals and oxidative stress.

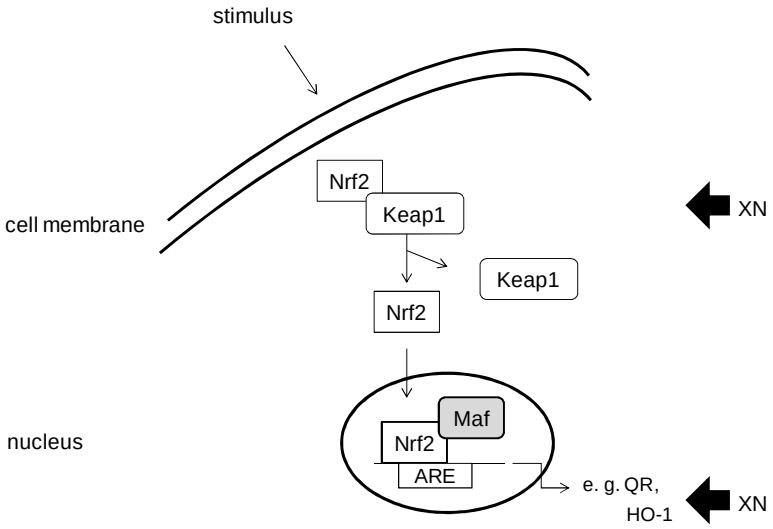


**Figure 1-4: Nfr2 Keap1 Pathway and the interaction with XN (the pathway is based on the information in [138])**

The ability of XN to induce the ARE was investigated using a luciferase assay in HepG2 cells. XN increased the response of the luciferase assay [134]. In order to investigate the effect of XN on the Nrf 2-Keap 1 pathway in detail, the alkylation of the Keap 1 was checked by mass spectrometry. XN alkylated the Keap 1 [134,136] and reacted mostly with the sulfhydryl group of C151 of the Keap 1 [137]. These results strengthened the theory that a Michael like reaction might be responsible for the induction of phase II enzymes. However, this might not be the full explanation. Miranda et al. [135] determined the structure-response relationship between prenylated and non-prenylated flavanones and chalcones. Flavanones without a prenyl group showed no QR induction. Prenylated flavanones led to a weak QR induction [135].

In a recent study XN was found to induce also the transcription of haeme-oxygenase 1 (HO 1), which is a phase II enzyme [139]. HO 1 is correlated with anti-oxidative, anti-inflammatory and anti-proliferative properties [140].

Summing up, XN induces phase II enzymes such as the QR and HO 1 via the Nrf 2-Keap 1 pathway. XN protects cells from genotoxic damage by HAAs. An inhibitory effect on phase I enzymes has to be confirmed in further *in vivo* experiments.

### 1.1.5. (Anti)-oxidative effect

Reactive oxygen species (ROS) are either radicals or non-radicals. ROS can lead to oxidation of substances and harmful reactions. There are also other types of reactive species such as reactive nitrogen, reactive chlorine and reactive bromine species [141]. The reactivity and harmfulness of radicals is dependent on the radical species. ROS such as hydrogen peroxide and superoxide radical anions exhibit a high reaction rate. However, they

are less harmful than hydroxyl radicals. Unfortunately there is no scavenger in biological systems that react preferentially with hydroxyl radicals [142].

In the respiratory chain of mitochondria, oxygen is needed to transfer electrons and build up water as well as ATP. During this process ROS can be released. It is for this reason that organisms built up defense mechanism in order to scavenge ROS. In a healthy organism the production and the scavenging of radicals is in balance. An overproduction of ROS can be induced by exogenic factors such as UV radiation and the uptake of toxic compounds such as cigarette smoke. In addition, ROS can be released during the response of the immune system, which is referred to as “respiratory burst”. Intracellular enzymes, that are known to produce ROS, include the cytochrome P 450, xanthine, and the NAPDH oxidase. ROS are also produced during the Fenton reaction [143,144]. ROS are correlated with the development and promotion of cancer as well as neurodegenerative and cardiovascular diseases. Humans exhibit various defensive strategies based on superoxide dismutase, glutathione peroxidase, ascorbic acid, α-tocopherol and glutathione. But the capacity of the body´s own defense is limited and ingestion of natural phenolic compounds, which exhibit an antioxidant activity, is claimed to be beneficial. Quercetin, one of the most potent scavengers of the flavonoids, exhibit three important structural characteristics for scavenging activity: the catechol structure of the B ring, the 2-3 diene structure and an oxo-structure in position 4 of the C ring [145].

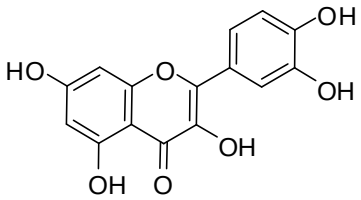


**Figure 1-5: Quercetin is one of the most potent radical scavengers within the flavonoids. The catechol structure of the B ring, the 2-3 diene structure and a keto functionality in position 4 of the C ring [145] are important features for the scavenging activity.**

Chelation of metal cations, stimulation or inhibition of enzymes and neutralization of radicals can also lead to an anti-oxidant effect [142]. The anti-oxidant properties of XN were investigated in a variety of assays including the LDL peroxidation assay. The peroxidation of LDL is an essential factor for the formation of atherosclerosis. The oxidation of LDL can be assessed by the formation of diene and thiobarbituric acid-reactive substances (TBARS) [146,147].

A structure-response relationship study with 13 chalcones and the corresponding flavonoids as well as α-tocopherol was performed. XN showed anti–oxidant activity already at 5 µM. But XN`s anti-oxidant activity on the formation of dienes was lower compared to quercetin.

However, it was higher than that of the other tested compounds. Interestingly, the inhibition of the formation of TBARS was more effective if a combination of XN and α-tocopherol was used instead of each compound on its own [146].

In another, study the anti-oxidative properties of XN were compared to 12 polyphenolic substances in a liver microsomal lipid peroxidation assay and in rat hepatocytes. $Fe^{2+}$/ascorbate, $Fe^{3+}$-ADP/NADPH, and tert-butylhydroperoxide (TBH) were used as inducers for the lipid peroxidation. XN showed an anti-oxidant effect at 5 and 25 µM in the microsomal lipid peroxidation assay with $Fe^{2+}$/ascorbate > $Fe^{3+}$-ADP/NADPH >TBH. XN also inhibited cytotoxic effects induced by TBH in primary rat hepatocytes. In order to investigate the underlying mechanism of the protective effects of the compounds, two additional assays were performed. In doing so, their influence on the activity of the NADPH-cytochrome P 450-reductase and the chelation of iron was investigated. Quercetin showed an effect in both assays. XN did not show any activity. Thus XN has to act through another mechanism [148].

Stevens et al. [147] investigated the scavenging effect of several chalcones and flavonoids. In this study the inhibition of the LDL peroxidation, which was induced by 3-morpholino sydnonimine (SIN-1), was measured. The prenylated chalcones showed the highest anti-oxidant activity [147]. This correlation was also be observed by Miranda et al. [146] and Rodriguez et al. [148].

In addition to the structure-response relationship study, Stevens et al. [147] also investigated the structures of the XN metabolites, which were formed after incubation with SIN-1 and peroxynitrite. In the former set-up auronxanthohumol and endoperoxyxanthohumol were found to be the main XN metabolites. In the latter set-up solely endoperoxyxanthohumol was formed. Based on these results it was discussed that the α,β-unsaturated keto functionality of XN is important for the anti-oxidant activity. In addition the prenyl group has an electron donating effect, which on his part contributes to the anti-oxidant activity [147].

Peroxidation of erythrocytes leads to their immediate shrinkage followed by subsequent cell death. As a consequence of this, anemia, vascular injury and metabolic syndrome can occur. XN was tested concerning its potential to inhibit the peroxidation of erythrocytes by their co-incubation with TBH. XN was an inhibitor of the TBH induced lipid peroxidation [149].

In further studies the anti-oxidant activity of XN and XN metabolites were investigated in an oxygen radical absorbance capacity fluorescein assay (ORAC). In this assay set up 2,2′-azobis(2-methylpropionamide) dihydrochloride (AAPH) is used for the generation of radicals and fluorescein as the fluorescent dye. The anti-oxidant activity is correlated with the inhibition of fluorescence decrease. The results are compared to the anti-oxidant activity of Trolox. XN showed lower anti-oxidant activity than ferulic acid and p-coumaric acid. XN exhibited $2.3 \pm 0.2$ Trolox equivalents in a concentration range of 0.25-1.5 µM [150–152].

Ferulic acid exhibited 4.47 ± 0.21 Trolox equivalents in a concentration range of 0.3-1.0 µM [153]. These results compared well to the ORAC assay results obtained by Gerhäuser et al. [36].

Beside this ORAC assay, three more assays were performed in order to determine the anti-oxidant activity of XN. In the first assay the fluorescence decrease of β-phycocrythrins induced by hydroxyl radicals was studied. The hydroxyl radicals were formed with $H_2O_2$-$CuSO_4$. This assay yielded 8.9 Trolox equivalents for XN at a concentration of 1 µM. In the second assay, the scavenging of superoxide radical anions formed from 12-*O*-tetradecanoylphorbol-13-acetate (TPA) by XN was measured in differentiated HL-60 human promyelocytic leukemia cells. XN inhibited the superoxide radical anion production with an $IC_{50}$ value of 2.6 ± 0.4 µM. In the third assay the inhibition of the superoxide formation was measured in a xanthine/xanthine oxidase assay. XN inhibited the superoxide radical anion production with an $SC_{50}$ value of 27.7 ± 4.9 µM. The detection dye used in the xanthine/xanthine oxidase assay was nitro blue tetrazolium chloride (NBT). The concentration of NBT was 25 µM [36].

Schempp et al. [154] re-evaluated the anti-oxidant activity of XN in the xanthine/xanthine oxidase assay. In this study the anti-oxidant activity of XN disappeared at a concentration of 100 µM NBT. The authors suggested that XN might form radicals upon autooxidation and thus scavenge the NBT radicals which are formed by the superoxide radical anions. A change of the detection system to cytochrome c confirmed that XN is not a superoxide scavenger [154].

Hartkorn et al. [155] investigated the ability of XN to affect the oxidation of luminol *in vitro*. The anti-oxidant activity was determined in a xanthine/xanthine oxidase assay. The determined $IC_{50}$ value was 15 µM [155]. Schempp et al. [154] could confirm the results but discussed mismatches within the assay. XN can absorb light in wavelength range that includes the light emitted by luminol. In addition XN might scavenge the luminal radicals [154].

In the second part of the study of Hartkorn et al. [155], the influence of XN on the superoxide dismutase (SOD), 8-isoprostane, which is a marker for lipid peroxidation and GSH were studied under hepatic ischemia reperfusion conditions [155]. The hepatic ischemia reperfusion is an accepted model to investigate the anti-oxidant effects of compounds *in vivo* [156]. SOD and 8-isoprostane were positively affected by XN. But no influence on the GSH levels under hepatic ischemia reperfusion was observed. In addition NF-κB and Akt as well as the anti-apoptotic marker Bcl-xl, the proapoptotic marker caspase-3 and the liver injury markers aspartate aminotransferase (AST), alanine aminotransferase (ALT) were determined. The NF-κB and Akt level was not significantly decreased, whereas the level of the anti-apoptotic marker Bcl-xl was markedly reduced. After the ischemia reperfusion the

proapoptotic marker caspase-3 was increased. During the reperfusion period a slightly increase of AST, ALT and LDH was determined. A cytotoxic effect of XN in the hepatic ischemia and reperfusion system was discussed [155].

The production of superoxide radical anion in XN treated cells was also determined by the dihydroethidium to 2-hydroxyethidium (DHE) assay and the formation of the thiol disulfide GSSG. XN produced superoxide radical anions in dose dependent manner in BPH-1, PC-3, LNCaP, SkBr3 and RAW 264.7 cell lines (The $EC_{50}$ value of maximal superoxide radical anion induction were $2.3 \pm 0.1$ µM to $4.0 \pm 0.5$ µM, respectively). This effect could not be observed in cell free conditions. An involvement of mitochondria within the superoxide radical anion production by XN and a correlation within the induction of apoptosis was discussed. In order to verify this theory, isolated mouse liver mitochondria were used to perform a DHE assay. The production of superoxide radical anion could be confirmed. In addition an effect on the respiratory chain, ATP concentration, mitochondrial potential and the cytochrome c release was observed at 12.5 µM XN. PARP cleavage was detected [157]. These effects were also observed in a T98G human malignant glioblastoma cell line and were associated with an activation of mitogen activated protein kinase (MAPK)-pathway/p38 [158]. The increased production of ROS by XN was also confirmed in a study conducted by Yang et al. [114]. An increase in the ROS concentration of $1509 \pm 125$% was measured in 3T3-L1 mouse embryo fibroblasts after 20 min. A cytochrome c release, a diminished mitochondrial potential and PARP cleavage were also detected [114].

In another study the inhibition of the TBH induced DNA strand break was examined in a comet-assay. No scavenging effect of XN could be detected. Nevertheless, a pre-incubation revealed significant DNA protection in HepG2 cells. A stimulation of cellular mechanism such as phase II enzymes, which lead to a protective effect, was discussed [130]. No scavenging activity of XN could be observed in a 1,1-diphenyl-2-picrylhydrazyl (DPPH) radical assay [130,134].

Summing up the ability of XN to scavenge superoxide radicals should be abandoned, but a scavenging of peroxynitrite and hydroxyl radicals appears likely. It must be kept in mind that dietary products are transformed to metabolites after ingestion. The investigation of the type of XN metabolites revealed metabolites with a catechol substructure in the B ring [159,160], which can also contribute to the scavenging of radicals. XN was also found to induce the production of ROS that trigger cells into apoptosis (see 1.1.7 Pro-apoptotic mechanism).

### 1.1.6. Anti-inflammatory effect

Today it is obvious that chronic inflammation increases the risk for cancer. It is discussed that 15-20% of cancer correlated death are induced by inflammation. A chronic inflammation

can be caused e.g. by *Helicobacter pylori*, Barrett´s esophagus, alcoholic liver diseases [161]. Beside cancer other diseases such as metabolic syndrome [162], diabetes [163], inflammation bowel disease [164] and Alzheimer´s disease [165] are also correlated with chronic inflammation.

Inflammation is, under normal conditions, a temporary reaction and can be induced, for instance, by viruses, asbestos, bacteria and tissue injury. Macrophages and neutrophil granulocytes are the first inflammatory cells at the site of infection. They segregate chemokines, interleukins and ROS to orchestrate the adaptive immune system and induce inflammation. This reaction is referred to as innate immune system and causes inflammation with dolor, calor, rubor and tumor [166]. Molecular response of the immune system was shown to be involved in the carcinogenesis as well as the angiogenesis, metastasis and invasion of cancer. ROS can act as bacterial harmful agent but can also induce DNA and protein damage in healthy cells. DNA damage itself can cause mutation and can lead to cancer. Tumor-associated macrophages and cancer cells can secrete TNF-α, vascular endothelial growth factor (VEGF) and chemokine/cytokines, which leads to proliferation, angiogenesis and metastasis of cancer cells [34]. The transcription factor NF-κB plays a central role in the inflammatory processes in autoimmune diseases [167] as well as the tumor initiation and progression [168]. Thus a therapy strategy for chronic inflammatory bowel diseases is the inhibition of the NF-κB translocation and the transcription of mRNA [167]. There are two major release pathways of NF-κB, the canonical and the non-canonical pathway. NF-κB is a dimer which is located in the cytosol and bound to IκB. It is activated by a variety of substances including the tumor necrosis factor (TNF), LPS, receptor activator of NF-κB ligand (RANKL), UV-C radiation, epidermal growth factor (EGF), and ROS [168]. During the activation, the IκB kinase phosphorylates (IKK) the IκB unit of NF-κB/IκB and thus allows the degradation by the ubiquitin ligase complex (see Figure 1-6). NF-κB is then translocated to the nucleus and advances the transcription and subsequent expression of about 200 different proteins [34]. These proteins are involved in the defense of apoptosis (Bcl-2), the prostaglandin synthesis (COX-2, 5-LOX), in inflammatory mechanism (i-NOS, TNF-α, interleukins (IL)) and in the production of adhesion molecules (ICAM-1) [168].

As described above, the inhibition of NF-κB degradation might leads to the suppression of tumor cells and the inhibition of autoimmune diseases.

XN´s influence on the NF-κB pathway was investigated in a variety of studies and showed an inhibitory effect in “healthy” and cancer cells [155,169–174,175–177]. The inhibition of NF-κB leads to a decrease in the expression of downstream proteins and proinflammatory markers. XN inhibited the production of monocyte chemo-attractant protein-1 (MCP-1) in THP-1 monocytes [178], hepatic stellate cells, primary human hepatocytes [171], RAW 264.7 and U937 human monocytes [179]. The production of interleukins such as interleukin-6 (IL-6)

[178], mRNA levels of IL-8 and IL-1 [171], IL-2 [176] and IL-1β [172,173,180] as well as cytokine TNF [171], TNF-α [172,176] and IFN—γ [176] were decreased by XN. Inflammatory modulating enzymes which are regulated through NF-κB were affected by XN also. Examples include the cyclooxygenases (COX)-2 and COX-1 [36], N-acetylglucosaminidase (NAG) in wistar rats [180] and inducible NO synthase (iNOS) in RAW 264.7 glia cells [181].
Interestingly in ionomycin and phorbol 12-myristate 13-acetate activated EL-4 T cells, XN increased the production of IL-2 as well as other cytokines via the NF-AT and AP-1. But it had no effect on NF-κB [177]. No effect on NF-κB could be also observed in MCF7 cells [173]. In addition to these aforementioned effects of XN, proinflammatory factors and enzymes as well as angiogenic factors were affected by XN too (see 1.1.9 Anti-angiogenesis, -metastasis and –invasive properties).

The mechanism of NF-κB inhibition by XN was studied in myeloid and leukemic cells [178,182]. XN inhibited the activation of NF-κB, which was induced by TNF, IL-1β, LPS, $H_2O_2$ and okadaic acid. Because XN inhibited the induction of NF-κB independent of the stimulus it was concluded that there must be a similar underlying mechanism. The IKK and p65 unit of NF-κB were significantly affected by XN. The mutation of specific cysteine residues reversed the inhibition and anti-inflammatory effect. XN contains an electrophilic unsaturated carbonyl structure that reacts with sulfhydryl groups in a Michael addition. The sulfhydryl groups are located in the cysteine 179 of the IKK and the cysteine 38 of p65 [182]. Descriptive studies supported this theory. It was shown that IκBα degradation was decreased during the co-incubation with XN [169,171,176].
In the study of Peluso et al. [178] the influence of XN, XN metabolites and hydrated XN on the expression of MCP-1 and IL-6 was investigated in LPS activated monocytic THP-1 cells. MCP-1 and IL-6 are downstream signals of the LPS induced NF-κB pathway [168]. Hydrogenated XN inhibited the expression of the MCP-1 and IL-6. For this reason it was discussed that the α,β-unsaturated carbonyl structure might not be the only explanation for the observed effects. The LPS-binding protein associates with LPS, binds to CD14, and clusters with Toll-like receptor 4 (TLR4) [166,183]. MD-2 is essential for the initiation of the activation of the NF-κB cascade via the TLR4. XN inhibited the expression of TLR4 [172,178]. The fitting of the tested compounds with the MD-2 unit was calculated in a molecular docking simulation. It was shown that the increased inhibition of the MCP-1 and IL-6 is correlated with the fitting accuracy to MD-2 [178]. Cho et al. [172] showed an inhibition of the MD-2 expression by XN.
Beside the inhibition via the LPS induced pathway, XN inhibited the IFN-γ activated Januskinase/Signal transducers and activators of transcription (JAK/STAT) signaling. IFN-γ binds to the IFN receptors thereby leading to a conformation change and

auto-phosphorylation of the JAK. The JAK phosphorylates tyrosin residues within the receptor thereby creating docking sites for the STAT. The STAT homodimer modulates the expression of IRF-1, inflammatory enzymes such as iNOS and adhesion molecules such as ICAM-1 [184]. RAW 264.7 cells were stimulated with IFN-γ and showed reduced binding activity of STAT-1α and IRF-1, which was revealed by the measurement of decreased mRNA levels [172].

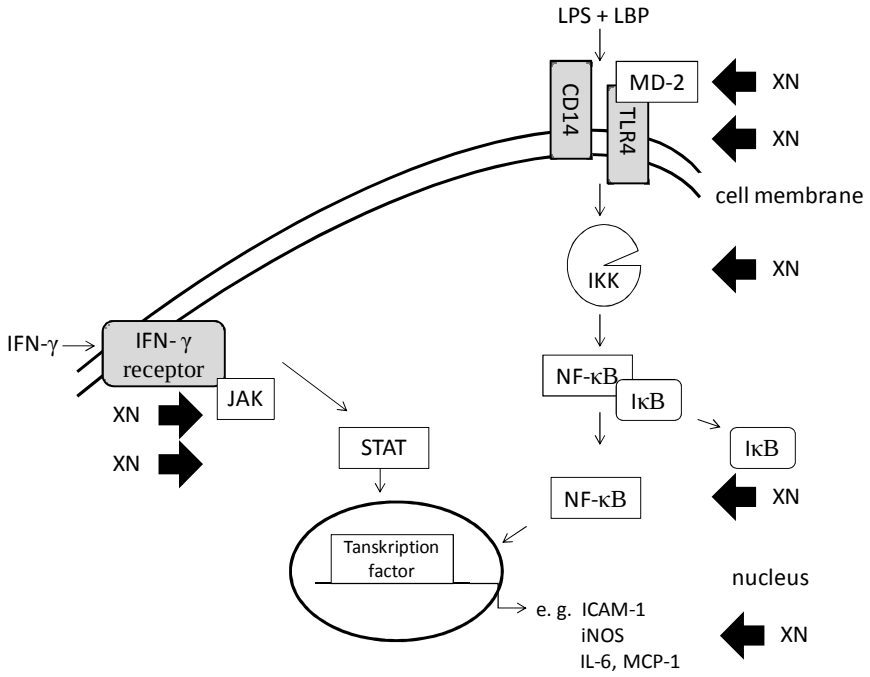


**Figure 1-6: Postulated mechanism of the anti-inflammatory effect of xanthohumol. (The JAK/STAT as well as the LPS and IFN-γ signal transduction through TLR4 is simplified pictured from [184]).**

Because of the anti-inflammatory effect of XN it was also tested concerning its ability to affect osteoarthritis. Examples include a study of the effect of XN and its metabolites on IL-stimulated bovine chondrocytes. XN inhibited the hyaluronan export via the ATP-binding cassette transporter multi-drug resistance associated protein 5 (MRP5) as well as proteoglycan and collagen loss [185].

XN was also investigated for the treatment of chronic allergic contact dermatitis and showed positive effects in BALB/c mice [177].

Of course, not every inflammatory/autoimmune disease initiates cancer and the inflammation in the proximity of cancer is not always associated with a bad prognosis. Nevertheless, the inhibition of NF-κB by XN showed beneficial effects on the initiation, progression, metastasis and invasion of cancer in a variety of cell types (see 1.1.9 Anti-angiogenesis, -metastasis and –invasive properties).

### 1.1.7. Pro-apoptotic mechanism

A balance between cell death and proliferation is indispensable to life. An abnormal cell-life time can lead to auto immune diseases, tumor generation and at worst to malignancy. An option for the treatment of cancer might be the inhibition of the proliferation by cell death induction. Thus the study of the cell death induction by compounds in malignant cells is a key for a successful tumor therapy. There are a variety of mechanisms that induce cell death such as necrosis, autophagy and apoptosis. Apoptosis is the most regulated mechanism and is characterized by a defined cascade of steps towards cell death. The cell fragments obtained during apoptosis are recycled. The apoptotic mechanisms are mainly regulated by a variety of proteins that is switched “on” and “off”.

XN was found to trigger death in a broad panel of cancer cell lines. Examples include human breast cancer MCF-7 [157,186,187], T47-D [187] and MDA-MB-435 cells [36], as well as the leukemic cells B-CLL [188], MM6, U937 [170,174,182], K562 [174], KBM-5 [182], Jurkat and HL-60 [36,182]. Furthermore, XN was effective in human colon cancer cells HT-29 [186], HCT-15 [189] and HCT116 derived 40-16 cells [190], prostate cancer cells LNCaP ($AR^+$) [191], DU145 and PC-3 [175,191,192], benign human cells BPH-1 [157,175], ovarian cancer cells A-2780 [186], SKOC3 [189] and OVCAR3 [193], hepatocellular cells HuH-7, HepG2 [194], AML12, HA22T/VGH, Hep3B [195] and hepatic stellate cells [171], human malignant glioblastoma cells T98G [158], fibroblasts HT-1080 [106], dendritic cells [196], medullary thyroid cancer cells TT7 [197], cervical cancer cells HeLa [150,151,152], human embryonic kidney cells HEK293 [155], adipocyte cells 3T3-L1 [114,116], macrophage microglia RAW 294.7 [157], lung cancer cell line A549 and melanoma cells SK-Mel-2 [189].

There are several cell death mechanisms of apoptosis which depend on the cell type, expressed receptors and modulating factors. In abnormal cells some of this apoptotic factors are mutated. In B-cell lymphoma, for instance, the anti-apoptotic protein Bcl-2 is over-expressed and leads to an abnormal survival. In 50% of colon cancers, the pro-apoptotic protein Bax is mutated [34]. Therefore the triggering of cancer cell apoptosis might be an effective tool to combat cancer. The most investigated signal pathways which lead to apoptosis are the extrinsic and the intrinsic apoptotic pathways. The intrinsic pathway is controlled by the mitochondria. Usually the extrinsic pathway is independent from the intrinsic pathway and mitochondria. In some cases however the extrinsic apoptotic signal on its own is not sufficient to induce apoptosis. In these cases the intrinsic pathway is induced too in order to potentiate the apoptotic stimulus [198].

The extrinsic pathway is activated by TNF and Fas ligands. The intrinsic is activated by DNA strand break, which can be induced by e.g. UV radiation [199]. In response to an extrinsic

signal the caspase cascade is initiated. Caspase is a zymogene protease that exhibits a cystein group in the active center and cleaves proteins after an aspartate residue. There are two forms of caspases, the initiator caspase and the effector caspase. The caspase cascade is started by a signal that activates the initiator caspase. The initiator caspase then activates the effector caspase. In the extrinsic pathway caspase-8 is the initiator caspase and procaspase-3 the effector caspase [200].

As a consequence of an extrinsic and/or intrinsic apoptotic stimulus proteases cleave other enzymes such as PARP and thus lead to a fast progression of apoptosis. PARP is therefore beside sphingomyelin used as a detection marker of apoptosis [201].

The intrinsic pathway is correlated with a release of cytochrome c. Cytochrome c is released from mitochondria via Bax. Bax is activated by pro-apoptotic factors of the Bcl-2 family and leads to the formation of pores in the mitochondrial membrane. The release of mitochondrial proteins activates caspase-9 by aggregation of the proteins with apoptosomes [200]. Cells that were treated with XN showed higher levels of the initiator caspase-9 [158,190,191,202] and an increased ROS production [114,157,158]. XN generated ROS via the inhibition of complex I to III of the respiratory chain and the inhibition of the electron flux between the complexes I or II and III [157].

During the stimulation of cells with XN a co-activation of the extrinsic and the intrinsic pathway could also be observed. Various research groups observed an up-regulation of the initiator caspases -8 and -9 and thus concluded that the apoptosis in the investigated prostate and human colon cancer cells was induced by the co-activation of the extrinsic and intrinsic apoptotic pathway [190,191].

In dentritic cells XN induced acid sphingomyelinase, caspase-8 and -3 and led to cell death solely via the extrinsic apoptotic pathway [196].

Further apoptotic pathways beside the extrinsic and the intrinsic are the endoplasmatic- and caspase independent pathway. The caspase independent pathway is correlated with apoptosis-inducing factors (AIF) which are excreted by mitochondria. Lust et al. [188] investigated the apoptotic mechanism of XN in B-CLL cells. No influence on caspase-3, p38 and Akt could be detected. Furthermore, XN induced apoptosis is not inhibitable with the caspase inhibitor zVAD-fmk [203]. Hence they discussed a caspase/caspase-3 independent apoptotic pathway. In addition Delmulle et al. [203] and Strathmann et al. [157] suggested autophagy as a further mechanism leading to cell death. Autophagosomes surround organelles and proteins. Upon fusion of these vesicles with lysosomes, the content gets degraded. The exact cascade of autophagy is not known yet. But it seems clear that proteases are also involved in the degradation of the cells by autophagy [34].

The induction of apoptosis by the endoplasmatic reticulum (ER) is less investigated. The ER is responsible for post translated modification and folding of proteins. ER stress leads to

higher misfolded and unfolded proteins which accumulate in the ER and activate the unfolded protein response (UDP). As a result the levels of chaperone glucose-regulated proteins (GRP) and heat-shock proteins are increased. This in turn leads to regulation of proteins such as the transmembrane kinase, which is also a stress responsible protein, RNA-activated protein kinase –like ER kinase (PERK), activating transcription factor 6 (ATF6) and inositol-requiring enzyme 1 (IRE1) transcription factor homologous protein (CHOP). The Up-regulation causes an activation of caspase-12 and cleavage of PARP [199,204]. XN induced the ER dependent factors such as GRP78, PERK, CCAAT/enhancer-binding protein (C/EBP), CHOP and IRE1 [202]. The ER dependent apoptosis was discussed by Lust et al [202] and Fribley et al. [205]. Fribley et al. [205] also discussed proteasomes as potential initiators.

Further signals/inducers are the C-Jun N-terminal kinase (JNK), p38, ceramide, granzyme B from cytotoxic T-cells, which discharge in the above described pathways [201]. JNK and p38 are mitogen-activated protein kinases (MAPK) which are involved in the activation of apoptosis [206]. The JNK phosphorylates proteins, which trigger the pro-apoptotic protein Bax [201]. An activation of ERK1/2 and p38 in a T98G human malignant glioblastoma cell line by ROS, which was induced by XN, was discussed [158].

Another substance that was determined to be a signaling factor towards apoptosis was ceramide. Ceramide is expressed at the cell surface after conversion of sphingomyelin by the acid sphingomyelinase (Asm). In addition ceramide is produced by *de novo* synthesis in cellular membranes. Thus the induction of Asm triggers apoptosis [207]. XN was shown to induce Asm and apoptosis in dendritic cells [196].

The protein kinase Akt is an important survival factor that effects proliferation, angiogenesis and apoptosis [34]. Akt is a regulating factor in the NF-κB pathway. Akt phosphorylates IKK that regulates the degradation of NF-κB/IκB and leads to a translocation of NF-κB to the nucleus. Hence the inhibition of Akt leads to apoptosis. Another pro-apoptotic factor that is regulated by Akt is Bad. Bad is a pro-apoptotic protein and belongs to the Bcl-2 family. An inhibition of Akt leads to dephosphorylation of Bad and the induction of apoptosis [201]. XN was found to be an Akt inhibitor. Deeb et al. [191] and Hartkorn et al. [155] showed an inhibition of Akt by XN. XN inhibited Akt in a hepatic ischemia/reperfusion model [155] and in a prostate cancer cell line [191]. An inhibition of NF-kB by XN was observed in leukemia cells [174].

XN triggers cancer cell into apoptosis, but shows rescue ambitions, too. Oxidative stress as well as energy exhausting can cause suicidal death of erythrocytes which is also referred to as eryptosis. Eryptosis is correlated with an increased activity of $Ca^{2+}$ and $K^{+}$ channels. In the process potassium chloride is effluxed which leads to a shrinkage of the erythrocytes. XN was found to prevent erythrocytes in dose dependent manner from suicidal death [149]. In

addition no viability inhibition in primary human hepatocytes at concentrations up to 100 µM could be observed [194]. Cancer cells exhibit an abnormal redox balance because of stress situations and elevated intercellular ROS levels [208]. This might explain the positive effects of XN on healthy cells and the induction of apoptosis in cancer cells. The in this chapter described apoptotic pathways that are influenced by XN are summarized in Figure 1-7.

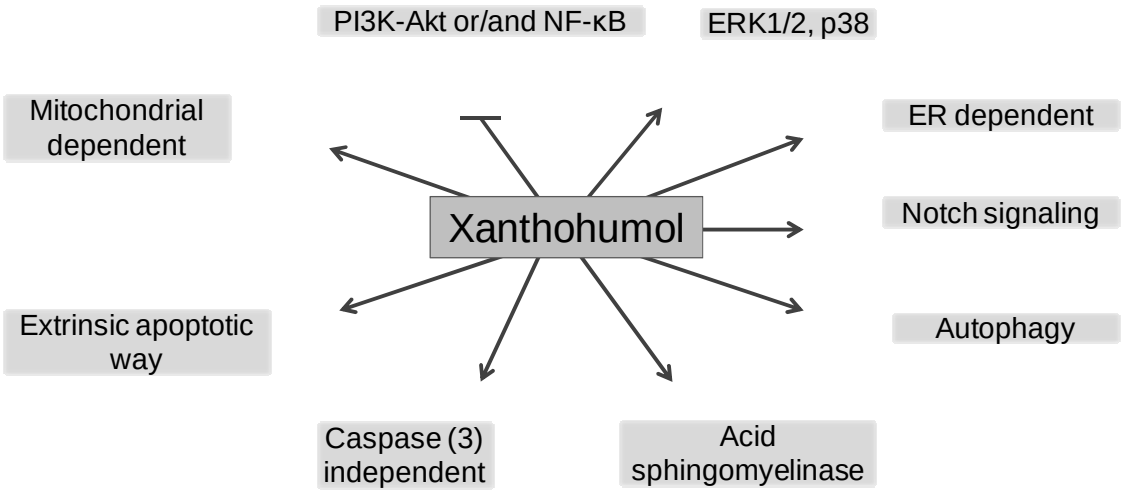


**Figure 1-7: XN induces apoptosis via different pathways: PI3K-Akt or/and NF-κB, ERK1/2, p38, ER dependent, Notch signaling, Autophagy, acid sphingomyelinase, caspase (3) independent, extrinsic apoptotic way and mitochondrial dependent.**

In principle the apoptotic mechanism depend on the cell type. However, the mechanisms for the induction of apoptosis by XN are not fully understood yet. XN induces apoptosis through multiple ways and is an extraordinary model compound for cancer treatment through the induction of apoptosis.

### 1.1.8. Estrogen modulating activity

Secondary metabolites of *H. lupulus* have been shown to have positive effects in the treatment of hormone dependent cancer. Estrogen is a ligand of estrogen receptors α or β (ER) which are located at the nucleus and leads to the expression of growth factors. Estrogen originates from the aromatization of testosterone and androstenedione. The underlying reaction is catalyzed by the aromatase (CYP19).

A target in the postmenopausal cancer therapy is the inhibition of aromatase in order to inhibit the estrogen-induced proliferation of the cancer cells. XN was investigated concerning its ability to inhibit the aromatase in choriocarcinoma JAR cells [209,210]. The aromatase

was inhibited by XN with an $IC_{50}$ value of 20.3 µM (95% confidence intervals of 15.3-26.9). However no significant influence of XN on the expression of aromatase was observed [209].
In addition to the proliferative effect, estrogen can also be converted to different *o*-quinones. The *o*-quinones can lead to malignance by binding to the DNA. Hemachandra et al. [211] investigated the influence of XN and 8-PN on the estrogen-induced expression of CYP 450 1B1 and CYP450 1A1 in MCF-10A cells. The expression of the CYP 450 was inhibited by 8-PN, but no effect of XN could be observed [211].
Estrogen modulates different pathways including those with an alkaline phosphatase expression. The alkaline phosphatase might be involved in tumorigenesis [212]. In pathological conditions, the alkaline phosphatase level is increased and may point to cancer [213,214]. The expression of intestines alkaline phosphatase as well as the proliferation of MCF-7 cells was inhibited by XN in mice [212].

### 1.1.9. Anti-angiogenesis, -metastasis and –invasive properties

Cancer is an uncontrolled proliferation of cells and can basically be grouped in two forms, the benign and the malignant form. The ability to metastasize, invade and impair organ functions is correlated with the malignancy of a cancer type. Hence the inhibition of metastasis, invasion and angiogenesis is a key approach in the treatment of malignant cancer. The process of metastasis can be divided in several steps such as migration, intravasation, transport, extravasation, metastatic colonization and angiogenesis. At first cancer cells have to separate from a solid tumor. Thus, the junctions of the tumor cells and the neighbor cells (catenin-cadherin junctions) as well as of the extracellular matrix (integrin junctions) have to be breached. An alteration in the junctions can lead to independent, cancer cell movement and adherence to other extracellular matrices. Mutations in the extracellular domain as well as methylation in the promotor section of E-cadherin gene was observed in some cancers. It is discussed that E-cadherin acts as a tumor suppressor by the securing of cell-cell junctions and suppresses metastasis of tumor cells into other body sections [34]. XN showed an anti-invasive effect mainly by growth inhibition and by the adhesion enhancement between breast cancer cells via the E-cadherin/catenin in a chicken heart invasion assay. This was implicated because the XN effect was abolished if the cells were treated with a monoclonal antibody for E-cadherin [187].
However other research groups could not observe an anti-invasive effect of XN [169,174,215].
In a study of Negrão et al. [216] XN was found to affect the proliferation, apoptosis and invasion of human aortic smooth muscle cells (HASMC). No effect on the invasion of human umbilical vein endothelial cells (HUVEC) could be observed. However an influence on the

proliferation and apoptosis could be detected [216]. Thus XNs effect on the cell invasion seems to be cell dependent.

XN was also found to influence enzymes and the expression of proteins that are correlated with metastasis. In brief, XN inhibited several matrix metalloproteases that break the connection between the extracellular matrix and the intestine in CML, HUVC [170], K562 CML [174], dermal fibroblasts [217], and HUVECs [169].

After the separation of tumor cells from a solid tumor and the extracellular matrix, malignant cells can penetrate blood and lymphatic vessels (intravasation) in order to reach the next organ. The extravasation is regulated by signals between cancer cells and endothelial cells. This process is also referred to as “seed and soil”. During the extravasation cancer cells adhere to the endothelium, penetrate the vessels, and infiltrate the intestine. If the cells penetrate the vessels from the interior side they can begin to colonize. The maximum distance between the cancer cells and the surrounding vessels that allows for the supply with oxygen and nutrients is 200 µm. In case of larger distances new vessels are formed (angiogenesis). Angiogenesis is a ubiquitous process e.g. during embryogenesis, organ development and wound healing. However the formation of blood vessels by endothelial cells in order to supply cancer cells with nutrients is fatal. Thus the control of the tumor-associated angiogenesis is another key approach in the treatment of cancer. The tumor-associated angiogenesis is regulated by a variety of pro-angiogenetic and anti-angiogenetic factors. The first include the vascular endothelial growth factors (VEGF) [34]. Imbalance between the pro-angiogenetic and anti-angiogenetic factors can cause extended vascularization which is also referred to as “sprouting” [218,34]. Sprouting is an effect that orchestrates matured endothelial cells in a way that they detach, move and built up new vessels. VEGF are one of the main activators that lead to a variety of pro-angiogenetic effects such as an increase in the permeability of blood vessels. The expression of VEGF is regulated not only but also by MAPK and PI3K/Akt [219]. XN was investigated concerning its ability to inhibit Akt in HUVECs which were stimulated with IGF-1 [169]. XN was found to be an Akt and NF-κB inhibitor (1.1.6 Anti-inflammatory ). An inhibition of the VEGF production by XN was observed in HUVEC, U 937 CML [170] and K562 cells [174]. In addition an inhibition of the VEGF production was observed in rats that ingested stout beer supplemented with XN [180].

The anti-angiogenetic potential of XN was investigated in a variety of *in vitro* and *in vivo* models. Examples include MCF7 xenografts in mice [173], a matrigel model and matrigel injected in mice [169,216], a wound healing model [180,216] and mice models for endometriosis [220]. XN significantly decreased the vascularization [169,173,180,216,220]. Additionally, in one of the studies a decreased factor VIII expression was detected [173]. The mechanism of the inhibition of the vascularization by XN was discussed from different perspectives. On the one hand a significant inhibition of the vascularization was correlated

with an inhibition of ROS and VEGF [169,180,220]. On the other hand an induction of apoptosis was discussed [173,220]. Dell'Eva et al. discussed a combination of both effects [170].

Summing up, XN is a potent anti-inflammatory and anti-angiogenetic substance due to the inhibition of Akt, NF-κB and correlated signals such as VEGF. The underlying mechanisms depend on the cancer cell type, the environment and the concentration of XN.

## 1.2 Safety studies

The use of XN as a therapeutic agent requires investigation of the effects on healthy cells and organisms in *in vitro* and *in vivo* models. Up to now only a few studies are available so far that addresses the safety of XN. In the following a short overview of these studies will be given. Albini et al. [169] investigated the effect of the supplementation of 200 µM XN in water on the health parameters of male nude mice. No effect of XN on the investigated parameters could be detected [169]. In another study human bone marrow progenitor cells isolated from healthy volunteers were incubated with XN in the colony-forming-unit assay. XN up to a concentration of 5 µM did not inhibit the proliferation of the cells [170]. Moreover XN up to a concentration of 100 µM showed no effect on the viability of primary human hepatocytes [194].

However cancer cell lines seem to be more sensitive to XN. A significant difference in the viability between normal and malignant astrocytes by XN could be detected. The observed lower viability of the malignant astrocytes was attributed to a more pronounced induction of apoptosis in the malignant cells [215].

In an *in vivo* safety study in Female Sprague Dawley rats the toxicity of XN on the liver, kidney, lung, heart, stomach and spleen was investigated. In this study, the rats obtained a XN supplemented starch suspension (1000 mg XN/kg body weight) every day by gavage. The feeding period was 28 days. The fed XN induced a slight hepatotoxicity and led to less developed mammary glands. Hence during the additionally performed fertility study the XN feeding dose was decreased to 100 mg XN/kg body weight per day. In the first as well as in the second generation no difference in the fertility was observed. However the sex ratio tended towards the female offspring [221].

A safety study with BALB/c mice revealed no difference in organ weight, appearance and function. The mice were fed with chows supplemented with 0.5% (w/w) XN which equates to 1000 mg XN/kg body weight [222]. The differences in the studies of Hussong et al. [221] and Dorn et al. [222] might be ascribed to the different animal species. In addition different analytical methods were used.

In another study the influence of XN (100 mg XN/kg body weight per day, 28 days) on the enterobacteria of Sprague Dawley rats was investigated. No influence on the flora composition could be observed [223].

## 1.3 Bioavailability, metabolism and cell uptake

It is of utmost importance to investigate the bioavailability of XN in order to determine suitable XN concentration ranges, which allow achieving the desired effects. The bioavailability of a substance is dependent on its liberation, absorption, distribution, metabolism and excretion.

The lipophilic XN was shown to have a low bioavailability after oral administration [224,225]. However the results differ depending on the way of ingestion and the sample preparation. Avula et al. [224] fed male wistar rats with 10, 20, 50, 100, 200, 400, 500 mg XN/kg body weight. Legette et al. [225] fed Sprague-Dawley rats and dissolved the XN in self-emulsifying isotropic mixtures of oleic acid, propylene glycol and Tween 80 (0.9:1:1). The oral gavage dose was 16.9 mg/kg body weight. Avula et al. [224] could not detect XN in the serum after oral application. Legette et al. [225] measured maximal concentrations of $0.42 \pm 0.03$ µM conjugated and unconjugated XN in the serum. A lipophilic solvent was used for the sample preparation [225]. Avula et al. [224] used methanol as extraction medium.

XN as a lipophilic compound adsorb not only at vessels [226] but probably also at proteins [227,228]. A high lipophilic elution solvent is necessary to dissolve XN in the extraction solutions. Thus the methods used for the quantification of XN can differ in the limit of detection (LOD) and limit of quantification (LOQ).

However the bioavailability can also be a matter of the concentration as Legette et al. [225] observed a dependency between the amount of XN in the serum and the ingested amount of XN. A double amount of XN fed did not lead to a twofold higher bioavailability of XN [225].

In order to give a reliable statement of the behavior of compounds in the organism it is also necessary to determine their metabolites. Unfortunately Avula et al. [224] did not determine the XN metabolites. Hence a conclusion concerning the non-detected XN in the serum is not possible [224].

The basic principle of biotransformation is well investigated. The main function of the biotransformation is the elimination of compounds from the organism. The enzymes, which are involved in the biotransformation, convert lipophilic compounds to more hydrophilic ones in order to allow for a fast excretion. The biotransformation takes place mainly in the liver and gut, but is also performed in other parts of the organism such as the kidney, muscle, lung, skin, spleen and blood. The biotransformation is usually a two step reaction. At first the haeme enzymes CYP 450 converts compounds by oxidation, reduction, alkylation and

dealkylation to reactive compounds. This process is also referred to as phase I reaction. In the phase II reaction, enzymes such as UDP-glucuronosyltransferases or sulfotransferases add glucuronic acid or sulfates. The enzymes are located in the mitochondria and cytosol, but especially in the endoplasmatic reticulum. Usually the metabolites which are produced during the biotransformation lose their activity. However the biotransformation can also lead to more reactive substances. This process is also referred to as bioactivation. Examples for substances that are bioactivated include HAA, morphine and some glucocorticoides [99,128]. Therefore it is of paramount importance to investigate the metabolites of phase I and phase II reactions concerning their pharmacological effects. However the pharmacological investigation of metabolites *in vivo* is rather sophisticated, because of their typically low concentrations. Hence structure identification studies are often performed *in vitro* with microsomes, microorganisms and the direct transformation with phase I and phase II enzymes. This applies also for XN.

Examples include the co-incubation of XN with human liver microsomes, rat liver microsomes, microorganisms and phase II enzymes [103,159,160,229,230,231,232]. Yilmazer et al. investigated phase I [159] and phase II metabolites [229]. XN was incubated with and without CYP inducers. Xanthohumol C (see Figure 3-1) and three further metabolic products were detected. This provided evidence that XN is a substrate for CYPs that are located in rat liver microsomes. Three of the metabolites were produced by epoxidation of the prenyl chain. The fourth by hydroxylation of the B ring [159]. The hydroxylated B ring of the XN metabolites is a catechol structure that might act as a radical scavenger [145] (see Figure 1-5).

In another study conducted by Yilmazer et al. [229] it was observed that glucuronidation is the main mechanism (89%) during the metabolism of XN in the phase II reaction [229]. The phase II enzymes UDP-glucuronyltransferases and sulfotransferases were not only found in the liver but also in the gastrointestinal tract. Hence it was suggested that XN is not only metabolized in the liver but with high evidence also in the gastrointestinal tract [230].

Unfortunately only few *in vivo* XN metabolism studies are available so far. One of these studies was conducted by Nookandeh et al. [233]. They detected 22 XN metabolites in the feces of female SD-rats. However 89% of non-metabolized XN were excreted and only 11% metabolites were produced. Several hitherto not reported metabolites such as xanthohumol H and 4-Methoxyxanthohumol (see Figure 3-1) were elucidated. XN was metabolized mainly by epoxidation of the prenyl chain, hydroxylation, *O*-methylation and *O*-acetylation [233]. In contrast to the *in vitro* studies conducted by Nikolic et al. [160] and Yilmazer et al. [159], no hydroxylation of the B ring was observed.

However IXN was detected in one *in vivo* study [233] as well as in one *in vitro* study [160]. IXN is an isomerization product of XN that is produced in beer during fermentation [9]. The

stomach was discussed as a possible place of isomerization. However this could not be confirmed in a study conducted by Possemiers et al. [234]. The consensus is a spontaneous isomerization of XN to IXN [225,235,236].

Another XN metabolite is 8-PN. 8-PN is a phytoestrogen with remarkable estrogenic activity. The formation of 8-PN was investigated in the artificial human intestinal microbial ecosystem. A dependency between the human gut microflora and the production of 8-PN was observed [234]. In further *in vitro* studies *Eubacterium limosum,* a resident of the human gut flora, was found to *O*-demethylate IXN to 8-PN. Supplementation of non 8-PN converter feces with *E. limosum* resulted in increased 8-PN levels [235]. The transformation of IXN to 8-PN was also observed in i*n vivo* studies. Human microbiota-associated Sprague-Dawley rats produced 8-PN, whereas Germ-free Sprague-Dawley rats did not. The IXN concentration in the serum of human microbiota-associated rats was found to be higher than in germ-free rats. Stability tests with gastric fluids yielded in decreased XN concentrations but no production of IXN [236].

The conversion of IXN to 8-PN was also observed in humans and thus confirmed the *in vitro* results as well as the *in vivo* rat experiments. The conversion was found to be mediated by the human gut [237] and CYP enzymes [238].

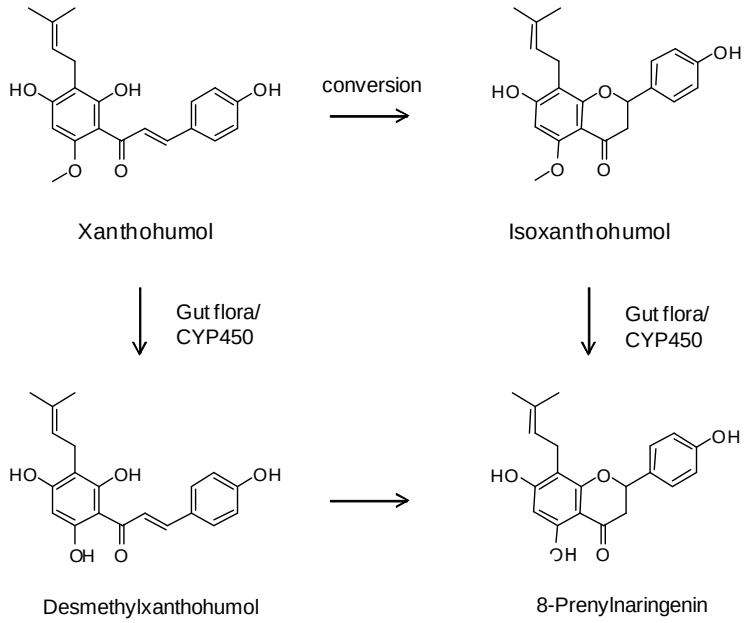


**Figure 1-8: Overview of the 8-prenylnaringenin (8-PN) production. Xanthohumol (XN) can be spontaneously converted to isoxanthohumol (IXN) and subsequently to 8-PN by gut flora or the CYP450. XN can be transformed to desmethylxanthohumol and subsequently to 8-PN.**

There are two principle ways for cellular excretion of hydrophobic compounds. One way is the aforementioned biotransformation. The second is the immediate efflux [239]. The phase II metabolites which are produced during the biotransformation are usually excreted

into the bile or the sinusoidal blood by membrane transporters such as multidrug resistance-associated proteins Mrp2, Mrp3 and Abcc2 [240]. ABC-transporter are ATP-dependent and are located in the cell membrane. The original function of the ABC-transporter is the transport of hydrophobic compounds across the cellular membrane [239]. The P-glycoprotein is a known transporter and is encoded by the *MDR1* gene. It plays a major role in drug resistance of cancer cells [34].

It is probable that XN metabolites are also excreted by membrane transporters. However the mechanism of the XN uptake and excretion is not fully known yet.

In the uptake study of Rodriguez-Proteau et al. [241] the influence of XN on the uptake of digoxin and cyclosporine A was investigated in Caco-2 and Madin-Darby canine kidney (MDCKII)–multidrug resistant (MDR) cells. The efflux of cyclosporine A was inhibited by XN. Nevertheless the intracellular cyclosporine A concentration was decreased. The efflux of digoxin was not impaired by XN. However the intracellular concentration increased. Rodriguez-Proteau et al. [241] discussed a competition between XN and cyclosporine A for the MDR1. A final conclusion could not be drawn since XN did not affect the efflux of digoxin [241]. However a competition might be an explanation, because XN was shown to accumulate up to 93% in Caco-2 cells [227] and hepatic cell lines [228] (see also chapter 4).

An influence of XN on ABC-transporter was also observed by further research groups [189,242]. XN was shown to decrease the mRNA levels of ABC-transporter such as the ABCB1, ABCC1, ABCC2 and ABCC3 [189]. In addition XN reduced the efflux of cimetidin by the P-glycoprotein in Caco-2 and porcine kidney epithelial LLC-PK1 cells [242].

Summing up the low bioavailability of XN might be explained by its comparably high lipophilicity and the fast and concentrated uptake of XN in different cell lines and cells avoiding the penetration into the blood stream, but the exact mechanism of the XN uptake is still unrevealed.

## 1.2. Aims

XN is a lipophilic compound and exhibits low water solubility. In order to use XN as model compound and to measure effects of XN in *in vitro* assays it was necessary to investigate suitable handling and experimental set-ups.

At first it should be determined which FCS concentration is necessary to achieve a suitable recovery of XN under cell culture conditions. Three different FCS concentrations (0, 1 and 10%) were chosen to mediate the solubility of XN. Because of its lipophilicity XN bind not only to proteins but also to different materials used in cell culture work. The dependency between the XN concentrations, the FCS amount and cell culture material were investigated

and are described in chapter 2. After establishing the experimental set-ups the behavior of minor hop chalcones, XN metabolites and related compounds were studied in *in vitro* assays. First the compounds were tested concerning their ability to influence the growth of cancer cell lines in chapter 3. MTT assays and CV assays were performed in order to measure the influence of the compounds on the cell viability, proliferation and concerning cytotoxic effect in three hepatic and one colorectal cancer cell line. The NO production was measured in a Griess assay and the iNOS expression with an iNOS activation kit using a fluorescence microscope.

Up to now, little is known about XN´s uptake and intracellular behavior. Therefore the uptake of XN was studied *in vitro* in two hepatic cancer cell lines HuH-7 and HSZ-B, primary hepatic cells and Caco-2 cells to mimic a part of the entero-hepatic circulation and is described in chapter 4.

Following the *in vitro* experiments, the absorption, distribution and metabolism of XN was investigated *in vivo* after oral intake by BALB/c mice and is described in chapter 5. The BALB/c mice were fed with 100 mg/kg, 500 mg/kg and 1000 mg/kg body weight of an XN enriched extract (73%) for 3 and 7 days. After the feeding period the concentrations of conjugated and unconjugated XN were determined in serum, urine, feces, bile and liver. In addition the absorption, distribution, metabolism and the XN concentration in dependency of the ingested XN amount were determined. Furthermore the influence of the matrix on the absorption, distribution and metabolism of XN was investigated on the basis of two different chows supplemented with either 98% XN (pure XN) or 73% XN (enriched extract with polyphenolic matrix, XE). The BALB/c mice were fed for either 3 or 7 days (1000 mg/kg body weight). After the feeding period the serum, liver, urine, feces and bile samples were analyzed concerning the amount of unconjugated and conjugated XN.

# 2 Pitfalls in cell culture work with xanthohumol [1)]

## 2.1 Abstract

Xanthohumol (XN), the most abundant prenylated chalcone in hop (*Humulus lupulus* L.) cones, is well known to exert several promising pharmacological activities *in vitro* and *in vivo*. Among these, the chemopreventive, anti-inflammatory and anti-cancer effects are probably the most interesting. As XN is hardly soluble in water and able to undergo conversion to isoxanthumol (IXN) we determined several handling characteristics for cell culture work with this compound. Recovery experiments revealed that working with XN under cell culture conditions requires a minimal amount of 10% fetal calf serum (FCS) to increase its solubility to reasonable concentration (~50-75 µmol/l) for pharmacological *in vitro* tests. Additionally, more than 50% of XN can be adsorbed to various plastic material routinely used in the cell culture using FCS concentrations below 10%. In contrast, experiments using fluorescence microscopy in living cells revealed that detection of cellular intake of XN is hampered by concentrations above 1% FCS.

## 2.2 Introduction

Triggered by the work of Gerhäuser et al. [36] the pharmacological characterization of the prenylated chalcone XN (Figure 2-1) strongly advanced in the last decade. It has been found that XN, which is the most abundant chalcone in hop (*H. lupulus* L.) cones, shows among others chemopreventive [36], anti-inflammatory [171], cytotoxic [150,192] and anti-angiogenic effects [169].

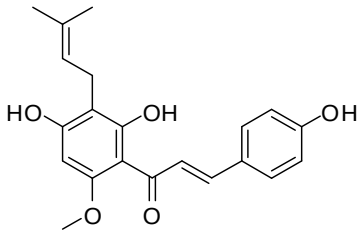


**Figure 2-1: Structure of xanthohumol (XN).**

[1)] The data of this chapter is published in: M. Motyl, B. Kraus, J. Heilmann, Pitfalls in cell culture work with xanthohumol, Pharmazie 67 (2012) 91–94.

Mechanistically, it has been observed that XN is able to influence the transcription factors NF-κB, NF-AT, Akt and Nrf2 [139,169,177] and to trigger apoptosis [157,191]. Furthermore, the modulation of enzymes involved in carcinogen metabolism and detoxification has been reported [36,134].

Interestingly, it has been noticed that handling of XN is difficult as the water solubility is low with only 1.3 mg/l at 23 °C [9], what is always a drawback for pharmacological *in vitro* and *in vivo* studies. Moreover, the stability of XN depends on the milieu, leading to the formation of the better water-soluble flavanone IXN under the influence of heat and water. Both aspects results in low XN contents in beer and consequently, IXN is much more abundant after brewing in comparison to XN itself. As the same process is observable for the chalcone desmethylxanthohumol, which is converted to the phytoestrogen 8-prenylnaringenin [9], stability of chalcones and their conversion to the corresponding flavanones is a topic of general importance.

A very recent study showed that not only brewing processes, but also *in vitro* assay conditions can initiate instability of XN and thus artificially influence the pharmacological activity. The presence of FCS is supposed to catalyze the formation of XN dependent radicals leading to degradation of XN as well as to radical processes with assay detector reagents and thus to false positive results [154]. As a first consequence of this investigation, XN cannot longer be classified only as a radical scavenger, but also as an inducer of radical producing pathways. This was also supported by very recent in vitro data from cellular test systems [157]. These handling difficulties prompted us to further investigate the behavior of XN in cell culture to give helpful suggestions for the reliable design of cellular experiments with XN. In our investigations, we first determined the solubility of XN in cell culture medium (Dulbeccos Minimum Essential Medium, DMEM) containing different concentrations of FCS. In a second step, the recovery of XN from medium was determined as a function of FCS concentration. Additionally, the recovery of XN from medium supplemented with 10% FCS was measured using different plastic materials routinely applied in cell culture like Petri dishes, cell culture flasks, centrifuge tubes and 96-well plates. Likewise, the feasible conversion of XN to IXN was investigated. As fluorescence microscopy, especially fluorescence imaging in living cells, is a tool with increasing importance for cellular studies we also analyzed the fluorescence behavior of XN in a cellular system at different concentration of FCS.

## 2.3 Material and Methods

XN was provided by NATECO$_2$ (Wolznach, Germany) with a purity >98% determined by HPLC as described as stated below. For determination of XN solubility and recovery, the same method was applied. All solvents (MeOH/$H_2O$) used were of HPLC quality. DMEM

(Gibco, Invitrogen, Grand Island N.Y., U.S.A.) was supplemented with different concentration (1-15%) of FCS (Biochrom AG Berlin, Germany) for the solubility and recovery experiments. For recovery experiments, stock solution of XN was added to the medium and incubated in Petri dishes d 100 x 20 mm, 96 well plates, culture flasks 75 $cm^2$ (all from TPP, Trasadingen, Switzerland), culture flasks 25 $cm^2$ (Greiner bio-one, Frickenhausen, Germany), tubes 1.5 ml and 2 ml (Eppendorf, Hamburg, Germany) and centrifuge tubes 15 ml (MEUS s.r.l., Piove di Sacco, Italy) for 3 or 24 h (37 °C, 5% $CO_2$, humidified incubator). After addition of two volumes (v/v) of acetone, the samples were vortexed and centrifuged at 20,000 g (4 °C). To purify the samples, the supernatants were centrifuged through NanoSep centrifugal devices (Cat. 5168502 VWR, Darmstadt, Germany) at 20,000 g (4 °C).

The analytical HPLC system consisted of an Elite La Chrom system (VWR-Hitach, Germany) equipped with an L-2455 diode array detector, a thermostated L-2200 autosampler, an L-2130 pump and an L-2350 column oven. A Purospher® Star RP-18e (column size: 250 x 4.0, particle size: 5 µM, Merck, Darmstadt, Germany) was used as column. Detection wavelength was 368 nm. The eluents were water/0.1% formic acid (A) and acetonitril/water (95/5, B). The injection volume of the sample was 20 µl and the following elution-programm was used with a flow rate of 1.0 ml per min (at 30 °C): 0-9 min 57.8-68.2% B 9-14 min followed by equilibration to 57.8%.

Solubility of XN was determined according to the method of Li et al. (modified, [243]). Shortly, 1 mg XN was continuously vortexed for 3 h or 24 h with 100 µl DMEM containing 1%, 5% or 10% FCS. Subsequently, 300 µl were filtered through a 0.45 µm Acrodisc® 13 mm syringe filter (PALL, Ann Arbor, MI USA) and then extracted as described above.

Fluorescence imaging experiments were performed using a computer controlled research microscope (Carl Zeiss Cell Observer®), consisting of a Zeiss Axio Observer (Carl Zeiss Göttingen, Germany) with Software AxioVision 4.8.1 (Carl Zeiss MicroImaging, Germany), following the protocol published by Wolff et al. [228]. For imaging of XN, a custom-built filter set was used (460/80 FT 475 BP605/40). Quantification of cellular XN fluorescence at individual time points was done automatically by the ASSAYbuilder® Physiology Analyst software (Carl Zeiss MicroImaging, Germany), using a phase contrast image to determine the cell boundaries. Values are presented as mean ± SD as indicated (with $n = 3$ or 4). Comparison between groups was made using one-way ANOVA, followed by Tukey´s Multiple Comparison Test as post test. A $p$ value $< 0.05$ was considered statistically significant. For elimination of outliers, the test according to Grubbs was applied. All calculations were performed using GraphPad.

## 2.4 Investigation, results and discussion

The solubility tests for XN in pure DMEM, according to the standard method of Li et al. [243] resulted in a solubility of less than 0.05 mg/l (3 h, 37 °C, centrifugation and filtration). This is in consideration of the moderately different experimental design in the same range as determined by [9] with 1.3 mg/l (water, 4.5 h, 23 °C and centrifugation), underlining again the bad solubility of XN in aqueous medium. Addition of FCS resulted in an increase of solubility to 2, 5 and 16 mg/l for DMEM containing 1, 5 and 10% FCS (after 3 h). As assays often required a longer incubation time, XN solubility was also determined after 24 h (37 °C) leading to an increased solubility of 4, 10 and 24 mg/l, respectively (Table 2-1).

**Table 2-1: Solubility of XN in DMEM after 3 and 24 h (37 °C, 5% $CO_2$, centrifuge tubes), and effect of FCS supplementation**

| Medium | Incubation time (h) | Solubility (mg/ml) |
|---|---|---|
| DMEM | 3 | < 0.05 |
| | 24 | < 0.05 |
| DMEM + 1% FCS | 3 | 2 |
| | 24 | 4 |
| DMEM + 5% FCS | 3 | 5 |
| | 24 | 10 |
| DMEM + 10% FCS | 3 | 16 |
| | 24 | 24 |

Accordingly, the maximal solubility of XN under cell culture conditions for 3-24 h (37 °C, 10% FCS) can be estimated to be 50-75 µmol/l. Consequently, the application of test concentrations clearly higher than 75 µM XN [150,186] renders the results somewhat uncertain as the accurate concentration of XN in the assay is not exactly determinable due to a clear exceeding of the solubility. In such cellular systems, an equilibration between solved, unsolved and intracellular XN can be expected dequalifying for example a determined $IC_{50}$ value of a cytotoxicity assay.

To verify the effective XN concentration in an assay a recovery experiment was performed by subjecting 10 µM XN to DMEM supplemented with different FCS concentrations (1-15%). After 3 h incubation at 37 °C (in centrifuge tubes) XN was extracted from the medium and quantified by HPLC. As expected, results showed that the measured XN concentration is a function of the percentile amount of FCS in medium (Figure 2-2 A).

**A**

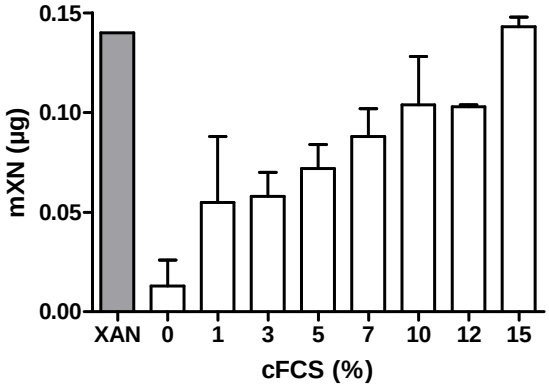


**B**

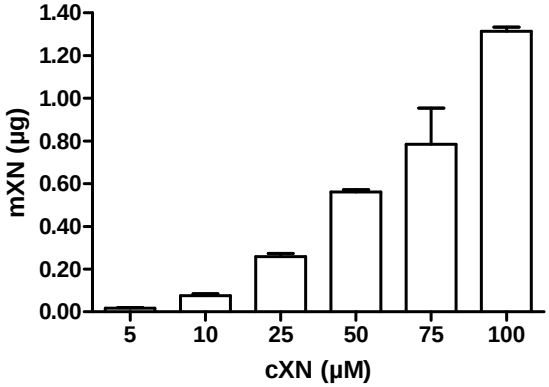


**C**

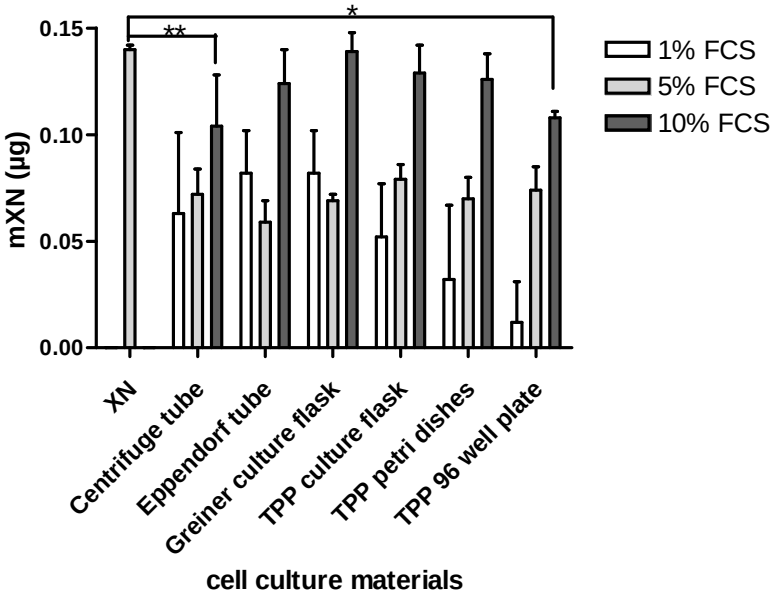


**Figure 2-2: A. Recovery of XN (10 µM) after incubation (3 h, 37 ℃) in DMEM supplemented with**

**-Figure 2-2 continues on page 43-**

**-Continuance of Figure 2-2-**

**different concentrations of FCS (1-15%) in centrifuge tubes (n=4). B. Recovery of XN from different concentrations (5, 10, 25, 50, 75 and 100 µM) incubated in DMEM supplemented with 10% FCS (n=4). C. Recovery of XN after incubation of 10 µM XN (3 h, 37 °C) in DMEM supplemented with 1, 5 and 10% FCS in different cell culture material like Petri dishes, flasks, centrifuge tubes and 96 well plates from different suppliers (n=3). All values in comparison to control (XN).**

Surprisingly, the measured XN concentration is significantly lower in comparison to the applied 10 µM even in FCS concentrations sufficient for an entire solution of the compound. A series of recovery experiments with XN concentrations of 5, 10, 25, 50, 75 and 100 µM (3 h, 37 °C, 10% FCS) showed that the reduced amount of recovered XN is not due to a reduced solubility as higher concentrations of dissolved XN can be easily obtained (Figure 2-2 B). We therefore concluded that most likely also absorption phenomena on plastic materials can be obtained for XN under normal assay conditions. This was pursued by incubating 10 µM XN (3 h, 37 °C) in DMEM supplemented with 1, 5 and 10% FCS in different cell culture material like Petri dishes, flasks, centrifuge tubes and 96 well plates from different suppliers (Figure 2-2 C). Experiments revealed remarkable differences concerning the recovery of XN from the medium depending on the used cell culture material. For all materials, a satisfying recovery (>90%) of XN requires a minimum of 10% FCS in the medium, whereas 1 or 5% FCS resulted in a server loss (~50% or more) of the test compound (Figure 2-2 C).

On the other hand, high FCS concentrations can also hamper results from cellular *in vitro* experiments, as the fluorescence properties of substances can be affected. As shown by Wolff et al. [228] the cellular intake of XN into cells can be followed by imaging of XN fluorescence. In our experiments, we followed the time dependent cellular intake of 10 µM XN in immortalized human hepatic stellate cells [244] with fluorescence microscopy (Figure 2-3 A) varying the FCS concentrations from 1-10%.

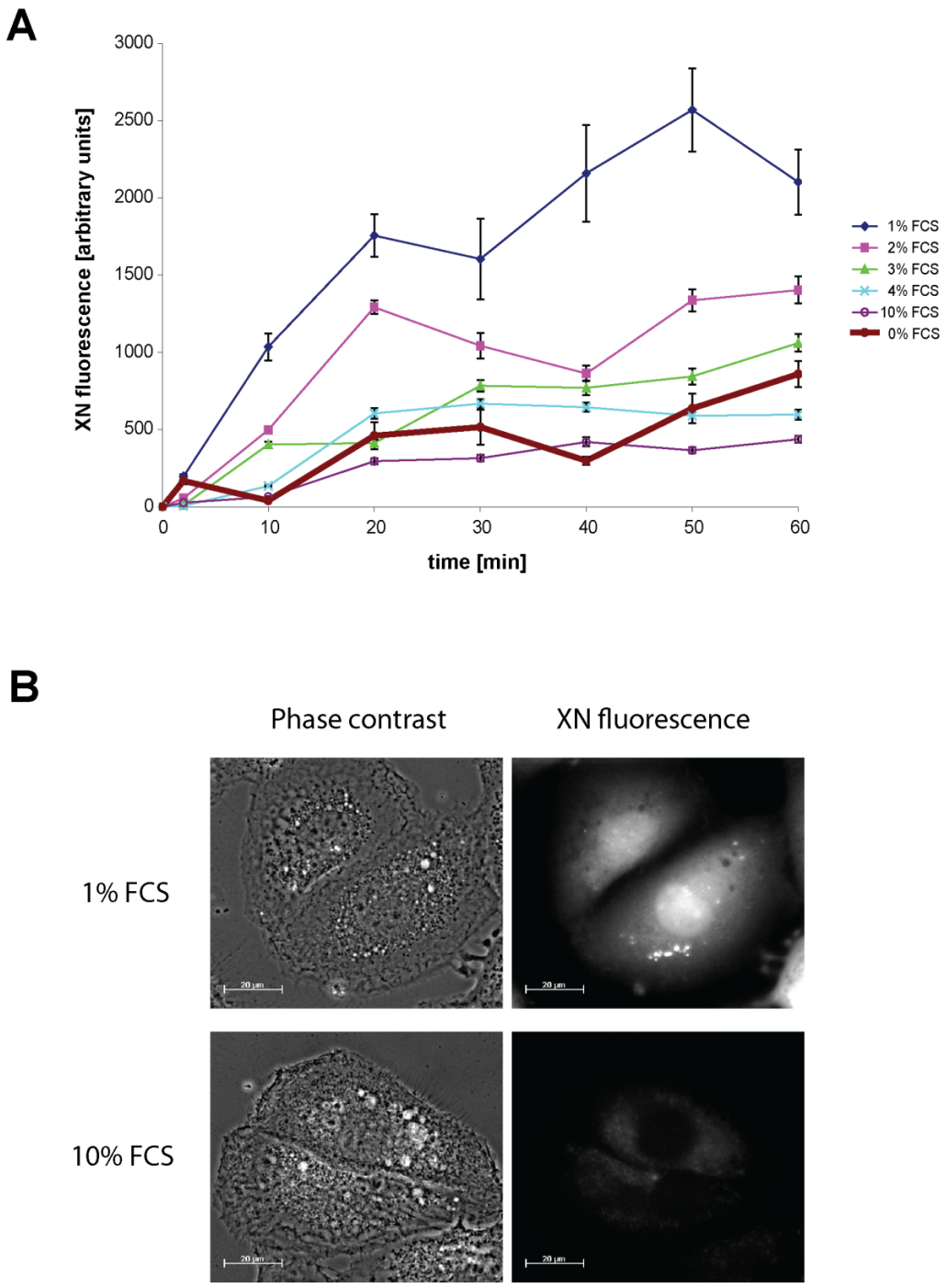


**Figure 2-3 Measurement of the time-dependents increase of XN fluorescence in human hepatic stellate cells by fluorescence microscopy. A. XN fluorescence in hepatic stellate cells incubated with 10 µM XN in DMEM containing 1, 2, 3, 4, 10% or no FCS over a period of 60 min. Intensity values for all timepoints after XN addition were corrected for background fluorescence present at time point 0. Data points represent means of multiple cells ± SD. B. XN fluorescence in hepatic stellate cells after 60 min incubation with 10 µM XN in DMEM with 1% (upper images) and 10% FCS (lower images). The weak fluorescence present in cells incubated with 10% FCS in medium is mostly autofluorescence, which is also present in cells that received no XN (not shown). Scale bars: 20 µM. (is published in [226])**

Results showed that a reasonable increase was only observable with 1% FCS in medium. At higher FCS concentrations, XN fluorescence inside the cells was impaired, probably due to quenching or a spectral shift. In cells incubated with 10% FCS in culture medium hardly any XN fluorescence was visible (Figure 2-3 B) even though it could be detected and quantified via HPLC, as shown by Wolff et al. [228].

Likewise, the complete emission of FCS impaired the detectable XN fluorescence inside the cells. This may be caused by different factors. On the one hand, increased absorption to the culture dish or decreased solubility of XN could alter the available amount of XN to be taken up by the cells. On the other hand, binding of XN at least to some proteins contained in the FCS could be a premise for its unimpaired uptake into cells.

The reported conversion of chalcones to flavanones prompted us to look also for the appearance of IXN besides XN under the above mentioned cell culture conditions. This reaction is not observable after 3 h (DMEM, 10% FCS, 37 °C), whereas the longer incubation time (24 h) resulted in the generation of IXN even in non-cellular conditions (data not shown).

Experiments on the solubility of XN in FCS supplemented DMEM showed that under normal cell culture conditions the solved concentration can reach 50-75 µM. The concentration of solved XN is further reduced by its absorption to plastic material. The recovery experiments clearly revealed that a minimum concentration of 10% FCS in medium is necessary to reduce the observed absorption to the plastic to a tolerable value. In contrast, FCS concentrations higher than 1% hampered fluorescence measurements with XN rigorously. As a general conclusion, we suppose that for several lipophilic natural products a limited solubility under assay conditions, absorption to plastic material and a possible interaction with FCS in cellular *in vitro* experiments have to be assumed. A routine determination of the maximal FCS concentration seems to be an appropriate parameter for the generation of reliable *in vitro* results.

## 2.5 Acknowledgments

Gabi Brunner (Pharmaceutical Biology, University of Regensburg) is gratefully acknowledged for excellent technical support. Special thanks got to the Hopfenverwertungsgenossenschaft (HVG, Wolnzach) for financial support. NATECO$_2$ (Dr. M. Gehrig) is gratefully acknowledged for providing pure XN.

# 3 Characterization of minor hop compounds, XN metabolites and related compounds

## 3.1 Abstract

Xanthohumol (XN, **1**) is ingested in human's diet with beer as well as related chalcones. After ingestion, XN (**1**) is metabolized via biotransformation. The biotransformation might produce compounds, which are more active and/or more toxic as the precursor molecules. For this reason, the minor hop chalcones, XN (**1**) metabolites and related compounds were tested on their influence on viability and proliferation and thus their induction of cytotoxicity in cancer cell lines using the MTT viability assay and crystal violet staining (CV). Furthermore, the impact on lipopolysaccharide (LPS)-induced NO production by inducible nitric oxide synthase (iNOS) was studied using Griess assay and the influence on iNOS expression was determined by immunofluorescence.

Xanthohumol H (**2**) lead to lower $IC_{50}$ in the MTT assay as XN in HuH-7, HSC and Caco-2 cells. Xanthohumol C (**6**) and dihydroxanthohumol C **7** were more active in the CV assay. In the Griess assay (10 ng/ml LPS as stimulus) the highest activity to inhibit the NO production was observed for **3**, alpinetin chalcone (**18**) and helichrysetin (**13**). In a modified set-up of the Griess assay (10 ng/ml LPS and 200 ng/ml IFN-$\gamma$ as stimulus) the highest activity was observed for **6**. All compounds showed activity against the iNOS expression with exception of 3-OHhelichrysetin (**14**). The most active compounds were **18**, **6**, flavokawain B (**16**), **2** and helichrysetin (**13**). Non-prenylated chalcones and tetrahydropyran chalcones exhibited better inhibitory activity against NO production or iNOS expression.

## 3.2 Introduction

XN (**1**) is the main prenylated chalcone in *H. lupulus* L.. Since the nineteen's compound **1** has been intensively investigated. It shows a wide range of effects such as anti-infective, anti-inflammatory and anti-cancer activity (see also 1.1 Xanthohumol). In human's diet **1** and minor hop compounds such as prenylated chalcones are ingested with beer. Bioavailability studies showed a low disposability [224,225] and substantial metabolism of XN (**1**, Chapter 5). The data on pharmacological effects of **1** as well as of phase I and phase II metabolites and minor hop chalcones were scarce. The reasons are: 1. The low concentration of minor hop compounds and XN (**1**) metabolites in hops, body fluids and organs; 2. The low amount of body fluids and organs available for extraction; 3. The lack of synthesis routes for **1** phase II metabolites to provide sufficient amounts for *in vivo* and *in vitro* testing.

However, XN metabolites and structural derivatives might have distinct pharmacological effects compared to **1** itself. Thus, a thorough evaluation of their properties is highly desirable.

### 3.2.1 Minor hop compounds, XN metabolites and related compounds

The minor hop compounds, XN metabolites and structurally related compounds, which were investigated in this chapter, are summarized in Figure 3-1.

XN (**1**) was isolated for the first time from *H. lupulus* L. by Power et al. [80]. The minor hop compounds xanthohumol C (**6**), dihydroxanthohumol C (**7**), desmethylxanthohumol (**5**) and flavokawain C (**17**) were identified by Stevens et al. [12,82].

In order to investigate the metabolism of **1** a variety of *in vitro* and *in vivo* studies were performed [159,160,233]. The *in vivo* study performed by Nookandeh et al. revealed several XN metabolites such as xanthohumol H (**2**), 4-acetoxyxanthohumol (**3**) and 4-methoxyxanthohumol (**4**) in feces of female SD-rats [233].

Flavokawain A (**15**) and flavokawain B (**16**) [245], alpinetin chalcone (**18**) [246,247], helichrysetin (**13**) and 3-OHhelichrysetin (**14**) were included in this study in order to look for structure response relationship studies. Compounds **15** and **16** were found in *Piper methysticum* but occur also in other plants [245]. Compound **13** is a genuine chalcone from *Helichrysum heterolasium* and was isolated by Bohlmann et al. [248]. A synthesis route for **13** and **14** was developed by Vogel et al. [150].

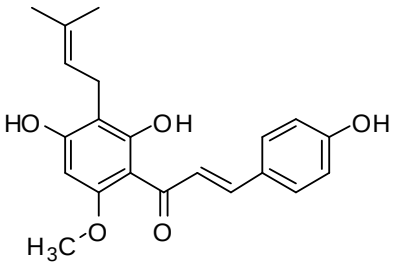

**1**

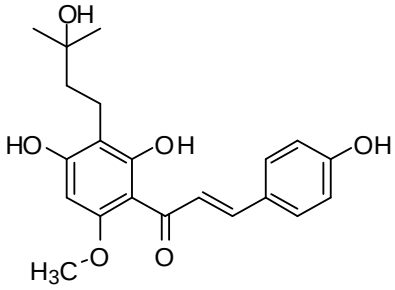

**2**

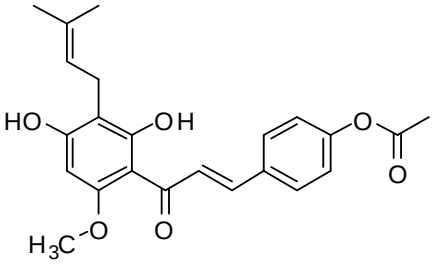

**3**

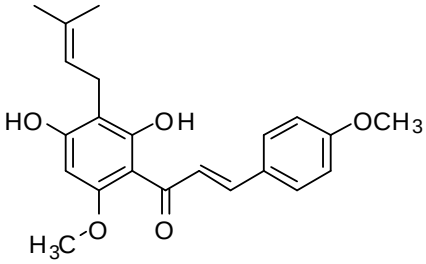

**4**

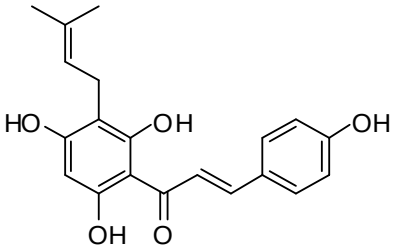

**5**

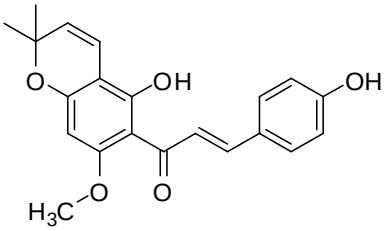

**6**

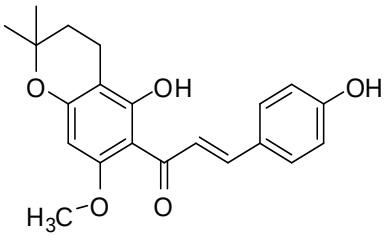

**7**

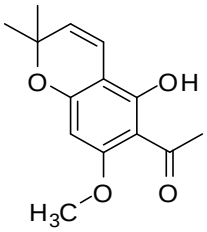

**8**

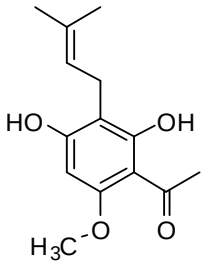

**9**

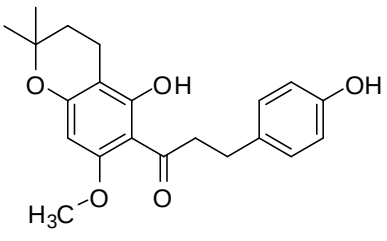

**10**

-**Figure 3-1 continues on page 49-**

**-Continuance of Figure 3-1-**

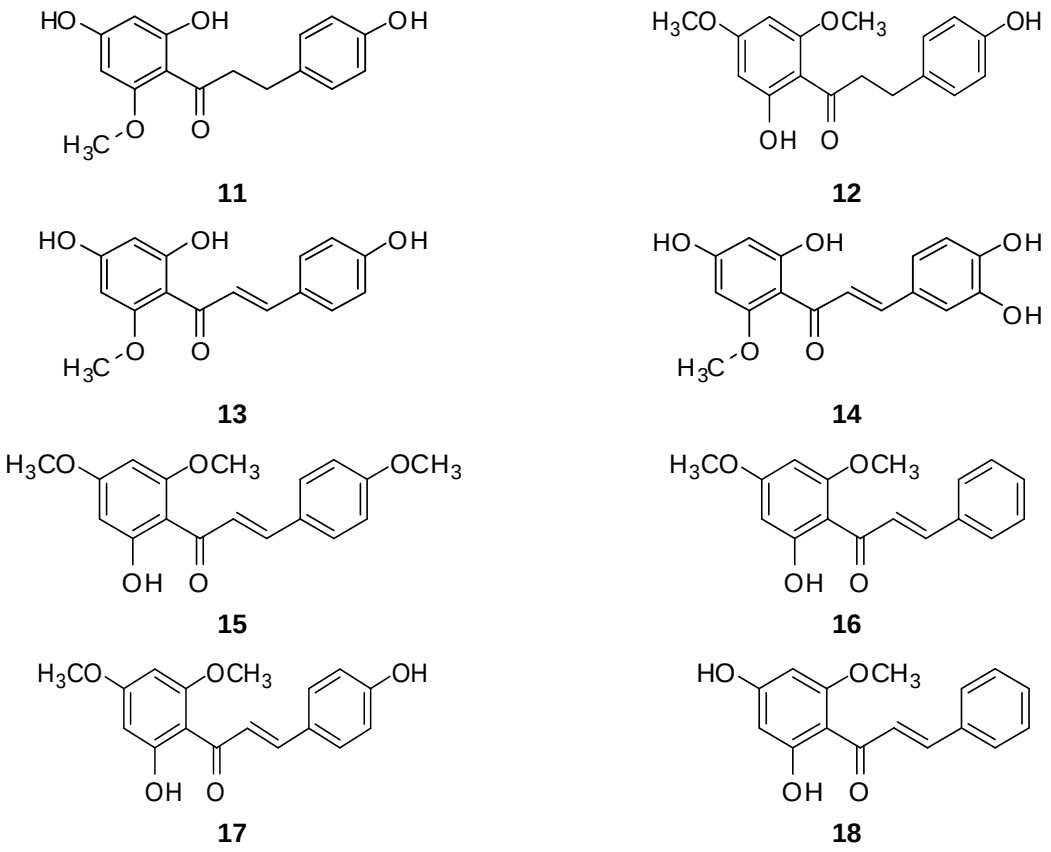


**Figure 3-1: Structures of the investigated minor hop compounds, XN metabolites and related compounds. 1: Xanthohumol (XN), 2: Xanthohumol H, 3: 4-Acetoxyxanthohumol, 4: 4-Methoxyxanthohumol, 5: Desmethylxanthohumol, 6: Xanthohumol C, 7: Dihydroxanthohumol C, 8: Acetylchroman, 9: Prenylacetophenon, 10: Tetrahydroxanthohumol C, 11: Dihydrohelichrysetin, 12: Dihydroflavokawain C, 13: Helichrysetin, 14: 3-OHhelichrysetin, 15: Flavokawain A, 16: Flavokawain B, 17: Flavokawain C, 18: Alpinetin chalcone.**

### 3.2.2 Biological effects of XN metabolites

Diseases such as the metabolic syndrome [162], diabetes [163], inflammation bowel disease [164], Alzheimer´s disease [165] and cancer [161] are correlated with chronic inflammation. The expression of proinflammatory proteins is modulated amongst others by the transcription factor NF-κB. NF-κB plays a central role in the inflammatory process and is correlated with oncogenic activation in cancer [34]. It has been observed that the inhibition of the transcription factor leads to apoptosis [182]. NF-κB is a dimer, which is located in the cytosol and bound to IκB. During activation, the IκB kinase phosphorylates (IKK) the IκB unit of NF-κB/IκB and thus allows the degradation by the ubiquitin ligase complex (see 1.1.6 Anti-inflammatory effect). NF-κB is then translocated to the nucleus and leads to the

expression of about 200 different proteins, which are involved in the prevention of apoptosis [34]. Examples include Bcl-2, enzymes of the prostaglandin synthesis (COX-2, 5-LOX), proteins involved in inflammatory mechanisms (inducible nitric oxide synthase (iNOS), TNF-α, interleukins (IL)) and adhesion molecules (ICAM-1) [168].

In the study of Peluso et al. [178] they investigated the effect of different compounds such as **1**, **5** and **17** on the expression of MCP-1 and IL-6. MCP-1 and IL-6 are downstream signals of the LPS induced NF-κB pathway [168]. Both cytokines were inhibited by **1**, **5** and **17** at 20 µM. **17** exhibited the highest inhibitory activity on MCP-1. IL-6 was comparably inhibited by **1** and **17**. Interestingly, the dihydro compounds and the flavanones showed also activity in both, the NO and the MCP-1/IL-6 assay systems [178,181]. It seems that the α,β-unsaturated structure is not absolutely required for the NF-κB inhibition. Peluso and co-workers [178] proposed an interaction with the MD-2 and Toll-like receptor 4 (TLR4). The fitting of the tested compounds with the MD-2 unit was calculated in a molecular docking study. It has been shown that the increase in the inhibition of the MCP-1 and IL-6 is correlated with the fitting accuracy to MD-2 [178]. MD-2 is needed for the induction of the NF-κB cascade by LPS. Compound **1** was shown to reduce the expression of the TLR4 [172,178] and MD-2 [172].

The expression of iNOS has been reported to correlate with chronic inflammation found in bowel disease [164] and diabetes mellitus [249]. The iNOS produces NO in micromolar amounts by L-arginine depletion and L-citrullin production (Figure 3-2) [250].

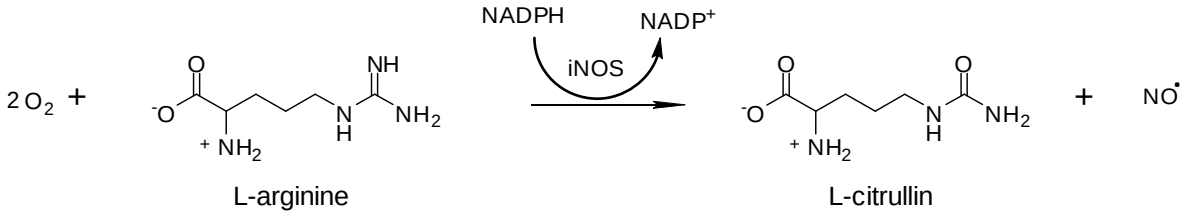


**Figure 3-2: The NO production by iNOS. iNOS catalyze the NO production through L-arginine depletion to L-citrullin with $O_2$ and the coenzyme NDPH.**

It is controlled by the transcription factors NF-κB and STAT-1. The iNOS expression is induced by LPS via the NF-κB pathway and by the cytokine IFN-γ via the JAK/STAT pathway. The expression of iNOS is calcium/calmodulin independent and it is constitutively expressed. The LPS-binding protein associates with LPS, binds to CD14, and clusters with Toll-like receptor 4 (TLR4) [166,183]. MD-2 is essential for the initiation of the NF-κB cascade via the TLR4. In the JAK/STAT pathway, IFN-γ binds to the IFN receptors thereby leading to a conformation change and auto-phosphorylation of the JAK. The JAK

phosphorylates tyrosin residues within the receptor thereby creating docking sites for the STAT. The STAT homodimer modulates the expression of IRF-1, inflammatory enzymes such as iNOS and adhesion molecules such as ICAM-1 [184].

High concentrations of NO can lead to the formation of reactive nitrogen species (RNS). RNS can nitrate proteins and DNA, trigger apoptosis and mutagenesis, and maintain cancer [250,251]. Studies showed that iNOS activation leads to survival of colorectal cancer [252]. The correlation between the iNOS expression and survival was also observed in human gastric cancer. The investigation revealed a correlation between the angiogenesis, COX-2 and tumor progression. The expression of both enzymes, iNOS and COX-2, led to a worse prognosis and was correlated with angiogenesis. The prognosis gets better if only one or none of the two enzymes was expressed [253]. In ameloblastoma higher iNOS levels were correlated with higher VEGF concentrations [254]. However, iNOS seems to have beneficial effects, too. NO showed antibacterial effects [255]. In addition, a beneficial interaction with cancer was discussed. IFN-γ stimulated leukemia cell lines could be triggered to apoptosis by the induction of NO and caspase-3 [256]. In human pancreatic cancer, the induction of iNOS led to a higher apoptotic index [257]. The effects of the expression of iNOS are controversial discussed in the literature. The outcome depends probably on the molecular status of cancer and the NO concentration [250]. Beside the dichotomy of the iNOS, the iNOS can be used for the screening of compounds and their ability to influence the expression pathways.

Zhao et al. [181] investigated the effect of chalcones and flavanones on the NO production in LPS and IFN-γ stimulated RAW 264.7 cells. The production of NO was inhibited by compound **1** and tetrahydroxanthohumol (**10**) at 5 µM, but the effect was more pronounced for **1**. The underlying mechanism was not investigated [181].

Flavokawains and **18** were tested on their activity to inhibit iNOS, for instance. Compound **15** has been shown to influence a variety of pro-inflammatory proteins. Compound **16** inhibited the expression of iNOS, COX-2, the production of NO and $PGE_2$ as well as the secretion of TNF-α in LPS stimulated RAW 264.7 macrophages and mice [258]. Compound **16** inhibited the expression of COX-1 [259]. Zhou et al. [260] investigated the influence of **16** on NF-κB in TNF-α stimulated human hepatoma HepG2 cells and cervical carcinoma HeLa cells. Compound **16** influenced NF-κB mostly in hepatocytes. Decreased levels of free IκBα units, a decreased transcriptional activity of NF-κB and decreased nuclear translocation were observed. An either direct or indirect inhibition of IKK by **16** was discussed [260]. An IKKβ inhibition by **15** but not by **16** could be observed in an *in vitro* kinase assay. However **15** and **16** inhibited the TNF-α induced NF-κB transcriptional activity in a luciferase assay. The inhibitory mechanism of both flavokawains was based on the inhibition of the IκB degradation and the translocation of the subunits p50 and p65 of NF-κB [261]. Compound **18** that carries

one *O*-methoxy group at the C-6´ and a non-substituent B ring, was found to lead to remarkable NO inhibition in LPS stimulated RAW 264.7 cells. The $IC_{50}$ value of **18** was 1.5 µM (without a SD) [262]. The inhibitory mechanism seems to be similar to that of **16**. Qin et al. described an inhibition of the IκB degradation [263]. Lee et al. and Israf et al. showed an inhibition of the NF-κB translocation induced by **18** [262,264].
The IKK is regulated by the Akt. Compound **18** inhibited the Akt and thus the IKK. In addition **18** indirectly inhibited the transcriptional activity as well as the phosphorylation of RelA/p65. Thus, the expression of NF-κB down-regulated enzymes such as iNOS and COX-2 were inhibited [262] but without a loss in activity [264]. The production of thromboxane and prostaglandins is mainly catalyzed by the COXs. Hence the synthesis of thromboxan $B_2$ and prostaglandin $E_2$ was inhibited by **18** in LPS activated blood monocytes [265]. An inhibition of the COX--2 was also observed in BV2 [266] and myeloma cells [263]. However an effect of **18** on the degradation of NF-κB/IκB and the COX-2 expression in THP-1 and RAW 264.7 cells could not be observed [262–265,267].

In order to orchestrate the immune response macrophages and neutrophil granulocytes segregate chemokines, interleukins and ROS. This leads to an inflammation that is characterized by rubor, calor, tumor and dolor, which are the cause of an enhanced permeabilization of the vascular system and the infiltration of fluids. In order to orchestrate the adaptive cells, endothelial cells produce selective lectins, chemokines and integrins (adhesion molecules) on their surface. The adaptive cells can then roll, be activated, adhere, and infiltrate the tissue. The whole process is termed homing. The last step of the homing is the diapedese and is correlated with a loss of connectivity between the endothelial cells. Diapedese allows the entry of the immune cells. Homing is associated with three digit postal codes, every cell needs a proper code in order to roll, be activated and adhere to the endothelium [268]. Endothelial cells express the adhesion molecule integrin ICAM-1. The expression of the adhesion molecule is non-constitutive and is induced by IL-1 and TNF-α [166]. A variety of research groups established the ICAM assay, which assesses the inhibition of ICAM-1 by different compounds [269,270]. Compound **1**, **2**, **3**, **4**, **6**, **13** and **14** were investigated in the ICAM assay in order to determine their influence on the ICAM-1 production in human microvascular endothelial cells (HAMEC-1) [152]. Compound **14** showed the highest inhibition of the expression of ICAM-1. Compound **1**, **2**, **4** and **6** were the most ineffective compounds but nevertheless inhibited the ICAM-1 expression.

Beside the anti-inflammatory properties of **1**, minor hop chalcones and related compounds, they were investigated concerning their cytotoxicity in a few cancer cell lines. However the underlying mechanism of the proliferative, inhibitory and cytotoxic effects of XN metabolites

and related compounds, with exception of **17** and **18**, were not investigated so far. Compound **1**, **2**, **3**, **4**, **5**, **6**, **7**, **13**, **14** and **17** were found to be cytotoxic in Hela cells. The cytotoxicity was observed in a lower micromolar range, between 5.2 µM ± 0.8 µM (**13**) and 19.2 ± 1.2 µM (**17**) [150,151,152]. In another study the cytotoxicity of **1**, **5** and **6** in human breast cancer cells MCF-7, colon cancer cells HT-29 and ovarian cancer cells was investigated. **1** was the most active one followed by **5** and **6** (all 10 µM with SE pointed in diagram) [186].

There are also a few studies available concerning the cytotoxicity of XN (**1**) related compounds. **15-17** were investigated concerning their cytotoxic activity in L-02 and HepG2 cells [260,271,272]. In the study of Li et al. [271] compound **15** showed no cytotoxicity in both cell lines. **16** and **17** were equally toxic in HepG2 cells ($IC_{50}$ of compound **16:** 62.38 ± 5.04 µM and **17:** 59.48 ± 2.72 µM). In L-02 cells **16** showed higher cytotoxic activities ($IC_{50}$ of compound **16:** 35.15 ± 2.56 µM and **17:** 57.04 ± 2.32 µM) [271].

Compound **16** also influenced the growth of human oral squamous carcinoma HSC-3, human melanoma (A-2058), oral adenosquamous carcinoma (Cal-27), human non-small-cell lung cancer (A-549) [273]; wild type and $p53^{-/-}$ human colon cancer (HCT116), A-549, mouse fibroblast (NIH3T3), human fibroblast (HFW) [274]; androgen receptor(AR)-negative hormone-refractory prostate cancer (HRPC) DU145 and PC-3 as well as AR-positive HRPC LAPC4 and LNCaP cells [275]. Compound **16** triggered cells to regulated cell death by the MAPK (ERK, JNK and p38) signaling [260], mitochondrial dependent pathway [274], mitochondrial dependent and independent pathways [275] as well as the ER dependent pathway [273]. All cited studies discussed the possibility that the apoptotic ways were induced by ROS because the addition of NAC [273,274] and GSH [260] prevented apoptosis. Additionally cell death via autophagy was also discussed [274]. Interestingly, compound **16** was studied *in vivo* in Balb/c mice and exhibited a hepatotoxic effect (**16**: 25 mg/kg body weight for 1 week) which was abolished by GSH [260].

The influence of **15** on cellular mechanism was analyzed in urinary bladder cancer cell lines such as p53 wild type RT4 and mutated T24 [276], UMUC3, TCCSUP, 5637, HT1376-HT1197 [277] and Ej [276]. Zi and co-workers [276] investigated the effect of **15** and **16** on the cell proliferation and the underlying mechanism of **15** induced apoptosis. The p53 mutated urinary bladder cell lines were 3 to 4 times more sensitive to **15** than the wild type. Compound **15** showed the weakest inhibitory effect on the proliferation and **16** was the most potent proliferation inhibitor. The incubation with flavokawains led to typical apoptotic signs such as cell shrinking, rounding up, blebbing, nuclear fragmentation and condensation. The compound **15** was shown to influence apoptotic factors such as Bax and caspase-3/9. Zi et al. [276] determined the influence of **15** on the tumor growth in *in vivo* xenografts (Ej)

NCR-*nu*/*nu* mice. Mice were fed with 50 mg/kg **15** for 25 days. A tumor growth inhibition of 57% was observed [276].

The compound **18** is a simple chalcone which carries a non-substituted B ring and an *O*-methoxy group in the A ring (Figure 3-1). A viability inhibition of a human colon cancer cell line SW-480 by **18** was detected. The $IC_{50}$ value was 35 µM (without SD) [278]. The inhibition mechanism was studied in more detail *in vitro* [52] and *in vivo* [279]. Compound **18** induced apoptosis via the in- and extrinsic pathway by the up-regulation of the death receptor 5. The up-regulation of the death receptor 5 was discussed to be correlated with the NF-κB inhibition [52]. In the *in vivo* studies of Yadav et al. [279] the up-regulation was correlated with an increased ROS production. Furthermore, **18** was shown to inhibit TNF-α mediated cell death in L929 cells at an $IC_{50}$ value of 7 µM (without a SD) [280].

Summing up, the minor hop compounds **5**, **6** and **17** were investigated concerning their antioxidant and cytotoxic activity so far. The XN metabolites and other minor hop ingredients were less or not investigated concerning cytotoxic, hepatotoxic, proliferative, and inflammatory properties with the exception of **15, 16** and **18**. Furthermore, a structure-response relationship study with the metabolites, minor hop substances and structure related flavokawains, unprenylated chalcones (**13**, **14**) and dihydro compounds was not performed, yet.

## 3.3 Aims of the study

XN (**1**) is ingested in human's diet with beer as well as related chalcones. After ingestion, biotransformation might produce compounds, which are more active and/or more toxic as the precursor molecules. For this reason the minor hop chalcones, XN metabolites and related compounds were tested on their capability to influence viability and proliferation in cancer cell lines using the MTT and CV assay. Furthermore, the ability of the compounds to inhibit NO production by iNOS was determined by Griess assay. Expression of iNOS was analysed using immunofluorescence combined with fluorescence microscopy and image analysis.

## 3.4 Material

### 3.4.1 Chemicals

**Chemicals** Compounds **2**, **3**, **4**, **6-9**, **13**, **14**, **15-17**, **18** were obtained by synthesis (University of Regensburg) [150,152]. XN (**1**) was provided by the Nookandeh Institut (Hamburg, Germany) and exhibited a purity of 98%. The hydrogenations of **7**, **13**, **17** were performed by

Petr Jirásek (Pharmaceutical Biology, University of Regensburg) using a method described by Mori et al. [281] to obtain the compounds **10-12**. The purities of the tested compounds were between 86-99% (3.6.1 Purity degree, lipophilicity and structure determination). Ethanol (Order no. 8006) was bought from J.T. Baker (Deventer, Netherlands). Deuterated acetone and chloroform were obtained from the Deutero GmbH (Kastellaun, Germany).

Crystal violet (Order no. 1190210), tri-sodium citrate dihydrate (Order no. 1.06448.1000), dimethyl sulfoxide (DMSO) (Order no. 1.02931.1000), ortho-phosphoric acid (Order no. 1.00573.1000), sodium dodecyl sulfate (SDS) (Order no. 1.02931.1000), acetone (Order no. 1.00014.2511), formic acid (Order no. 1.00264.1000), glacial acetic acid (Order no. 1.00063.1000), sulfuric acid (Order no. 1.00731.1000), acetonitrile (Order no. 1.00030.2500), methanol (Order no. 1.06035.2500), sodium nitrite (Order no. 1.06549.0500) and HPTLC plates silica gel 60 $F_{254}$ (charge HX109045) were purchased from the Merck KGaA (Darmstadt, Germany).

Anisaldehyde (Order no. A8, 810-7), naphtyletyhlene diamine dihydrochloride (NED) (Order no. N-5889), sulfanilamid (Order no. S-9251), 3-(4,5-Dimethylthiazol-2-yl)-2,5-diphenyltetrazoliumbromide (MTT) (Order no. M-2128), trypan blue (Order no. T-0887), lipopolysaccharide (LPS) from *Escherichia coli* 055:B5 (LPS) (Order no. L-2880) and Interferon-γ (IFN-γ) mouse recombinant expressed in *E. coli* (Order no. I-4777) were obtained from Sigma-Aldrich (Steinheim, Germany).

Ethyl acetate (Order no. 232110025) and cyclohexane (Order no. 176810010) were purchased from Acros Organics (Geel, Belgium).

Deionized water (18 mS/cm) was obtained using a Millipore Milli-Q UF Plus equipment.

### 3.4.2 Cell lines and culture materials

**Cell lines.** The immortalized activated human hepatic stellate cell line (HSC) was obtained from the University Hospital of Regensburg, Department of Internal Medicine I [244]. The human hepatoma cell line (HepG2) (ATCC®-number HB-8065™) and the murine macrophage cell line (RAW 264.7) (ATCC®-number TIB-71™) were obtained from the American Typ Culture Collection (ATCC, USA). The human colorectal cell line (Caco-2, ATCC®-number HTB-37™) was a gift from the Institute of Virology, Helmholtz Zentrum München, Germany. The human hepatoma cell line (HuH-7, HSRRB-number JCRB0403) was obtained from the Health Science Research Resources Bank (HSRRB) of the Japan Health Sciences Foundation (JHSF, Japan).

**Media and supplements.** Roswell Prak Memorial Institute 1640 (RPMI 1640) medium without phenol red (Order no. F 1275), RPMI 1640 medium with phenol red (Order no. F 1215), Dulbecco's modified eagle medium (DMEM) with phenol red (Order no. FG 0415),

L-glutamine (Order no. K 0283), non essential amino acids 100 x (NEAA, Order no. K 0293), fetal calf serum (FCS, Order no. S 0115), phosphate buffered saline (PBS, Order no. L 1825), sodium pyruvate 100 mM (SP, Order no. L 0473) and trypsin 10 x (Order no. K 2135) were purchased from the Biochrom AG (Berlin, Germany).
DMEM without phenol red (Order no. 41965) and DMEM with phenol red (Order no. 31053) were bought from Invitrogen, GIBCO (Grand Island N.Y., U.S.A.).
**Material for routine cell culture work and experiments.** 96 well plates (Order no. 92096), cell scrapers (Order no. 99003), culture flasks 75 cm² (Order no. 90076) and 150 cm² (Order no. 90151) were purchased from TPP (Trasadingen, Switzerland), safe lock tubes 1.5 ml (Order no. 0030.102.002) and 2 ml (Order no. 0030 120.094) from Eppendorf (Hamburg, Germany) and centrifuge tubes 15 ml (Order no. 17020) from MEUS s.r.l. (Piove di Sacco, Italy). The Cellomics® iNOS activation kit (Order no. 8403802) was purchased from Thermo Scientific (Bonn, Germany).

## 3.5 Methods

### 3.5.1 Purity analysis

The purity of the used compounds was analyzed by HPLC. The HPLC-system consisted of an organizer Elite Lachrom, diode array detector L-2455, autosampler L-2200, pump L-2130 and a column oven L-2350 (all from VWR-Hitachi, Breda, Netherlands). A Purosphere® Star RP-18e 250 x 4.0 mm 5 µm column form Merck (Darmstadt, Germany) was used. The analytes were dissolved in acetone at a concentration of 10 mM and diluted to a final concentration of 10 µM in 50% acetone. A sample of 20 µl was injected and separated using a gradient program. Eluent A consisted of water supplemented with 0.1% formic acid. Eluent B was acetonitrile. UV-detection was performed at a wavelength of 368 nm. The gradient started with 55% eluent B and reached 85% after 27 minutes. During the following 3 min the initial conditions were reestablished and hold for 10 min. The HPLC was operated at a flow of 1.0 ml/min and a temperature of 30 °C.
The purity of the compounds was calculated as percent of the total peak area.

### 3.5.2 Comparison of lipophilicity by high performance thin layer chromatography (HPTLC)

The lipophilicity of the compounds was rated by HPTLC analysis (CAMAG, Muttenz, Switzerland). It was performed with a twin through chamber 200 x 100 mm, a Linomat 5 applicator, an ADC 2 automatic developing chamber and a Reprostar 3. 7.5 µl of 500 µM

solutions were applied in 1 cm lines on HPTLC plate Silica gel 60 $F_{254}$. The first/last compound and the start line had 1 cm distance from the respective borders of the silica plate. The solvent system was hexan:ethyl acetate:methanol 70:20:10 + 0.1% formic acid. After 11 min of separation, the compounds were heated up to 110 °C on a heatplate Thermoplate S (Desaga, Sarstedt AG & Co., Nümbrecht, Germany). After 5 min, the HPTLC plate was dipped into Naturstoff reagent (5 g/l in methanol). Then the HPTLC plate was dipped into macrogol 400 (50 g/l in methanol).

### 3.5.3 Hydrogenation and NMR analysis

The hydrogenation of **7**, **13** and **17** was performed by Petr Jirásek using a method described by Mori et al. [281]. The molecular structures were confirmed by NMR using a Bruker Avance spectrometer (400 MHz). $^1$H NMR spectra were recorded at ambient temperature. For this purpose, **10** and **12** were dissolved in deuterated chloroform. Compound **11** was dissolved in deuterated acetone.

### 3.5.4 FCS heat inactivation

FCS was inactivated in a water bath at 56 °C for 30 min. The FCS was cooled down to room temperature, and aliquoted in 50 ml portions. The aliquots were stored at -20 °C until used.

### 3.5.5 Cell cultivation and harvesting

HSCs, HuH-7 and HepG2 cells were cultivated in DMEM with phenol red from Invitrogen, GIBCO (Grand Island N.Y., U.S.A.), which was supplemented with 10% heat-inactivated FCS. Caco-2 cells were cultivated in DMEM with phenol red from Biochrom AG (Berlin, Germany), which was supplemented with 10% heat-inactivated FCS, 1% SP and 1% NEAA. The cells were cultivated in 150 $cm^2$ culture flasks and kept in a New Brunswick scientific cell incubator (Edison, N.J., U.S.A.) at 37 °C and 5% $CO_2$ in a humidified atmosphere. Once a week the cell lines were split and after four days the growth media were exchanged. For splitting, the exhausted media were aspirated and the confluent cells were carefully washed with 13 ml PBS. After aspiration of PBS, 2 ml of trypsin (1 x in PBS) were added to the culture flasks with confluent cells. The adherent cells were incubated for approximately 4 min at 37 °C. After carefully beating at the underside of the culture flask wall, cells were detached from the bottom of the culture flask. 5 ml medium were added to the trypsin/cell suspension to stop the trypsination.

Mouse macrophages RAW 264.7 were cultivated in RPMI 1640 medium supplemented with 10% heat-inactivated FCS and 1% L-glutamine. Three times a week RAW 264.7 were splitted. In order to detach RAW 264.7 from the culture flasks bottom, the cells were scrapped off with a cell scraper. For this, the exhausted growth medium was discarded and 5 ml medium were added to the adherent mouse macrophages. The cell suspension of each cell line was transferred to a 15 ml centrifuge tube. In order to remove dead cells and debris, the cell suspension was centrifuged in a centrifuge Megafuge 1.0 R (Heraeus Sepatech GmbH, Osterode, Germany) at 700 rpm for 5 min. The supernatant was discarded and the cells were resuspended in 5 ml medium. HSCs, HuH-7 and Caco-2 cells were diluted 1:10. HepG2 and RAW 264.7 cells were diluted 1:20.

### 3.5.6 Cell counting

The cell suspensions were counted in a Neubauer cell counting chamber and seeded in 96 well plates (TPP, Trasadingen, Switzerland) to determine the viability, proliferation, NO production and iNOS expression. Therefore, a small amount of the cell suspension (3.5.5 Cell cultivation and harvesting) was diluted with 0.4 mg/ml trypan blue PBS. 10 µl of the trypan blue cell suspension were pipetted under the glass lid of the Neubauer cell counting chamber. Cells in 4 large-scale quadrates were counted and the cell number was calculated by the following equation (Equation 3-1).

$$\frac{x\ cells}{4} \times 10^4 \times dilution\ factor = \frac{cells}{ml}$$

**Equation 3-1: Calculation of the cell numbers. Cells were counted with a Neubauer cell counting chamber.**

### 3.5.7 Dilution of test compounds

Prior to use the compounds were dissolved either in DMSO or in ethanol yielding either 100 mM or 10 mM stock solutions. In the next step, the stock solutions were diluted with medium without phenol red to their test concentrations. DMEM without phenol red was used for HSC, HuH-7, HepG2 and Caco-2 cells. RPMI 1640 medium without phenol red was used for RAW 264.7 cells. The dilutions were used for 3.5.8 Viability assay, 3.5.9 Proliferation assay, 3.5.10 Nitric oxide , and 3.5.11 iNOS .

The end concentrations of solvent were kept below 0.1% (DMSO) and 1% (ethanol) respectively.

### 3.5.8 Viability assay

The MTT viability assay was performed according to Mosmann et al. [282] with the following modifications. Each incubation step was performed in an incubator at 37 °C and 5% $CO_2$, in humidified atmosphere. Each well of a 96 well plate was filled with 100 µl medium with phenol red containing 5.000 HSC cells or 15.000 HuH-7 cells or 7.500 HepG2 cells or 15.000 Caco-2 cells or 5.000 RAW 264.7 cells (medium see 3.5.5 Cell cultivation and harvesting). The outer wells were filled only with medium (blank value). The whole pipetting scheme is summarized in Figure 3-13. The cells were kept for 24 h at 37 ℃ to allow sedimentation and adherence on the culture flask bottom. Afterwards the exhausted growth medium was aspirated and 100 µl of medium with the test compounds in different concentrations were added.

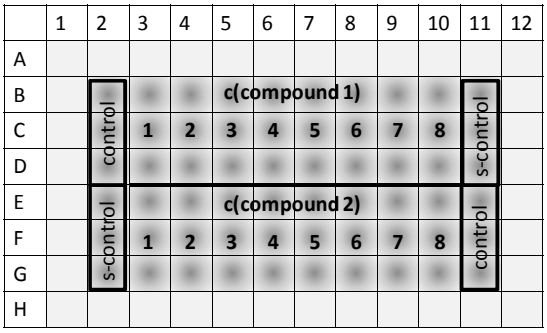


**Figure 3-3: Pipetting scheme of a 96 well plate used for viability testing. The outer wells (light gray) were filled with medium (blank value). 3 wells of column 2 and 11 were filled with either 100 µl medium without compounds (control abbreviation c) or with 100 µl medium with the highest solvent concentration (solvent control abbreviation s.c.). The interior wells from row B to G and column 3 to 10 were used for $IC_{50}$ determinations of two compounds. Eight different concentrations of compound 1 and compound 2 were measured. The rows B, C and D were filled with compound 1. E, F and G with compound 2. The compounds were diluted to their test concentration of 10, 20, 30, 40, 50, 60, 80 and 100 µM (see 3.5.7 Dilution of test compounds). Each well was filled with 100 µl.**

After 24 h incubation, the compound solutions were aspirated. Shortly before use, 4 mg/ml 3-(4,5-dimethylthiazol-2-yl)-2,5-diphenyltetrazoliumbromide (MTT)) in PBS were 1:10 diluted in medium (RPMI for RAW 264.7 and DMEM for the other cell lines). 100 µl of 0.4 mg/ml MTT solution were filled in each well followed by incubation for 3 h.

After conversion of MTT to formazan crystals by mitochondrial dehydrogenases (Scheme 3-1), the MTT solution and the medium of the outer wells (blank value) were removed and 100 µl of a 10% SDS solution were pipetted into the wells to solve the formazan crystals.

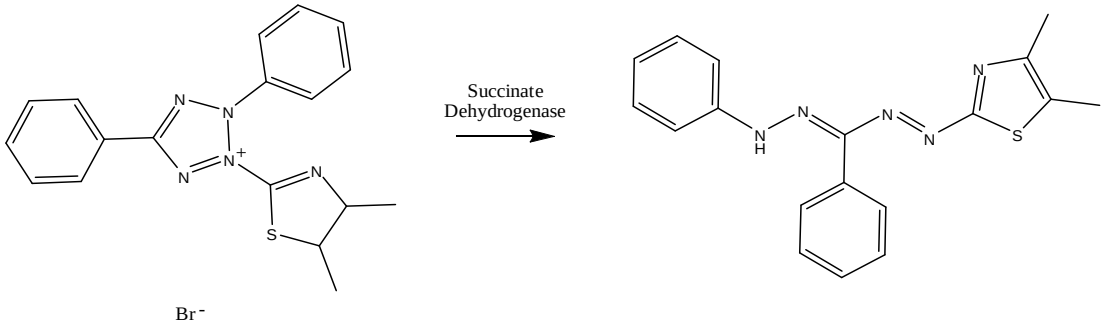


**Scheme 3-1: Reaction of the tetrazolium salt MTT to formazan catalyzed by succinat dehydrogenase.**

After 24 h, the formazan crystals were dissolved in SDS. The absorption A was measured with the microplate reader SpectraFluor Plus (TECAN, Hombrechtikon, Switzerland) at 560 nm.

For each compound, the determination was performed in 3 different experiments with

different passage numbers. For all compounds, the viability was determined with Equation 3-2.

$$Cell\ viability = \frac{A_{c(compound1)} - A_{blank\ value}}{A_{control} - A_{blank\ value}} \times 100\%$$

**Equation 3-2: Calculation of cell viability in % referring to untreated control cells.**

### 3.5.9 Proliferation assay

To analyse the influence of the test compounds on proliferation, cells were stained with crystal violet (CV, structure is depicted in Scheme 3-2). CV as a cationic dye intercalates in the histone free areas of the DNA. The crystal violet staining assay (CV) was adopted from [283].

At the beginning of the experiments cells were seeded into three 96 well plates. After 24 h cultivation one 96 well plate was stained with CV solution in order to determine the initial cell density prior to the addition of the test compounds. The two remaining 96 well plates were used to analyse the influence of the substances on cell proliferation. One of the remaining 96 well plates was handled as described in 3.5.8 Viability assay up to the removing step of the compound solution. The third 96 well plate only received culture medium in order to determine the 48 h blank values of untreated cells.

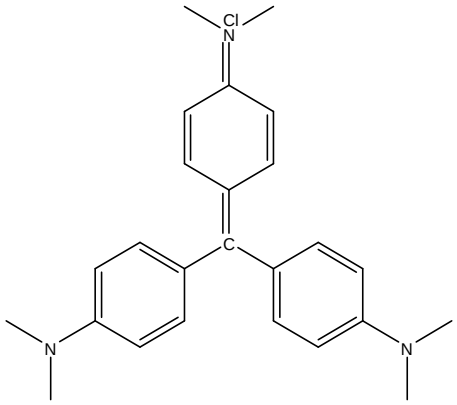


**Scheme 3-2: Structure of crystal violet.**

After the aspiration of the compound solutions the staining was performed with 50 µl 0.5% CV dissolved in 20% methanol for 10 min. After the removal of the CV solution, stained cells were washed 3 times with 250 µl deionized water in order to completely remove unbound CV. The plates were air-dried at room temperature. Subsequently, 100 µl of a 0.05 M sodium citrate/ethanol (1:1, v/v) solution were added to each well in order to dissolve the bound CV. Afterwards the absorption was measured with a SpectraFluor Plus microplate reader (TECAN, Hombrechtikon, Switzerland) at 560 nm.
For each compound the experiment was performed three times with different passage numbers. The control value of untreated cells after 48 h was defined as 100% proliferation. Inhibition of the proliferation was defined as the part of the values that were found in between the 24 h and the 48 h control values. Cytotoxicity was defined as the part of the values found below that one of the 24 h control.

### 3.5.10 Nitric oxide assay (Griess assay)

The nitric oxide assay was performed in order to determine the influence of the test compounds on the NO production by iNOS. The test method was adopted from [284].
For this assay, 100 µl RPMI 1640 medium with phenol red containing $8 \times 10^4$ RAW 264.7 cells were seeded in 96 well plates and cultured for 24 h. Then the media were aspirated and 100 µl of a mixture of 50 µl of the test solutions in concentrations that showed no effect on the cell viability and 50 µl of 20 ng/ml LPS (yielding a final concentration of 10 ng/ml LPS per well) were pipetted in each well. The plates were cultivated for another 24 h. The complete pipetting scheme is depicted in Figure 3.4.
Usually the used concentrations in both assays were 2, 5, 8, 10 and 15 µM. Desm XN was used up to 30 µM, A-chroman and P-acetophenon up to 50 µM.
In the second set-up of the nitric oxide assay the same pipetting scheme was used, but the testing solutions were supplemented with 20 ng/ml LPS plus 400 ng/ml IFN-$\gamma$ yielding a final concentration of 10 ng/ml LPS and 200 ng/ml IFN-$\gamma$ per well.

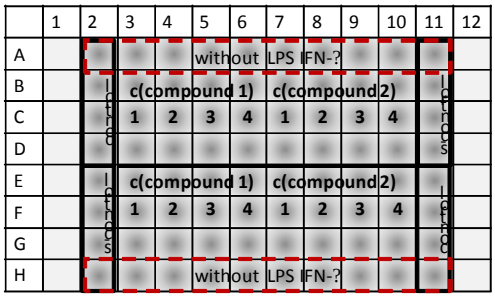


**Figure 3-4: Pipetting scheme of a 96 well plate used in the nitric oxide assay. The columns 1 and 12 (light gray) were filled with medium. Four wells of column 2 and 11 were filled with 100 µl medium without compounds (control), the other four wells in column 2 and 11 were filled with 100 µl medium supplemented with the highest solvent concentration (s-control). The interior wells of rows A to D in columns 3 to 6 were used to determine the influence of compound 1 on the nitric oxide. Usually the compound concentrations were 2, 5, 8, 10 and 15 µM. 100 µl were pipetted in each well. In order to check the appropriate stimulation the cells in row A and H were not stimulated.**

The intracellularly generated NO is released into the culture medium where it gets oxidized to nitrite. In order to determine the concentration of the accumulated nitrite in the supernatants, a 9 point nitrite calibration curve (serial dilution started with 100 µM) was prepared in RPMI 1640 without phenol red using a 100 µM sodium nitrite stock solution solved in RPMI 1640 without phenol red. After an incubation time of 24 h, 50 µl of each supernatant were transferred to a new 96 well plate. 50 µl Griess reagent were added to the supernatants and the nitrite solutions followed by incubation for 15 min.

The Griess reagent was composed of 0.1% naphtyletyhlene diamine dihydrochloride (NED, Sigma-Aldrich, Steinheim, Germany) and 1% sulfanilamide (Sigma-Aldrich, Steinheim, Germany) in 50 mM ortho-phosphoric acid (85%, Merck, Darmstadt, Germany). For easier dissolution of the components, the reagent was prepared in a hot waterbath, and then cooled down before use.

The Griess reagent reacts with nitrite to form an azo dye. The underlying reaction scheme is depicted in Scheme 3-3.

The absorbance of the colored solutions was measured at 560 nm using a SpectraFluor Plus microplate reader (TECAN, Hombrechtikon, Switzerland).

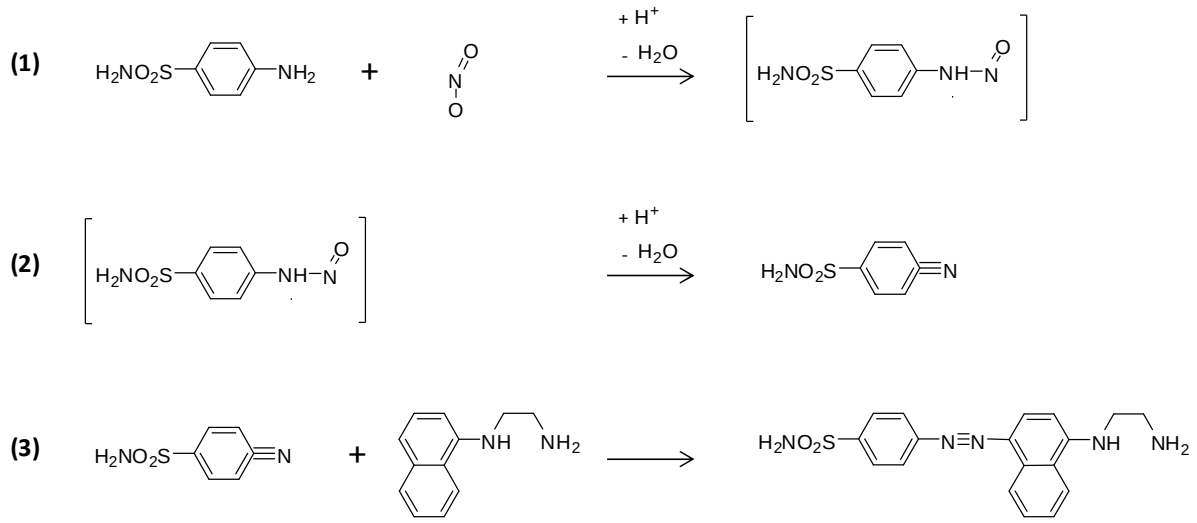

**Scheme 3-3: Griess reaction. The nitrite reacts with the amino group of sulfanilamide. A diazonium cation is formed which binds to naphtyletyhlenediamine and builds an azo dye [285]. The absorbance of the colored solutions is measured at 560 nm.**

For each compound the experiment was performed 3 times with different cell passage numbers. The nitrite content of the samples was calculated using the prepared calibration curve. Control c, which was incubated with medium and stimuli, was defined as 100% NO production.

### 3.5.11 iNOS protein expression

In order to determine if an inhibition of nitric oxide formation by the compounds was based on a reduced expression of iNOS protein, expression was analyzed by immunofluorescence using the Cellomics® iNOS Activation Kit (Thermo Scientific, Bonn, Germany). For this, 1 x $10^4$ RAW 264.7 cells were seeded, incubated and stimulated as described in 3.5.10 Nitric oxide assay. Most of the compounds were tested at concentrations of 5 and 10 µM. The dihydro compounds were also tested at 15 µM. Compounds **16**–**18** were also analysed at 2 µM. **5** and **9** were used up to 40 µM and **8** up to 50 µM. After incubation with the test compounds, immunostaining was performed as described in the kit instructions. Briefly, the cells were fixed and blocked. Staining the iNOS protein with the primary antibody and the staining solution the cells were permeabilized.

Fluorescence imaging was carried out with a computer-controlled Cell Observer® system consisting of a Zeiss Axio Observer (Carl Zeiss, Göttingen, Germany) with software AxioVision 4.8.1 (Carl Zeiss, MicroImaging, Munich, Germany), motorized scanning stage, AxioCam HRm and HXP 120 light source. Images were aquired using a 10x/0.3 Ph1 M27 EC

Plan-Neofluar objective (Carl Zeiss AG, Oberkochen, Germany). Image analysis was performed with the ASSAYbuilder® Physiology Analyst software. The valid object count (number of cell cores detected by the software) and mean ring spot total intensity were the parameters used for calculation. With the mean ring spot total intensity a ring is superimposed on the cell without the cell core and the intensity is measured by the software.
For each compound the experiment was performed 3 times with different cell passage numbers.

### 3.5.12 Statistical analysis and calculations

The statistical analysis was performed with Graph Pad Prism 4. Significant different averages ($p$ value < 0.05) were evaluated statistically with one-way ANOVA followed by Tukey's Multiple Comparison Post Test.
The $IC_{50}$ values were calculated with Graph Pad Prism 4. Therefore a sigmoidal dose-response were calculated with a variable hillslope, fixed bottom and top.
The results were expressed as mean ± standard deviation (SD). Results were checked for outliers using Grubbs test.

## 3.6 Results

### 3.6.1 Purity degree, lipophilicity and structure determination

The investigated compounds were analyzed by HPLC in order to determine their purity. The purity was 94 to 99% with exception of **5** (see Table 3-1: Purity and lipohilicity), which had a purity of 86%.

**Table 3-1: Purity and lipohilicity of the investigated compounds.**

| No. | Compound | IUPAC name | Rf-values | Purity % |
|---|---|---|---|---|
| **1** | Xanthohumol (XN) | 2',4'-Dihydroxy-6'-methoxy-3'prenylchalcone | 0.15 | 99 |
| **2** | Xanthohumol H | 2',4',4-Tri(hydroxy)-3'(3''-hydroxy-3''-methylbutyl)-6'-methoxychalcone | 0.08 | 97 |
| **3** | 4-Acetoxy-xanthohumol | 4-Acetoxy-2',4'-dihydroxy-6'-methoxy-3'-prenylchalcone | 0.25 | 96 |
| **4** | 4-Methoxy-xanthohumol | 2',4'-Dihydroxy-4,6-dimethoxy-3'-prenylchalcone | 0.29 | 96 |
| **5** | Desmethyl-xanthohumol | 2',4,4',6'-Tetrahydroxy-3'- prenylchalcone | 0.09 | 86 |
| **6** | Xanthohumol C | 2'',2''-Dimethylpyrano[2'',3'':3',4']-2',4-dihydroxy-6'-methoxychalcone | 0.33 | 97 |
| **7** | Dihydroxanthohumol C | 2'',2''-Dimethyl-3'',4''-dihydro-(2H)-pyrano[2'',3'':3',4']-2',4-dihydroxy-6'-methoxychalcone | 0.35 | 98 |
| **8** | Acetylchroman | 2,2-Dimethyl-5-hydroxy-7-methoxy-acetylchroman | 0.36 | 94 |
| **9** | Prenylacetophenon | 2,4-Dihydroxy-3-prenyl-6-methoxyacetophenon | 0.69 | 98 |
| **10** | Tetrahydroxanthohumol C | Dihydro 2'',2''-Dimethyl-3'',4''-dihydro-(2H)-pyrano[2'',3'':3',4']-2',4-dihydroxy-6'-methoxychalcone | 0.39 | 87 |
| **11** | Dihydro-helichrysetin | Dihydro 2',4,4'-Trihydroxy-6'-methoxychalcone | 0.15 | 88 |
| **12** | Dihydro-flavokawain C | Dihydro 2',4-Dihydroxy-4',6'-trimethoxychalcone | 0.28 | 94 |
| **13** | Helichrysetin | 2',4,4'-Trihydroxy-6'-methoxychalcone | 0.14 | 99 |
| **14** | 3-Hydroxy-helichrysetin | 2',3,4,4'-Tetrahydroxy-6'-methoxychalcone | 0.07 | 98 |
| **15** | Flavokawain A | 2'-Hydroxy-4,4',6'-trimethoxychalcone | 0.49 | 99 |
| **16** | Flavokawain B | 2'-Hydroxy-4',6'-dimethoxychalcone | 0.56 | 94 |
| **17** | Flavokawain C | 2',4-Dihydroxy-4',6'-trimethoxychalcone | 0.25 | 99 |
| **18** | Alpinetin chalcone | 2',4'-Dihydroxy-6'-methoxy-chalcone | 0.31 | 99 |

Furthermore, the lipophilicity of the compounds was estimated by HPTLC in order to identify a possible relationship between the lipophilicity and the biological activity of the used compounds. The results of the HPTLC are depicted in Figure 3-5 and the Rf-values are in Table 3-1, starting with the most lipophilic **9** > **15** > **14** > **10** > **8** > **7** > **6** > **18** > **4** > **12** > **17** = **3** > **1** = **11** > **13** > **5** > **2** > **14**.

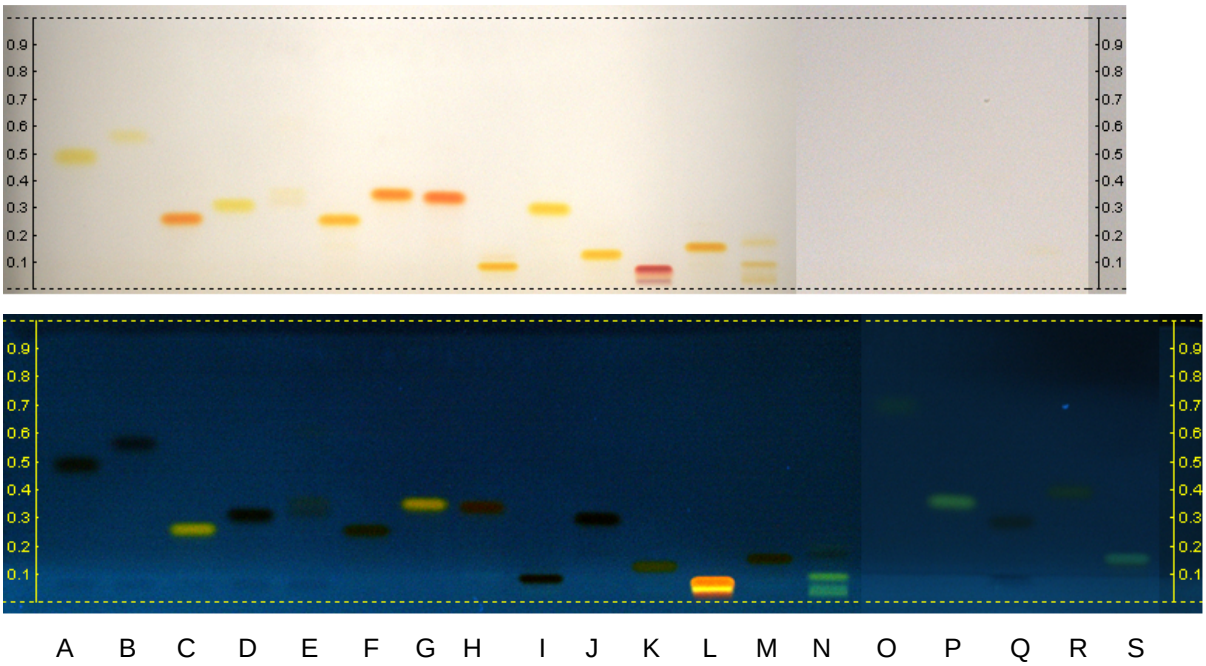


**Figure 3-5: The lipophilicity of 18 compounds was estimated by HPTLC. A: Flavokawain A (14), B: Flavokawain B (15), C: Flavokawain C (17), D: Alpinetin chalcone (18), E: Pinostrobin, F: 4-Acetoxyxanthohumol (3), G: Dihydroxanthohumol C (7), H: Xanthohumol C (6), I: Xanthohumol H (2), J: 4-Methoxyxanthohumol (4), K: Helichrysetin (13), L: 3-OHHelichrysetin (14), M: Xanthohumol (1), N: Desmethylxanthohumol (5), O: Acetylchroman (8), P: Prenylacetophenon (9), Q: Dihydro-Flavokawain C (12), R: Tetrahydroxanthohumol C (10), S: Dihydro-Helichrysetin (11). The solvent system consisted of hexan:ethyl acetate:methanol (70:20:10) + 0.1% formic acid. The HPTLC plates were derivatized with Naturstoff reagent and macrogol.**

In the majority the inhibition of the NF-κB pathway is attributed to the Michael system. In order to analyze if the Michael system is solely responsible for the iNOS inhibition, **7**, **13** and **17** were hydrogenated to obtain **10**-**12**. The hydrogenation reaction was verified by $^{1}$H NMR spectroscopy. The $^{1}$H NMR spectra confirmed the complete hydrogenation (see Figure 9-1).

### 3.6.2 Effect on the cell viability and proliferation

Compounds **1**-**4**, **6**, **7**, **13** and **14** (3.2.1 Minor hop compounds, XN metabolites and related compounds) were tested in two cell based assays, the cell viability MTT assay and the proliferation assay CV. The compounds were tested concerning their effects in 3 hepatoma

HSC, HepG2, HuH-7 cell lines, and a colon carcinoma Caco-2 cell line as well as immortalized mouse macrophages RAW 264.7.

**$IC_{50}$ values determined in MTT and CV assay.** In order to determine $IC_{50}$ values for the viability and proliferation data, the different cell lines were incubated with the compounds at concentrations of 10, 20, 30, 40, 50, 60, 80 and 100 µM. Based on the concentration response curves, the $IC_{50}$ values were calculated for both assays as mean ± SD (three different experiments). The $IC_{50}$ values are summarized in five diagrams in Figure 3-6. In A-D, the $IC_{50}$ proliferation and viability values of **1**-**4**, **6**, **7**, **13** and **14** are depicted for HSC, HepG2, HuH-7 and Caco-2 cells. In Figure 3-6, the $IC_{50}$ viability values for RAW 254.7 cells concerning the above mentioned eight substances plus additional derivatives are summarized.

**A** HSC

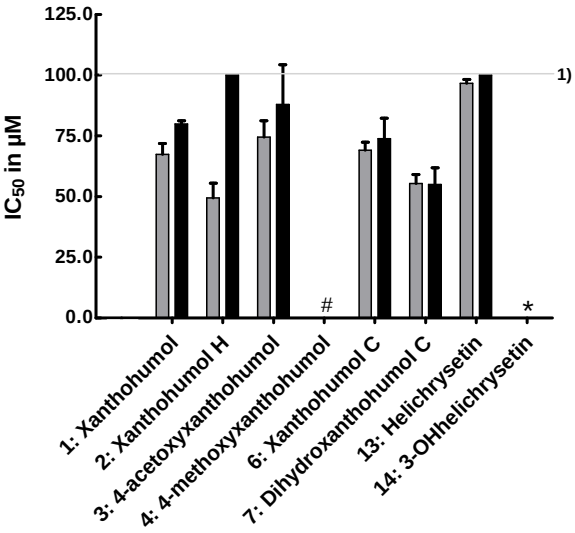


**B** HepG2

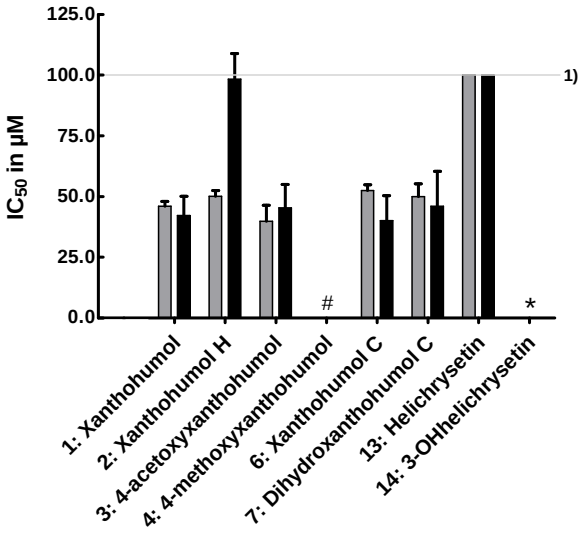


-**Figure 3-6 continues on page 72-**

**-Continuance of Figure 3-6-**

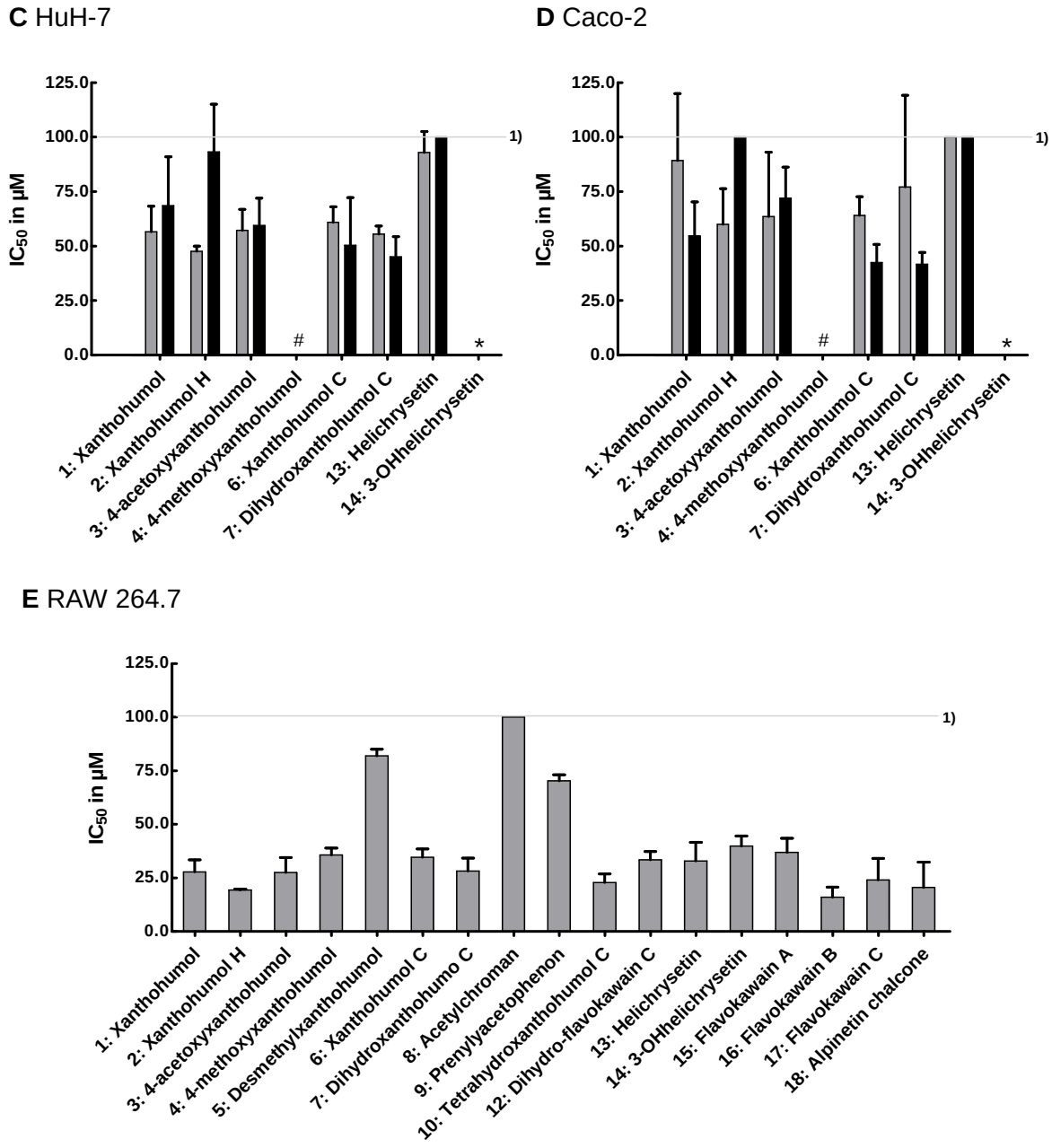


**Figure 3-6: $IC_{50}$ values of the compounds determined from off dose response proliferation (■) and viability curves (■). No $IC_{50}$ value could be calculated for the compound 4 (#) and compound 14 (*). Compound 14 (*) showed no toxicity up to the highest tested concentration of 100 µM ([1)]). A: HSC, B: HepG2, C: HuH-7, D: Caco-2, E: RAW 264.7. Mean ± SD n ≥ 4.**

The $IC_{50}$ values of **14** (*) and **4** (#) could not be calculated for the cell lines (A-D) in both assays (MTT/CV). The hydrophilic compound **14** showed no effect on the cell viability, cell proliferation or cell behavior up to a concentration of 100 µM ([1)] display the upper measurement concentration see Figure 3-6). However, compound **4** caused a measurable effect in both assays but no $IC_{50}$ value could be determined. In almost all cell lines 20 µM of **4**

induced a decrease in the viability, a proliferation inhibition and exhibited cytotoxicity. The effects of **4** were very similar at concentrations between 20-100 µM (see Figure 3-7). Hence, no $IC_{50}$ value of **4** could be calculated.

**A** Viability assay

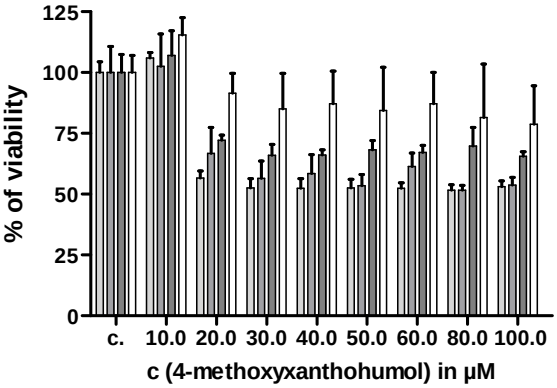


**B** Proliferation assay

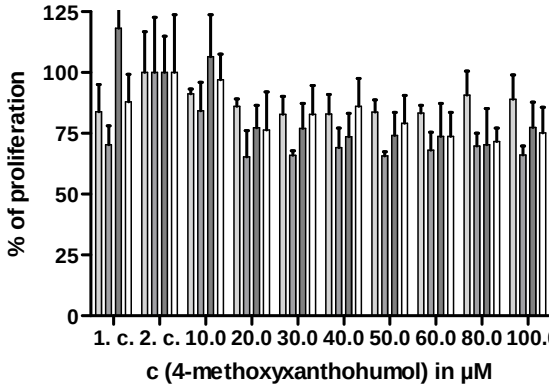


**Figure 3-7: The behavior of 4-methoxyxanthohumol (4) in the MTT (A) and CV (B) assay in four cell lines. The first light grey bar displays the HSC, the second darker grey bar the HepG2, the third dark grey bar the HuH-7 and the fourth white bar the Caco-2 cells. Abbreviation c. and 1 c. display the control of untreated cells after 24 h incubated with medium 2. c. Control of untreated cells after 48 h of incubation.**

Nevertheless, compound **4** showed a strong effect, but not a sigmoidal behavior (Figure 3-7). A low activity on the cell viability and proliferation was detected for compound **13**. The $IC_{50}$ values (MTT) of **13** were 33.0 ± 8.6 µM (**E**: RAW 264.7), 93.0 ± 9.5 µM (**C**: HuH-7), 96.7 ± 1.6 µM (**A**: HSC) and >100 µM (**B**: HepG2, **D**: Caco-2) (Figure 3-6). Summing up **13** showed marginal and **14** no biological activity in all cell lines and both assays.

The compound (concerning prenylated chalcones and those with tetrahydropyran ring annuleted to the A-ring) **2** reached the lowest $IC_{50}$ value in HuH-7, HSC and Caco-2 cells determined with MTT assay. Compound **2** showed $IC_{50}$ values of 49.4 ± 6.1 µM (**A**: HSC), 47.7 ± 2.3 µM (**C**: HuH-7) and 60.1 ± 16.2 µM (**D**: Caco-2). Only in HSC cells a significant difference could be measured between **2** and the other prenylated chalcones. The compounds **2** and **7** ($IC_{50}$ of 55.4 ± 3.7 µM) were the compounds which reached significantly the lowest $IC_{50}$ values in the MTT assay. The highest $IC_{50}$ values in HSCs reached **6** and **3**. The compound **6** showed $IC_{50}$ value of 69.1 ± 3.3 µM and **3** of 74.5 ± 6.8 µM (**A**: HSC). Quite the opposite direction for **3** was determined in HepG2 cells. Compound **3** reached the lowest $IC_{50}$ values of 39.8 ± 6.6 µM, but a significant difference in the values could be only measured between **3** and **6** (52.6 ± 2.2 µM). The other chalcones such as the prenylated and tetrahydropyran-chalcone exhibited an $IC_{50}$ value of 46.0 ± 2.1 µM (XN, **1**), 50.2 ± 2.2 µM (**2**) and 50.0 ± 5.3 µM (**7** (**A**: HSC)).

In the macrophages cell line RAW 264.7 **16** showed the lowest $IC_{50}$ value of 16.0 ± 4.7 µM. Not only **16** exhibited remarkable $IC_{50}$ values in RAW 264.7, also the structural related chalcones **17** (24.1 ± 10.0 µM) and **18** (20.6 ± 11.7 µM). In the group of the prenylated chalcones **2** (19.4 ± 0.3 µM) and **10** (22.9 ± 4.0 µM) reached the lowest $IC_{50}$ values.

In the CV assay a quite opposite behavior was measured for **2** and **7** as well as for **6**. The compound **2** showed the highest $IC_{50}$ values concerning the proliferation e. g. >100 µM (**A**: HSC), 98.4 ± 10.5 µM (**B**: HepG2), 93.3 ± 21.9 µM (**C**: HuH-7) and >100 µM (**D**: Caco-2). Compound **7** showed the lowest $IC_{50}$ values of 55.1 ± 6.8 µM (**A**: HSC), 45.2 ± 9.1 µM (**C**: HuH-7) and 41.7 ± 5.4 µM (**D**: Caco-2). Compound **7** was significant different from compound **2** in HSC and Caco-2. A similar trend was observed for **6**. In HSC (73.8 ± 8.5 µM), HuH-7 (50.4 ± 21.8 µM) and Caco-2 (42.4 ± 8.4 µM) cells the $IC_{50}$ values of **6** were higher as for **7** but lower compared to the other compounds. In HepG2 cells **6** reached the lowest $IC_{50}$ value of 40.2 ± 10.2 µM.

**Sensitivity of the cells incubated with the compounds.** Already low concentrations of the investigated compounds led to a cell viability decrease in RAW 264.7 macrophages. The $IC_{50}$ value of **2** was 19.4 ± 0.3 µM compared to 49.4 ± 6.1 µM in HSC, 47.7 ± 2.3 µM in HuH-7 and 60.1 ± 16.2 µM in Caco-2 cells. HSC and Caco-2 were the most unsusceptible cell lines. The HSC and Caco-2 cells were robust against incubation with high concentrations of all tested chalcones except of Heli.

### 3.6.3 Nitric oxide assay

All compounds were screened concerning their ability to inhibit the NO production using a Griess assay. Two different stimuli were used to induce the NO production and thus allow for the measurement of the influence of the tested compounds on the NO production. One of the stimuli was 10 ng/ml LPS. The second was a combination of 10 ng/ml LPS and 200 ng/ml IFN-γ. The results of the Griess assay are summarized in Table 3-2.

**Table 3-2: Influence of 18 compounds (1-18) on the NO production by iNOS in RAW 264.7 cells determined by Griess assay. NO formation was induced either with LPS or with a combination of LPS and INF-γ. The compounds were tested at their non-toxic concentration. In the table the remaining NO production in % from the control is depicted.**

| Compound | 10 ng/ml LPS | | 10 ng/ml LPS and 200 ng/ml IFN-γ | |
|---|---|---|---|---|
| | Concentration in µM | % remaining NO production | Concentration in µM | % remaining NO production |
| **1** | 10 | 65.4 ± 12.0 | 15 | 84.1 ± 6.0 |
| **2** | 5 | 65.4 ± 17.3 | 15 | 78.3 ± 3.0 |
| **3** | 10 | 74.0 ± 8.1 | | no inhibition |
| **4** | 5 | 75.5 ± 7.5 | | no inhibition |
| **5** | 15 | 25.6 ± 21.4 | 15 | 87.8 ± 3 |
| **6** | 2 | 72.1 ± 4.1 | 5 | 84.7 ± 5.3 |
| **7** | 5 | 62.3 ± 16.7 | 8 | 76.8 ± 10.5 |
| **8** | 30 | 49.9 ± 2.8 | | no inhibition |
| **9** | 50 | 55.1 ± 5.8 | | no inhibition |
| **10** | | no inhibition | 8 | 87.5 ± 2.1 |
| **11** | | no inhibition | | no inhibition |
| **12** | | no inhibition | | no inhibition |
| **13** | 2 | 77.7 ± 2.3 | 8 | 80.5 ± 0.5 |
| **14** | 2 | 91.2 ± 3.8 | 10 | 87.2 ± 6.3 |
| **15** | 15 | 23.7 ± 15.7 | | no inhibition |
| **16** | 5 | 40.0 ± 13.4 | 8 | 80.9 ± 7.6 |
| **17** | 5 | 38.4 ± 4.3 | 8 | 80.1 ± 10.5 |
| **18** | 2 | 70.2 ± 1.6 | 10 | 66.8 ± 15.6 |

After induction with 10 ng/ml LPS, **18**, **6** and **13** showed the highest inhibition of NO formation followed by **14** (all at 2 µM). At 5 µM **16** and **17** showed a significantly higher inhibitory activity than **4** ($p<0.05$). **7**, **2** and **4** were less active in inhibiting the NO production

than the aforementioned compounds. At 10 µM XN (**1**) and **3** exhibited a significant higher inhibitory activity than **15** and **5**. The compound **8** and **9** showed an inhibitory effect on the NO production at 30 µM and 50 µM. No inhibition was observed for the dihydro-chalcones.
In order to compare the results of the Griess assay with those of the iNOS protein expression assay, it was necessary to conduct both experiments under the same conditions. A second version of the assay was conducted with 10 ng/ml LPS and 200 ng/ml IFN-γ as stimuli. No inhibitory activity on the NO production could be observed for **3**, **4**, **8**, **9**, **11**, **12**, and **15** under these conditions. At 2 µM a significant NO inhibition of the compounds **18**, **6**, **13** and **14** could be already detected during the activation with solely 10 ng/ml LPS. Using 10 ng/ml LPS and 200 ng/ml IFN-γ, the first inhibitory activity was observable at 5 µM for compound **6**. At 8 µM an inhibitory effect was also observed for **7**, **17**, **13**, **16** and **10**. The statistical analysis revealed no significant difference between these compounds. **18** and **14** inhibited the NO production at 10 µM. At 15 µM no significant difference could be observed between **1**, **2** and **5**.

### 3.6.4 iNOS protein expression

The nitric oxide assay only reveals whether a compound is able to inhibit the NO production or not. It gives no information about the underlying mechanism. Reduction of NO formation can for example be caused by reaction of NO with the test compounds, by inhibition of iNOS enzym activity or by reduction of iNOS protein expression.
Thus, the purpose of this study was to also determine if the inhibition of the NO production is caused by a decrease in iNOS expression. iNOS expression was analyzed with a fluorescently labeled antibody (Cellomics® iNOS Activation Kit). The positive control (activated cells without test compound) acted as a 100% reference point in order to allow for a comparison of the tested compounds. The results are summarized in Table 3-3.

**Table 3-3: Influence of compounds 1-18 on iNOS expression determined by fluorescence immunostaining. The compounds were tested at their non-toxic concentration. In the table the remaining iNOS expression in % from the control is depicted**

| | 10 ng/ml LPS and 200 ng/ml IFN-γ | |
|---|---|---|
| Compound | Concentration in µM | % remaining iNOS expression |
| **1** | 10 | 18.2 ± 8.9 |
| **2** | 5 | 39.6 ± 12.5 |
| **3** | 5 | 56.0 ± 11.0 |
| **4** | | no inhibition |
| **5** | | no inhibition |
| **6** | 5 | 35.2 ± 2.6 |
| **7** | 10 | 16.8 ± 14.6 |
| **8** | 50 | 76.3 ± 7.7 |
| **9** | | no inhibition |
| **10** | 10 | 65.4 ± 9.1 |
| **11** | 10 | 62.3 ± 16.8 |
| **12** | 5 | 72.1 ± 8.3 |
| **13** | 5 | 41.1 ± 17.9 |
| **14** | | no inhibition |
| **15** | 10 | 30.2 ± 6.7 |
| **16** | 5 | 35.5 ± 12.5 |
| **17** | 10 | 22.9 ± 9.0 |
| **18** | 5 | 10.7 ± 6.6 |

All compounds except of **4**, **5**, **9** and **14** showed an inhibitory effect on the iNOS expression. The compounds were tested in concentrations without an effect on the cell viability. The most active chalcones at 5 µM were **18**, **6**, **16**, **2** and **13** followed by **3** and **12**. At 10 µM **7**, **1** and **15** showed the highest inhibition of the iNOS expression followed by **11** and **12**. At 50 µM **8** reduced the iNOS expression to a remaining level of 76.3 ± 7.7%.

## 3.7 Discussion

### 3.7.1 Effect on the cell viability and proliferation

The effect of minor hop compounds, XN (**1**) metabolites and structure related chalcones on the viability, proliferation and the cell survival was investigated in HuH-7, HepG2 and HSC, RAW 264.7 and Caco-2 cells.

The murine macrophage cells RAW 264.7 were much more sensitive to the tested compounds than the other cell lines. The defense and the activation of further immune-cells against toxic products and harmful organisms is their main function in the body. In contrast to the macrophages, hepatic stellate cells were not less sensitive to the tested compounds. Hepatic stellate cells are non parenchymal cells and located in the liver. Under healthy conditions, they store vitamin A. Under pathologic conditions, they start to build up extracellular matrix and lose vitamin A storage. This process is in many cases correlated with alcohol abuses and viral infections. The production of extracellular matrix causes a partial loss of the liver function and can lead to reversible fibrosis and at worst to necrosis and organ failure [286]. Therefore, HSC are more resistant to toxic substances than other cells, which was also confirmed in this study. HSC, colon cancer Caco-2 cells were also less sensitive to the compound exposure. The same non-sensitive behavior was observed in the sulforhodamine assay performed by Miranda and co-workers [186]. They incubated human breast cancer MCF-7, colon cancer HT-29 and ovarian cancer A-2780 cells with different chalcones for 48, 96 and 144 h. The ovarian cancer cell line was the most sensitive followed by human breast and the colon cancer cells. Interestingly, the cytotoxicity was more pronounced in HT-29 and A-2780 cells after 48 h compared to 96 h of incubation. It was discussed that the cells became less sensitive to the chalcones because of the detoxification process and/or the efflux by P-glycoproteins [186]. In further studies it was shown that **1** inhibit P-glycoprotein transport in Caco-2 [242] and MDCKII cells [241]. Furthermore, compound **1** inhibited the mRNA levels of the efflux transporter genes, too [189]. Nevertheless, the influence of **1** on the P-glycoprotein transporter is not fully understood yet [241] (1.3 Bioavailability, metabolism and cell uptake). However, compound **1** and other chalcones can be biotransformated and lose their cytotoxic effects. Thus, proliferation and cytotoxicity assays should be performed time-resolved in order to reach a more significant conclusion on the effect of the substances.

This may also explain the different behavior of HeLa cells in the studies conducted by Vogel et al. [150-152] and this study. In the latter, the HeLa cells were incubated with the minor hops compounds and XN metabolites for 72 h in the MTT assay. **13** showed the strongest viability inhibition ($IC_{50}$ value 5.2 ± 0.8 µM) followed by **2** > **1** > **6** > **14** > **7** = **4** > **3** > **5** and **17** [150-152]. In this study, a partially different behavior was observed probably because of the different cell types. **13** and **14** were found to be the compounds with the least cytotoxic effects. Compound **2** exhibited in this study the lowest $IC_{50}$ value (Figure 3-6: A, C and D). The incubation time in this MTT assay was 24 h.

A correlation between the lipophilicity of the tested substances and their cytotoxicity could be partially observed. The HPTLC study revealed that **5**, **2**, **13** and **14** were the most hydrophilic among the investigated compounds (see Table 3-1). The compound **13** and **14** were found to

have the lowest cytotoxicity. In contrast the lipohilic **16** exhibited the lowest $IC_{50}$ values in RAW 264.7 cells in the MTT assay. This is also in agreement with a study conducted by Li and co-workers [271]. In their study **15** showed the weakest effects on the viability of RAW 264.7. Compounds **16** and **17**, which are more lipophilic, were more potent. Further examples include a local anesthetics study [287] and a study with heat shock proteins [288]. The studies showed that lipophilic chemicals exhibit higher cytotoxicity in human T-lymphoma cells [287] or induce heat shock proteins [288].

The lipophilicity plays not only an important role for the cytotoxicity of substances, but has also been shown to provide protection against *in vitro* LDL oxidation. Lipophilic compounds were more potent in the inhibition of the LDL oxidation due to the physical capability to approximate to the LDL particles [146]. The same effect was observed for proteins. Lipophilic compounds can approximate to and interact with lipophilic centers of enzymes [288,289]. Compound **1** can interact with mitochondrial proteins, induce the release of ROS and thus lead to apoptosis [157]. In addition **1** can change the membrane fluidity [290]. This process might lead to a faster infiltration and a higher cytotoxicity. Compound **1** was found to penetrate the cell membrane of different cell lines but the exact access mechanism are still unknown [227,228]. It seems that **1** might affect the transport by ABC-transporters [189,241].

As aforementioned a correlation between the lipophilicity and cytotoxicity of the investigated substances could only be partially observed in this study. Compound **2** as an outlier showed a high inhibitory activity concerning the viability, but only weak effects on the proliferation and cytotoxicity. Compound **2** however was determined to be as hydrophil as **14**. The prenyl chain of **2** might be an explanation for this behavior. Prenyl chains were shown to lead to a variety of effects. For example compounds with a prenyl chain showed a higher antioxidant capability in oxidative injury models [148]. In addition, prenylated compounds possessed noteworthy activity against gram-negative bacteria [19], exhibited antimicrobial effects [291] and induced phase II enzymes [135]. Furthermore, they were shown to inhibit beta-side APP cleaving enzyme 1 (BACE1) [292], the invasion of cancer cells [187] as well as their proliferation and 5-LOX activity [289]. In addition, prenylation of apigenin and liquiritigenin has been shown to increase their cytotoxicity in different cell lines [293]. This correlation was also observed in a cytotoxicity study of prenylated isoflavonoids from *Bituminaria morisiana* (PIGNATTI & METLESICS) GREUTER. The prenyl chain in C-8 position enhanced the cytotoxicity of the pterocarpans [294].

The lipophilicity of compounds increases with the number of prenyl groups. However, lipophilicity can not only be attributed to prenyl groups. As aforementioned compounds with prenyl groups were usually more active compared to those without prenyl groups, but **16** was the most active compound in the MTT assay in RAW 264.7 cells and possesses no prenyl

group. Thus, neither the lipophilicity nor the number of prenyl groups is solely responsible for the inhibition of the viability and the proliferation of cancer cells by a substance.
In the present study, the mechanisms which induce cytotoxicity were not investigated in detail, but two distinct assays were used to get some hints. The MTT assay measures an increase or decrease in the cell viability, which can be caused by a drop of the cell count and/or a decrease in mitochondrial activity. The CV assay is only based on the cell count.
With increasing concentrations **2** first inhibited the viability and then the cell count (Figure 3-6 **A**, **B**, **C** and **D**). This might point to an involvement of the mitochondria. Compounds **6** and **7** showed the opposite behavior. First, a decrease in the cell count was observed, which was then followed by a decrease in viability. Thus, **6** and **7** might induce cell death via a different mechanism. The behavior of **1**, **3** and **13** depends on the used cell line. It is known that compound **1** induces apoptosis by different pathways depending on the cell type. This includes the intrinsic, extrinsic, and the endoplasmatic reticulum- and NF-κB dependent pathway (1.1.7 Pro-apoptotic mechanism). XN (**1**) was shown to induce the ROS production which triggers cells into apoptosis [157,154]. In this study **1** showed moderate effects on the cell viability and proliferation of the investigated cell lines. Thus the mechanism that are influenced by XN (**1**) might be different from those influenced by **2**, **4**, **6**, and **7** and should be studied in more detail in order to reveal which cell death mechanism are responsible for the observed effects.

### 3.7.2 Nitric oxide assay and iNOS protein expression

The tumor initiation and promotion is correlated with chronic inflammation [161]. The expression of iNOS was correlated with lower chance of survival depending on the type of cancer and chronic inflammatory diseases (see 3.2.2 Biological effects of XN metabolites). In the present study the inhibition of the NO production and iNOS by the minor hop chalcones, XN metabolites and related compounds was investigated concerning the structure-response relationship.
All compounds except of the dihydro compounds **10**, **11** and **12** showed a significant inhibition of the NO production in the performed Griess assay (10 ng/ml LPS). It is discussed in the literature that, the inhibition of the NO production might be mediated by endogenous electrophils via an α,β-unsaturated carbonyl moiety [181,295]. Compounds without this moiety led to no or only little decreases in the NO production [181]. In the present study, the same was observed in the nitric oxide assay using 10 ng/ml LPS as stimuli.
In order to compare the data from the Griess assay with that of the iNOS expression the assay was additionally performed with 10 ng/ml LPS and 200 ng/ml IFN-γ. In this case **10** showed a significant inhibitory effect on the NO production at 8 µM. The observed inhibition

of NF-κB regulated factors by dihydro compounds is in agreement with the study of Peluso et al. [178]. In their study monocytic THP-1 cells were stimulated with LPS and co-incubated with or without prenylated and non-prenylated chalcones as well as with flavanones. The influence on the MCP-1 and IL-6 production was investigated. Dihydroxanthohumol compared to **1** showed a higher inhibition of the IL-6 and the MCP-1 production. MCP-1 and IL-6 are cytokines which are regulated by the NF-κB pathway [178]. In the present study, the inhibition of NF-κB regulated factors by dihydro compounds could not be detected solely using 10 ng/ml LPS as stimulus, but it could be confirmed in the assay version with 10 ng/ml LPS plus 200 ng/ml IFN-γ as stimuli. Possibly the compounds are more potent to inhibit the NO production via the JAK/STAT pathway compared to the NF-κB pathway. It is discussed and pruposed in the literature that **1** inhibits the NF-κB pathway via its α,β-unsaturated moiety [169,171,176] and there is no such moiety in the dihydro compounds. XN (**1**) was also shown to influence the JAK/STAT pathway but a clear mechanism is not known, yet and thus hinders a comparison with the dihydro compounds (1.1.6 Anti-inflammatory effect).

A correlation between the inhibition of NF-κB or related proteins and tetrahydropyrans (A ring of **6** and **7**) has, not been discussed in the literature, yet. Compound **6** significantly inhibited the NO production irrespective of the used stimuli. The compound **8** showed higher inhibitory effects compared to **9**. The compound **10** inhibited the NO production in case of the stimulation of the cells with 10 ng/ml LPS and 200 ng/ml IFN-γ. This effect could also be observed during the determination of the iNOS expression. Compound **6** belongs to the effective iNOS inhibitors in this study. Therefore it is suggested that the A ring with the tetrahydropyran is conducted for the inhibition of the NO production and iNOS expression independent regardless of the used stimuli.

In the study of Zhao et al. [181] the prenylation was not found to enhance the inhibition of the NO production. This was also confirmed in the present study. Prenylated chalcones mostly exhibited a lesser inhibition of iNOS expression than non-prenylated chalcones with the exception of **2**. Compound **2**, which possesses a hydroxylated prenyl chain, was the most active chalcone in the group of prenyl chain carrying chalcones. Compound **5** however, also a prenylated chalcone, showed the weakest effect. One reason might be the lower purity of 86% of **5**. In the study of Peluso et al. [178] **5** also was less active compared to **1** and **16**.

In the group of prenylated chalcones the ability to inhibit the NO production was also dependent on the substituent of the B ring. Compounds exhibiting a free hydroxyl group inhibited the NO production more efficient than an *O*-methoxylated or an *O*-acetylated one. Peluso et al. observed an increase in the IL-6 and MCP-1 inhibition with an increasing number of prenyl groups and an *O*-methoxylation of the A ring (LPS stimulated THP-1 cells) [178]. IL-6 and MCP-1 are regulated via the NF-κB pathway. This could not be observed in

this study. One reason might be the used cells or the factors which were determined in the study of Peluso et al. [178].

Compound **13**, a non-prenylated chalcone, exhibited the highest inhibitory effect on NO production and iNOS protein expression. In general, the non-prenylated and the tetrahydropyran-chalcones showed a higher inhibitory activity in the NO production and the iNOS expression. Compound **18** does not contain a hydroxyl group in the B ring, but it was as active as **13** in the Griess assay with 10 ng/ml LPS stimulation and the iNOS expression assay. In the second version of the NO assay with 10 ng/ml LPS and 200 ng/ml IFN-γ as stimuli, **18** showed a lesser inhibition of the NO production than **13**. The iNOS expression is stimulated by LPS via the NF-κB pathway and by IFN-γ via Jak/STAT signaling (1.1.6 Anti-inflammatory effect). The compound **18** might be more potent in the inhibition of the NO production via the NF-κB pathway. One hydroxyl group in the non-prenylated chalcones seems to lead to a more effective inhibition of the NO production and the iNOS expression than two or no hydroxyl groups. A similar correlation was also observed for the flavokawains. The compound **16** and **17** were more potent than **15** with an *O*-methoxy group at the B ring. Interestingly, **16** was more potent to inhibit the iNOS expression. One outliner is **14**. Compound **14** showed inhibitory effects in the NO assays but no effect on the iNOS expression. There was no correlation between the lipophilicity of the compounds and the NO production as well as the iNOS expression.

## 3.8 Summary

In the present study, the influence of XN (**1**), minor hop constituents and XN metabolites concerning their influence on cell viability and proliferation was analyzed using MTT assay and CV. Compound **2** exhibited the lowest $IC_{50}$ value in the cell viability and **6** and **7** in the proliferation assay. The higher lipophilicity of **6** and **7** might be one explanation. However **2** is more hydrophilic than XN (**1**) but exhibited stronger anti-viability effects. Thus these XN metabolites and related compounds are possible candidates for advanced studies in order to reveal the underlying mechanism that led to the cell death.

The influence of the compounds on the NO production and iNOS expression was determined by Griess assay and the iNOS immunostaining. iNOS expression was induced with 10 ng/ml LPS and 200 ng/ml IFN-γ as stimuli. The NO formation was stimulated with 10 ng/ml LPS and 200 ng/ml IFN-γ stimuli to compare the effects in the iNOS expression assay and with 10 ng/ml LPS to evaluate the efficiency of inhibition and the possible pathways. In the first version of Griess assay (10 ng/ml LPS), the dihydro compounds did not inhibit the NO production. In the second version of the assay (10 ng/ml LPS and 200 ng/ml IFN-γ as stimuli) however, **10** inhibited the NO production. The

tetrahydropyran-chalcones **6** and **7** as well as the non-prenylated **13** were the compounds with the highest inhibitory activity on NO production and iNOS expression. In addition, non-prenylated chalcones with one hydroxyl group seem to be more effective in inhibiting the NO production and the iNOS expression compared to those with two or no hydroxyl groups. The prenyl chain seems to be less importance for this effect. In the iNOS assay all compounds, with exception of **14**, showed an inhibition of the iNOS expression on the protein level.

# 4 *In vitro* uptake of xanthohumol in hepatic and colorectal cancer cell lines and primary hepatocytes [2)]

## 4.1 Abstract

Xanthohumol (XN), a prenylated chalcone found in hops, has been reported to show anti-inflammatory and anti-infective properties. In addition, it possesses anti-cancer activity, affecting all development stages of cancer cells including cancer initiation, promotion and progression. In order to achieve these activities *in vivo* adequate XN concentrations have to be reached. Different studies revealed a low bioavailability of XN and in Caco-2 cells a fast and high cellular uptake has been reported. The exact uptake mechanism as well as the uptake in hepatic cell lines and primary hepatocytes has not been investigated yet. For this reason, we studied the cellular uptake and accumulation of XN in different hepatic and colorectal (cancer) cell lines and primary hepatocytes. Caco-2, HuH-7, HSC and primary hepatocytes were incubated with medium supplemented with 10 µM XN.

In order to determine the XN amount per cell a calibration curve was prepared. The calibration curve was based on the ratio between the protein amount per HuH-7, HSC and Caco-2 cells.

This study revealed that HuH-7 cells had the lowest protein concentration per cell. HSC had the highest. HuH-7 was the weakest uptaker followed by HSC, Caco-2 and primary hepatocytes. HSC, Caco-2 and primary hepatocytes accumulated a 52, 63 and 47 fold higher XN amount compared to the outer medium. However, the exact uptake mechanism is still not known and should be a topic of further studies.

## 4.2 Introduction

XN is one of the ingredients in hops and shows a wide range of effects such as anti-inflammatory, anti-cancer and anti-infective activity. The exact cell uptake mechanism of XN is not completely investigated, yet. Four studies investigated the absorption and/or protein binding or transporter interference for XN in different cell models [227,228,241,242].

[2)] The data of this chapter is pulished in: H. Wolff, M. Motyl, C. Hellerbrand, J. Heilmann, B. Kraus, Xanthohumol uptake and intracellular kinetics in hepatocytes, hepatic stellate cells, and intestinal cells, J. Agric. Food Chem 59 (2011) 12893–12901.

In the study of Pang and co-workers [227] the absorption of XN was determined in Caco-2 monolayers. The permeability of XN was measured in two directions from the AP to BL and from the BL to AP. The permeability coefficient of XN was similar to that of the low permeability marker sucrose (AP to BL, XN $1.33 \pm 0.03\ 10^{-7}$ cm/s, sucrose $1.96 \pm 0.5\ 10^{-7}$ cm/s). After 1 h the amount of XN was 0.8 ± 0.1% of 10 µM on the acceptor side, from the AP to the BL direction at 37 °C. Interestingly, 73. 0 ± 2.3% of XN accumulated in the Caco-2 cells. Quantification showed that 94 ± 1.0% of the intracellular accumulated XN was located in the cytosol. In order to determine the time course of the XN uptake, Caco-2 cells were incubated with 10 µM XN at 37 °C for 10 min. During the first minutes, XN was fastly absorbed. After the XN concentration decreased in the donor side the absorption stagnated [227]. In the same study a XN uptake depending on the XN concentration in the surrounded medium and the temperature was observed. Thus, investigation was performed in order to determine the type of transport. The treatment with various transporter inhibitors revealed a non-facilitated and energy-independent transport. In addition during the incubation with the transporter inhibitors the XN uptake increased 2 to 3 fold compared to the uptake of XN in the medium. This implicates that under normal conditions XN is actively moved out of the Caco-2 cells. Efflux of drug and xenobiotics from cells is correlated with ABC-transporters (1.3 Bioavailability, metabolism and cell uptake). Lee et al. [189] showed an influence of XN on the mRNA levels of ABC-transporters [189]. Taur et al. [242] showed that XN as well as quercetin, naringenin and genistein reduced the transport of the P-glycoprotein and increased the cimetidine absorption but did not influence the cimetidin uptake on organic cation transporters [242]. In another study of Rodriguez-Proteau et al. [241] the influence of XN on the uptake of cyclosporine A and digoxin in Caco-2 and MDCKII cells was measured. There was a quite different behavior of XN on the uptake of the substances. The efflux of cyclosporine A was inhibited, but the intracellular concentration was decreased whilst the opposite was observed for digoxin [241].

It is known that XN interacts with proteins such as Keap 1 [137,139], NF-κB [176,182] and IKK [182], most likely via its α,β-unsaturated carbonyl structure that can react with thiols [137]. Thus, it seems not surprising that studies showed a bounding of XN to proteins. Pang et al. [227] determined the capability of XN to bind to isolated cytosolic native or denaturized proteins. XN bound 20 fold higher to native cytosolic proteins compared to the denatured proteins. This was confirmed by the observations of Wolff et al. [228] investigating the movement of XN with fluorescence recovery after photobleaching (FRAP). It was observed that XN moves like a heavier molecule with a mean size of 27 kDa. It seems that XN bound to proteins. After bleaching XN movement was not only detected in the cytosol but much more interesting in the nucleus, too [228]. This might explain the effect of XN on the regulation of transcription.

## 4.3 Aim

The exact uptake mechanism of XN is not fully understood yet. The uptake has to the best of our knowledge never been investigated in hepatic cancer cell lines and primary hepatocytes. In order to determine the amount of XN that is taken up per mg of cell proteins two hepatic cancer cell lines and primary hepatocytes were incubated with XN supplemented medium. Simultaneously calibration curves and cell volumes were determined in order to calculate the absorbed XN per cell.

## 4.4 Material

### 4.4.1 Chemicals

**Chemicals** Xanthohumol was provided by the Nookandeh Institut Hamburg with a purity of 98%. Ethanol (Order no. 8006) was bought from J.T. Baker (Deventer, Netherlands). Dimethyl sulfoxide (DMSO) (Order no. 1.02931.1000), sodium dodecyl sulfate (SDS) (Order no. 1.02931.1000), acetone (Order no. 1.00014.2511), formic acid (Order no. 1.00264.1000) and acetonitrile (Order no. 1.00030.2500) were purchased from Merck KGaA (Darmstadt, Germany). The Bradford reagent was obtained from Bio-Rad (Munich, Germany). Bovine serum albumin (BSA) (Order no. A-6003) was purchased from Sigma-Aldrich (Steinheim, Germany).
Deionized water (18 mS/cm) was obtained from Millipore Milli-Q UF Plus equipment.

### 4.4.2 Cell lines and culture materials

**Cell lines** The immortalized activated human hepatic stellate cell line (HSC) was obtained from University Hospital of Regensburg, Department of Internal Medicine I [212] The human hepatoma cell line (HepG2) (ATCC®-number HB-8065™) was obtained from the American Type Culture Collection (ATCC, USA). The human colorectal cell line (Caco-2) (ATCC®-number HTB-37™) was a gift from the Institute of Virology, Helmholtz Zentrum München, Germany. The human hepatoma cell line (HuH-7) (HSRRB-number JCRB0403) was obtained from the Health Science Research Resources Bank (HSRRB) of the Japan Health Sciences Foundation (JHSF, Japan).
Human liver tissue samples are obtained and experimental procedures were performed according to the guidelines of the charitable state controlled foundation HTCR (HUMAN

TISSUE AND CELL RESEARCH, Gemeinnützige Stiftung bürgerlichen Rechts), with the informed patient's consent. Isolation of primary human hepatocytes was carried out at the Center of Liver Cell Research, University Hospital of Regensburg.

**Medium and supplements** Dulbecco's modified eagle medium (DMEM) with phenol red (Order no. FG 0415), L-glutamine (Order no. K 0283), non essential amino acids 100 x (NEAA) (Order no. K 0293), fetal calf serum (FCS) (Order no. S 0115), phosphate buffered saline (PBS) (Order no. L 1825), sodium pyruvate 100 mM (SP) (Order no. L 0473) and trypsin 10 x (Order no. K 2135) were ordered from Biochrom AG (Berlin).

DMEM high glucose without phenol red (Order no. 41965) and DMEM high glucose with phenol red (Order no. 31053) were obtained from Invitrogen, GIBCO (Grand Island N.Y., U.S.A.).

**Material for cell culture** 96 well plates (Order no. 92096), cell scrapers (Order no. 99003), culture flasks 75 cm² (Order no. 90076) and 150 cm² (Order no. 90151) were purchased from TPP (Trasadingen, Switzerland), safe lock tubes 1.5 ml (Order no. 0030.102.002) and 2 ml (Order no. 0030 120.094) from Eppendorf (Hamburg) and centrifuge tubes 15 ml (Order no. 17020) from MEUS s.r.l. (Piove di Sacco, Italy).

## 4.5 Methods

### 4.5.1 FCS heat inactivation

FCS was inactivated in a water bath at 56 ℃ for 30 min. Then FCS was cooled down to room temperature, and portioned into 50 ml aliquots. The aliquots were stored at -20 ℃ until use.

### 4.5.2 Cell cultivation and harvesting

HSC, HuH-7 and Caco-2 were cultivated and harvested as described in chapter 3 (3.5.5 Cell cultivation and harvesting).

Primary hepatocytes (PH) were isolated in the Center of Liver Cell Research, University Hospital of Regensburg. $5 \times 10^6$ PH cells were seeded in 100 mm collagen coated BIOCOAT® culture dishes (Becton Dickinson labware, Bedfrod, MA, U.S.A.). The cells were cultivated as described in [296,297]. In Brief, the cells were for 24 h with and the next 24 h with FCS. After that the cells were incubated with XN to determine the XN uptake (4.5.3 Measurement of XN uptake).

### 4.5.3 Measurement of XN uptake

$6 \times 10^6$ HuH-7, $1 \times 10^6$ HSC or Caco-2 were seeded in Petri dishes d 100 x 20 mm in 6 ml DMEM with phenol red and were cultivated for 36 h. The medium of HuH-7, Caco-2, HSC and PH was aspirated and replaced with DMEM without phenol red supplemented with 10 µM XN for 3 h. The supplemented XN medium was aspirated and the cells were washed three times with 6 ml PBS. Subsequently, the cells were incubated with 1 ml trypsin (1 x in PBS) for approximately 4 min at 37 °C. After carefu lly beating at the underside of the culture flask wall, cells were detached from the bottom of the culture flask. 5 ml medium were added to the trypsin cell suspension to stop the trypsination. The suspension was transferred into centrifuge tubes and was centrifuged at 700 rpm for 5 min. The supernatant was discarded and the cell pellet was resuspended in 5 ml PBS. 80 µl of the resuspended PBS suspension were taken and homogenized with 50 µl glas beads (0.75-1.0 mm). After the homogenization one equivalent amount (v/v) of acetone was added. The homogenized cells were spin down at 1,000 rpm for 4 min at 4 °C. After the centrifug ation step, the supernatant was transferred in NanoSep centrifugal devices (catalog no. 5168502, VWR, Darmstadt, Germany) and were centrifuged at 14,800 rpm and 4 °C for 20 min. Subs equently, the purified solution was analyzed by HPLC.

### 4.5.4 Quantification of XN

Quantification of XN was performed with a LaChrom Elite system (Hitachi) equipped with a Purosphere® Star RP-18e column (5 µm 250 x 4 mm) column with a precolumn (LiChroCART 4-4). The HPLC system (VWR Hitachi, Breda Netherlands) was composed of an organizer Elite Lachrom, diode array detector L-2455, autosampler L-2200, pump L-2130 and a column oven L-2350. The mobile phase A consisted of water with 0.1% formic acid and B of pure acetonitrile. The detachment of 20 µl sample was performed with a flow rate of 1 ml/min and a column oven temperature of 30 °C. In order to separate and to quantify the XN amount, the following gradient course was used: 0-9 min, 35-65% B; 9-11 min, 65%-35% B. After 11 min the column was equilibrated to 35% B.

The quantification was performed with DAD at a wavelength of 368 nm. A calibration range of 0.1-100.0 µM; typical retention time for XN was 10.7 min. Calibration curves for the quantification of XN were measured with 11 different concentrations (n=6 for every concentration) resulting in a $R^2$ of 0.9999.

### 4.5.5 Determination of protein content per cell

In order to determine the protein amount per cell, cells were treated as described in 4.5.3 Quantification of XN. In contrast to the determination of the uptake, the cells were not stimulated with XN.

After 3 h the cells were harvested and the cell count as well as the protein amount was determined. The cell count was determined as described in 3.5.6 Cell counting. The protein amount was determined with the Bradford reagent. In order to develop a BSA calibration curve, 10 mg/ml BSA were weighed out and were dissolved in PBS. The BSA calibration curve was performed in serial dilution with 6 concentrations, 1.0, 0.75, 0.5, 0.25, 0.125 and 0 mg/ml BSA solved in PBS. The measurement was performed in a 96 well plate. 2.5 µl of the BSA solution was added to 125.5 µl Bradford reagent. After 5 min the absorption was measured with a microplate reader SpectraFluor Plus (TECAN, Hombrechtikon, Switzerland) at 590 nm.

### 4.5.6 Determination of the cell volumes

The cell volumes were determined as described by Wolff et al. [228].

### 4.5.7 Calculation and statistical analysis

The statistical analysis and the calculation of results were performed with Graph Pad Prism 4. Significant different averages ($p$ value $< 0.05$) were evaluated statistically with one-way ANOVA followed by Tukey's Multiple Comparison Post Test. The results are expressed as mean ± standard deviation. The test according to Grubbs was applied to remove outliers.

## 4.6 Results

At first the XN uptake per mg protein was determined in HuH-7, HSC, Caco-2 and PH cells. The highest XN uptake was found in HSC and Caco-2 cells, followed by PH and HuH-7 (Table 4-1). The uptake measurements were performed in 9, 8, 6 and 2 independent experiments for HSC, HuH-7, Caco-2 and PH cells respectively.

**Table 4-1: The XN uptake in HuH-7, HSC, Caco-2 and PH cells. Data are shown as mean ± SD. The concentration of XN was determined per cell and per protein content. In order to determine the concentration per cell the cell volume was measured with a fluorescent microscope as it is described in the paper of Wolff et al. [228].**

| | Cell type | | | |
|---|---|---|---|---|
| | HuH-7 | HSC | Caco-2 | Primary hepatocytes |
| XN per cell (pg/cell) | 0.03 ± 0.02 | 0.83 ± 0.22 | 0.72 ± 0.13 | 0.39 ± 0.26 |
| XN per protein (µg/mg) | 0.21 ± 0.18 | 1.49 ± 0.39 | 2.13 ± 0.38 | 0.56 ± 0.07 |
| Cell volume (pL) | 3.53 ± 0.84 | 4.88 ± 1.42 | 4.25 ± 2.39 | 2.04 ± 0.27 |
| XN per cell (µM) | 25 ± 6 | 511 ± 132 | 625 ± 132 | 469 ± 149 |
| approximated accumulation (fold) | 3 | 52 | 63 | 47 |

In order to determine the XN concentration per cell calibration curves for the protein content were recorded. The calibration curves describe the correlation between the protein content and the cell number allowing the determination of the average protein content per cell (see Figure 4-1). The HSC (**A**) contained the most protein per cell followed by Caco-2 (**A**) and HuH-7 (**B**) cells (see Figure 4-1). A calibration curve for the PH could not been generated, because of the different protein amounts per cell. The amount of XN per PH cells was determined directly. After the harvesting of the PH cells the cell count as well as the protein concentration was determined. The HuH-7, HSC and Caco-2 calibration curves were prepared with data of at least 3 independent measurements.

**A** HSC, Caco-2

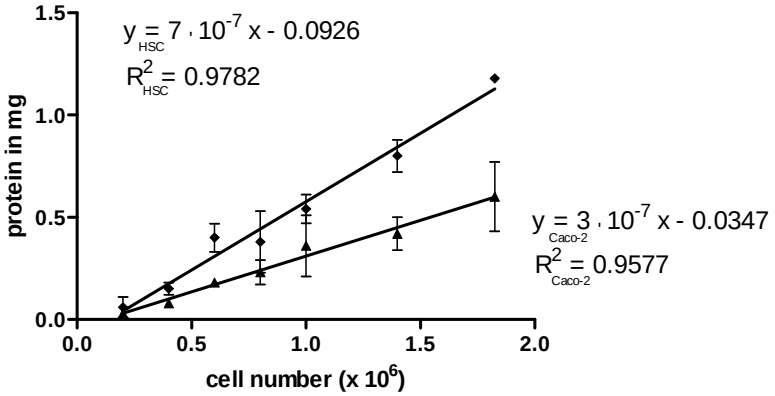


**B** HuH-7

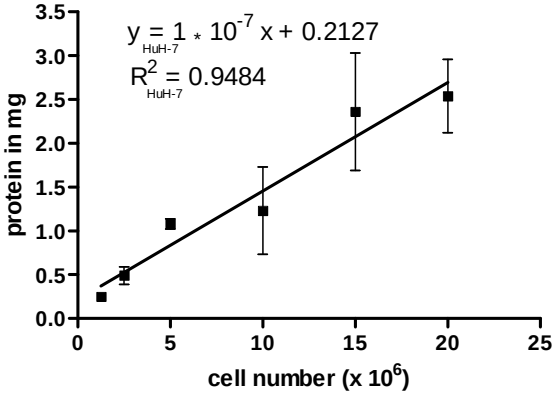


**Figure 4-1: Correlation of protein content with the cell number for HSC, Caco-2 (A) and HuH-7 cells (B).**

The coefficient between cell number and protein content was between 0.9484 and 0.9782. HSC which have the highest ratio between protein amount and cell count exhibit the best correlation coefficient (0.9782).

The cell volume was determined by fluorescence microscopy as it is described in the paper of Wolff et al. [228]. The XN concentration even for single cells could be calculated. For the uptake investigations the cell lines and the PH´s were incubated with 10 µM XN in DMEM for 3 h. HuH-7 cells exhibited a concentration of 25 ± 6 µM XN and were the weakest uptaker. HSC, Caco-2 and PH cells accumulated 52, 63 and 47 fold higher XN concentrations compared to the medium (see Figure 4-2).

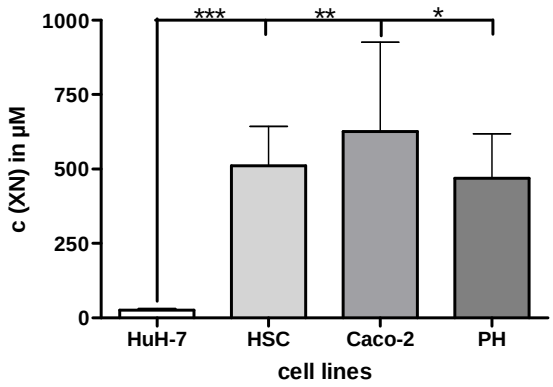


**Figure 4-2: XN uptake in HuH-7, HSC, Caco-2 and PH cells in µM. The cells were incubated with 10 µM XN in DMEM for 3 h. HuH-7 was the weakest uptaker. HuH-7 cells exhibited 3 fold higher XN concentrations if compared to the outer medium. HSC, Caco-2 and PH exhibited 47 to 63 fold higher XN concentrations. The XN uptake was determined in 9, 8, 6 and 2 independent experiments for HuH-7, HSC, Caco-2 and PHs respectively.**

The uptake of XN in HuH-7 differs significantly from that of HSC, Caco-2 and PH. No significantly different intracellular XN concentration was observed comparing the HSC, Caco-2 and PH.

## 4.7 Discussion

In order to determine the amount of XN that was taken up per cell and protein, cell volumes and protein contents of the different cell lines were determined. HuH-7 had the lowest protein amounts per cell and HSC the highest. Because the protein amount per cell differs depending on the patients, no average protein content per cell was determined for the PH.

The XN concentration per cell was determined using the cell volume [228]. The measurements revealed a weaker XN uptake in HuH-7 cells. HSC, Caco-2 and PH exhibited a 52, 63 and 47 fold higher XN concentration compared to the XN concentration in the medium. HuH-7 cells exhibited only a 3 fold higher XN concentration compared to the medium.

The reason for different XN up-take is most likely the varying density and type of ABC-transporters in HuH-7 cells compared to HSC, Caco-2 and PH. For example the uptake of cyclosporine A in co-stimulation with XN was found to differ in Caco-2 and MDCKII-MDR cell lines. MDCKII-MDR cells took up cyclosporine in a dose dependent manner. In Caco-2 cells the cyclosporine A uptake decreased in case of co-incubation with XN [241]. A stronger activation and different types or densities of ABC-transporters might lead to a higher efflux of XN out of HuH-7 cells. Furthermore, studies also revealed that XN influences the mRNA values of multidrug proteins [189] and the efflux of cimetidine by P-glycoproteins [242]. The

effects of XN on ABC-transporter seem to be complex and are not fully investigated yet. Another reason for the different XN uptake in HuH-7 cells might be the existence of other transporters which are involved in the XN uptake. Pang et al. [227] incubated Caco-2 cell with transporter inhibitors such as dipyramidamole, sodium azide, oligomycin and rotenone. The experiment revealed an increased uptake of XN [227].

The lower XN uptake might also be the cause of a higher metabolism of XN in HuH-7. It is known that XN is metabolized in high quantities. However in this study this was rather not the case. The quantification of XN was performed by HPLC (4.5.3 Measurement of XN). This method had the advantage that metabolites with similar chromophor could be detected. As phase II metabolites are more hydrophilic compared to their precursor they eluted earlier on a reversed phase column. But at early retention times the chromatograms of the extracts of HuH-7 did not differ from the ones of the HSC.

Uptake and movement studies showed that XN binds to proteins [227,228]. Wolff et al. [228] showed with FRAP measurements that XN moved slowly in the cell such as a molecule with a mean size of 27 kDa. In another study it was shown that XN bound rather to native cytosolic proteins (94%) than to cellular membranes or organelles, with sizes bigger than 10 kDa [227]. HuH-7 showed a lower amount of proteins per cell compared to HSC and Caco-2. If the protein amount per cell is lower, XN is possibly faster excreted via higher efflux and absorbed in smaller quantities.

## 4.8 Summary

This study revealed that hepatic cancer cell lines as well as primary hepatic cells absorb XN in high concentrations. But there was a clear dependency on the cell type. HuH-7 cells exhibited only 3 fold higher intracellular concentrations of XN compared to the medium. This might have different reasons such as different ABC-transporters, other protein amounts per cell and different transporter densities, but the clear mechanism of XN´s uptake is not known, yet. The understanding of the uptake mechanism might lead to new approaches to increase the bioavailability of XN and structure related compounds. Moreover, a thorough investigation could explain whether a XN metabolite is able to reach his target in humans compared to his precursor.

# 5 Influence of dose and phenolic congeners on absorption and distribution of the hop chalcone xanthohumol after oral application in mice [3)]

## 5.1 Abstract

Hop cones contain several structurally related chalcones with xanthohumol (XN) being the most abundant. We elucidated the dose dependent absorption of XN in mice after oral application with regard to its phase II metabolism and its distribution in serum, liver, urine, bile and feces. A matrix effect on the absorption of XN was addressed by feeding pure XN in comparison to a phenolic hop extract highly enriched with XN.

Application of 0.5% XN in diet for 3 and 7 days resulted in biologically relevant concentrations of XN phase II metabolites in all excretes and investigated tissues. The concentrations of XN phase II metabolites in serum did not show a linear relationship to dose, as escalating plasma levels were observed with highly enriched XN diet (0.5%). Results showed a high concentration of XN conjugates in bile and pointed to a possible relevance of the entero-hepatic circulation. Feeding of a XN enriched phenolic extract derived from hops (XE) showed that absorption of XN is positively influenced by its congeners. HPLC-HRMS analysis revealed the presence of several minor chalcones and flavanones in the XN enriched extract.

Data indicate that phase II metabolites are the biologically relevant compounds after oral consumption of XN. For the use of XN as a functional nutrient application of a standardized extract is recommended instead of pure compound.

## 5.2 Introduction

Since the Middle Ages the female inflorescences (cones) of the plant (*Humulus lupulus* L. Cannabaceae) have been an essential ingredient in beer brewing, and about 95% of worldwide cultivated hop is used for brewing purposes with the rest largely utilized for the production of phytomedicines and dietary supplements [298]. There are basically three classes of secondary metabolites present in hop cones: prenylated acylphloroglucinols

[3)] M.Motyl, C. Dorn, B. Kraus, M. Gehring, C. Hellerbrand, and J. Heilmann, Influence of dose and phenolic congeners on absorption and distribution of the hop chalcone xanthohumol after oral application in mice – manuscript in preparation

(so-called bitter acids) represented by e. g. humulon and lupulon, essential oil components and phenolic compounds with xanthohumol (XN, Figure 5-1) being the most abundant prenylated chalcone in hops.

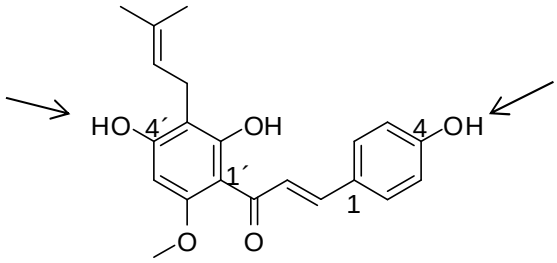


**Figure 5-1: Structure of xanthohumol (XN); observed glucuronidation and sulphatation positions are indicated with arrows.**

Recently much attention has been paid to the polyphenolic content of hops, and especially, XN has been identified as a compound with multiple biological activities [299]. Limited availability of the more than 10 minor chalcones like demethylxanthohumol or xanthohumol C which occur at 5-1,000 fold lower concentration relative to XN [82] resulted in less pharmacological information on these compounds [150,151]. Most of the chalcones contain a free 2`-hydroxy group, and thus, also the corresponding flavanones like isoxanthohumol, 6-prenylnaringenin and 8-prenylnaringenin are present in hop cones, extract and beer [82]. Of special importance is the conversion of XN to the flavanone isoxanthohumol during the brewing process [9] making isoxanthohumol the quantitatively predominating prenylated flavonoid in beer. Furthermore, hops contain significant amounts of flavonol glycosides and proanthocyanidines [300,301].

The bad solubility of XN in aqueous solutions together with the conversion into isoxanthohumol results in relatively low contents in beer. For example, Stevens et al. reported on XN contents ranging from 0.009 to 0.69 mg/l [84]. Nevertheless, XN is a pharmacologically extremely interesting compound mainly due to its reported chemopreventive and anti-cancer activity [36,169] and thus a candidate of product development in the functional food domain. Several *in vitro* studies have been done on the metabolism of XN using microorganisms [232] and liver microsomes [160], leading to the identification of a couple of phase I metabolites like 3-hydroxyxanthohumol and xanthohumol H. Furthermore, the production of xanthohumol-4-O-glucuronide and xanthohumol-4´-O-glucuronide as phase II metabolites and the conversion to isoxanthohumol have also been reported *in vitro* and *in vivo* [159,233]. Very recently, the role of human intestinal bacteria on the *in vivo* metabolism of XN has been addressed in germ-free and human microbiota-associated rats by Hanske et al. [236].

Still, little is known about the *in vivo* absorption and metabolism of XN, particularly after oral administration. A previous study in rats indicated that the bioavailability of XN is low. Avula et al. determined the XN concentration in rat plasma, urine and fecal samples after a single i.v. or oral application of pure XN [224]. Choosing a HPLC method with a detection limit of 0.013 µg/ml, XN was not detectable in urine and feces. The authors also addressed the matrix effect no absorption by feeding one rat with hop extract containing either 20 or 50 mg/g XN, but no difference was observed between application of pure XN and the hop extract. However, the authors did not investigate phase II metabolites by direct quantification of the glucuronides and sulphates or indirect quantification *via* addition of glucuronidases and sulphatases and subsequent determination of entire XN. Furthermore, several studies in flavonoids can be strongly source dependent and both are often significantly different comparing various extracts or the application of a pure compound with a food product (e.g. vegetables, fruits and beverages) containing the same amount accompanied by other secondary metabolites [302–304] reviewed in [305]. The plasma levels of flavonols and their phase II metabolites are sometimes reported to be lower after application of the pure compound in comparison to the applied food product [303,305]. As the epidemiological impact of flavonols in the diet (especially in the case of quercetin glucosides) is supposed to be very high, studies on absorption and metabolism focused in the last years on the consumption of flavonols from several edibles and not on the application of pure compounds [305,306].

## 5.3 Aim

The aim of our study was to elucidate the absorption of XN with regard to its distribution in liver, urine, bile, feces and serum, its phase II metabolism, as well as to investigate the influence of other hop phenolics on the absorption and metabolism of XN. To find the optimal dose for the feeding experiments, different concentrations of a XN enriched phenolic hop extract (73%, XE) were mixed with the diet to yield 0.05, 0.25 and 0.5% of XN and fed to BALB/c mice. To evaluate the influence of a short time as well as a more continuous polyphenol intake on metabolism and absorption, mice were fed for 3 and 7 days with XE, and the resulting concentration of XN and its quantification before and after addition of glucuronidase and sulphatase. To investigate a possible effect of phenolic congeners on the absorption, also pure XN (>98%) was mixed with the diet in the most applicable concentration of XN and its metabolites in liver, serum, bile and feces were also measured after 3 and 7 days in comparison to the respective extract group.

## 5.4 Material and Methods

### 5.4.1 Chemicals

Glucuronidase (bovine liver, Type B-10, G0501) and sulphatase (from *Helix pomatia*, Type H-1 S9626) were obtained from Sigma-Aldrich (Deisenhofen/St. Louis, MO, USA). XN was from Alexis Biochemicals (Lausen, Switzerland) or from Nookandeh Institute (Homburg/Saar, Germany) with a purity $\geq$ 98%, determined by HPLC.

XN-enriched phenolic hop extract (XE) was a gift from NATECO$_2$ (Wolnzach, Germany) and contained 73% XN determined by HPLC with UV detection. The extract was obtained after extraction of dried hop cones with supercritical $CO_2$ (300 bar, 50-60 °C) to remove the essential oil and the bitter acids. After wards the residue was extracted again with supercritical $CO_2$ (600-900 bar, 60-90 °C) to obtain a polyphenolic e xtract with 10-30 °C XN content. Further enrichment of XN and polyphenols resulted from pH-dependent precipitation and filtration of the associated compounds. Data sheet on extract information can be obtained via NATECO$_2$. For better characterization of the secondary metabolite spectrum in XE, the extract was fractionated on Sephadex LH-20 (MeOH) and resulting fractions were analyzed by TLC, HPLC-DAD and HPLC-HRMS (Figure 5-8: HPLC chromatogram of fraction 8. Solvent A: 5 mM $NH_4OOCH$, solvent B: acetonitrile/water 95/5; column: Purospher® Star RP-18e (size: 250 x 4.0, particle size: 5 µm); flow: 0.8; 0-15 min 40 to 100% B, 15-22 min 100% B; detection wavelength: 368 nm.Figure 5-7, Figure 5-8, Figure 5-9). Analysis revealed the presence of several hydroxyl cinnamic acids, prenylated chalcones and flavanols according [307].

### 5.4.2 Animals, animal treatment and sample asservation

Female BALB/c mice were purchased from Charles River Laboratories (Sulzfeld, Germany) at 6 weeks of age and housed in a 22 °C controlled room under a 12 h light-dark cycle with free access to food and water. After 1 week of acclimatization, mice were divided into different groups (4-5 mice per group). The groups were fed for 3 and 7 days either with a diet supplemented with three different concentrations of XE leading to a 0.05, 0.25 and 0.5% (w/w) content of XN or supplemented with an equivalent dose of pure XN (0.5%), Afterwards the 0.5% content diets were fed in the main experiment to a second group (8-10 mice) for both XE and pure XN under the same conditions. Both chows were prepared by Ssniff (Soest, Germany) and are based on the Ssniff® R/M-H chow (Cat. V1534-0). At the end of the experimental time, mice were killed by heart puncture under ketamine/xylazine (2:1) anaesthesia, and blood samples and organs were collected for further analyses. Liver tissue

sections were frozen in liquid nitrogen immediately after organ explantation and stored at -80 ℃. For serum analysis, blood was centrifuged at 2,000 g to remove cellular components. Serum (supernatant) was used immediately for further analysis or stored at -80 ℃- As 4-5 (8-10 in the second experiment) mice lived in one cage, the feces was first pooled and than divided into 4-5 (8-10) samples to generate in overall average for each group in a cage. Urine and bile were collected by puncture of the bladder and gall bladder, respectively, under deep anaesthesia, and stored at -80 ℃ until processing for further analysis.

### 5.4.3 Sample preparation

For HPLC analysis of XN content in liver, tissue samples (~200 mg) were thoroughly homogenized in 800 µl of 2 M sodium acetate buffer (pH 4.7) containing 10 mg/ml ascorbic acid at 4 ℃ using a MICCRA D1 homogenizer (ART Prozess- & Labortechnik GmbH & Co. KG, Müllheim, Germany). Afterwards the samples were homogenized with an ultrasonic homogenized in 1 ml buffer. Urine (5 µl) and bile [5 µl, pooled from 5 (8-10) animals of one cage as one gives not enough volume for sample preparation] samples were diluted with buffer to 25 µl. Serum (45 µl) samples were used undiluted. For enzymatic hydrolysis of conjugated XN-metabolites an aliquot of the samples were spiked with an equivalent volume of sodium acetate buffer containing β-glucutonidase and sulphatase). Resulting sample were incubated in sealed vials for 3 h at 37 ℃ with continuous shaking (400 rpm). After addition of an equivalent amount (v/v) of acetone the processed samples were vortexed and centrifugated at 20,000 x g; 4 ℃) using NanoSep centrifugal devices (Cat. 5168502 VWR, Darmstadt, Germany). Recovery of XN in the samples was reproducible and at 90-105% (Table 5-1).

### 5.4.4 Analytical methods

Quantification of XN was done by HPLC in analogy to [230]. The analytical HPLC system consisted of an Elite LaChrom system (VWR-Hitachi, Germany) equipped with a L-2455 diode array detector, a thermostated L-2200 autosampler, a L-2130 pump and a L-2350 column oven. A Purospher® Star RP-18e (column size: 250 x 4.0, particle size: 5 µm, Merck, Darmstadt, Germany) was used as column. Detection wavelength was 368 nm. The eluents were water/0.1% formic acid (A) and acetonitrile (95/5, B). The injection volume of the sample was 20 µl and the following elution-program was used with a flow rate of 1.0 ml per min (at 30 ℃): 0-9 min 57.8%-68.2% B, 9-14 min up to 100% B and equilibration to 57.8%. Typical retention time for XN was 11.0 min. Calibration curves for the quantification of XN were measured with 11 different concentrations (n=6 for every concentration) resulting in a

$R^2$ of 0.9999. For validation of the extraction process raw samples of the used tissues and excretes were spiked with different XN concentrations and extracted. Performance parameters of the method (e. g. LOD, LOQ and recovery) are given in Table 5-1.

### 5.4.5 Statistical analysis

Values are presented as means ± SD. Comparison between groups was made using ANOVA, followed by Tukey´s Multiple Comparison Test as post test. A $p$ value < 0.05 was considered statistically significant. For elimination of outliers the test according to Grubbs was applied. All calculations were performed using GraphPad Prism 4.

## 5.5 Results and Discussion

To obtain valid information concerning the concentrations of unconjugated XN as well as of its phase II metabolites the concentration of XN with and without supplements of β-glucuronidase and sulphatase was determined. We started with the method of Wang and Morris [308], developed for the quantification of quercetin conjugates, to optimize the deconjugation process. Experiments with random liver and serum samples resulted in a β-glucuronidase concentration of 10 U/µl, a sulphatase concentration of 1 U/µl and an incubation time to 3 h to guarantee a quantitative hydrolysis of the conjugated compounds and a uniform working procedure (Figure 5-2). A further increase of the enzyme concentrations or incubation time respectively did not result in higher deconjugation efficiency of XN (Figure 5-2). Legette et al. [225] also used the same time (3 h) and temperature (37 °C) for the deconjugation process.

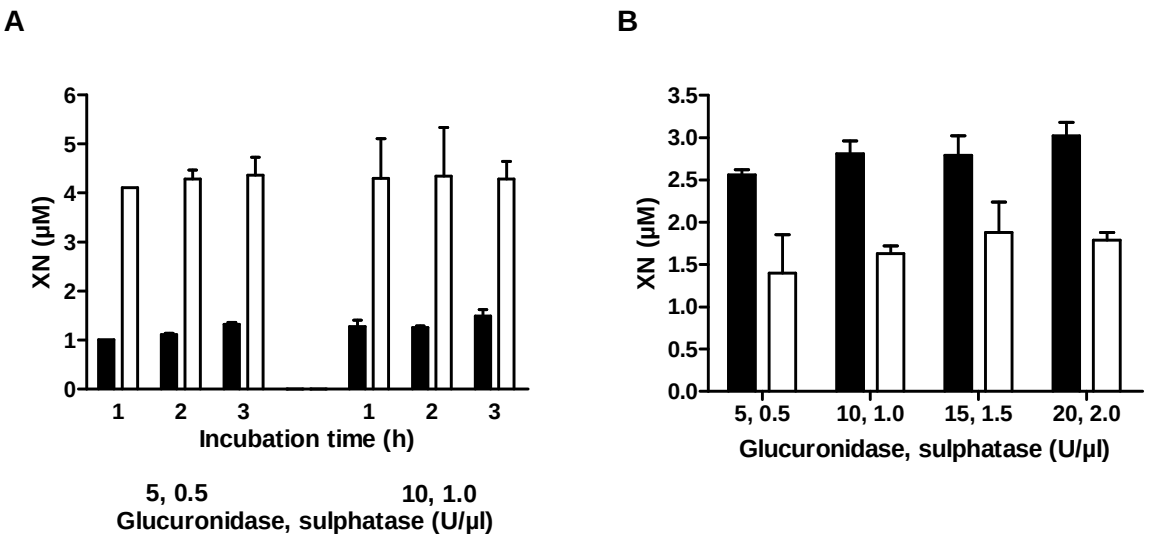


**Figure 5-2: Hydrolysis of the conjugated XN metabolites by β-glucuronidase and sulphatase. Optimization of incubation time and enzyme concentration in random liver (black column) and serum (white columns) samples. A XN concentration depending on the incubation time (1, 2 and 3 h) for two different enzyme activities (glucuronidase/sulphatase activity: 5/0.5 and 10/1 U/µl). B XN concentration depending on the variation of enzyme activity at a constant incubation time of 3 h (glucuronidase/sulphatase 5/ 0.5, 10/1; 15/1.5, 20/2.0 U/µl). Values are expressed as mean ± SD from 3 different experiments.**

For further work it was necessary to determine the recovery rate of the external standard XN in the sample matrix. In doing so the target was to reach a low LOD and LOQ and to achieve a recovery of ± 10%. Blank serum, urine, bile, feces and tissue like liver were used to spike XN into the samples and to determine the LOD, LOQ, and the recovery. In addition the coefficient of the determination ($R^2$) was calculated. The results are summarized in Table 5-1.

**Table 5-1 Performance parameters of the HPLC method for the quantification of xanthohumol (XN)**

| Tissue/excretion | LOD (µM) | LOQ (µM) | Recovery (%) | Calibration range recovery (µM) | $R^2$ (calibration line) |
|---|---|---|---|---|---|
| | 0.006* | 0.02* | | | 0.9999 |
| Serum | | | 90-112 | 2.5-25 | 0.9971 |
| Liver | | | 92-105 | 0.31-59 | 0.9999 |
| Urine | | | 90-108 | 0.08-270 | 0.9986 |
| Bile | | | 89-94 | 1.25-1000 | 0.9991 |
| Feces | | | 88-112 | 6.25-313 | 0.9954 |

*Calibration range: 0.001-3 µM

$R^2$ was between 0.9954 and 0.9999. It should be noted that the calibration curve, depending on the sample matrix, is processed over a range of 0.08 µM to 1000 µM. The recovery rate

was ± 12%. Avula et al. [224] reached a LOD of 0.04 µM and a LOQ of 0.1 µg/ml using methanol for the sample extraction. In this study we showed that using methanol as the extraction solvent only a 50% recovery of XN could be reached (Figure 5-3). Avula et al. [224] determined a recovery rate of 98.5%. Unfortunately, it is not clear if this result was obtained for all calibration points. In the study of Legette et al. [225] the relative standard deviation was 12% or better, the accuracy was between 90% and 110% and the LOQ 0.4-0.5 nM. In their study the XN quantification was performed with MS. For this reason the LOQ is lower than the one obtained in this study.

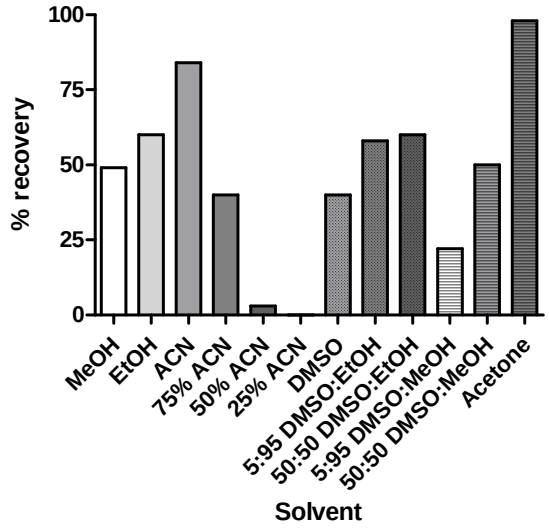


**Figure 5-3: Sample extraction**

The poor solubility of XN in aqueous solutions prompted us to supplement the diet and not the water with XN and XE, respectively. XN content in diet samples was analyzed by HPLC to ensure a sufficient stability as well as a homogenous XN distribution during the chow preparation (data not shown). Mice were fed for 3 and 7 days with different concentrations of XE (0.05, 0.25 and 0.5% XN) in the chow. Food consumption did not vary significantly between the different experimental groups, and in line with our previous safety study on XN no signs if toxicity were observable in the mice with the highest XE/XN concentration used [222]. Feeding of different concentrations of XE did neither after 3 nor after 7 days led to a linear increase of the serum and urine concentrations of XN or its conjugated metabolites (Figure 5-4).

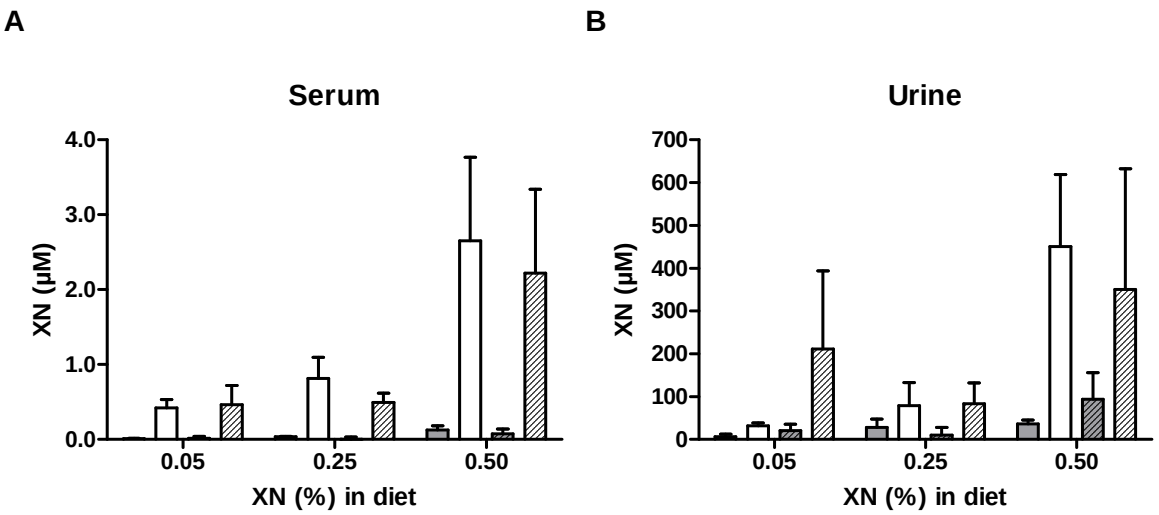


**Figure 5-4: Concentration of conjugated (white columns) and unconjugated (grey columns) XN in A serum and B urine after feeding of diet enriched XE equivalent to 0.05, 0.25 and 0.5% (w/w) XN for 3 (plain columns) and 7 (shaded columns) days. Values are expressed as mean ± SD obtained from 4-5 animals in each group.**

For example, after 7 days serum levels of conjugated XN in the 0.25% group reached 0.5 ± 0.1 µM in comparison to 2.2 ± 0.9 µM in the 0.5% group. Thus, the highest concentration applied led to an over proportional increase of the serum and urine XN levels. A similar trend was observed by Legette et al. [225]. However no further body fluids or tissues were investigated. Interestingly, they gavaged the feed in liquid form which led to a similar pattern of XN in the sera. However to the best of our knowledge the distribution of XN in the urine, bile, feces as well as the liver after oral ingestion of chow was not investigated so far.

The comparability and reproducibility of *in vivo* studies concerning the bioavailability of further chalcones should be supported by the realization of a pilot experiment to evaluate the dose dependent absorption behavior of the respective compound. Interestingly, several studies on the bioavailability of other more widespread polyphenols did not address this problem as only a single dose was applied. The existing data concerning the dose-dependent investigation of flavonoid bioavailability point to the fact that there is a dose-dependent absorption for the main flavonols, but probably heterogeneous absorption behavior among the different classes of polyphenols. Egert et al. [309] reported on a dose dependent increase of quercetin concentration in plasma, and Barve et al. [310] found the same for orally administered kaempferol. However, for the main tea catechin epigallocatechin-3-O-gallate (EPCG) a linear dose relationship to the plasma concentration is only observable for lower dosing, whereas higher doses resulted in a dose-independent plateau of EPCG plasma level [311]. Furthermore, Ullmann et al. [312] reported in line with our results on XN a dose escalating effect for the plasma levels of EPCG after repeated

application of higher EPCG doses. Based in the food intake the daily intake of XN in mice fed with 0.05, 0.25 and 0.5% diet can be translated to approximately 100, 500 and 1000 mg/kg body weight, respectively [222].

Mechanistically, a variation of XN absorption depending on the applied dose and escalating plasma levels with the highest XN concentration dependent transport mechanisms. In contrast to the report of Avula et al. [224] detectable concentrations of free, unmetabolized XN were present not only in the urine, but also in serum in our setup. This can be likely explained by the continuous XN intake over several days or the higher dose of XN used, whereas Avula and colleagues investigated a single dose design. Furthermore, the extraction of biological samples with MeOH chosen in [224] is not suitable to recover low concentration of XN quantitatively (Figure 5-1). Nevertheless, also in our study the concentration of free XN in serum was very low and did not exceed 1 µM in all groups. Interestingly, in contrast to the phase II metabolites the concentrations of free XN in serum did not significantly increase with the time or a higher dose of applied XN (Figure 5-4, Figure 5-5).

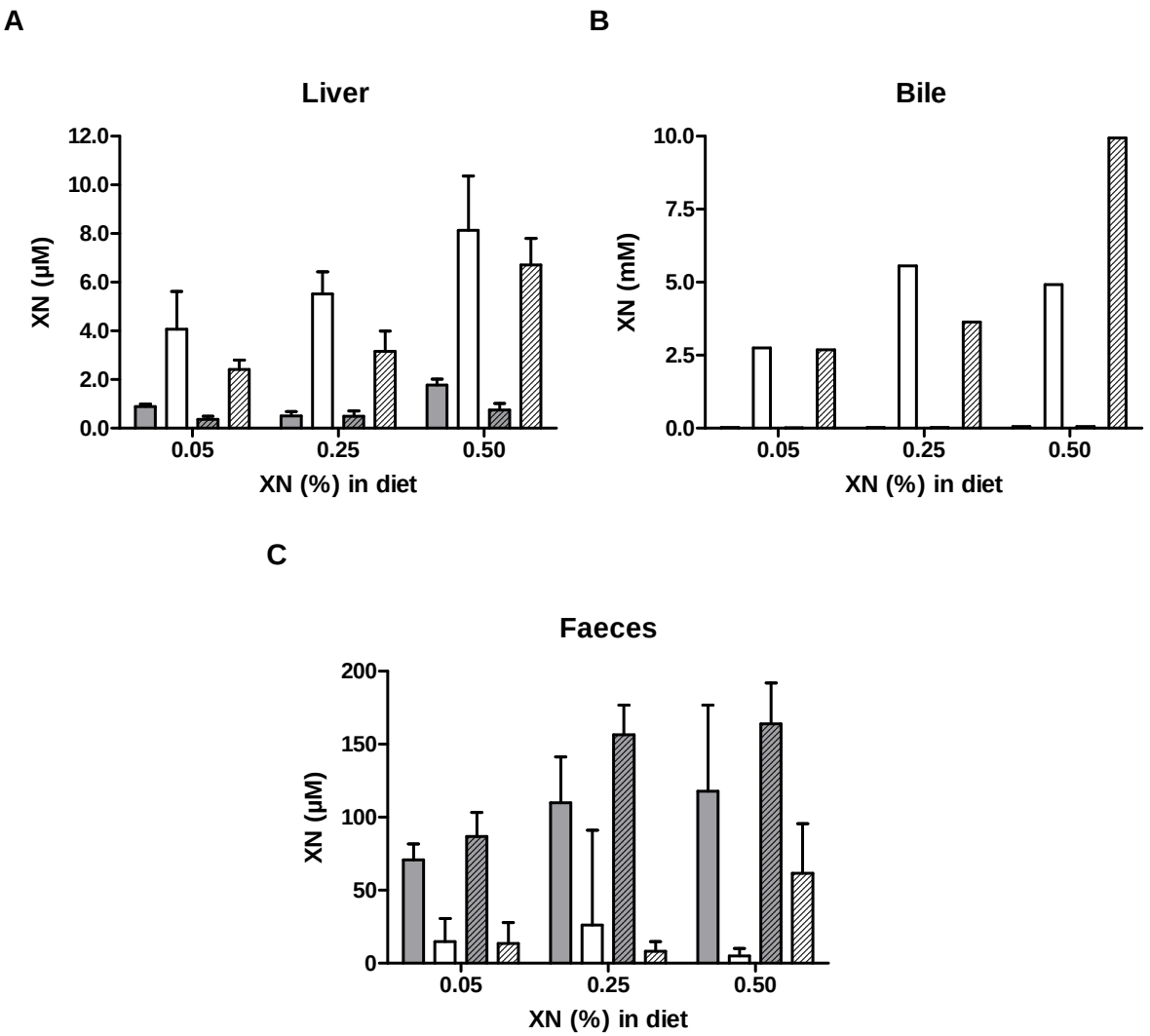


**Figure 5-5: Concentration of conjugated (white columns) and unconjugates (grey columns XN in A liver, B bile and C feces after feeding of diet enriched with XE equivalent to 0.05, 0.25 and 0.5% (w/w) XN for 3 (plain columns) and 7 (shaded columns) days. Values are expressed as mean ± SD obtained from 4-5 animals in each group. As the bile value resulted from a pooled sample no standard deviation is given.**

Figure 5-5 shows the amount of pure XN and XN metabolites present in liver and bile after 3 and 7 days feeding of XE at different concentrations. In all groups hepatic concentrations of conjugated XN were found to be significantly higher than corresponding serum concentrations as we found that the bile is highly enriched with XN containing mmolar concentrations. In line with serum and urine concentrations of XN and its phase II metabolites in liver and bile did not linearly increase with higher intake of XN. An enrichment of XN-conjugates in liver was observable for all groups irrespective of the time span of XN intake and increase with higher XN content in the diet (Figure 5-6 A). A comparison of the 3 and 7 days groups revealed a remarkable decrease of conjugated XN after linger application of XE (e. g. containing 0.5% XN from 8.1 ± 2.2 µM to 6.7 ± 2.4 µM). This result was confirmed with statistical significance in the second experimental setup comparing the

application of 0.5% XN in the XE group (Figure 5-6 C, 11.5 ± 2.3 µM in the 3 days group vs. 5.6 ± 1.6 µM in the 7 days group) with the 0.5% pure XN group.

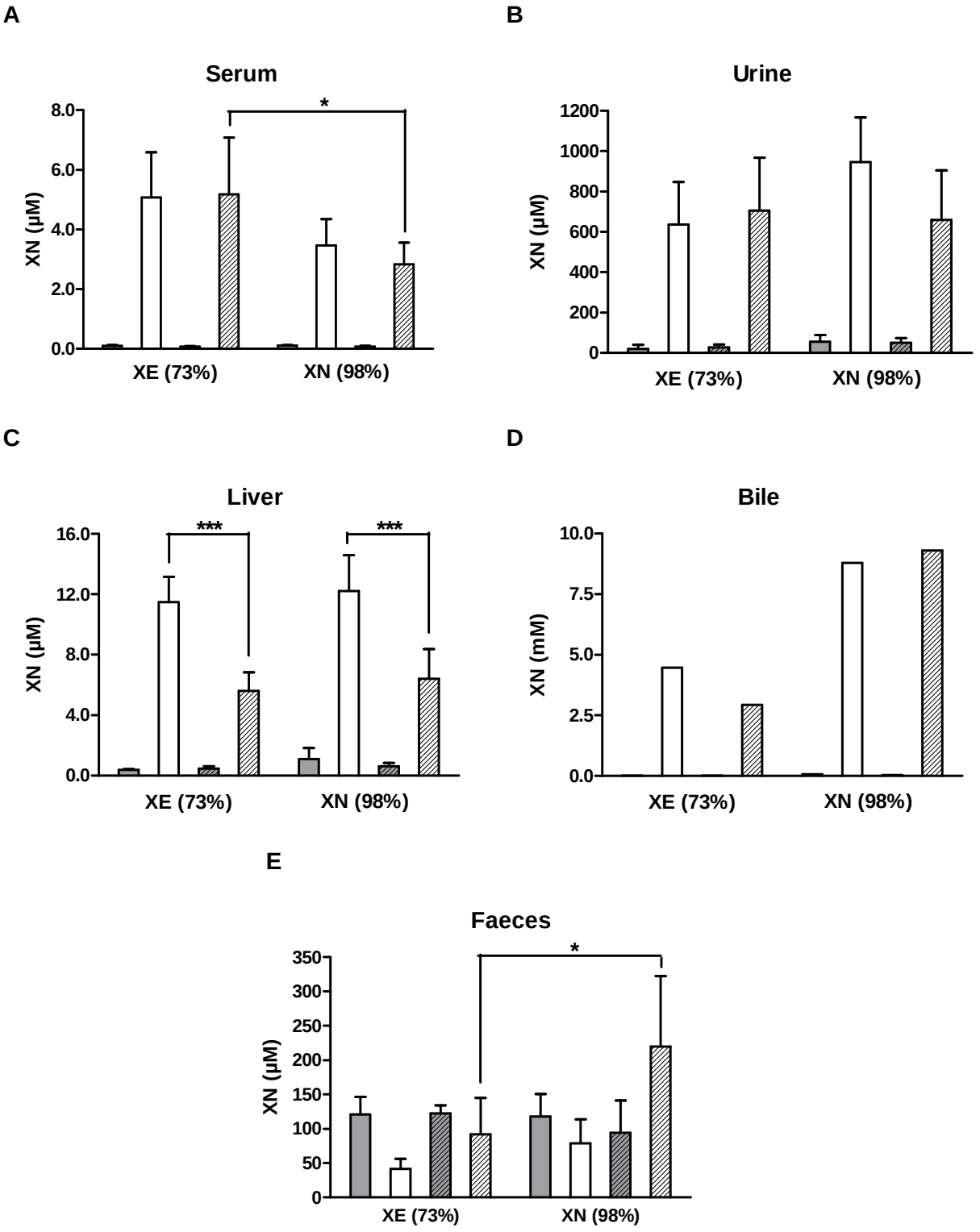


**Figure 5-6: Concentration of conjugated (white columns) and unconjugated (grey columns) XN in A serum, B urine, C liver, D bile after feeding of diet enriched with 0.5% (w/w) pure XN or XN in XN in XE for 3 (plain columns) and 7 (shaded columns) days. Values are expressed as mean ± SD obtained from 8-10 animals in each group. Bile is given without SD as it was pooled from all animals due to the low volume. * Significant on the $p < 0.05$ level, ***significant on the $p < 0.001$ level.**

In the bile the enrichment of XN-conjugates was more heterogeneous (Figure 5-5 B). For animals fed with 0.05% XN there is no significant difference between the 3 and the 7 days group. In the case of the 0.25 and 0.5% groups we observed some differences depending on the feeding time, however, results are not conclusive. Further, as compared to serum, urine and hepatic tissue concentration of conjugated XN in bile showed a quite high variation of XN in the two 7 days groups (Figure 5-5 B, Figure 5-6 D, 10.0 mM in the dose finding set up vs. 2.9 mM in the XE/pure XN comparison set up) that received the XE diet with 0.5% XN, a phenomenon for which we do not have a plausible explanation up to now. However, there appears to be a dose dependent increase of XN concentration in the bile, at least comparing mice fed with 0.05% XN diet and the 0.25 and 0.5% groups, respectively. Most impressive is the extremely pronounced content of XN conjugates in bile, which can be likely explained by the very good solubilization of the lipophilic XN and its amphiphilic glucuronides by bile acids. Furthermore, it points to the existence of an entero-hepatic circulation of XN and its metabolites. Similar to the other specimen the analyzed concentration of free XN in bile was low in comparison to the concentration of phase II metabolites in all groups (micromolar range). These results underline, in accordance with several publications on other polyphenols [313–315], that for studies on absorption of XN (and most likely also for other chalcones) the determination of phase II metabolites is indispensable.

Based on these data the gut and the liver appear as favorable organs to use the chemopreventive and anti-cancer activity of XN. Naturally, intestinal epithelial cells are exposed to the highest XN concentrations after oral application. In addition, also hepatic concentrations are higher than in other organs since after oral application XN concentrations in the portal circulation are higher than in the systemic circulation, and enterohepatic circulation of the bile further augments this situation.

The shape of the concentration curve of XN excreted with the feces is closely coupled to the bile concentration to the bile concentration with the highest concentration of XN and its phase II metabolites after 7 days and a feeding concentration of 0.5% (m/m) XN in XE (Figure 5-6). As no metabolic cages were used a defined mapping of feces to single mice was not possible. In contrast to the other investigated samples the excreted XN belonged mainly to the free XN content and the phase II metabolite concentrations were generally lower. A comparatively high concentration of phase II metabolites was observable 7 days application of 0.5% XN in both experimental setups (Figure 5-5, Figure 5-6). The increasing content of phase II metabolites in these samples in comparison to the 3 days measurement and the 0.25% XN concentration after 7 days, gives striking evidence that XN undergoes an

induced excretion to bile especially after application of higher doses and a longer oral intake of XN, respectively.

In order to investigate the effect of the extract on the absorption of XN also pure XN was fed to mice for 3 and 7 days with a concentration of 0.5% XN in the same chow as used for the feeding experiments applying XE. Figure 5-6 shows that absorption of XN is positively influences by extract application (and likely the polyphenolic congeners) as the concentration in the serum is significantly lower after application of the same amount of pure XN. The concentration in the serum is significantly lower after application of the same amount of pure XN. The concentration of conjugated XN metabolites decreased from 5.1 ± 2.0 µM (in case of XE diet) to 3.5 ± 0.8 µM (in case of XN diet) after 3 and from 5.2 ± 2.7 µM (XE diet) to 2.8 ± 0.9 µM (XN diet) after 7 days. In contrast, the concentration of overall (conjugated and free) XN in the feces samples (Figure 5-6) was significantly higher after the application of pure XN in comparison to the extract. After 3 days the group fed with 0.5% XN in XE revealed an entire (conjugated + unconjugated) level of 115.9 ± 24.9 µg XN per mg feces, whereas the group fed with 0.5% pure XN showed a value of 135.1 ± 62.2 µg/mg. After 7 days the extract-group revealed an entire concentration of XN 129.8 ± 29.5 µg/mg feces in comparison to 185.4 ± 77.1 µg/mg in the pure XN group. It is of general importance and in line with the XN content in feces that the distribution of XN and its metabolites is also influenced as the concentration of XN in bile is dramatically increasing after feeding of pure XN in the 3 and 7 days groups the interpretation is difficult to explain as we have no results for the single individuals. Urine and hepatic concentration of XN were not significantly different in the animals receiving the extract or the pure XN diet neither after 3 nor after 7 days (Figure 5-6). The positive influence on the absorption of pharmacologically active metabolites by other polyphenolic compounds has been also reported in the case of *Hypericum perforatum* extracts for hypericin [316] and was explained by better solubilization of lipophilic compounds by the polyphenolic congeners [317]. As XN reveals also relatively high lipophilicity this is plausible explanation for the better absorption of XN, too. Nevertheless, also several other factors modulating absorption and degredation of flavonoids can be discussed for the positive effect after XE application. Congeners with antioxidant activity are able to protect XN from oxidative degradation, the degree of microbial degradation by the gut can be structure- and concentration-dependently modulated [318], or the number of bacteria in the gut and thus the activity of the microbial flora can be influenced [319].

As several compounds of the overcritical $CO_2$ hop extract are polyphenols according the TLC, HPLC/DAD and HPLC/HRESIMS analysis (Figure 5-7, Figure 5-8, Figure 5-9) the increased absorption of XN from the extract suggests that application of a spectrum of

multiple phenolic substances contribution to an increased XN bioavailability. Contribution of polyphenols to pharmacokinetic parameters has been reported by Moon and Morris [320], who showed increased bioavailability, reduced clearance and induced entero-hepatic cycling of biochanin A after co-administration of quercetin and EPCG.

## 5.6 Summary

Summing up, our results show that biologically relevant concentration of XN phase II metabolites could be obtained in all excretes and investigated tissues of mice in the case of both application schemes, pure XN and a XN-enriched phenolic hop extract (XE), after 3 and 7 days, whereas the concentration of unconjugated XN was significantly lower. An enrichment of XN and its phase II metabolites was detected in the liver and particularly in the bile. A dose dependent absorption for XN was not observable as escalating plasma levels for XN with highly enriched XN diet (0.5%) were measured. Furthermore, with the latter dose an induced entero-hepatic circulation of XN can be observed. The ongoing research, using LC coupled to high resolution ESI-MS/MS analyses as well as isolation, will focus now on the extract characterization of the metabolic spectrum after the application of pure XN and XE to clarify whether there is not only a quantitative, but also a qualitative variation of the XN metabolism caused by the application matrix. This question is of special interest as a recent publication of Jirasko et al. [321] reported on hitherto unknown phase II metabolites of XN derivatives after modification in a phase I reaction after the application of a XN containing hop extract. Another question of relevance is the variable conversion of XN into isoxanthohumol and also the recently reported conversion to the demethylation product 8-prenylnaringenin by human bacteria [236,322]. This is of pharmacological relevance as isoxanthohumol often showed markedly lower effects in pharmacological assays, whereas 8-prenylnaringenin showed significant estrogenic effects. Also an influence on human P450 enzymes by hops secondary metabolites has been reported [133] and should be investigated after application of XE. Furthermore, the synthesis, pharmacological characterization of XN phase II metabolites as well as investigation on their transport behavior on cellular levels is absolutely necessary to address the biological importance due to their high content in the investigated tissues. As the metabolism of polyphenols can be quantitatively and qualitatively different between rodents and humans *in vivo* studies in man are still a lacking brick in the investigation of XN metabolism.

## 5.7 Appendix

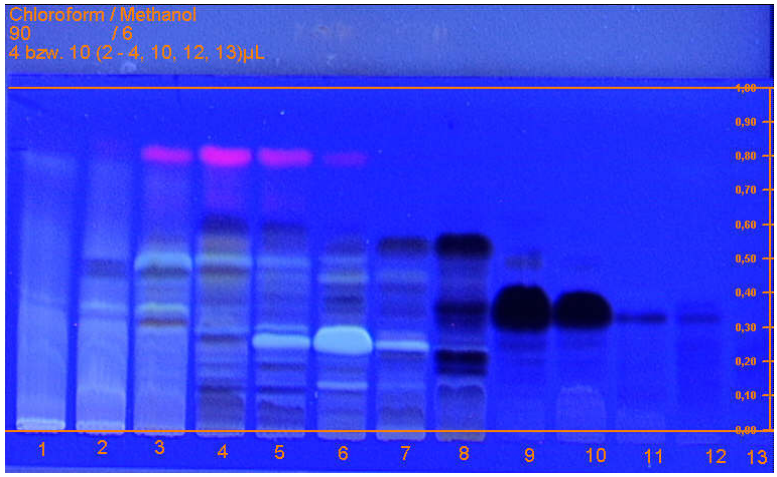


**Figure 5-7: TLC chromatogram of the main fractions obtained from CC of XE 73% (1.7 g) on Sephadex LH-20 (155 g, L 53 cm Ø 3.5 cm) with MeOH as mobile phase. 190 fractions (5 ml, combined after TLC analysis). TLC conditions: silica gel (Merck), mobile phase: $CHCL_3$/MeOH 90:6, detection: 366 nm; dark spots belong mainly to prenylated chalcones and flavanones; main spot fraction 9 and 10: xanthohumol.**

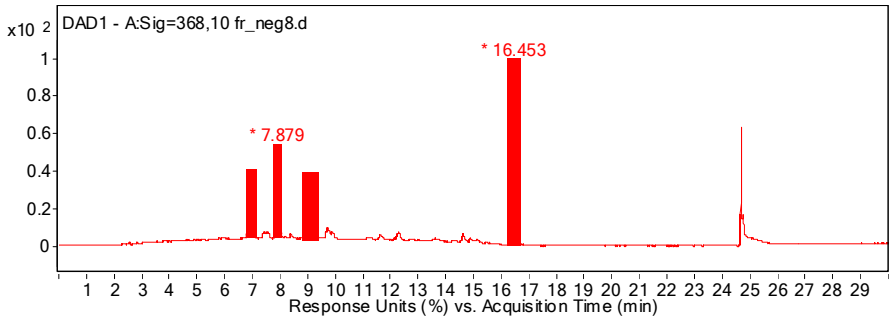


**Figure 5-8: HPLC chromatogram of fraction 8. Solvent A: 5 mM $NH_4OOCH$, solvent B: acetonitrile/water 95/5; column: Purospher® Star RP-18e (size: 250 x 4.0, particle size: 5 µm); flow: 0.8; 0-15 min 40 to 100% B, 15-22 min 100% B; detection wavelength: 368 nm.**

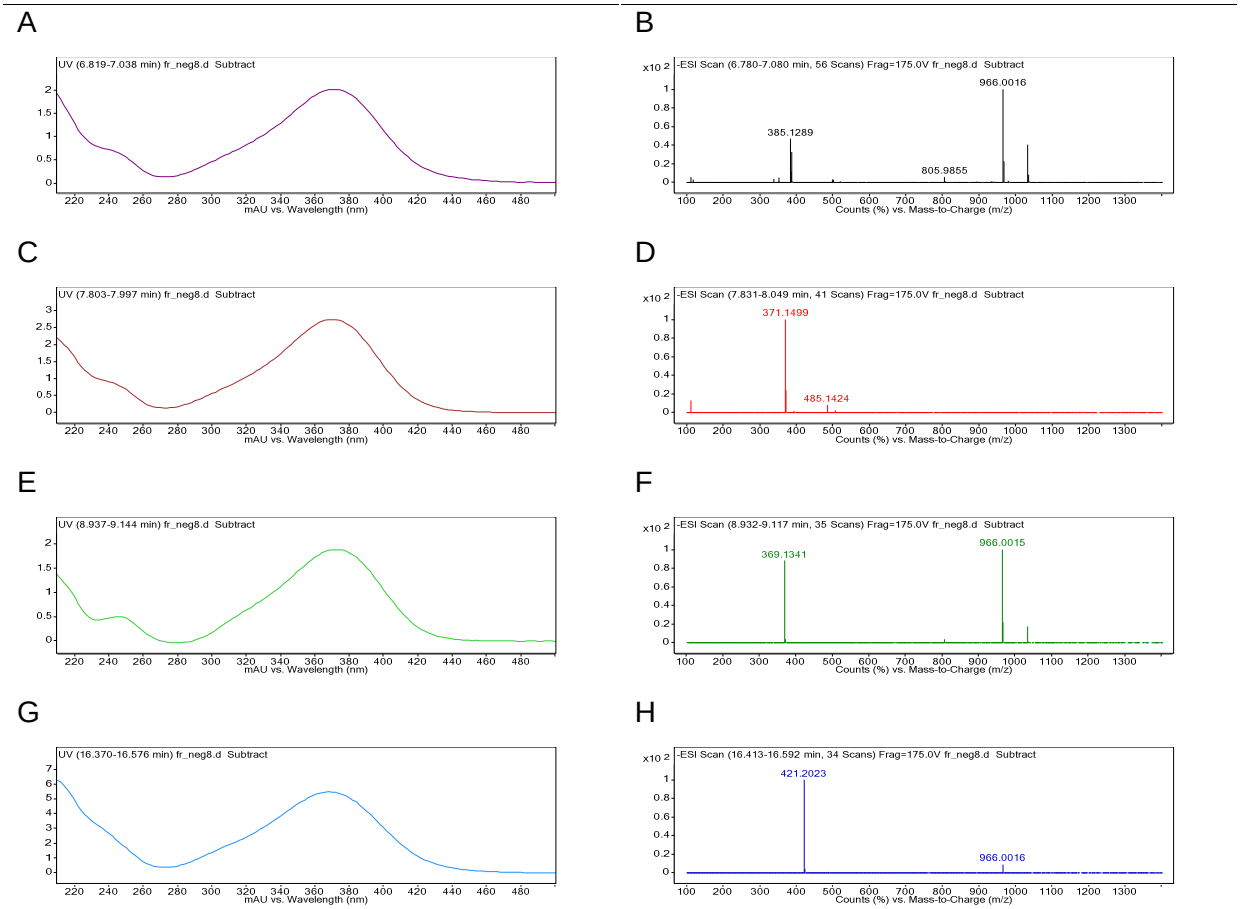


**Figure 5-9: UV- and HRESIMS spectra of selected polyphenols in fraction 8 (XE 73%). Data (lambda$_{max}$ and $[M+H]^+$) points to the presence of several prenylated chalcones as congeners of xanthohumol. UHD Accurate Mass Q-TOF LC/MS System; with Ultra-High-Definition Q-TOF, JetStream-Technology, MS-ESI (Agilent).**

# 6 Discussion

XN is a small molecule with a prenyl chain and belongs to the huge family of polyphenols and the subgroup of chalcones. In comparison to other chalcones such as hydroxysafflor yellow A and isoliquiritin, XN exhibits no sugar moiety. XN is a lipophilic compound that is poorly soluble in water and medium [82,226] with a solubility of < 0.05 mg/ml XN in cell culture medium after 3 h incubation time [226]. A low solubility was also observed for other flavonoids such as silymarin [323]. In order to use the prenylated chalcones as reference substances in pharmacological studies, it is necessary to establish appropriate experimental set-ups in order to reach the requested XN concentrations in the medium. There are different methods to enhance the solubility of compounds e.g. by complexation, micellization, cosolvency [324], adjustment of the pH [325] and BSA optimization [326]. In this thesis the solubility of XN was adjusted with FCS. FCS is a complex solution of different proteins and factors [327]. With higher FCS concentrations the solubility of XN increased in a dose dependent manner. A minimum FCS concentration of 10% was necessary in order to reach XN concentrations of 10 µM. The absorption of XN to proteins was shown in different studies [227,228]. Pang et al. [227] investigated the ability of XN to bind to native isolated cytosolic proteins. The ability of XN to bind to proteins was also studied in cells by FRAP measurements [228]. Moreover XN was also shown to interact with proteins such as Keap 1 [137,139], NF-κB [176,182] and IKK [182], but the proteins which are responsible for the mediation of the solubility are not identified yet. But high FCS concentrations might also lead to interference with detection methods such as fluorescence measurements [226] (Chapter 2). FCS contains different proteins and factors [327] which might quench the fluorescence or induce a spectral shift. However, XN adsorb not only to proteins but also to cell culture materials. In Greiner culture flasks, TPP culture flasks and Petri dishes but not in centrifuge tubes and 96 well plates the required XN concentration of 10 µM could be reached using 10% FCS. The adsorption of small molecules to culture materials was also shown in other studies. The adsorption of different small molecules was examined, for instance, on different UV-ozone treated materials such as poly(methyl methacrylate), polysterne, polycarbonate, poly(dimethylsiloxane) and cyclic olefin copolymers. It was shown that the treatment of thermoplastics with UV-ozone reduced the adsorption of the compounds on some of the thermoplastics [328]. The required experimental set-up for lipophilic compounds should be checked at the beginning of *in vitro* as well as *in vivo* experiments. The supplementation of pure water without any solubilizers with XN is inadvisable for *in vivo* studies [169,220]. The supplementation of chow might solve the solubility problem of XN in *in vivo* studies (see also Chapter 5). Summing up it is

necessary to determine the effective concentration of lipophilic compounds in the used media at the beginning of the experiments.

XN exhibits a low bioavailability. Only a few studies were performed that investigate the XN uptake *in vitro.* Pang et al. [227] determined the XN uptake in Caco-2 cells. Wolff et al. [228] (see also Chapter 4) investigated the time course and manner of the XN uptake in hepatic and colorectal cancer cell lines as well as primary hepatocytes. In addition the XN concentration per cell was determined. Both studies detected a fast and concentrated uptake of XN. XN absorption reached a steady state between 30 and 60 min in HSC, HuH-7, PH [228] and Caco-2 cells [228,227].

In order to determine the XN concentration per cell in this thesis, the XN amount per protein was measured and a correlation curve that describes the ratio between the protein per cell and the cell volumes prepared for each cell line as well as the PH. The measurements revealed that HSC, Caco-2 and PH took up 52, 63 and 47 fold higher XN concentrations compared to the XN supplemented medium. In HuH-7 the uptake was only 3 fold higher compared to the medium (see Chapter 4) [228]. Reasons for the low XN uptake in HuH-7 cells might be the existence of different transporter types and densities in the cell lines. ABC-transporters are ATP-dependent and are located in the cell membrane. A function of the ABC-transporters is the transport of hydrophobic compounds across the cellular membrane [239]. XN was shown to influence ABC-transporters and reduce their mRNA levels [189] as well as the efflux of compounds mediated by P-glycoproteins [242,241,227]. Pang et al. [227] incubated Caco-2 cells with transporter inhibitors and detected an increased uptake of XN. However a clear mechanism is not known yet.

Another possible reason of the low XN uptake in HuH-7 cells would be a higher phase I or phase II metabolism of XN in HuH-7 cells. The detoxification of XN and metabolites was also discussed in the study of Miranda et al. [186]. They determined the cytotoxic effects of XN and metabolites in different cell lines. The cells were incubated with the compounds for 48, 96 and 144 h. The longer the incubation time the lower was the observed cytotoxicity. In this thesis a higher metabolic rate in HuH-7 cells might be not the mode of action. The intracellular concentration of XN was determined by HPLC. This method had the advantage that metabolites with a similar chromophor could be detected and observed during the XN quantification (see Chapter 5). Rather no difference concerning the phase II metabolism was observed between the cell lines. The exact mechanism for the low XN uptake in HuH-7 is not known.

Nevertheless XN, showed a fast and comprehensive up-take by the liver cells. This fact might also lead to a low bioavailability. E.g. Avula et al. [224] did not detect XN after oral application of 10, 20, 50, 100, 200, 400, 500 mg XN/kg body weight and XN enriched hops

extract in rat's serum. Legette et al. [225] detected 0.42 ± 0.03 µM conjugated and unconjugated XN after a single oral gavages dose of 16.9 mg/kg body weight. In this thesis BALB/c mice were fed with two different chows. In a first experiment the chow was supplemented with 73% XN (27% phenolic matrix). BALB/c mice were fed with 100 mg XN/kg, 500 mg XN/kg and 1000 mg XN/kg body weight of the 73% XN chow for 3 and 7 days. After the feeding period the serum, liver, urine, feces and bile samples were analyzed concerning their XN content (unconjugated and conjugated XN). The concentrations of unconjugated XN were between 0.01 and 0.12 µM (see Chapter 5). The slight differences between the studies might be attributed to different experimental designs. The concentration of unconjugated XN in serum is generally low and a suitable lipophilic solvent had to be chosen in order to effectively extract XN from the matrix. Different solvents might lead to different recoveries from serum with differing LOQs and varying results. Apart from the optimal extraction solvent, the detection method is also relevant. Legette et al. [225] worked with a LOQ of 0.4-0.5 nM, Avula et al. [224] with 0.04 µM. In this thesis a LOQ of 0.02 µM was achieved. Legette et al. [225] determined the XN amount with MS and probably for this reason reached lower LOQ [225]. Furthermore, in comparison to the study of Avula et al. [224], Legette et al. [225] determined the sum of unconjugated and conjugated XN. In our study the unconjugated, conjugated and the sum of XN was determined. The ratio between unconjugated and conjugated XN was between 21 and 163 (see Chapter 5). This might be one reason why Avula et al. [224] did not detect XN, because the phase II metabolites were not determined. The investigation of phase II metabolites is of great importance. After oral ingestion the flavonoids can be absorbed in the small intestine and the colon as aglycones and in some cases also as glycosides [329–331]. After the uptake they are transported to the liver by the venous gastrointestinal blood. Metabolism such as glucuronidation and deglucuronidation can take place in the small intestine and/or in the liver [332–334]. One example for deglucoronidation in the liver is the toxic metabolite mycophenolate mofetil acyl glucuronide, which is deglucuronidated in the liver by α,β hydrolase domain containing 10 [332]. The precursor flavonoids and their metabolites can reach the bile and colon after they passed the liver and may be absorbed again (entero-hepatic circulation). The complex mechanism of the metabolism of flavanoids is not fully understood and is still under investigation. However metabolites can spread higher, lesser or the same activity compared to their precursors. Thus phase II metabolites should always be investigated in order to determine the bioavailability and behavior of polyphenols *in vivo*. The concentrations of unconjugated XN ranged between 0.01 and 0.12 µM in serum (see Chapter 5). Thus the bioavailability of unconjugated XN was low, but a high phase II metabolism rate was observed. Similar results were described for quercetin (single oral dose of 350 mg/kg body weight). No free quercetin was detected but a metabolite concentration of 30.0 ± 3.8 µM after

24 h [335]. The same high phase II metabolism was also observed for further lipophilic flavonoid aglyca in a Caco-2 cell model. This study revealed a good permeability of aglycones and a comprehensive metabolization to their glucuronic acid and sulfate derivatives [336]. Similar behavior was observed for XN in cellular uptake and in *in vivo* studies. XN showed a rapid uptake in hepatic cancer cell lines, Caco-2 and PHs [227,228] (see also Chapter 4). The fast and high uptake might be an explanation for the low bioavailability and absorption of XN [224,225] (see also Chapter 5).

In our study the dose dependent distribution of unconjugated and conjugated XN was investigated in serum, bile, urine, feces and liver 3 and 7 days after daily intake with the chow. In all samples of the body fluids, secretions and tissues the concentration of unconjugated and conjugated XN was not linearly increasing with the ingested amount of XN. A similar pattern was also observed in the study of Legette et al. [225] for XN and in the study of Yang et al. [337] for epicatechin-3-gallate (ingestion of 1.5, 3.0 and 4.5 g decaffeinated green tea solids). In contrast a linear correlation between the ingested dose and the absorption was described for other flavonoids like isorhamnetin [338]. The determination of the bioavailability on the basis of only one dose as it was performed in different studies e.g. [335,339] might lead to only limited conclusions. Thus it seems to be beneficial to investigate the dose dependent absorption rather than conducting single dose experiments.

In our study the concentration of XN metabolites in the liver was lower after 7 days of administration compared to 3 days, but higher in bile and feces (1000 mg/kg body weight). No difference in the XN metabolite concentrations depending on the feeding period was observed for serum and urine samples. Interestingly, the XN concentration was highest (unconjugated and conjugated) in the bile followed by feces, urine, liver and serum. This pointed to an entero-hepatic circulation. Quercetin metabolites were also found to be excreted through the bile [340]. Compounds with a molecular weight of less than 300 Da are commonly excreted via the urine. Molecular weights above 300 Da commonly lead to an excretion via the bile [99].

Noteworthy is also the high concentration of conjugated XN in the serum. Only a small amount of unconjugated XN reaches the systemic circulation (ratio of conjugated/unconjugated XN ranges between 21-163).

In the second part of the study the influence of the matrix on the bioavailability and uptake was studied, because it was shown in the literature that compounds are better ingested with matrix as without [303,341,342]. One group of BALB/c mice was fed with a diet supplemented with 98% XN (XN). The second group was fed with a diet supplemented with 73% XN (XE) (27% phenolic matrix). The feeding period was either 3 or 7 days (1000 mg/kg

body weight). After the feeding period the serum, liver, urine, feces and bile samples were analyzed for the amount of unconjugated and conjugated XN. It was observed that with the ingestion of XE significantly more conjugated XN was found in the systemic circulation. Furthermore, the excretion of conjugated XN via the bile and feces was higher for the XN diet compared to XE. The same trend was observed for the urine but could not be statistically confirmed. The observed effects were attributed to the remaining matrix in the XE diet. Matrix effects on the absorption of compounds were also observed in other studies about flavanoids. E.g. the bioavailability of polyphenols (e. g. epigallocatechin-3-gallate) was increased in case of the ingestion with decaffeinated green tea [341]. Wiczkowski and co-workers [303] discussed matrix effects as a possible explanation for a higher uptake of quercetin in shallots. Matrix effects were also discussed by Egert et al. [342]. They determined the uptake of quercetin in cereal bars and quercetin powder-filled hard capsules [342]. There are many different explanations for the higher absorption and bioavailability which are observed in case of ingestion of substances with matrix. One explanation might be the regulation of the efflux or influx of the compounds by transporters e.g. ABC-transporter by the matrix [343,344]. Another explanation might be lower metabolism of polyphenols caused by the matrix. Chen et al. [341] investigated the absorption of polyphenols (e. g. epigallocatechin-3-gallate) with decaffeinated green tea matrix or without in rats. The results pointed to higher absorption of polyphenols with matrix as without. They discussed a competition of matrix tea polyphenols with the metabolism enzymes such as glucuronosyl- and sulfotransferase. This might lead to higher concentration of polyphenols and lower elimination [341]. Flavonoids can be also absorbed in the colon [329,330] and are transformed by the colon microflora. The matrix might also prevent the molecule against destruction and oxidation by the microflora [318]. Another explanation might be the higher solubility of a polyphenol facilitated by the matrix. This was also discussed in several studies [309,316,341,345]. In the study of Egert and co-workers [309] the bioavailability of quercetin in quercetin-enriched cereal bars and quercetin powder-filled hard capsules was investigated. The ingestion of quercetin-enriched cereal bars yielded higher area under the curve compared to the ingestion of quercetin powder-filled hard capsules and a higher solubility of quercetin in the cereal bars was discussed. An increase in the solubility is one of the main factors for an increase of the bioavailability. There are a variety of methods that are used to increase the solubility of lipophilic compounds such as complexetion, micellization, coselvency [324], adjustment of the pH [325] and BSA optimization [326]. The increase of the solubility of XN by cyclodextrines is described in the patent application of Yamaguchi et al. [346].

In this thesis it was shown that XN is taken up by liver cell lines (*in vitro*) and is highly metabolized (*in vivo*). As the pharmacological data of XN metabolites and related compounds are scarce, the effect of a series of chalcones on the viability, proliferation and cytotoxicity was investigated in three hepatic and one colorectal cancer cell line using MTT and CV assay. Compounds **13** and **14** were found to be less toxic compounds. Compound **2** was the compound with the lowest $IC_{50}$ value. A different effect of the compounds was observed in the study of Vogel et al. using HeLa cells [150–152]. Compound **13** showed the strongest viability inhibition ($IC_{50}$ value 5.2 ± 0.8 µM) followed by **2** > XN > **6** > **14** > **7** = **4** > **3** > **5** and **17** [152,151,150]. The differences in the effectiveness are probably explainable because of the different cell lines and method handling.

In this thesis a correlation between the lipophilicity of the tested substances and their cytotoxicity could be partially observed. The lipophilicity was compared by HPTLC. E. g. **15** was one of the more lipophilic compounds and showed the lowest $IC_{50}$ value in RAW 264.7. A correlation between the cytotoxicity and lipophilicity was also observed in a variety of other studies. For example **15** showed the weakest viability inhibitory activity in RAW 264.7 cells followed by **16** and **17** [271]. The latter flavokawains are more lipohilic than **15**. These results for the flavokawains were also confirmed in this study. The studies of local anesthetics [287] and heat shock proteins [288] revealed a similar correlation between the cytotoxicity and lipophilicity. The studies showed that lipophilic chemicals exhibit higher cytotoxicity in human T-lymphoma cells [287] or induce heat shock proteins [288]. An explanation might be the ability of lipophilic substances to approximate to and interact with lipophilic centers of enzymes [288,289]. XN can interact with mitochondrial proteins, induce the release of ROS and lead to apoptosis [157]. In addition XN (**1**) can change the membrane fluidity [290]. This process might lead to a faster infiltration and a higher cytotoxicity, but the exact mechanism is not investigated yet. Nevertheless, the lipophilicity might not to be the only explanation. Compound **2** is less lipophilic and showed comparatively high reduction of the cell viability. It carries a prenyl chain with a hydroxyl group which might be responsible for the observed effects. The presence of a prenyl chain was also correlated with the effect to inhibit the growth of microorganism [19,291], phase II enzymes [135], BACE1 [292], the invasion of cancer cells [187] as well as their proliferation and 5-LOX activity [289]. In addition the adherence of prenyl groups to apigenin and liquiritigenin was shown to increase the cytotoxicity in different cell lines [293].

The molecular mechanism of the effects of XN (**1)**, XN metabolites and related compounds was not investigated in this study. Each assay investigates different aspects of cellular behavior. The MTT assay describes an increase or decrease in the viability which can be caused by a drop of the cell count and a decrease in mitochondrial activity. The CV assay is only based on the cell count. With increasing concentrations **2** first inhibited the viability and

then the cell count in the MTT and CV assay. This might point to an inhibition of the mitochondria function by **2** without a decrease of the cell count. The compounds **6** and **7** showed the opposite behavior. First a decrease in the cell count was observed followed by a decrease in the viability. Thus, the mechanism of **6** and **7** might be another as by **2**. The behavior of **1**, **3** and **13** concerning cell viability and cell count depends on the cell line. It is known that XN induces cell death in different cancer cell lines and through different mechanisms (see 1.1.7 Pro-apoptotic mechanism). The behavior of **2**, **6** and **7** differed from XN in most cell lines and thus might be investigated in further detail in following studies.

In addition the NO production and the iNOS expression were investigated for XN, XN metabolites and related compounds (see Chapter 3). The compounds were tested on their activity to inhibit the NO production which was induced with 10 ng/ml LPS in the first assay. In order to compare the influence on the NO production with the iNOS expression the second Griess assay was performed with 10 ng/ml LPS and 200 ng/ml IFN-γ

All compounds except of the used hydrogenated derivatives showed a significant inhibition of the NO production in the performed Griess assay (10 ng/ml LPS). In the literature it is discussed that the α,β-unsaturated carbonyl moiety is responsible for the inhibition [181,295]. Compounds without this moiety led to no or only little decreases in the NO production [181]. Therefore the hydrogenated compounds in comparison to the other XN metabolites and related compounds were tested. In the second Griess assay (10 ng/ml LPS and 200 ng/ml IFN-γ) compound **10** a hydrogenated chalcone showed a significant inhibitory effect on the NO production at 8 µM. This is in agreement with the study of Peluso et al. [178]. Peluso et al. studied the influence of flavonoids and dihydro flavonoids on the expression of MCP-1 and IL-6 in LPS stimulated monocytic THP-1 cells. As aforementioned the activity to inhibit the NO production were not observed in solely LPS (10 ng/ml LPS) stimulated cells in the Griess assay by the hydrogenated compounds. LPS stimulates the NO production via the NF-κB pathway. IFN-γ activates the NO production via the JAK/STAT pathway. Compound **10** may inhibit the NO production more effective through the JAK/STAT pathway with its tetrahydropyran structure characteristics.

Compound **6** significantly inhibited the NO production and carry a closed prenyl chain at the A ring. The correlation between the higher NO inhibition activity and the open prenyl chain at the A ring of the chalcone were investigated with compound **9** and the closed prenyl chain in the Acetylchroman **8**. Compound **8** led to higher inhibitory effects compared to **9**. As aforementioned **10** spread effective inhibitory activity on the NO production compared to the other hydrogenated chalcones (10 ng/ml LPS and 200 ng/ml IFN-γ). Thus the A ring with the closed prenyl chain at the A ring might be beneficial for the inhibition of the NO production and the iNOS expression independent of the used stimuli.

Further comparison of the structure of the investigated compounds revealed that the prenyl chain did not enhance the inhibition of the NO production. The same was observed by Zhao et al. [181]. However **2** was an outlier of this conclusion and the most active compound of the prenylated chalcones. Compound **5** showed the weakest activity. A similar correlation was also observed in the study of Peluso et al. [178]. Compound **5** was found to be less active than XN and **17** [178]. There is no explanation for this behavior up to now

Furthermore, **13** which is a non-prenylated chalcone showed the highest inhibitory activity on the NO production and iNOS expression. Compound **18** spread higher activity as **13** but was less active in the second NO assay (10 ng/ml LPS and 200 ng/ml IFN-γ). Compound **18** might inhibit the NO production predominantly through the NF-κB pathway. No correlation between the lipophilicity and the inhibitory effects on the NO production and the iNOS expression could be observed.

# 7 Summary

XN is an abundant chalcone in hops and spread a wide range of pharmacological effects. The lipophilicity of XN is a challenge for water based *in vitro* studies. For this reason suitable experimental set-ups for *in vitro* experiments were established. A content of 10% FCS in the cell culture medium was found to efficiently increase the solubility of XN. However the application of 10% FCS did not fully prevent the adsorption of XN to several cell culture materials. In Greiner culture flasks, TPP culture flasks and Petri dishes but not in centrifuge tubes and 96 well plates a solubility concentration of 10 µM XN could be reached.

XN is mainly found in beer in the human diet and is ingested with other minor hop compounds. After ingestion XN is highly metabolized (see Chapter 5). For this reason it is necessary to determine the effects of minor hop chalcones, XN metabolites and related compounds in order to investigate if the compounds are more or less active compared to XN. XN is a potent anti-inflammatory compound that leads to the inhibition of inflammatory and angiogenetic factors and exhibits anti-cancer effects. The compounds were investigated concerning their ability to influence the viability, proliferation and cytotoxicity in MTT and CV assays.

Compound **2** had the lowest $IC_{50}$ values in the MTT assay. In the CV assay **6** and **7** showed the lowest $IC_{50}$ values in most of the investigated cell lines. Thus these XN metabolites and related compounds might be candidates for advanced studies.

The ability to influence inflammatory factors such as the NO production and iNOS expression was determined in a Griess assay and an iNOS expression assay. Compound **10** effectively inhibited the NO production in RAW 264.7 cells stimulated with 10 ng/ml LPS. The iNOS expression was significantly inhibited by the tested hydrogenated chalcones. In the group of

the chalcones the tetrahydropyran-chalcone **6** had a remarkable potential to inhibit the NO production and iNOS expression. The non-prenylated chalcones **13** and **14** showed a higher activity to inhibit the NO production with both stimuli compared to the prenylated chalcones. In the group of the non-prenylated chalcones the chalcones with one hydroxyl group led to more effective inhibition of the NO production and iNOS expression compared to those with two or no hydroxyl groups. In the group of the prenylated chalcones **2** showed the highest and **5** the lowest activity in inhibiting the NO production (stimulus 10 ng/ml LPS) and iNOS expression. Prenylated chalcones with free hydroxyl groups inhibited the NO production more efficient than the *O*-methoxylated and *O*-acetylated derivatives.

Compounds **2**, **4**, **6** and **7** differ in their activity in the performed assays and might be candidates for the study of molecular mechanism in more detail.

XN exhibits a low bioavailability. The exact uptake mechanism of XN is not fully understood yet. In this thesis the XN uptake was studied in hepatic and colorectal cancer cell lines and primary hepatocytes. HSC, Caco-2 and PH cells exhibited a 52, 63 and 47 fold higher XN concentration compared to the medium which was initially supplemented with 10 µM XN. In HuH-7 cells the measured XN concentration was only 3 fold higher. This might be explained by differences in the ABC-transporters, metabolism and amount of proteins per cell. But the reason is not known yet and needs to be further investigated. The results showed that XN is accumulated in hepatic cancer cell lines and primary hepatocytes and might thus exhibit a low bioavailability. This prompted us to investigate the bioavailability as well as the distribution and metabolism of XN in the liver, serum, bile, feces and urine of BALB/c mice.

The BALB/c mice were fed with 100 mg XN/kg, 500 mg XN/kg and 1000 mg XN/kg body weight (73% XN) for 3 and 7 days respectively. There was no linear correlation between the fed amount of XN and the XN concentration in serum. Thus it seems advisable to determine suitable concentration ranges for every compound prior to *in vivo* experiments. The distribution measurements revealed that the highest XN concentrations were detected in the bile followed by the feces, urine, liver and serum. This pointed to an entero-hepatic circulation of XN. The serum XN (unmetabolized) concentration was between 0.01 and 0.12 µM. XN was highly metabolized. The ratio between conjugated and unconjugated XN was between 21 and 163.

In order to investigate the influence of the matrix on the XN absorption, BALB/c mice were fed with 73% XN (27% matrix) and 98% XN. The BALB/c mice received a diet with 1000 mg XN/kg body weight for 3 and 7 days respectively. The absorption of XN was significantly higher in the group that was fed with 73% XN. In addition the studies showed that XN is highly metabolized. The highest XN concentrations were detected in the bile followed by the serum, liver, urine and feces.

# 8 References

[1] J. Nagel, L.K. Culley, Y. Lu, E. Liu, P.D. Matthews, J.F. Stevens, J.E. Page, EST analysis of hop glandular trichomes identifies an O-methyltransferase that catalyzes the biosynthesis of xanthohumol, Plant Cell 20 (2008) 186–200.

[2] H. Grisebach, Die Biosynthese der Flavonoide 1, Planta Med. 10 (1962) 385–397.

[3] E. Wellmann, D. Baron, H. Grisebach, Two different enzymes for the biosynthesis of UDP-xylose from UDP-glucuronic acid in cell suspension cultures of parsley (*Petroselinum hortense*), Biochim. Biophys. Acta 244 (1971) 1–6.

[4] F. Kreuzaler, K. Hahlbrock, Enzymatic synthesis of aromatic compounds in higher plants: formation of naringenin (5,7,4'-trihydroxyflavanone) from p-coumaroyl coenzyme A and malonyl coenzyme A, FEBS Lett. 28 (1972) 69–72.

[5] N. Yadav, S.K. Dixit, A. Bhattacharya, L.C. Mishra, M. Sharma, S.K. Awasthi, V.K. Bhasin, Antimalarial activity of newly synthesized chalcone derivatives in vitro, Chem. Biol. Drug Des. 80 (2012) 340–347.

[6] A. Kamal, A. Mallareddy, P. Suresh, T.B. Shaik, V. Lakshma Nayak, C. Kishor, R.V.C.R.N.C. Shetti, N. Sankara Rao, J.R. Tamboli, S. Ramakrishna, A. Addlagatta, Synthesis of chalcone-amidobenzothiazole conjugates as antimitotic and apoptotic inducing agents, Bioorg. Med. Chem. 20 (2012) 3480–3492.

[7] I. Łącka, M.T. Konieczny, A. Bułakowska, T. Rzymowski, S. Milewski, Antifungal action of the oxathiolone-fused chalcone derivative, Mycoses 54 (2011) e407-14.

[8] Y. Tsurumaru, K. Sasaki, T. Miyawaki, Y. Uto, T. Momma, N. Umemoto, M. Momose, K. Yazaki, HlPT-1, a membrane-bound prenyltransferase responsible for the biosynthesis of bitter acids in hops, Biochem. Biophys. Res. Commun. 417 (2012) 393–398.

[9] J.F. Stevens, A.W. Taylor, J.E. Clawson, M.L. Deinzer, Fate of xanthohumol and related prenylflavonoids from hops to beer, J. Agric. Food Chem. 47 (1999) 2421–2428.

[10] R. Slimestad, M. Verheul, Properties of chalconaringenin and rutin isolated from cherry tomatoes, J. Agric. Food Chem. 59 (2011) 3180–3185.

[11] Y. Iwase, M. Takahashi, Y. Takemura, M. Ju-ichi, C. Ito, H. Furukawa, M. Yano, Isolation and identification of two new flavanones and a chalcone from *Citrus kinokuni*, Chem. Pharm. Bull. 49 (2001) 1356–1358.

[12] J.F. Stevens, M. Ivancic, V.L. Hsu, M.L. Deinzer, Prenylflavonoids from *Humulus lupulus,* Phytochemistry 44 (1997) 1575–1585.

[13] J. Vaya, P.A. Belinky, M. Aviram, Antioxidant constituents from licorice roots: isolation, structure elucidation and antioxidative capacity toward LDL oxidation, Free Radic. Biol. Med. 23 (1997) 302–313.

[14] M.R. Meselhy, S. Kadota, Y. Momose, N. Hatakeyama, A. Kusai, M. Hattori, T. Namba, Two new quinochalcone yellow pigments from *Carthamus tinctorius* and Ca2+ antagonistic activity of tinctormine, Chem. Pharm. Bull. 41 (1993) 1796–1802.

[15] J.-S. Jiang, J. He, Z.-M. Feng, P.-C. Zhang, Two new quinochalcones from the florets of *Carthamus tinctorius,* Org. Lett. 12 (2010) 1196–1199.

[16] R. Köck, A. Mellmann, F. Schaumburg, A.W. Friedrich, F. Kipp, K. Becker, The epidemiology of methicillin-resistant *Staphylococcus aureus* (MRSA) in Germany, Dtsch. Arztebl. Int. 108 (2011) 761–767.

[17] B.C.-L. Chan, H. Yu, C.-W. Wong, S.-L. Lui, C. Jolivalt, C. Ganem-Elbaz, J.-M. Paris, B. Morleo, M. Litaudon, C.B.-S. Lau, M. Ip, K.-P. Fung, P.-C. Leung, Q.-B. Han, Quick identification of kuraridin, a noncytotoxic anti-MRSA (methicillin-resistant *Staphylococcus aureus*) agent from *Sophora flavescens* using high-speed counter-current chromatography, J. Chromatogr. B Analyt. Technol. Biomed. Life Sci. 880 (2012) 157–162.

[18] T. Hatano, M. Kusuda, K. Inada, T.-o. Ogawa, S. Shiota, T. Tsuchiya, T. Yoshida, Effects of tannins and related polyphenols on methicillin-resistant *Staphylococcus aureus,* Phytochemistry 66 (2005) 2047–2055.

[19] K. Sugamoto, Y.-i. Matsusita, K. Matsui, C. Kurogi, T. Matsui, Synthesis and antibacterial activity of chalcones bearing prenyl or geranyl groups from *Angelica keiskei,* Tetrahedron 67 (2011) 5346–5359.

[20] A. Friis-Møller, M. Chen, K. Fuursted, S.B. Christensen, A. Kharazmi, *In Vitro* Antimycobacterial and Antilegionella Activity of Licochalcone A from Chinese Licorice Roots, Planta Med. 68 (2002) 416–419.

[21] R.-I. Tsukiyama, H. Katsura, N. Tokuriki, M. Kobayashi, Antibacterial Activity of Licochalcone A against Spore-Forming Bacteria, Antimicrob. Agents Ch. 46 (2002) 1226–1230.

[22] H. Isomoto, H. Furusu, K. Ohnita, C.-Y. Wen, K. Inoue, S. Kohno, Sofalcone, a mucoprotective agent, increases the cure rate of *Helicobacter pylori* infection when combined with rabeprazole, amoxicillin and clarithromycin, World J. Gastroenterol. 11 (2005) 1629–1633.

[23] T. Fukai, A. Marumo, K. Kaitou, T. Kanda, S. Terada, T. Nomura, Anti-*Helicobacter pylori* flavonoids from licorice extract, Life Sci. 71 (2002) 1449–1463.

[24] J.-Y. Park, H.J. Jeong, Y.M. Kim, S.-J. Park, M.-C. Rho, K.H. Park, Y.B. Ryu, W.S. Lee, Characteristic of alkylated chalcones from *Angelica keiskei* on influenza virus neuraminidase inhibition, Bioorg. Med. Chem. Lett. 21 (2011) 5602–5604.

[25] S. Shibata, A drug over the millennia: pharmacognosy, chemistry, and pharmacology of licorice, Yakugaku Zasshi 120 (2000) 849–862.

[26] S. Frölich, C. Schubert, U. Bienzle, K. Jenett-Siems, *In vitro* antiplasmodial activity of prenylated chalcone derivatives of hops (*Humulus lupulus*) and their interaction with haemin, J. Antimicrob. Chemother. 55 (2005) 883–887.

[27] M.-L. Go, Novel antiplasmodial agents, Med. Res. Rev. 23 (2003) 456–487.

[28] M. Nkunya, H. Weenen, D. Bray, Q. Mgani, L. Mwasumbi, Antimalaria activity of Tanzanian plants and their active constituents: the genus *Uvaria,* Planta Med. 57 (1991) 341–343.

[29] M. Chen, S.B. Christensen, J. Blom, E. Lemmich, L. Nadelmann, K. Fich, T.G. Theander, A. Kharazmi, Licochalcone A, a novel antiparasitic agent with potent activity against human pathogenic protozoan species of *Leishmania*, Antimicrob. Agents Chemother. 37 (1993) 2550–2556.

[30] L. Jayasinghe, B.A.I.S. Balasooriya, W.C. Padmini, N. Hara, Y. Fujimoto, Geranyl chalcone derivatives with antifungal and radical scavenging properties from the leaves of *Artocarpus nobilis*, Phytochemistry 65 (2004) 1287–1290.

[31] S. Gafner, J.L. Wolfender, S. Mavi, K. Hostettmann, Antifungal and antibacterial chalcones from *Myrica serrata*, Planta Med. 62 (1996) 67–69.

[32] H.N. ElSohly, A.S. Joshi, A.C. Nimrod, L.A. Walker, A.M. Clark, Antifungal chalcones from *Maclura tinctoria,* Planta Med. 67 (2001) 87–89.

[33] C. Messier, D. Grenier, Effect of licorice compounds licochalcone A, glabridin and glycyrrhizic acid on growth and virulence properties of *Candida albicans*, Mycoses 54 (2011) e801-6.

[34] L. Pecorino, Molecular biology of cancer. Mechanisms, targets, and therapeutics, Oxford University Press, Oxford University Press; New York, second edition, (2008).

[35] D. Hanahan, R.A. Weinberg, The Hallmarks of Cancer, Cell 100 (2000) 57–70.

[36] C. Gerhäuser, A. Alt, E. Heiss, A. Gamal-Eldeen, K. Klimo, J. Knauft, I. Neumann, H.-R. Scherf, N. Frank, H. Bartsch, H. Becker, Cancer chemopreventive activity of Xanthohumol, a natural product derived from hop, Mol. Cancer Ther. 1 (2002) 959–969.

[37] C. Theisen, Chemoprevention: What's in a name?, J. Natl. Cancer Inst. 93 (2001) 743.

[38] S.G. Maher, J.V. Reynolds, Basic concepts of inflammation and its role in carcinogenesis, Recent Res. Cancer 185 (2011) 1–34.

[39] D. Ziech, R. Franco, A. Pappa, M.I. Panayiotidis, Reactive oxygen species (ROS)--induced genetic and epigenetic alterations in human carcinogenesis, Mutat. Res. 711 (2011) 167–173.

[40] J.-M. Yun, M.-H. Kweon, H. Kwon, J.-K. Hwang, H. Mukhtar, Induction of apoptosis and cell cycle arrest by a chalcone panduratin A isolated from *Kaempferia pandurata* in

androgen-independent human prostate cancer cells PC3 and DU145, Carcinogenesis 27 (2006) 1454–1464.

[41] M. Cuendet, J. Guo, Y. Luo, S. Chen, C.P. Oteham, R.C. Moon, R.B. van Breemen, L.E. Marler, J.M. Pezzuto, Cancer chemopreventive activity and metabolism of isoliquiritigenin, a compound found in licorice, Cancer Prev. Res. (Phila) 3 (2010) 221–232.

[42] V.R. Yadav, S. Prasad, B. Sung, B.B. Aggarwal, The role of chalcones in suppression of NF-κB-mediated inflammation and cancer. Immunopharmacology of Synthetic Natural Products, Int. Immunopharmacol. 11 (2011) 295–309.

[43] Z.J. Cheng, S.C. Kuo, S.C. Chan, F.N. Ko, C.M. Teng, Antioxidant properties of butein isolated from *Dalbergia odorifera,* Biochim. Biophys. Acta 1392 (1998) 291–299.

[44] S. Tsukamoto, M. Aburatani, T. Yoshida, Y. Yamashita, A.A. El-Beih, T. Ohta, CYP3A4 inhibitors isolated from Licorice, Biol. Pharm. Bull. 28 (2005) 2000–2002.

[45] C. Pohl, F. Will, H. Dietrich, D. Schrenk, Cytochrome P450 1A1 expression and activity in Caco-2 cells: modulation by apple juice extract and certain apple polyphenols, J. Agric. Food Chem. 54 (2006) 10262–10268.

[46] A.D. Kinghorn, B.-N. Su, D.S. Jang, L.C. Chang, D. Lee, J.-Q. Gu, E.J. Carcache-Blanco, A.D. Pawlus, S.K. Lee, E.J. Park, M. Cuendet, J.J. Gills, K. Bhat, H.-S. Park, E. Mata-Greenwood, L.L. Song, M. Jang, J.M. Pezzuto, Natural inhibitors of carcinogenesis, Planta Med. 70 (2004) 691–705.

[47] J.-Q. Gu, E.J. Park, J.S. Vigo, J.G. Graham, H.H.S. Fong, J.M. Pezzuto, A.D. Kinghorn, Activity-guided isolation of constituents of *Renealmia nicolaioides* with the potential to induce the phase II enzyme quinone reductase, J. Nat. Prod. 65 (2002) 1616–1620.

[48] B.-N. Su, E. Jung Park, J.S. Vigo, J.G. Graham, F. Cabieses, H.H.S. Fong, J.M. Pezzuto, A.D. Kinghorn, Activity-guided isolation of the chemical constituents of *Muntingia calabura* using a quinone reductase induction assay, Phytochemistry 63 (2003) 335–341.

[49] M. Cuendet, C.P. Oteham, R.C. Moon, J.M. Pezzuto, Quinone reductase induction as a biomarker for cancer chemoprevention, J. Nat. Prod. 69 (2006) 460–463.

[50] H.C. Chang, H.-W. Chen, H.-S. Tung, K.-L. Liu, C.-W. Tsai, C.-K. Lii, Butein Up-Regulates the Expression of the pi Class of Glutathione S-Transferase in Rat Primary Hepatocytes through the ERK/AP-1 Pathway, J. Agric. Food Chem. 58 (2010) 8994-9000.

[51] S.H. Lee, J.Y. Kim, G.S. Seo, Y.-C. Kim, D.H. Sohn, Isoliquiritigenin, from *Dalbergia odorifera*, up-regulates anti-inflammatory heme oxygenase-1 expression in RAW264.7 macrophages, Inflamm. Res. 58 (2009) 257–262.

[52] T. Ohtsuki, H. Kikuchi, T. Koyano, T. Kowithayakorn, T. Sakai, M. Ishibashi, Death receptor 5 promoter-enhancing compounds isolated from *Catimbium speciosum* and their enhancement effect on TRAIL-induced apoptosis, Bioorg. Med. Chem. 17 (2009) 6748–6754.

[53] E. Szliszka, Z.P. Czuba, B. Mazur, A. Paradysz, W. Krol, Chalcones and dihydrochalcones augment TRAIL-mediated apoptosis in prostate cancer cells, Molecules 15 (2010) 5336–5353.

[54] I. Park, K.-K. Park, J.H.Y. Park, W.-Y. Chung, Isoliquiritigenin induces G2 and M phase arrest by inducing DNA damage and by inhibiting the metaphase/anaphase transition, Cancer Lett. 277 (2009) 174–181.

[55] E. Szliszka, Z.P. Czuba, B. Mazur, L. Sedek, A. Paradysz, W. Krol, Chalcones enhance TRAIL-induced apoptosis in prostate cancer cells, Int. J. Mol. Sci. 11 (2009) 1–13.

[56] M.-S. Kim, J.Y. Kwon, N.J. Kang, K.W. Lee, H.J. Lee, Phloretin induces apoptosis in H-Ras MCF10A human breast tumor cells through the activation of p53 via JNK and p38 mitogen-activated protein kinase signaling, Ann. N. Y. Acad. Sci. 1171 (2009) 479–483.

[57] N. Nakatani, M. Ichimaru, M. Moriyasu, A. Kato, Induction of apoptosis in human promyelocytic leukemia cell line HL-60 by C-benzylated dihydrochalcones, uvaretin, isouvaretin and diuvaretin, Biol. Pharm. Bull. 28 (2005) 83–86.

[58] G. Chen, X. Hu, W. Zhang, N. Xu, F.-Q. Wang, J. Jia, W.-F. Zhang, Z.-J. Sun, Y.-F. Zhao, Mammalian target of rapamycin regulates isoliquiritigenin-induced autophagic and apoptotic cell death in adenoid cystic carcinoma cells, Apoptosis 17 (2012) 90–101.

[59] T. Akihisa, H. Tokuda, D. Hasegawa, M. Ukiya, Y. Kimura, F. Enjo, T. Suzuki, H. Nishino, Chalcones and other compounds from the exudates of *Angelica keiskei* and their cancer chemopreventive effects, J. Nat. Prod. 69 (2006) 38–42.

[60] V. Jhanji, H. Liu, K. Law, V.Y.-W. Lee, S.-F. Huang, C.-P. Pang, G.H.-F. Yam, Isoliquiritigenin from licorice root suppressed neovascularisation in experimental ocular angiogenesis models, Br. J. Ophthalmol. 95 (2011) 1309–1315.

[61] S. Yamazaki, T. Morita, H. Endo, T. Hamamoto, M. Baba, Y. Joichi, S. Kaneko, Y. Okada, T. Okuyama, H. Nishino, A. Tokue, Isoliquiritigenin suppresses pulmonary metastasis of mouse renal cell carcinoma, Cancer Lett. 183 (2002) 23–30.

[62] C.-Y. Ma, W.-T. Ji, F.-S. Chueh, J.-S. Yang, P.-Y. Chen, C.-C. Yu, J.-G. Chung, Butein inhibits the migration and invasion of SK-HEP-1 human hepatocarcinoma cells through suppressing the ERK, JNK, p38, and uPA signaling multiple pathways, J. Agric. Food Chem. 59 (2011) 9032–9038.

[63] A.W.L. Chua, H.S. Hay, P. Rajendran, M.K. Shanmugam, F. Li, P. Bist, E.S.C. Koay, L.H.K. Lim, A.P. Kumar, G. Sethi, Butein downregulates chemokine receptor CXCR4 expression and function through suppression of NF-κB activation in breast and pancreatic tumor cells, Biochem. Pharmacol. 80 (2010) 1553–1562.

[64] J.-K. Kim, E.K. Shin, J.H. Park, Y.H. Kim, J.H.Y. Park, Antitumor and antimetastatic effects of licochalcone A in mouse models, J. Mol. Med. 88 (2010) 829–838.

[65] Y.H. Kim, E.K. Shin, D.H. Kim, H.H. Lee, J.H.Y. Park, J.-K. Kim, Antiangiogenic effect of licochalcone A, Biochem. Pharmacol. 80 (2010) 1152–1159.

[66] Y.H. Choi, G.H. Yon, K.S. Hong, D.S. Yoo, C.W. Choi, W.-K. Park, J.Y. Kong, Y.S. Kim, S.Y. Ryu, *In vitro* BACE-1 inhibitory phenolic components from the seeds of *Psoralea corylifolia,* Planta Med. 74 (2008) 1405–1408.

[67] M.Y. Chung, M.-C. Rho, J.S. Ko, S.Y. Ryu, K.H. Jeune, K. Kim, H.S. Lee, Y.K. Kim, *In vitro* inhibition of diacylglycerol acyltransferase by prenylflavonoids from *Sophora flavescens,* Planta Med. 70 (2004) 258–260.

[68] J.R.L. Ehrenkranz, N.G. Lewis, C.R. Kahn, J. Roth, Phlorizin: a review, Diabetes Metab. Res. Rev. 21 (2005) 31–38.

[69] M. Najafian, M.Z. Jahromi, M.J. Nowroznejhad, P. Khajeaian, M.M. Kargar, M. Sadeghi, A. Arasteh, Phloridzin reduces blood glucose levels and improves lipids metabolism in streptozotocin-induced diabetic rats, Mol. Biol. Rep. 39 (2012) 5299–5306.

[70] S.N. Kim, S.J. Bae, H.B. Kwak, Y.K. Min, S.-H. Jung, C.-H. Kim, S.H. Kim, *In vitro* and *in vivo* osteogenic activity of licochalcone A, Amino Acids 42 (2012) 1455–1465.

[71] L. Zhu, H. Wei, Y. Wu, S. Yang, L. Xiao, J. Zhang, B. Peng, Licorice isoliquiritigenin suppresses RANKL-induced osteoclastogenesis *in vitro* and prevents inflammatory bone loss *in vivo,* Int. J. Biochem. Cell B. 44 (2012) 1139-1152.

[72] O. Nerya, R. Musa, S. Khatib, S. Tamir, J. Vaya, Chalcones as potent tyrosinase inhibitors: the effect of hydroxyl positions and numbers, Phytochemistry 65 (2004) 1389–1395.

[73] J.K. Son, J.S. Park, J.A. Kim, Y. Kim, S.R. Chung, S.H. Lee, Prenylated flavonoids from the roots of *Sophora flavescens* with tyrosinase inhibitory activity, Planta Med. 69 (2003) 559–561.

[74] L. Fan, X. Dang, Z. Shi, C. Zhang, K. Wang, Hydroxysafflor yellow A protects PC12 cells against the apoptosis induced by oxygen and glucose deprivation, Cell. Mol. Neurobiol. 31 (2011) 1187–1194.

[75] H. Zhu, Z. Wang, C. Ma, J. Tian, F. Fu, C. Li, D. Guo, E. Roeder, K. Liu, Neuroprotective effects of hydroxysafflor yellow A: *in vivo* and *in vitro* studies, Planta Med. 69 (2003) 429–433.

[76] Y. Tian, Z.-F. Yang, Y. Li, Y. Qiao, J. Yang, Y.-Y. Jia, A.-D. Wen, Pharmacokinetic comparisons of hydroxysafflower yellow A in normal and blood stasis syndrome rats, J. Ethnopharmacol. 129 (2010) 1–4.

[77] A. Wen, J. Yang, Y. Jia, Z. Yang, Y. Tian, Y. Wu, Z. Wang, Z. He, A rapid and sensitive liquid chromatography-tandem mass spectrometry (LC-MS/MS) method for the

determination of hydroxysafflor yellow A in human plasma: application to a pharmacokinetic study, J. Chromatogr. B Analyt. Technol. Biomed. Life Sci. 876 (2008) 41–46.

[78] H.W. Lee, H.Y. Ji, H.I. Lee, H.-K. Kim, D.H. Sohn, Y.-C. Kim, H.T. Chung, H.S. Lee, Determination of butein in rat serum by high performance liquid chromatography, J. Pharm. Biomed. Anal. 34 (2004) 227–231.

[79] M. Verzele, J. Stockx, F. Fontijn, M. Anteunis, Xanthohumol, a New Natural Chalkone, Bull. Soc. Chim. Belges 66 (1957) 452–475.

[80] F.B. Power, F. Tutin, H. Rogerson, CXXXV.?The constituents of hops, J. Chem. Soc., Trans. 103 (1913) 1267.

[81] H. Jung, S. Kang, S. Hyun, J. Choi, *In vitro* free radical and ONOO- scavengers from *Sophora flavescens,* Arch. Pharm. Res. 28 (2005) 534–540.

[82] J.F. Stevens, A.W. Taylor, G.B. Nickerson, M. Ivancic, J. Henning, A. Haunold, M.L. Deinzer, Prenylflavonoid variation in *Humulus lupulus*: distribution and taxonomic significance of xanthogalenol and 4´-O-methylxanthohumol, Phytochemistry 53 (2000) 759–775.

[83] P.J. Magalhães, L.F. Guido, J.M. Cruz, A.A. Barros, Analysis of xanthohumol and isoxanthohumol in different hop products by liquid chromatography-diode array detection-electrospray ionization tandem mass spectrometry, J. Chromatogr. A 1150 (2007) 295–301.

[84] J.F. Stevens, A.W. Taylor, M.L. Deinzer, Quantitative analysis of xanthohumol and related prenylflavonoids in hops and beer by liquid chromatography–tandem mass spectrometry, J. Chromatogr. A 832 (1999) 97–107.

[85] S. Wunderlich, A. Zürcher, W. Back, Enrichment of xanthohumol in the brewing process, Mol. Nutr. Food Res. 49 (2005) 874–881.

[86] S. Bhattacharya, S. Virani, M. Zavro, J.G. Haas, Inhibition of *Streptococcus mutans* and other oral Streptococci by hop (*Humulus Lupulus* L.), Econ. Bot. 57 (1) (2003) 118–125.

[87] N. Yamaguchi, K. Satoh-Yamaguchi, M. Ono, *In vitro* evaluation of antibacterial, anticollagenase, and antioxidant activities of hop components (*Humulus lupulus*) addressing acne vulgaris, Phytomedicine 16 (2009) 369–376.

[88] C. Davis, Normal Flora. Medical Microbiology, 4th edition in: Galveston (TX): University of Texas Medical Branch at Galveston, Baron S (Eds.), (1996) Chapter 6.

[89] S. Mizobuchi, Y. Sato, A New Flavanone with Antifungal Activity Isolated from Hops, Agric. Biol. Chem. 48 (11) (1984) 2771–2775.

[90] K. Sakai, N. Koyama, T. Fukuda, Y. Mori, H. Onaka, H. Tomoda, Search Method for Inhibitors of Staphyloxanthin Production by Methicillin-Resistant *Staphylococcus aureus*, Biol. Pharm. Bull. 35 (2012) 48–53.

[91] G.Y. Liu, A. Essex, J.T. Buchanan, V. Datta, H.M. Hoffman, J.F. Bastian, J. Fierer, V. Nizet, *Staphylococcus aureus* golden pigment impairs neutrophil killing and promotes virulence through its antioxidant activity, J. Exp. Med. 202 (2005) 209–215.

[92] H. Gollnick, W. Cunliffe, D. Berson, B. Dreno, A. Finlay, J. Leyden, A. Shalita, D. Thiboutot, Management of acne: a report from a Global Alliance to Improve Outcomes in Acne, J. Am. Acad. Dermatol. 49 (2003) S1-37.

[93] S. Läuchli, Acne vulgaris, Curr. Probl. Dermatol. 42 (2011) 140–146.

[94] V. Srinivasan, D. Goldberg, G. Haas, Contributions to the antimicrobial spectrum of hop constituents, Econ. Bot. 58 (2004) S230.

[95] M.T. Madigan, J.M. Martinko, J. Parker, T.D. Brock, W. Goebel, Mikrobiologie, Spektrum Akad. Verl., Berlin [u.a.], 2. corrected edition (2001).

[96] V.E. Buckwold, R.J.H. Wilson, A. Nalca, B.B. Beer, T.G. Voss, J.A. Turpin, R.W. Buckheit, J. Wei, M. Wenzel-Mathers, E.M. Walton, R.J. Smith, M. Pallansch, P. Ward, J. Wells, L. Chuvala, S. Sloane, R. Paulman, J. Russell, T. Hartman, R. Ptak, Antiviral activity of hop constituents against a series of DNA and RNA viruses, Antiviral Res. 61 (2004) 57–62.

[97] Q. Wang, Z.-H. Ding, J.-K. Liu, Y.-T. Zheng, Xanthohumol, a novel anti-HIV-1 agent purified from Hops *Humulus lupulus,* Antiviral. Res. 64 (2004) 189–194.

[98] N. Zhang, Z. Liu, Q. Han, J. Chen, S. Lou, J. Qiu, G. Zhang, Inhibition of bovine viral diarrhea virus *in vitro* by xanthohumol: comparisons with ribavirin and interferon-alpha and implications for the development of anti-hepatitis C virus agents, Eur. J. Pharm. Sci. 38 (2009) 332–340.

[99] E. Mutschler, Arzneimittelwirkungen. Lehrbuch der Pharmakologie und Toxikologie ; mit einführenden Kapiteln in die Anatomie, Physiologie und Pathophysiologie ; 264 Tabellen und 1357 Strukturformeln, Wiss. Verl.-Ges, Stuttgart, 9th edition (2008).

[100] N. Zhang, Z. Liu, Q. Han, J. Chen, Y. Lv, Xanthohumol enhances antiviral effect of interferon alpha-2b against bovine viral diarrhea virus, a surrogate of hepatitis C virus, Phytomedicine 17 (2010) 310–316.

[101] World Malaria Report 2011, World Health Organization, 2012.

[102] D.A. Fidock, T. Nomura, A.K. Talley, R.A. Cooper, S.M. Dzekunov, M.T. Ferdig, L.M. Ursos, A.B. Sidhu, B. Naudé, K.W. Deitsch, X.Z. Su, J.C. Wootton, P.D. Roepe, T.E. Wellems, Mutations in the *P. falciparum* digestive vacuole transmembrane protein PfCRT and evidence for their role in chloroquine resistance, Mol. Cell 6 (2000) 861–871.

[103] W. Herath, D. Ferreira, S.I. Khan, I.A. Khan, Identification and biological activity of microbial metabolites of xanthohumol, Chem. Pharm. Bull. 51 (2003) 1237–1240.

[104] W.P.T. James, The epidemiology of obesity: the size of the problem, J. Intern. Med. 263 (2008) 336–352.

[105] N. Tabata, M. Ito, H. Tomoda, S. Omura, Xanthohumols, diacylglycerol acyltransferase inhibitors, from *Humulus lupulus,* Phytochemistry 46 (1997) 683–687.

[106] K. Goto, T. Asai, S. Hara, I. Namatame, H. Tomoda, M. Ikemoto, N. Oku, Enhanced antitumor activity of xanthohumol, a diacylglycerol acyltransferase inhibitor, under hypoxia, Cancer Lett. 219 (2005) 215–222.

[107] M.M. Hussain, J. Shi, P. Dreizen, Microsomal triglyceride transfer protein and its role in apoB-lipoprotein assembly, J. Lipid Res. 44 (2003) 22–32.

[108] A. Casaschi, G.K. Maiyoh, B.K. Rubio, R.W. Li, K. Adeli, A.G. Theriault, The chalcone xanthohumol inhibits triglyceride and apolipoprotein B secretion in HepG2 cells, J. Nutr. 134 (2004) 1340–1346.

[109] H. Nozawa, Xanthohumol, the chalcone from beer hops (*Humulus lupulus* L.), is the ligand for farnesoid X receptor and ameliorates lipid and glucose metabolism in KK-A(y) mice, Biochem. Biophys. Res. Commun. 336 (2005) 754–761.

[110] B. Goodwin, S.A. Jones, R.R. Price, M.A. Watson, D.D. McKee, L.B. Moore, C. Galardi, J.G. Wilson, M.C. Lewis, M.E. Roth, P.R. Maloney, T.M. Willson, S.A. Kliewer, A regulatory cascade of the nuclear receptors FXR, SHP-1, and LRH-1 represses bile acid biosynthesis, Mol. Cell 6 (2000) 517–526.

[111] Y. Zhu, F. Li, G.L. Guo, Tissue-specific function of farnesoid X receptor in liver and intestine, Pharmacol. Res. 63 (2011) 259–265.

[112] S. Galic, J.S. Oakhill, G.R. Steinberg, Adipose tissue as an endocrine organ, Mol. Cell. Endocrinol. 316 (2010) 129–139.

[113] H. Oberkofler, N. Fukushima, H. Esterbauer, F. Krempler, W. Patsch, Sterol regulatory element binding proteins: relationship of adipose tissue gene expression with obesity in humans, Biochim. Biophys. Acta 1575 (2002) 75–81.

[114] J.-Y. Yang, M.A. Della-Fera, S. Rayalam, C.A. Baile, Effect of xanthohumol and isoxanthohumol on 3T3-L1 cell apoptosis and adipogenesis, Apoptosis 12 (2007) 1953–1963.

[115] F.M. Gregoire, C.M. Smas, H.S. Sul, Understanding adipocyte differentiation, Physiol. Rev. 78 (1998) 783–809.

[116] J.-Y. Yang, M.A. Della-Fera, S. Rayalam, C.A. Baile, Enhanced effects of xanthohumol plus honokiol on apoptosis in 3T3-L1 adipocytes, Obesity (Silver Spring) 16 (2008) 1232–1238.

[117] P.G. Kopelman, Obesity as a medical problem, Nature 404 (2000) 635–643.

[118] Y. Zhang, C. Huang, Targeting adipocyte apoptosis: a novel strategy for obesity therapy, Biochem. Biophys. Res. Commun. 417 (2012) 1–4.

[119] V. Mendes, R. Monteiro, D. Pestana, D. Teixeira, C. Calhau, I. Azevedo, Xanthohumol influences preadipocyte differentiation: implication of antiproliferative and apoptotic effects, J. Agric. Food Chem. 56 (2008) 11631–11637.

[120] T. Scholzen, J. Gerdes, The Ki-67 protein: from the known and the unknown, J. Cell. Physiol. 182 (2000) 311–322.

[121] W. Wuttke, H. Jarry, T. Becker, A. Schultens, V. Christoffel, C. Gorkow, D. Seidlová-Wuttke, Phytoestrogens: endocrine disrupters or replacement for hormone replacement therapy?, Maturitas 61 (2008) 159–170.

[122] V. Coxam, Phyto-oestrogens and bone health, Proc. Nutr. Soc. 67 (2008) 184–195.

[123] S.R. Milligan, J.C. Kalita, A. Heyerick, H. Rong, L. de Cooman, D. de Keukeleire, Identification of a potent phytoestrogen in hops (*Humulus lupulus* L.) and beer, J. Clin. Endocrinol. Metab. 84 (1999) 2249–2252.

[124] H. Tobe, Y. Muraki, K. Kitamura, O. Komiyama, Y. Sato, T. Sugioka, H.B. Maruyama, E. Matsuda, M. Nagai, Bone resorption inhibitors from hop extract, Biosci. Biotechnol. Biochem. 61 (1997) 158–159.

[125] K.E. Effenberger, S.A. Johnsen, D.G. Monroe, T.C. Spelsberg, J.J. Westendorf, Regulation of osteoblastic phenotype and gene expression by hop-derived phytoestrogens, J. Steroid Biochem. Mol. Biol. 96 (2005) 387–399.

[126] H.M. Jeong, E.H. Han, Y.H. Jin, Y.H. Choi, K.Y. Lee, H.G. Jeong, Xanthohumol from the hop plant stimulates osteoblast differentiation by RUNX2 activation, Biochem. Biophys. Res. Commun. 409 (2011) 82–89.

[127] F. Long, Building strong bones: molecular regulation of the osteoblast lineage, Nat. Rev. Mol. Cell Biol. 13 (2012) 27–38.

[128] M.E. McManus, W.M. Burgess, M.E. Veronese, A. Huggett, L.C. Quattrochi, R.H. Tukey, Metabolism of 2-acetylaminofluorene and benzo(a)pyrene and activation of food-derived heterocyclic amine mutagens by human cytochromes P-450, Cancer Res. 50 (1990) 3367–3376.

[129] C.L. Miranda, Y.H. Yang, M.C. Henderson, J.F. Stevens, G. Santana-Rios, M.L. Deinzer, D.R. Buhler, Prenylflavonoids from hops inhibit the metabolic activation of the carcinogenic heterocyclic amine 2-amino-3-methylimidazo[4, 5-f]quinoline, mediated by cDNA-expressed human CYP1A2, Drug Metab. Dispos. 28 (2000) 1297–1302.

[130] J. Plazar, B. Zegura, T.T. Lah, M. Filipic, Protective effects of xanthohumol against the genotoxicity of benzo(a)pyrene (BaP), 2-amino-3-methylimidazo[4,5-f]quinoline (IQ) and tert-butyl hydroperoxide (t-BOOH) in HepG2 human hepatoma cells, Mutat. Res. 632 (2007) 1–8.

[131] O. Viegas, B. Zegura, M. Pezdric, M. Novak, I.M.P.L.V.O. Ferreira, O. Pinho, M. Filipič, Protective effects of xanthohumol against the genotoxicity of heterocyclic aromatic amines MeIQx and PhIP in bacteria and in human hepatoma (HepG2) cells, Food Chem. Toxicol. 50 (2011) 949–955.

[132] F. Ferk, W.W. Huber, M. Filipic, J. Bichler, E. Haslinger, M. Misík, A. Nersesyan, B. Grasl-Kraupp, B. Zegura, S. Knasmüller, Xanthohumol, a prenylated flavonoid contained in beer, prevents the induction of preneoplastic lesions and DNA damage in liver and colon induced by the heterocyclic aromatic amine amino-3-methyl-imidazo[4,5-f]quinoline (IQ), Mutat. Res. 691 (2010) 17–22.

[133] M.C. Henderson, C.L. Miranda, J.F. Stevens, M.L. Deinzer, D.R. Buhler, *In vitro* inhibition of human P450 enzymes by prenylated flavonoids from hops, *Humulus lupulus,* Xenobiotica 30 (2000) 235–251.

[134] B.M. Dietz, Y.-H. Kang, G. Liu, A.L. Eggler, P. Yao, L.R. Chadwick, G.F. Pauli, N.R. Farnsworth, A.D. Mesecar, R.B. van Breemen, J.L. Bolton, Xanthohumol isolated from Humulus lupulus Inhibits menadione-induced DNA damage through induction of quinone reductase, Chem. Res. Toxicol. 18 (2005) 1296–1305.

[135] C.L. Miranda, G.L. Aponso, J.F. Stevens, M.L. Deinzer, D.R. Buhler, Prenylated chalcones and flavanones as inducers of quinone reductase in mouse Hepa 1c1c7 cells, Cancer Lett. 149 (2000) 21–29.

[136] G. Liu, A.L. Eggler, B.M. Dietz, A.D. Mesecar, J.L. Bolton, J.M. Pezzuto, R.B. van Breemen, Screening method for the discovery of potential cancer chemoprevention agents based on mass spectrometric detection of alkylated Keap1, Anal. Chem. 77 (2005) 6407–6414.

[137] Y. Luo, A.L. Eggler, D. Liu, G. Liu, A.D. Mesecar, R.B. van Breemen, Sites of alkylation of human Keap1 by natural chemoprevention agents, J. Am. Soc. Mass Spectrom. 18 (2007) 2226–2232.

[138] I.M. Copple, C.E. Goldring, N.R. Kitteringham, B.K. Park, The keap1-nrf2 cellular defense pathway: mechanisms of regulation and role in protection against drug-induced toxicity, Handb. Exp. Pharmacol. 196 (2010) 233–266.

[139] I.-S. Lee, J. Lim, J. Gal, J.C. Kang, H.J. Kim, B.Y. Kang, H.J. Choi, Anti-inflammatory activity of xanthohumol involves heme oxygenase-1 induction via NRF2-ARE signaling in microglial BV2 cells, Neurochem. Int. (Neurochemistry international) 58 (2011) 153–160.

[140] R. Ollinger, H. Wang, K. Yamashita, B. Wegiel, M. Thomas, R. Margreiter, F.H. Bach, Therapeutic applications of bilirubin and biliverdin in transplantation, Antioxid. Redox Signal. 9 (2007) 2175–2185.

[141] B. Halliwell, Reactive species and antioxidants. Redox biology is a fundamental theme of aerobic life, Plant Physiol. 141 (2006) 312–322.

[142] B. Halliwell, How to characterize an antioxidant: an update, Biochem. Soc. Symp. 61 (1995) 73–101.

[143] J.F. Curtin, M. Donovan, T.G. Cotter, Regulation and measurement of oxidative stress in apoptosis, J. Immunol. Methods 265 (2002) 49–72.

[144] C. Bubici, S. Papa, K. Dean, G. Franzoso, Mutual cross-talk between reactive oxygen species and nuclear factor-kappa B: molecular basis and biological significance, Oncogene 25 (2006) 6731–6748.

[145] P.G. Pietta, Flavonoids as antioxidants, J. Nat. Prod. 63 (2000) 1035–1042.

[146] C.L. Miranda, J.F. Stevens, V. Ivanov, M. McCall, B. Frei, M.L. Deinzer, D.R. Buhler, Antioxidant and prooxidant actions of prenylated and nonprenylated chalcones and flavanones *in vitro,* J. Agric. Food Chem. 48 (2000) 3876–3884.

[147] J.F. Stevens, C.L. Miranda, B. Frei, D.R. Buhler, Inhibition of peroxynitrite-mediated LDL oxidation by prenylated flavonoids: the alpha,beta-unsaturated keto functionality of 2'-hydroxychalcones as a novel antioxidant pharmacophore, Chem. Res. Toxicol. 16 (2003) 1277–1286.

[148] R.J. Rodriguez, C.L. Miranda, J.F. Stevens, M.L. Deinzer, D.R. Buhler, Influence of prenylated and non-prenylated flavonoids on liver microsomal lipid peroxidation and oxidative injury in rat hepatocytes, Food Chem. Toxicol. 39 (2001) 437–445.

[149] S.M. Qadri, H. Mahmud, M. Föller, F. Lang, Inhibition of suicidal erythrocyte death by xanthohumol, J. Agric. Food Chem. 57 (2009) 7591–7595.

[150] S. Vogel, S. Ohmayer, G. Brunner, J. Heilmann, Natural and non-natural prenylated chalcones: Synthesis, cytotoxicity and anti-oxidative activity, Bioorgan. Med. Chem. 16 (2008) 4286–4293.

[151] S. Vogel, J. Heilmann, Synthesis, cytotoxicity, and antioxidative activity of minor prenylated chalcones from *Humulus lupulus,* J. Nat. Prod. 71 (2008) 1237–1241.

[152] S. Vogel, M. Barbic, G. Jürgenliemk, J. Heilmann, Synthesis, cytotoxicity, anti-oxidative and anti-inflammatory activity of chalcones and influence of A-ring modifications on the pharmacological effect, Eur. J. Med. Chem. 45 (2010) 2206–2213.

[153] A. Dávalos, C. Gómez-Cordovés, B. Bartolomé, Extending applicability of the oxygen radical absorbance capacity (ORAC-fluorescein) assay, J. Agric. Food Chem. 52 (2004) 48–54.

[154] H. Schempp, S. Vogel, R. Hückelhoven, J. Heilmann, Re-evaluation of superoxide scavenging capacity of xanthohumol, Free Radic. Res. 44 (2010) 1435–1444.

[155] A. Hartkorn, F. Hoffmann, H. Ajamieh, S. Vogel, J. Heilmann, A.L. Gerbes, A.M. Vollmar, S. Zahler, Antioxidant effects of xanthohumol and functional impact on hepatic ischemia-reperfusion injury, J. Nat. Prod. 72 (2009) 1741–1747.

[156] C. Li, R.M. Jackson, Reactive species mechanisms of cellular hypoxia-reoxygenation injury, Am. J. Physiol., Cell Physiol. 282 (2002) C227-41.

[157] J. Strathmann, K. Klimo, S.W. Sauer, J.G. Okun, J.H.M. Prehn, C. Gerhäuser, Xanthohumol-induced transient superoxide anion radical formation triggers cancer cells into apoptosis via a mitochondria-mediated mechanism, FASEB J. 24 (2010) 2938–2950.

[158] M. Festa, A. Capasso, C.W. D'Acunto, M. Masullo, A.G. Rossi, C. Pizza, S. Piacente, Xanthohumol induces apoptosis in human malignant glioblastoma cells by increasing reactive oxygen species and activating MAPK pathways, J. Nat. Prod. 74 (2011) 2505–2513.

[159] M. Yilmazer, J.F. Stevens, M.L. Deinzer, D.R. Buhler, *In vitro* biotransformation of xanthohumol, a flavonoid from hops (*Humulus lupulus*), by rat liver microsomes, Drug Metab. Dispos. 29 (2001) 223–231.

[160] D. Nikolic, Y. Li, L.R. Chadwick, G.F. Pauli, R.B. van Breemen, Metabolism of xanthohumol and isoxanthohumol, prenylated flavonoids from hops (*Humulus lupulus* L.), by human liver microsomes, J. Mass. Spectrom. 40 (2005) 289–299.

[161] A. Mantovani, P. Allavena, A. Sica, F. Balkwill, Cancer-related inflammation, Nature 454 (2008) 436–444.

[162] M. Fujimoto, N. Shimizu, K. Kunii, J.A.J. Martyn, K. Ueki, M. Kaneki, A role for iNOS in fasting hyperglycemia and impaired insulin signaling in the liver of obese diabetic mice, Diabetes 54 (2005) 1340–1348.

[163] Y. Du, M.A. Smith, C.M. Miller, T.S. Kern, Diabetes-induced nitrative stress in the retina, and correction by aminoguanidine, J. Neurochem. 80 (2002) 771–779.

[164] R.K. Cross, K.T. Wilson, Nitric oxide in inflammatory bowel disease, Inflamm. Bowel Dis. 9 (2003) 179–189.

[165] U.N. Das, Acetylcholinesterase and butyrylcholinesterase as possible markers of low-grade systemic inflammation, Med. Sci. Monit. 13 (2007) RA214-21.

[166] C.A. Janeway, Immunologie, Spektrum, Akad. Verl., Heidelberg [u.a.], 5th edition (2002).

[167] F. Autschbach, J.C. Hoffmann, Chronisch entzündliche Darmerkrankungen. Das CED-Handbuch für Klinik und Praxis, Thieme, Stuttgart [u.a.], 1. edition (2004).

[168] S.C. Gupta, C. Sundaram, S. Reuter, B.B. Aggarwal, Inhibiting NF-κB activation by small molecules as a therapeutic strategy, Biochim. Biophys. Acta 1799 (2010) 775–787.

[169] A. Albini, R. Dell'Eva, R. Vené, N. Ferrari, D.R. Buhler, D.M. Noonan, G. Fassina, Mechanisms of the antiangiogenic activity by the hop flavonoid xanthohumol: NF-kappaB and Akt as targets, FASEB J. 20 (2006) 527–529.

[170] R. Dell'Eva, C. Ambrosini, N. Vannini, G. Piaggio, A. Albini, N. Ferrari, AKT/NF-kappaB inhibitor xanthohumol targets cell growth and angiogenesis in hematologic malignancies, Cancer 110 (2007) 2007–2011.

[171] C. Dorn, B. Kraus, M. Motyl, T.S. Weiss, M. Gehrig, J. Schölmerich, J. Heilmann, C. Hellerbrand, Xanthohumol, a chalcon derived from hops, inhibits hepatic inflammation and fibrosis, Mol. Nutr. Food Res. 54 Suppl 2 (2010) S205-13.

[172] Y.-C. Cho, H.J. Kim, Y.-J. Kim, K.Y. Lee, H.J. Choi, I.-S. Lee, B.Y. Kang, Differential anti-inflammatory pathway by xanthohumol in IFN-γ and LPS-activated macrophages, Int. Immunopharmacol. 8 (2008) 567–573.

[173] R. Monteiro, C. Calhau, A.O.E. Silva, S. Pinheiro-Silva, S. Guerreiro, F. Gärtner, I. Azevedo, R. Soares, Xanthohumol inhibits inflammatory factor production and angiogenesis in breast cancer xenografts, J. Cell. Biochem. 104 (2008) 1699–1707.

[174] S. Monteghirfo, F. Tosetti, C. Ambrosini, S. Stigliani, S. Pozzi, F. Frassoni, G. Fassina, S. Soverini, A. Albini, N. Ferrari, Antileukemia effects of xanthohumol in Bcr/Abl-transformed cells involve nuclear factor-kappaB and p53 modulation, Mol. Cancer Ther. 7 (2008) 2692–2702.

[175] E.C. Colgate, C.L. Miranda, J.F. Stevens, T.M. Bray, E. Ho, Xanthohumol, a prenylflavonoid derived from hops induces apoptosis and inhibits NF-kappaB activation in prostate epithelial cells, Cancer Lett. 246 (2007) 201–209.

[176] X. Gao, D. Deeb, Y. Liu, S. Gautam, S.A. Dulchavsky, S.C. Gautam, Immunomodulatory activity of xanthohumol: inhibition of T cell proliferation, cell-mediated cytotoxicity and Th1 cytokine production through suppression of NF-kappaB, Immunopharmacol. Immunotoxicol. 31 (2009) 477–484.

[177] J.M. Choi, H.J. Kim, K.Y. Lee, H.J. Choi, I.-S. Lee, B.Y. Kang, Increased IL-2 production in T cells by xanthohumol through enhanced NF-AT and AP-1 activity, Int. Immunopharmacol. 9 (2009) 103–107.

[178] M.R. Peluso, C.L. Miranda, D.J. Hobbs, R.R. Proteau, J.F. Stevens, Xanthohumol and related prenylated flavonoids inhibit inflammatory cytokine production in LPS-activated THP-1 monocytes: structure-activity relationships and in silico binding to myeloid differentiation protein-2 (MD-2), Planta Med. 76 (2010) 1536–1543.

[179] E. Lupinacci, J. Meijerink, J.-P. Vincken, B. Gabriele, H. Gruppen, R.F. Witkamp, Xanthohumol from hop (*Humulus lupulus* L.) is an efficient inhibitor of monocyte chemoattractant protein-1 and tumor necrosis factor-alpha release in LPS-stimulated RAW 264.7 mouse macrophages and U937 human monocytes, J. Agric. Food Chem. 57 (2009) 7274–7281.

[180] R. Negrão, R. Costa, D. Duarte, T.T. Gomes, P. Coelho, J.T. Guimarães, L. Guardão, I. Azevedo, R. Soares, Xanthohumol-supplemented beer modulates angiogenesis and inflammation in a skin wound healing model. Involvement of local adipocytes, J. Cell. Biochem. 113 (2012) 100–109.

[181] F. Zhao, H. Nozawa, A. Daikonnya, K. Kondo, S. Kitanaka, Inhibitors of nitric oxide production from hops (*Humulus lupulus* L.), Biol. Pharm. Bull. 26 (2003) 61–65.

[182] K.B. Harikumar, A.B. Kunnumakkara, K.S. Ahn, P. Anand, S. Krishnan, S. Guha, B.B. Aggarwal, Modification of the cysteine residues in IkappaBalpha kinase and NF-kappaB (p65) by xanthohumol leads to suppression of NF-kappaB-regulated gene products and potentiation of apoptosis in leukemia cells, Blood 113 (2009) 2003–2013.

[183] M. Triantafilou, K. Brandenburg, S. Kusumoto, K. Fukase, A. Mackie, U. Seydel, K. Triantafilou, Combinational clustering of receptors following stimulation by bacterial products determines lipopolysaccharide responses, Biochem. J. 381 (2004) 527–536.

[184] K. Schroder, P.J. Hertzog, T. Ravasi, D.A. Hume, Interferon-gamma: an overview of signals, mechanisms and functions, J. Leukoc. Biol. 75 (2004) 163–189.

[185] D. Stracke, T. Schulz, P. Prehm, Inhibitors of hyaluronan export from hops prevent osteoarthritic reactions, Mol. Nutr. Food Res. 55 (2011) 485–494.

[186] C.L. Miranda, J.F. Stevens, A. Helmrich, M.C. Henderson, R.J. Rodriguez, Y.-H. Yang, M.L. Deinzer, D.W. Barnes, D.R. Buhler, Antiproliferative and cytotoxic effects of prenylated flavonoids from hops (*Humulus lupulus*) in human cancer cell lines, Food Chem. Toxicol. 37 (1999) 271–285.

[187] B. Vanhoecke, L. Derycke, V. van Marck, H. Depypere, D. de Keukeleire, M. Bracke, Antiinvasive effect of xanthohumol, a prenylated chalcone present in hops (*Humulus lupulus* L.) and beer, Int. J. Cancer 117 (2005) 889–895.

[188] S. Lust, B. Vanhoecke, A. Janssens, J. Philippe, M. Bracke, F. Offner, Xanthohumol kills B-chronic lymphocytic leukemia cells by an apoptotic mechanism, Mol. Nutr. Food Res. 49 (2005) 844–850.

[189] S.H. Lee, H.J. Kim, J.S. Lee, I.-S. Lee, B.Y. Kang, Inhibition of topoisomerase I activity and efflux drug transporters' expression by xanthohumol. from hops, Arch. Pharm. Res. 30 (2007) 1435–1439.

[190] L. Pan, H. Becker, C. Gerhäuser, Xanthohumol induces apoptosis in cultured 40-16 human colon cancer cells by activation of the death receptor- and mitochondrial pathway, Mol. Nutr. Food Res. 49 (2005) 837–843.

[191] D. Deeb, X. Gao, H. Jiang, A.S. Arbab, S.A. Dulchavsky, S.C. Gautam, Growth inhibitory and apoptosis-inducing effects of xanthohumol, a prenylated chalone present in hops, in human prostate cancer cells, Anticancer Res. 30 (2010) 3333–3339.

[192] L. Delmulle, A. Bellahcène, W. Dhooge, F. Comhaire, F. Roelens, K. Huvaere, A. Heyerick, V. Castronovo, D. de Keukeleire, Anti-proliferative properties of prenylated

flavonoids from hops (*Humulus lupulus* L.) in human prostate cancer cell lines, Phytomedicine 13 (2006) 732–734.

[193] J.G. Drenzek, N.L. Seiler, R. Jaskula-Sztul, M.M. Rausch, S.L. Rose, Xanthohumol decreases Notch1 expression and cell growth by cell cycle arrest and induction of apoptosis in epithelial ovarian cancer cell lines, Gynecol. Oncol. 122 (2011) 396–401.

[194] C. Dorn, T.S. Weiss, J. Heilmann, C. Hellerbrand, Xanthohumol, a prenylated chalcone derived from hops, inhibits proliferation, migration and interleukin-8 expression of hepatocellular carcinoma cells, Int. J. Oncol. (International journal of oncology) 36 (2010) 435–441.

[195] Y.-C. Ho, C.-H. Liu, C.-N. Chen, K.-J. Duan, M.-T. Lin, Inhibitory effects of xanthohumol from hops (*Humulus lupulus* L.) on human hepatocellular carcinoma cell lines, Phytother. Res. 22 (2008) 1465–1468.

[196] N.T. Xuan, E. Shumilina, E. Gulbins, S. Gu, F. Götz, F. Lang, Triggering of dendritic cell apoptosis by xanthohumol, Mol. Nutr. Food Res. 54 Suppl 2 (2010) S214-24.

[197] M.R. Cook, J. Luo, M. Ndiaye, H. Chen, M. Kunnimalaiyaan, Xanthohumol inhibits the neuroendocrine transcription factor achaete-scute complex-like 1, suppresses proliferation, and induces phosphorylated ERK1/2 in medullary thyroid cancer, Am. J. Surg. 199 (2010) 315-8; discussion 318.

[198] C. Scaffidi, S. Fulda, A. Srinivasan, C. Friesen, F. Li, K.J. Tomaselli, K.M. Debatin, P.H. Krammer, M.E. Peter, Two CD95 (APO-1/Fas) signaling pathways, EMBO J. 17 (1998) 1675–1687.

[199] R.S.Y. Wong, Apoptosis in cancer: from pathogenesis to treatment, J. Exp. Clin. Cancer Res. 30 (2011) 87.

[200] G. Karp, Molekulare Zellbiologie. Mit 36 Tabellen, Springer, Berlin [u.a.], 1. edition (2005).

[201] E. Ulukaya, C. Acilan, Y. Yilmaz, Apoptosis: why and how does it occur in biology?, Cell Biochem. Funct. 29 (2011) 468–480.

[202] S. Lust, B. Vanhoecke, M. van Gele, J. Boelens, H. van Melckebeke, M. Kaileh, W. Vanden Berghe, G. Haegeman, J. Philippé, M. Bracke, F. Offner, Xanthohumol activates the proapoptotic arm of the unfolded protein response in chronic lymphocytic leukemia, Anticancer Res. 29 (2009) 3797–3805.

[203] L. Delmulle, T. Vanden Berghe, D. de Keukeleire, P. Vandenabeele, Treatment of PC-3 and DU145 prostate cancer cells by prenylflavonoids from hop (*Humulus lupulus* L.) induces a caspase-independent form of cell death, Phytother. Res. 22 (2008) 197–203.

[204] J. Boelens, S. Lust, F. Offner, M.E. Bracke, B.W. Vanhoecke, Review. The endoplasmic reticulum: a target for new anticancer drugs, In Vivo 21 (2007) 215–226.

[205] A. Fribley, C.-Y. Wang, Proteasome inhibitor induces apoptosis through induction of endoplasmic reticulum stress, Cancer Biol. Ther. 5 (2006) 745–748.

[206] W. Kolch, Meaningful relationships: the regulation of the Ras/Raf/MEK/ERK pathway by protein interactions, Biochem. J. 351 Pt 2 (2000) 289–305.

[207] A. Carpinteiro, C. Dumitru, M. Schenck, E. Gulbins, Ceramide-induced cell death in malignant cells, Cancer Lett. 264 (2008) 1–10.

[208] G.T. Wondrak, Redox-directed cancer therapeutics: molecular mechanisms and opportunities, Antioxid. Redox Signal. 11 (2009) 3013–3069.

[209] R. Monteiro, H. Becker, I. Azevedo, C. Calhau, Effect of hop (*Humulus lupulus* L.) flavonoids on aromatase (estrogen synthase) activity, J. Agric. Food Chem. 54 (2006) 2938–2943.

[210] R. Monteiro, A. Faria, I. Azevedo, C. Calhau, Modulation of breast cancer cell survival by aromatase inhibiting hop (*Humulus lupulus* L.) flavonoids, J. Steroid Biochem. Mol. Biol. 105 (2007) 124–130.

[211] L.P. Hemachandra, P. Madhubhani, R. Chandrasena, P. Esala, S.-N. Chen, M. Main, D.C. Lankin, R.A. Scism, B.M. Dietz, G.F. Pauli, G.R.J. Thatcher, J.L. Bolton, Hops (*Humulus lupulus*) inhibits oxidative estrogen metabolism and estrogen-induced malignant transformation in human mammary epithelial cells (MCF-10A), Cancer Prev. Res. (Phila) 5 (2012) 73–81.

[212] S. Guerreiro, R. Monteiro, M.J. Martins, C. Calhau, I. Azevedo, R. Soares, Distinct modulation of alkaline phosphatase isoenzymes by 17beta-estradiol and xanthohumol in breast cancer MCF-7 cells, Clin. Biochem. 40 (2007) 268–273.

[213] A. Ben-Arie, Z. Hagay, H. Ben-Hur, M. Open, R. Dgani, Elevated serum alkaline phosphatase may enable early diagnosis of ovarian cancer, Eur. J. Obstet. Gyn. R. B. 86 (1999) 69–71.

[214] J.L. Millán, W.H. Fishman, Biology of human alkaline phosphatases with special reference to cancer, Crit. Rev. Clin. Lab. Sci. 32 (1995) 1–39.

[215] I. Zajc, M. Filipič, T.T. Lah, Xanthohumol Induces Different Cytotoxicity and Apoptotic Pathways in Malignant and Normal Astrocytes, Phytother. Res. not known (2012) not known, yet.

[216] R. Negrão, R. Costa, D. Duarte, T. Taveira Gomes, M. Mendanha, L. Moura, L. Vasques, I. Azevedo, R. Soares, Angiogenesis and inflammation signaling are targets of beer polyphenols on vascular cells, J. Cell. Biochem. 111 (2010) 1270–1279.

[217] N. Philips, M. Samuel, R. Arena, Y.-J. Chen, J. Conte, P. Natarajan, P. Natrajan, G. Haas, S. Gonzalez, Direct inhibition of elastase and matrixmetalloproteinases and stimulation of biosynthesis of fibrillar collagens, elastin, and fibrillins by xanthohumol, J. Cosmet. Sci. 61 (2010) 125–132.

[218] S.M. Weis, D.A. Cheresh, Tumor angiogenesis: molecular pathways and therapeutic targets, Nat. Med. 17 (2011) 1359–1370.

[219] K. Xie, D. Wei, Q. Shi, S. Huang, Constitutive and inducible expression and regulation of vascular endothelial growth factor, Cytokine Growth F. R. 15 (2004) 297–324.

[220] J. Rudzitis-Auth, C. Körbel, C. Scheuer, M.D. Menger, M.W. Laschke, Xanthohumol inhibits growth and vascularization of developing endometriotic lesions, Hum. Reprod. 27 (6) (2012) 1735-44.

[221] R. Hussong, N. Frank, J. Knauft, C. Ittrich, R. Owen, H. Becker, C. Gerhäuser, A safety study of oral xanthohumol administration and its influence on fertility in Sprague Dawley rats, Mol. Nutr. Food Res. 49 (2005) 861–867.

[222] C. Dorn, F. Bataille, E. Gaebele, J. Heilmann, C. Hellerbrand, Xanthohumol feeding does not impair organ function and homoeostasis in mice, Food Chem. Toxicol. 48 (2010) 1890–1897.

[223] L. Hanske, R. Hussong, N. Frank, C. Gerhäuser, M. Blaut, A. Braune, Xanthohumol does not affect the composition of rat intestinal microbiota, Mol. Nutr. Food Res. 49 (2005) 868–873.

[224] B. Avula, M. Ganzera, J.E. Warnick, M.W. Feltenstein, K.J. Sufka, I.A. Khan, High-performance liquid chromatographic determination of xanthohumol in rat plasma, urine, and fecal samples, J. Chromatogr. Sci. 42 (2004) 378–382.

[225] L. Legette, L. Ma, R.L. Reed, C.L. Miranda, J.M. Christensen, R. Rodriguez-Proteau, J.F. Stevens, Pharmacokinetics of xanthohumol and metabolites in rats after oral and intravenous administration, Mol. Nutr. Food Res. 56 (2011) 466-474.

[226] M. Motyl, B. Kraus, J. Heilmann, Pitfalls in cell culture work with xanthohumol, Pharmazie 67 (2012) 91–94.

[227] Y. Pang, D. Nikolic, D. Zhu, L.R. Chadwick, G.F. Pauli, N.R. Farnsworth, R.B. van Breemen, Binding of the hop (*Humulus lupulus* L.) chalcone xanthohumol to cytosolic proteins in Caco-2 intestinal epithelial cells, Mol. Nutr. Food Res. 51 (2007) 872–879.

[228] H. Wolff, M. Motyl, C. Hellerbrand, J. Heilmann, B. Kraus, Xanthohumol uptake and intracellular kinetics in hepatocytes, hepatic stellate cells, and intestinal cells, J. Agric. Food Chem. 59 (2011) 12893–12901.

[229] M. Yilmazer, J.F. Stevens, D.R. Buhler, *In vitro* glucuronidation of xanthohumol, a flavonoid in hop and beer, by rat and human liver microsomes, FEBS Lett. 491 (2001) 252–256.

[230] C.E. Ruefer, C. Gerhäuser, N. Frank, H. Becker, S.E. Kulling, *In vitro* phase II metabolism of xanthohumol by human UDP-glucuronosyltransferases and sulfotransferases, Mol. Nutr. Food Res. 49 (2005) 851–856.

[231] W.H.M.W. Herath, D. Ferreira, I.A. Khan, Microbial transformation of xanthohumol, Phytochemistry 62 (2003) 673–677.

[232] H.J. Kim, I.-S. Lee, Microbial metabolism of the prenylated chalcone xanthohumol, J. Nat. Prod. 69 (2006) 1522–1524.

[233] A. Nookandeh, N. Frank, F. Steiner, R. Ellinger, B. Schneider, C. Gerhäuser, H. Becker, Xanthohumol metabolites in faeces of rats, Phytochemistry 65 (2004) 561–570.

[234] S. Possemiers, S. Bolca, C. Grootaert, A. Heyerick, K. Decroos, W. Dhooge, D. de Keukeleire, S. Rabot, W. Verstraete, T. van de Wiele, The prenylflavonoid isoxanthohumol from hops (*Humulus lupulus* L.) is activated into the potent phytoestrogen 8-prenylnaringenin *in vitro* and in the human intestine, J. Nutr. 136 (2006) 1862–1867.

[235] S. Possemiers, A. Heyerick, V. Robbens, D. de Keukeleire, W. Verstraete, Activation of proestrogens from hops (*Humulus lupulus* L.) by intestinal microbiota; conversion of isoxanthohumol into 8-prenylnaringenin, J. Agric. Food Chem. 53 (2005) 6281–6288.

[236] L. Hanske, G. Loh, S. Sczesny, M. Blaut, A. Braune, Recovery and metabolism of xanthohumol in germ-free and human microbiota-associated rats, Mol. Nutr. Food Res. 54 (2010) 1405–1413.

[237] S. Bolca, S. Possemiers, V. Maervoet, I. Huybrechts, A. Heyerick, S. Vervarcke, H. Depypere, D. de Keukeleire, M. Bracke, S. de Henauw, W. Verstraete, T. van de Wiele, Microbial and dietary factors associated with the 8-prenylnaringenin producer phenotype: a dietary intervention trial with fifty healthy post-menopausal Caucasian women, Br. J. Nutr. 98 (2007) 950–959.

[238] J. Guo, D. Nikolic, L.R. Chadwick, G.F. Pauli, R.B. van Breemen, Identification of human hepatic cytochrome P450 enzymes involved in the metabolism of 8-prenylnaringenin and isoxanthohumol from hops (*Humulus lupulus* L.), Drug Metab. Dispos. 34 (2006) 1152–1159.

[239] K. Ueda, ABC proteins protect the human body and maintain optimal health, Biosci. Biotechnol. Biochem. 75 (2011) 401–409.

[240] M.J. Zamek-Gliszczynski, K.A. Hoffmaster, K.-i. Nezasa, M.N. Tallman, K.L.R. Brouwer, Integration of hepatic drug transporters and phase II metabolizing enzymes: mechanisms of hepatic excretion of sulfate, glucuronide, and glutathione metabolites, Eur. J. Pharm. Sci. 27 (2006) 447–486.

[241] R. Rodriguez-Proteau, J.E. Mata, C.L. Miranda, Y. Fan, J.J. Brown, D.R. Buhler, Plant polyphenols and multidrug resistance: effects of dietary flavonoids on drug transporters in Caco-2 and MDCKII-MDR1 cell transport models, Xenobiotica 36 (2006) 41–58.

[242] J.-S. Taur, R. Rodriguez-Proteau, Effects of dietary flavonoids on the transport of cimetidine via P-glycoprotein and cationic transporters in Caco-2 and LLC-PK1 cell models, Xenobiotica 38 (2008) 1536–1550.

[243] P. Li, S.E. Tabibi, S.H. Yalkowsky, Combined effect of complexation and pH on solubilization, J. Pharm. Sci. 87 (1998) 1535–1537.

[244] B. Schnabl, Y.H. Choi, J.C. Olsen, C.H. Hagedorn, D.A. Brenner, Immortal activated human hepatic stellate cells generated by ectopic telomerase expression, Lab. Invest. 82 (2002) 323–333.

[245] V.S. Parmar, S.C. Jain, K.S. Bisht, R. Jain, P. Taneja, A. Jha, O.D. Tyagi, A.K. Prasad, J. Wengel, C. Olsen, P.M. Boll, Phytochemistry of the genus *Piper*, Phytochemistry 46 (1997) 597–673.

[246] C. Bheemasankara Rao, T. Namosiva Rao, S. Suryaprakasam, Cardamonin and alpinetin from the seeds of *Amomum subulatum*, Planta. Med. 29 (1976) 391–392.

[247] P. Boeck, C.A. Bandeira Falcão, P.C. Leal, R.A. Yunes, V.C. Filho, E.C. Torres-Santos, B. Rossi-Bergmann, Synthesis of chalcone analogues with increased antileishmanial activity, Bioorg. Med. Chem. 14 (2006) 1538–1545.

[248] F. Bohlmann, W.-R. Abraham, Neue diterpene und weitere inhaltsstoffe aus *Helichrysum calliconum* und *Helichrysum heterolasium*, Phytochemistry 18 (1979) 889–891.

[249] E.C. Leal, A. Manivannan, K.-I. Hosoya, T. Terasaki, J. Cunha-Vaz, A.F. Ambrósio, J.V. Forrester, Inducible nitric oxide synthase isoform is a key mediator of leukostasis and blood-retinal barrier breakdown in diabetic retinopathy, Invest. Ophthalmol. Vis. Sci. 48 (2007) 5257–5265.

[250] S. Singh, A.K. Gupta, Nitric oxide: role in tumour biology and iNOS/NO-based anticancer therapies, Cancer Chemother. Pharmacol. 67 (2011) 1211–1224.

[251] M. Murata, R. Thanan, N. Ma, S. Kawanishi, Role of nitrative and oxidative DNA damage in inflammation-related carcinogenesis, J. Biomed. Biotechnol. 2012 (2012) 623019 (11 pages).

[252] K. Zafirellis, A. Zachaki, G. Agrogiannis, K. Gravani, Inducible nitric oxide synthase expression and its prognostic significance in colorectal cancer, APMIS 118 (2010) 115–124.

[253] C.-N. Chen, F.-J. Hsieh, Y.-M. Cheng, K.-J. Chang, P.-H. Lee, Expression of inducible nitric oxide synthase and cyclooxygenase-2 in angiogenesis and clinical outcome of human gastric cancer, J. Surg. Oncol. 94 (2006) 226–233.

[254] W.-l. Chen, K.-x. Ouyang, H.-g. Li, Z.-q. Huang, J.-s. Li, J.-g. Wang, Expression of inducible nitric oxide synthase and vascular endothelial growth factor in ameloblastoma, J. Craniofac. Surg. 20 (2009) 171-5; discussion 176-7.

[255] J. MacMicking, Q.W. Xie, C. Nathan, Nitric oxide and macrophage function, Annu. Rev. Immunol. 15 (1997) 323–350.

[256] D. Siripin, S. Fucharoen, D.I. Tanyong, Nitric oxide and caspase 3 mediated cytokine induced apoptosis in acute leukemia, Asian Pac. J. Allergy Immunol. 29 (2011) 102–111.

[257] G. Kong, E.K. Kim, W.S. Kim, Y.W. Lee, J.K. Lee, S.W. Paik, J.C. Rhee, K.W. Choi, K.T. Lee, Inducible nitric oxide synthase (iNOS) immunoreactivity and its relationship to cell proliferation, apoptosis, angiogenesis, clinicopathologic characteristics, and patient survival in pancreatic cancer, Int. J. Pancreatol. 29 (2001) 133–140.

[258] C.-T. Lin, K.J. Senthil Kumar, Y.-H. Tseng, Z.-J. Wang, M.-Y. Pan, J.-H. Xiao, S.-C. Chien, S.-Y. Wang, Anti-inflammatory activity of Flavokawain B from *Alpinia pricei* Hayata, J. Agric. Food Chem. 57 (2009) 6060–6065.

[259] Di Wu, M.G. Nair, D.L. DeWitt, Novel compounds from *Piper methysticum* Forst (Kava Kava) roots and their effect on cyclooxygenase enzyme, J. Agric. Food Chem. 50 (2002) 701–705.

[260] P. Zhou, S. Gross, J.-H. Liu, B.-Y. Yu, L.-L. Feng, J. Nolta, V. Sharma, D. Piwnica-Worms, S.X. Qiu, Flavokawain B, the hepatotoxic constituent from kava root, induces GSH-sensitive oxidative stress through modulation of IKK/NF-kappaB and MAPK signaling pathways, FASEB J. 24 (2010) 4722–4732.

[261] F. Folmer, R. Blasius, F. Morceau, J. Tabudravu, M. Dicato, M. Jaspars, M. Diederich, Inhibition of TNFalpha-induced activation of nuclear factor kappaB by kava (*Piper methysticum*) derivatives, Biochem. Pharmacol. 71 (2006) 1206–1218.

[262] J.-H. Lee, H.S. Jung, P.M. Giang, X. Jin, S. Lee, P.T. Son, D. Lee, Y.-S. Hong, K. Lee, J.J. Lee, Blockade of nuclear factor-kappaB signaling pathway and anti-inflammatory activity of cardamomin, a chalcone analog from *Alpinia conchigera,* J. Pharmacol. Exp. Ther. 316 (2006) 271–278.

[263] Y. Qin, C.-Y. Sun, F.-R. Lu, X.-R. Shu, Di Yang, L. Chen, X.-M. She, N.M. Gregg, T. Guo, Y. Hu, Cardamonin exerts potent activity against multiple myeloma through blockade of NF-κB pathway in vitro, Leuk. Res. 36 (2012) 514–520.

[264] D.A. Israf, T.A. Khaizurin, A. Syahida, N.H. Lajis, S. Khozirah, Cardamonin inhibits COX and iNOS expression via inhibition of p65NF-kappaB nuclear translocation and Ikappa-B phosphorylation in RAW 264.7 macrophage cells, Mol. Immunol. 44 (2007) 673–679.

[265] S. Ahmad, D.A. Israf, N.H. Lajis, K. Shaari, H. Mohamed, A.A. Wahab, K.T. Ariffin, W.Y. Hoo, N.A. Aziz, A.A. Kadir, M.R. Sulaiman, M.N. Somchit, Cardamonin, inhibits pro-inflammatory mediators in activated RAW 264.7 cells and whole blood, Eur. J. Pharmacol. 538 (2006) 188–194.

[266] Y.-L. Chow, K.-H. Lee, S. Vidyadaran, N.H. Lajis, M.N. Akhtar, D.A. Israf, A. Syahida, Cardamonin from *Alpinia rafflesiana* inhibits inflammatory responses in IFN-γ/LPS-stimulated BV2 microglia via NF-κB signalling pathway, Int. Immunopharmacol. 12 (2012) 657–665.

[267] S. Hatziieremia, A.I. Gray, V.A. Ferro, A. Paul, R. Plevin, The effects of cardamonin on lipopolysaccharide-induced inflammatory protein production and MAP kinase and NFkappaB signalling pathways in monocytes/macrophages, Br. J. Pharmacol. 149 (2006) 188–198.

[268] C. Schütt, B. Bröker, Grundwissen Immunologie, Spektrum Akademischer Verlag, Heidelberg, 3. edition (2011).

[269] V.M. Dirsch, H.-P. Keiss, A.M. Vollmar, Garlic metabolites fail to inhibit the activation of the transcription factor NF-kappaB and subsequent expression of the adhesion molecule E-selectin in human endothelial cells, Eur. J. Nutr. 43 (2004) 55–59.

[270] I. Caliş, M. Barbic, G. Jürgenliemk, Bioactive cycloartane-type triterpene glycosides from *Astragalus elongatus*, Z. Naturforsch., C, J. Biosci. 63 (2008) 813–820.

[271] N. Li, J.-H. Liu, J. Zhang, B.-Y. Yu, Comparative evaluation of cytotoxicity and antioxidative activity of 20 flavonoids, J. Agric. Food Chem. 56 (2008) 3876–3883.

[272] J.-W. Jhoo, J.P. Freeman, T.M. Heinze, J.D. Moody, L.K. Schnackenberg, R.D. Beger, K. Dragull, C.-S. Tang, C.Y.W. Ang, *In vitro* cytotoxicity of nonpolar constituents from different parts of kava plant (*Piper methysticum*), J. Agric. Food Chem. 54 (2006) 3157–3162.

[273] Y.-C. Hseu, M.-S. Lee, C.-R. Wu, H.-J. Cho, K.-Y. Lin, G.-H. Lai, S.-Y. Wang, Y.-H. Kuo, K.J. Senthil Kumar, H.-L. Yang, The Chalcone Flavokawain B Induces G(2)/M Cell-Cycle Arrest and Apoptosis in Human Oral Carcinoma HSC-3 Cells through the Intracellular ROS Generation and Downregulation of the Akt/p38 MAPK Signaling Pathway, J. Agric. Food Chem. 60 (2012) 2385–2397.

[274] Y.-F. Kuo, Y.-Z. Su, Y.-H. Tseng, S.-Y. Wang, H.-M. Wang, P.J. Chueh, Flavokawain B, a novel chalcone from *Alpinia pricei* Hayata with potent apoptotic activity: Involvement of ROS and GADD153 upstream of mitochondria-dependent apoptosis in HCT116 cells, Free Radic. Biol. Med. 49 (2010) 214–226.

[275] Y. Tang, X. Li, Z. Liu, A.R. Simoneau, J. Xie, X. Zi, Flavokawain B, a kava chalcone, induces apoptosis via up-regulation of death-receptor 5 and Bim expression in androgen

receptor negative, hormonal refractory prostate cancer cell lines and reduces tumor growth, Int. J. Cancer 127 (2010) 1758–1768.

[276] X. Zi, A.R. Simoneau, Flavokawain A, a novel chalcone from kava extract, induces apoptosis in bladder cancer cells by involvement of Bax protein-dependent and mitochondria-dependent apoptotic pathway and suppresses tumor growth in mice, Cancer Res. 65 (2005) 3479–3486.

[277] Y. Tang, A.R. Simoneau, J. Xie, B. Shahandeh, X. Zi, Effects of the kava chalcone flavokawain A differ in bladder cancer cells with wild-type versus mutant p53, Cancer Prev. Res. (Phila) 1 (2008) 439–451.

[278] M.J. Simirgiotis, S. Adachi, S. To, H. Yang, K.A. Reynertson, M.J. Basile, R.R. Gil, I.B. Weinstein, E.J. Kennelly, Cytotoxic chalcones and antioxidants from the fruits of a *Syzygium samarangense* (Wax Jambu), Food Chem. 107 (2008) 813–819.

[279] V.R. Yadav, S. Prasad, B.B. Aggarwal, Cardamonin sensitizes tumour cells to TRAIL through ROS- and CHOP-mediated up-regulation of death receptors and down-regulation of survival proteins, Br. J. Pharmacol. 165 (2012) 741–753.

[280] T. Morikawa, K. Funakoshi, K. Ninomiya, D. Yasuda, K. Miyagawa, H. Matsuda, M. Yoshikawa, Medicinal foodstuffs. XXXIV. Structures of new prenylchalcones and prenylflavanones with TNF-alpha and aminopeptidase N inhibitory activities from *Boesenbergia rotunda,* Chem. Pharm. Bull. 56 (2008) 956–962.

[281] A. Mori, T. Mizusaki, Y. Miyakawa, E. Ohashi, T. Haga, T. Maegawa, Y. Monguchi, H. Sajiki, Chemoselective hydrogenation method catalyzed by Pd/C using diphenylsulfide as a reasonable catalyst poison, Tetrahedron 62 (2006) 11925–11932.

[282] T. Mosmann, Rapid colorimetric assay for cellular growth and survival: Application to proliferation and cytotoxicity assays, J. Immunol. Methods 65 (1983) 55–63.

[283] K. Saotome, H. Morita, M. Umeda, Cytotoxicity test with simplified crystal violet staining method using microtitre plates and its application to injection drugs, Toxicol. In Vitro 3 (1989) 317–321.

[284] E. Park, Quinn, C.E. Wright, G. Schuller-Levis, Taurine chloramine inhibits the synthesis of nitric oxide and the release of tumor necrosis factor in activated RAW 264.7 cells, J. Leukoc. Biol. 54 (1993) 119–124.

[285] D. Tsikas, Analysis of nitrite and nitrate in biological fluids by assays based on the Griess reaction: appraisal of the Griess reaction in the L-arginine/nitric oxide area of research, J. Chromatogr. B Analyt. Technol. Biomed. Life Sci. 851 (2007) 51–70.

[286] H. Senoo, K. Yoshikawa, M. Morii, M. Miura, K. Imai, Y. Mezaki, Hepatic stellate cell (vitamin A-storing cell) and its relative--past, present and future, Cell Biol. Int. 34 (2010) 1247–1272.

[287] R. Werdehausen, S. Braun, S. Fazeli, H. Hermanns, M.W. Hollmann, I. Bauer, M.F. Stevens, Lipophilicity but not stereospecificity is a major determinant of local anaesthetic-induced cytotoxicity in human T-lymphoma cells, Eur. J. Anaesthesiol. 29 (2012) 35–41.

[288] U. Neuhaus-Steinmetz, L. Rensing, Heat shock protein induction by certain chemical stressors is correlated with their cytotoxicity, lipophilicity and protein-denaturing capacity, Toxicology 123 (1997) 185–195.

[289] N.P. Reddy, P. Aparoy, T.C.M. Reddy, C. Achari, P.R. Sridhar, P. Reddanna, Design, synthesis, and biological evaluation of prenylated chalcones as 5-LOX inhibitors, Bioorgan. Med. Chem. 18 (2010) 5807–5815.

[290] H. Tobe, T. Hata, M. Ishikawa, Study on possible mechanism of induction of nerve growth factor (NGF) by xanthohumol (XH) isolated from hop extract - action of XH on the membrane components of swine brain nerve cell, KKKSGGK 54 (2009) 45–54.

[291] D. Barron, R.K. Ibrahim, Isoprenylated flavonoids—a survey, Phytochemistry 43 (1996) 921–982.

[292] H.A. Jung, T. Yokozawa, B.-W. Kim, J.H. Jung, J.S. Choi, Selective inhibition of prenylated flavonoids from *Sophora flavescens* against BACE1 and cholinesterases, Am. J. Chin. Med. 38 (2010) 415–429.

[293] W. Wätjen, N. Weber, Y.-j. Lou, Z.-q. Wang, Y. Chovolou, A. Kampkötter, R. Kahl, P. Proksch, Prenylation enhances cytotoxicity of apigenin and liquiritigenin in rat H4IIE hepatoma and C6 glioma cells, Food Chem. Toxicol. 45 (2007) 119–124.

[294] F. Cottiglia, L. Casu, L. Bonsignore, M. Casu, C. Floris, M. Leonti, J. Gertsch, J. Heilmann, New cytotoxic prenylated isoflavonoids from *Bituminaria morisiana,* Planta Med. 71 (2005) 254–260.

[295] Y.-C. Liu, C.-W. Hsieh, C.-C. Wu, B.-S. Wung, Chalcone inhibits the activation of NF-kappaB and STAT3 in endothelial cells via endogenous electrophile, Life Sci. 80 (2007) 1420–1430.

[296] T.S. Weiss, B. Jahn, M. Cetto, K.-W. Jauch, W.E. Thasler, Collagen sandwich culture affects intracellular polyamine levels of human hepatocytes, Cell Prolif. 35 (2002) 257–267.

[297] T.S. Weiss, S. Pahernik, I. Scheruebl, K.-W. Jauch, W.E. Thasler, Cellular damage to human hepatocytes through repeated application of 5-aminolevulinic acid, J. Hepatol. 38 (2003) 476–482.

[298] M. van Cleemput, K. Cattoor, K. de Bosscher, G. Haegeman, D. de Keukeleire, A. Heyerick, Hop (*Humulus lupulus*)-derived bitter acids as multipotent bioactive compounds, J. Nat. Prod. 72 (2009) 1220–1230.

[299] P.J. Magalhães, D.O. Carvalho, J.M. Cruz, L.F. Guido, A.A. Barros, Fundamentals and health benefits of xanthohumol, a natural product derived from hops and beer, Nat. Prod. Commun. 4 (2009) 591–610.

[300] M. Sägesser, M.L. Deinzer, HPLC-ion spray-tandem mass spectrometry of flavonol glycosides in hops, J. Am. Soc. Brew. Chem. 54 (1996) 129–134.

[301] H.-J. Li, M.L. Deinzer, Structural identification and distribution of proanthocyanidins in 13 different hops, J. Agric. Food Chem. 54 (2006) 4048–4056.

[302] P.C. Hollman, J.M. van Trijp, M.N. Buysman, M.S. van der Gaag, M.J. Mengelers, J.H. de Vries, M.B. Katan, Relative bioavailability of the antioxidant flavonoid quercetin from various foods in man, FEBS Lett. 418 (1997) 152–156.

[303] W. Wiczkowski, J. Romaszko, A. Bucinski, D. Szawara-Nowak, J. Honke, H. Zielinski, M.K. Piskula, Quercetin from shallots (*Allium cepa* L. var. aggregatum) is more bioavailable than its glucosides, J. Nutr. 138 (2008) 885–888.

[304] J.H. de Vries, P.C. Hollman, I. van Amersfoort, M.R. Olthof, M.B. Katan, Red wine is a poor source of bioavailable flavonols in men, J. Nutr. 131 (2001) 745–748.

[305] C. Manach, G. Williamson, C. Morand, A. Scalbert, C. Rémésy, Bioavailability and bioefficacy of polyphenols in humans. I. Review of 97 bioavailability studies, Am. J. Clin. Nutr. 81 (2005) 230S-242S.

[306] A. Crozier, J. Burns, A.A. Aziz, A.J. Stewart, H.S. Rabiasz, G.I. Jenkins, C.A. Edwards, M.E. Lean, Antioxidant flavonols from fruits, vegetables and beverages: measurements and bioavailability, Biol. Res. 33 (2000) 79–88.

[307] J.F. Stevens, J.E. Page, Xanthohumol and related prenylflavonoids from hops and beer: to your good health!, Phytochemistry 65 (2004) 1317–1330.

[308] L. Wang, M.E. Morris, Liquid chromatography-tandem mass spectroscopy assay for quercetin and conjugated quercetin metabolites in human plasma and urine, J. Chromatogr. B Analyt. Technol. Biomed. Life Sci. 821 (2005) 194–201.

[309] S. Egert, S. Wolffram, A. Bosy-Westphal, C. Boesch-Saadatmandi, A.E. Wagner, J. Frank, G. Rimbach, M.J. Mueller, Daily quercetin supplementation dose-dependently increases plasma quercetin concentrations in healthy humans, J. Nutr. 138 (2008) 1615–1621.

[310] A. Barve, C. Chen, V. Hebbar, J. Desiderio, C.L.-L. Saw, A.-N. Kong, Metabolism, oral bioavailability and pharmacokinetics of chemopreventive kaempferol in rats, Biopharm. Drug Dispos. 30 (2009) 356–365.

[311] J.D. Lambert, M.-J. Lee, L. Diamond, J. Ju, J. Hong, M. Bose, H.L. Newmark, C.S. Yang, Dose-dependent levels of epigallocatechin-3-gallate in human colon cancer cells and mouse plasma and tissues, Drug Metab. Dispos. 34 (2006) 8–11.

[312] U. Ullmann, J. Haller, J.D. Decourt, J. Girault, V. Spitzer, P. Weber, Plasma-kinetic characteristics of purified and isolated green tea catechin epigallocatechin gallate (EGCG)

after 10 days repeated dosing in healthy volunteers, Int. J. Vitam. Nutr. Res. 74 (2004) 269–278.

[313] W. Mullen, C.A. Edwards, A. Crozier, Absorption, excretion and metabolite profiling of methyl-, glucuronyl-, glucosyl- and sulpho-conjugates of quercetin in human plasma and urine after ingestion of onions, Br. J. Nutr. 96 (2006) 107–116.

[314] X. Chen, L. Cui, X. Duan, B. Ma, D. Zhong, Pharmacokinetics and metabolism of the flavonoid scutellarin in humans after a single oral administration, Drug Metab. Dispos. 34 (2006) 1345–1352.

[315] C. Gardana, S. Guarnieri, P. Riso, P. Simonetti, M. Porrini, Flavanone plasma pharmacokinetics from blood orange juice in human subjects, Br. J. Nutr. 98 (2007) 165–172.

[316] V. Butterweck, U. Liefländer-Wulf, H. Winterhoff, A. Nahrstedt, Plasma levels of hypericin in presence of procyanidin B2 and hyperoside: a pharmacokinetic study in rats, Planta Med. 69 (2003) 189–192.

[317] G. Jürgenliemk, A. Nahrstedt, Dissolution, solubility and cooperativity of phenolic compounds from *Hypericum perforatum* L. in aqueous systems, Pharmazie 58 (2003) 200–203.

[318] A.R. Rechner, M.A. Smith, G. Kuhnle, G.R. Gibson, E.S. Debnam, S.K.S. Srai, K.P. Moore, C.A. Rice-Evans, Colonic metabolism of dietary polyphenols: influence of structure on microbial fermentation products, Free Radic. Biol. Med. 36 (2004) 212–225.

[319] M. Blaut, L. Schoefer, A. Braune, Transformation of flavonoids by intestinal microorganisms, Int. J. Vitam. Nutr. Res. 73 (2003) 79–87.

[320] Y.J. Moon, M.E. Morris, Pharmacokinetics and bioavailability of the bioflavonoid biochanin A: effects of quercetin and EGCG on biochanin A disposition in rats, Mol. Pharm. 4 (2007) 865–872.

[321] R. Jirásko, M. Holcapek, E. Vrublová, J. Ulrichová, V. Simánek, Identification of new phase II metabolites of xanthohumol in rat *in vivo* biotransformation of hop extracts using high-performance liquid chromatography electrospray ionization tandem mass spectrometry, J. Chromatogr. A 1217 (2010) 4100–4108.

[322] S. Possemiers, S. Rabot, J.C. Espín, A. Bruneau, C. Philippe, A. González-Sarrías, A. Heyerick, F.A. Tomás-Barberán, D. de Keukeleire, W. Verstraete, *Eubacterium limosum* activates isoxanthohumol from hops (*Humulus lupulus* L.) into the potent phytoestrogen 8-prenylnaringenin *in vitro* and in rat intestine, J. Nutr. 138 (2008) 1310–1316.

[323] S. Javed, K. Kohli, M. Ali, Reassessing bioavailability of silymarin, Altern. Med. Rev. 16 (2011) 239–249.

[324] P. Li, S.E. Tabibi, S.H. Yalkowsky, Solubilization of flavopiridol by pH control combined with cosolvents, surfactants, or complexants, J. Pharm. Sci. 88 (1999) 945–947.

[325] S. Tommasini, M.L. Calabrò, D. Raneri, P. Ficarra, R. Ficarra, Combined effect of pH and polysorbates with cyclodextrins on solubilization of naringenin, J. Pharm. Biomed. Anal. 36 (2004) 327–333.

[326] M. Kusuda, T. Hatano, T. Yoshida, Water-soluble complexes formed by natural polyphenols and bovine serum albumin: evidence from gel electrophoresis, Biosci. Biotechnol. Biochem. 70 (2006) 152–160.

[327] T. Lindl, Zell- und Gewebekultur. Einführung in die Grundlagen sowie ausgewählte Methoden und Anwendungen, Spektrum, Akad. Verl., Heidelberg , Berlin, 5th edition (2002).

[328] P.M. van Midwoud, A. Janse, M.T. Merema, G.M.M. Groothuis, E. Verpoorte, Comparison of biocompatibility and adsorption properties of different plastics for advanced microfluidic cell and tissue culture models, Anal. Chem. 84 (2012) 3938–3944.

[329] P.C. Hollman, J.H. de Vries, S.D. van Leeuwen, M.J. Mengelers, M.B. Katan, Absorption of dietary quercetin glycosides and quercetin in healthy ileostomy volunteers, Am. J. Clin. Nutr. 62 (1995) 1276–1282.

[330] P.C. Hollman, M.N. Bijsman, Y. van Gameren, E.P. Cnossen, J.H. de Vries, M.B. Katan, The sugar moiety is a major determinant of the absorption of dietary flavonoid glycosides in man, Free Radic. Res. 31 (1999) 569–573.

[331] R. Hänsel, O. Sticher, Pharmakognosie - Phytopharmazie, Springer, Heidelberg, 8. edition (2007).

[332] A. Iwamura, T. Fukami, R. Higuchi, M. Nakajima, T. Yokoi, Human α/β hydrolase domain containing 10 (ABHD10) is responsible enzyme for deglucuronidation of mycophenolic acid acyl-glucuronide in liver, J. Biol. Chem. 287 (2012) 9240–9249.

[333] K.A. O'Leary, A.J. Day, P.W. Needs, F.A. Mellon, N.M. O'Brien, G. Williamson, Metabolism of quercetin-7- and quercetin-3-glucuronides by an *in vitro* hepatic model: the role of human beta-glucuronidase, sulfotransferase, catechol-O-methyltransferase and multi-resistant protein 2 (MRP2) in flavonoid metabolism, Biochem. Pharmacol. 65 (2003) 479–491.

[334] K.A. O'Leary, A.J. Day, P.W. Needs, W.S. Sly, N.M. O'Brien, G. Williamson, Flavonoid glucuronides are substrates for human liver beta-glucuronidase, FEBS Lett. 503 (2001) 103–106.

[335] C. Manach, O. Texier, C. Morand, V. Crespy, F. Régérat, C. Demigné, C. Rémésy, Comparison of the bioavailability of quercetin and catechin in rats, Free Radical Bio. Med. 27 (1999) 1259–1266.

[336] J.-y. Dai, J.-l. Yang, C. Li, Transport and metabolism of flavonoids from Chinese herbal remedy Xiaochaihu- tang across human intestinal Caco-2 cell monolayers, Acta Pharmacol. Sin. 29 (2008) 1086–1093.

[337] Z. Yang, J. Yang, Y. Jia, Y. Tian, A. Wen, Pharmacokinetic properties of hydroxysafflor yellow A in healthy Chinese female volunteers, J. Ethnopharmacol. 124 (2009) 635–638.

[338] K. Lan, X. Jiang, J. He, Quantitative determination of isorhamnetin, quercetin and kaempferol in rat plasma by liquid chromatography with electrospray ionization tandem mass spectrometry and its application to the pharmacokinetic study of isorhamnetin, Rapid Commun. Mass Spectrom. 21 (2007) 112–120.

[339] F.I. Kanaze, M.I. Bounartzi, M. Georgarakis, I. Niopas, Pharmacokinetics of the citrus flavanone aglycones hesperetin and naringenin after single oral administration in human subjects, Eur. J. Clin. Nutr. 61 (2007) 472–477.

[340] N. Matsukawa, M. Matsumoto, H. Hara, High biliary excretion levels of quercetin metabolites after administration of a quercetin glycoside in conscious bile duct cannulated rats, Biosci. Biotechnol. Biochem. 73 (2009) 1863–1865.

[341] L. Chen, M.J. Lee, H. Li, C.S. Yang, Absorption, distribution, elimination of tea polyphenols in rats, Drug Metab. Dispos. 25 (1997) 1045–1050.

[342] S. Egert, S. Wolffram, B. Schulze, P. Langguth, E.M. Hubbermann, K. Schwarz, B. Adolphi, A. Bosy-Westphal, G. Rimbach, M.J. Müller, Enriched cereal bars are more effective in increasing plasma quercetin compared with quercetin from powder-filled hard capsules, Br. J. Nutr. 107 (2012) 539–546.

[343] C.-P. Yu, P.-P. Wu, Y.-C. Hou, S.-P. Lin, S.-Y. Tsai, C.-T. Chen, P.-D.L. Chao, Quercetin and rutin reduced the bioavailability of cyclosporine from Neoral, an immunosuppressant, through activating P-glycoprotein and CYP 3A4, J. Agric. Food Chem. 59 (2011) 4644–4648.

[344] Y.-A. Cho, J.-S. Choi, J.-P. Burm, Effects of the antioxidant baicalein on the pharmacokinetics of nimodipine in rats: a possible role of P-glycoprotein and CYP3A4 inhibition by baicalein, Pharmacol. Rep. 63 (2011) 1066–1073.

[345] F. Vallejo, M. Larrosa, E. Escudero, M.P. Zafrilla, B. Cerdá, J. Boza, M.T. García-Conesa, J.C. Espín, F.A. Tomás-Barberán, Concentration and solubility of flavanones in orange beverages affect their bioavailability in humans, J. Agric. Food Chem. 58 (2010) 6516–6524.

[346] Patent No. US 2011/0086815 A1, N. Yamaguchi, M. Ono, Novel composition containing xanthohumol-cyclodextrin complexes, Application date 26.02.2009. Publication year 2011.

# 9 Appendix

## 9.1 Abbreviation

| | |
|---|---|
| **XN** | Xanthohumol |
| **(1,** is used additionally in chapter 3**)** | |
| **2** | Xanthohumol H |
| **3** | 4-Acetoxyxanthohumol |
| **4** | 4-Methoxyxanthohumol |
| **5** | Desmethylxanthohumol |
| **6** | Xanthohumol C |
| **7** | Dihydroxanthohumol C |
| **8** | Acetylchroman |
| **9** | Prenylacetophenon |
| **10** | Tetrahydroxanthohumol |
| **11** | Dihydro-Helichrysetin |
| **12** | Dihydro-Flavokawain C |
| **13** | Helichrysetin |
| **14** | 3-OHHelichrysetin |
| **15** | Flavokawain A |
| **16** | Flavokawain B |
| **17** | Flavokawain C |
| **18** | Alpinetin chalcone |
| **8-PN** | 8-prenylnaringenine |
| **AAPH** | 2,2′-azobis(2-methylpropionamide) dihydrochloride |
| **Ah receptor** | Aryl hydrocarbon receptor |
| **AIF** | Apoptosis-inducing factors |
| **ALT** | Alanine aminotransferase |
| **AP** | Apical |
| **aP2** | Adipocyte lipid binding protein |
| **AR** | Androgen receptor |
| **ARE** | Antioxidant response element |
| **Asm** | Acid sphingomyelinase |
| **AST** | Aspartate aminotransferase |
| **ATCC** | American type culture collection |

| | |
|---|---|
| **ATF6** | Activating transcription factor 6 |
| **BaP** | Benzo(a)pyrene |
| **BL** | Basolateral |
| **BSA** | Bovine serum albumine |
| **BSEP** | Bile salt export pump |
| **BVDV** | Bovine viral diarrhea virus |
| **C/EBP** | CCAAT/enhancer-binding protein |
| **C/EBPα** | CCAAT/enhancer binding protein α |
| **Caco-2** | Human colorectal cell line |
| **CD** | Concentration to double inducation |
| **CHOP** | Homologous protein |
| **CHS** | Chalcone synthase |
| **COX** | Cyclooxygenase |
| **CR** | Chloroquine-resistant |
| **CS** | Chloroquine-sensitive |
| **CV** | Crystal violet |
| **DHE** | 2-Hydroxyethidium |
| **DMEM** | Dulbecco's modified Eagle medium |
| **DPPH** | 1,1-diphenyl-2-picrylhydrazyl radical |
| **$EC_{50}$** | Effective concentration |
| **EGF** | Epidermal growth factor |
| **ER** | Endoplasmatic reticulum |
| **ER** | Estrogen receptor |
| **FACS** | Fluorescence activated cell sorter |
| **FCS** | Fetal calf serum |
| **FRAP** | Fluorescence recovery after photobleaching |
| **FXP** | Farneosid X receptor |
| **GPR** | Glucose-regulated proteins |
| **GS** | Glutathione synthetase |
| **GSH** | Glutathion |
| **GST** | Glutathione S-transferase |
| **HAA** | heterocyclic aromatic amine |
| **HASMC** | Human aortic smooth muscle cells |
| **HCV** | Hepatits C virus |
| **HepG2** | Human hepatoma cell line |
| **HIPT-1** | *Humulus lupulus* prenyltransferase-1 |
| **HO 1** | Heme-oxygenase 1 |

| | |
|---|---|
| **HPTLC** | High performance thin layer chromatography |
| **HSC** | Human hepatic stellate cell line |
| **HuH-7** | Human hepatoma cell line |
| **HUVEC** | Human umbilical vein endothelial cells |
| **Hydro XAN C** | Hydroxanthohumol C |
| **HYSA** | Hydroxysafflor yellow A |
| **$IC_{50}$** | Inhibition concentration |
| **ICAM-1** | Intracellular adhesion molecule-1 |
| **IKK** | IκB kinase |
| **IL-6** | Interleukin-6 |
| **iNOS** | Inducible NO synthase |
| **IQ** | 2-Amino-3-methylimidazol[4,5-f]quinoline |
| **IRE1** | Inositol-requiring enzyme 1 |
| **IXN** | Isoxanthohumol |
| **JAK** | Januskinase |
| **JNK** | C-Jun N-terminal kinase |
| **Keap 1** | Kelch-like ECH-associated protein 1 |
| **LDH** | Lactate dehydrogenase |
| **LOD** | Limit of detection |
| **LOQ** | Limit of quantification |
| **LOX** | Lipoxygenase |
| **LPS** | Lipopolysaccharides |
| **MAPK** | Mitogen activated protein kinase |
| **MCP-1** | Monocyte chemo-attractant protein-1 |
| **MDCKII-MDR** | Madin-Darby canine kidney-MDR |
| **MDR** | Multidrug resistant |
| **MeIQx** | 2-Amino-3,8-dimethylimidazol[4,5-*f*]quinoxaline |
| **MIC** | Minimum inhibitory concentration |
| **MRP5** | ATP-binding cassette transporter multi-drug resistance associated protein 5 |
| **MTP** | Microsomal triglyceride transfer protein |
| **MTT** | 3-(4,5-Dimethylthiazol-2-yl)-2,5-diphenyltetrazoliumbromide |
| **NAC** | N-Acetylcystein |
| **NBT** | Nitro blue tetrazolium chloride |
| **NEAA** | Non essential amino acids |
| **NED** | Naphtyletyhlene diamine dihydrochloride |

| | |
|---|---|
| **NF-κB** | Nuclear factor kappa light chain enhancer of activated B-cells |
| **NMR** | Nuclear magnetic resonance spectroscopy |
| **Nrf 2** | Nuclear factor-erythroid 2 (NF-E2)-related factor 2 |
| **OMT** | *O*-Methyltransferase |
| **ORAC** | Oxygen radical absorbance capacity assay |
| **PARP** | Poly (ADP-ribose) polymerase |
| **PBS** | Phosphate buffered saline |
| **PERK** | RNA-activated protein kinase –like ER kinase |
| **PfCRT** | *P. falciparum* chloroquine resistant transporter |
| **PH** | Primary hepatocytes |
| **PhIP** | 2-amino-1-methyl-6-phenylimidazol[4,5-*b*]pyridine |
| **PPARγ** | Peroxisome proliferator-activated receptor γ |
| **QR** | NAD(P)H:quinone reductase |
| **RANKL** | Receptor activator of NF-κB ligand |
| **RAW 264.7** | Mouse macrophage |
| **RNS** | Reactive nitrogen species |
| **ROS** | Reactive oxygen species |
| **RPMI** | Roswell Park Memorial Insitute |
| **RUNX2** | Runt-related transcription factor 2 |
| **SD** | Standard deviation |
| **SDS** | Sodium dodecyl sulfate |
| **SE** | Standard error |
| **SHP** | Small heterodimer partner |
| **SOD** | Superoxid dismutase |
| **SP** | Sodium pyruvate |
| **SREBP** | Sterol regulatory element binding protein |
| **STAT** | Signal transducers and activators of transcription |
| **TBH** | tert-Butylhydroperoxide |
| **$TCID_{50}$** | Tissue culture infection dose |
| **TI** | Therapeutic index |
| **TLR4** | Toll-like receptor 4 |
| **TNF** | Tumor necrosis factor |
| **TPA** | 12-*O*-Tetradecanoylphorbol-13-acetate (TPA) |
| **UDP** | Unfolded protein response |
| **UGT** | UDP-glucuronosyltransferase |
| **VEGF** | Vascular endothelial growth factor |

| | |
|---|---|
| **XE** | Extract with 73% Xanthohumol and 23% Matrix |

## 9.2 NMR spectra of hydrogenated chalcones

The $^{1}$H NMR spectra of the hydrogenated chalcones are depicted in Figure 9-1.

**A** Compound **10**

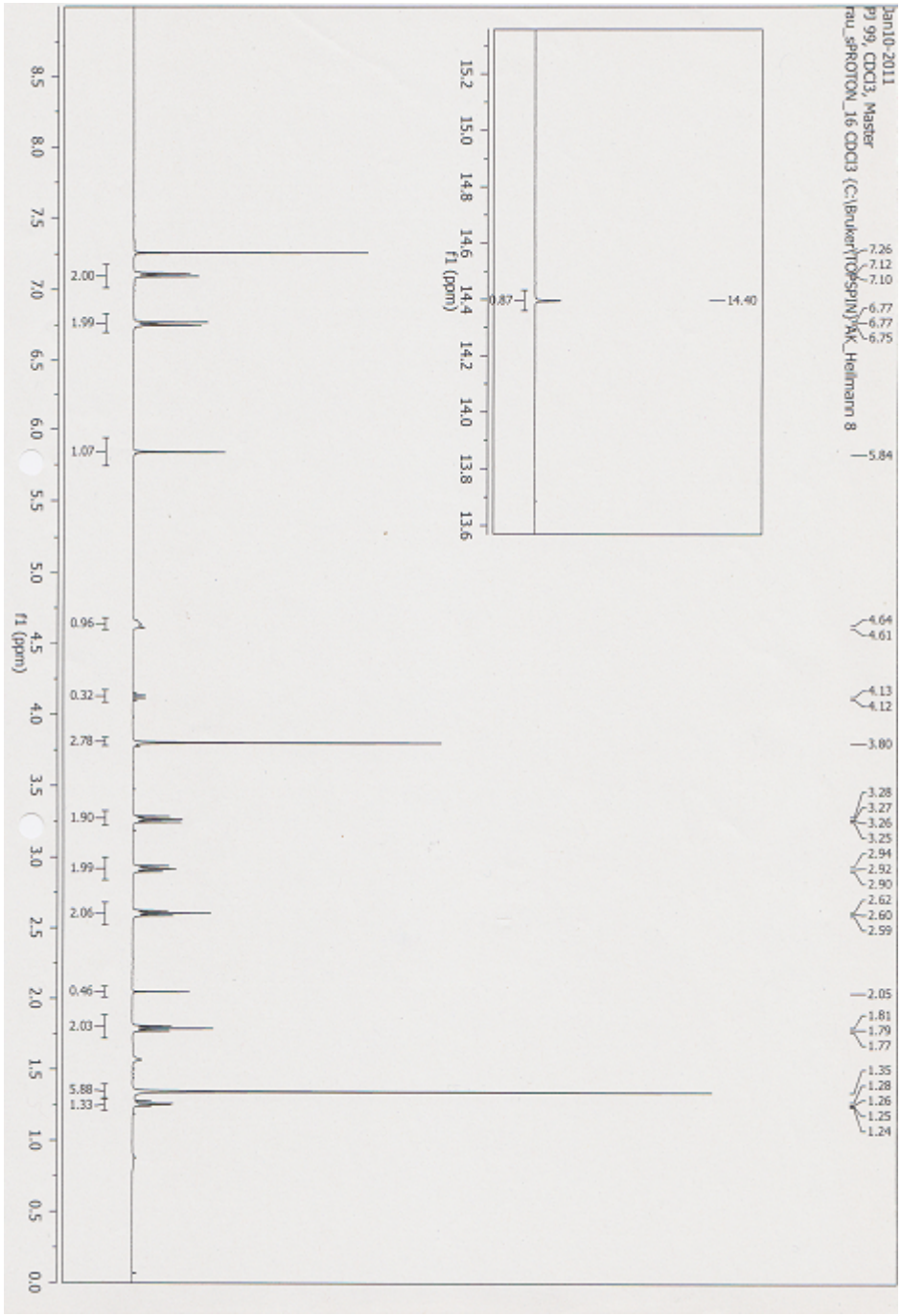

**B** Compound **12**

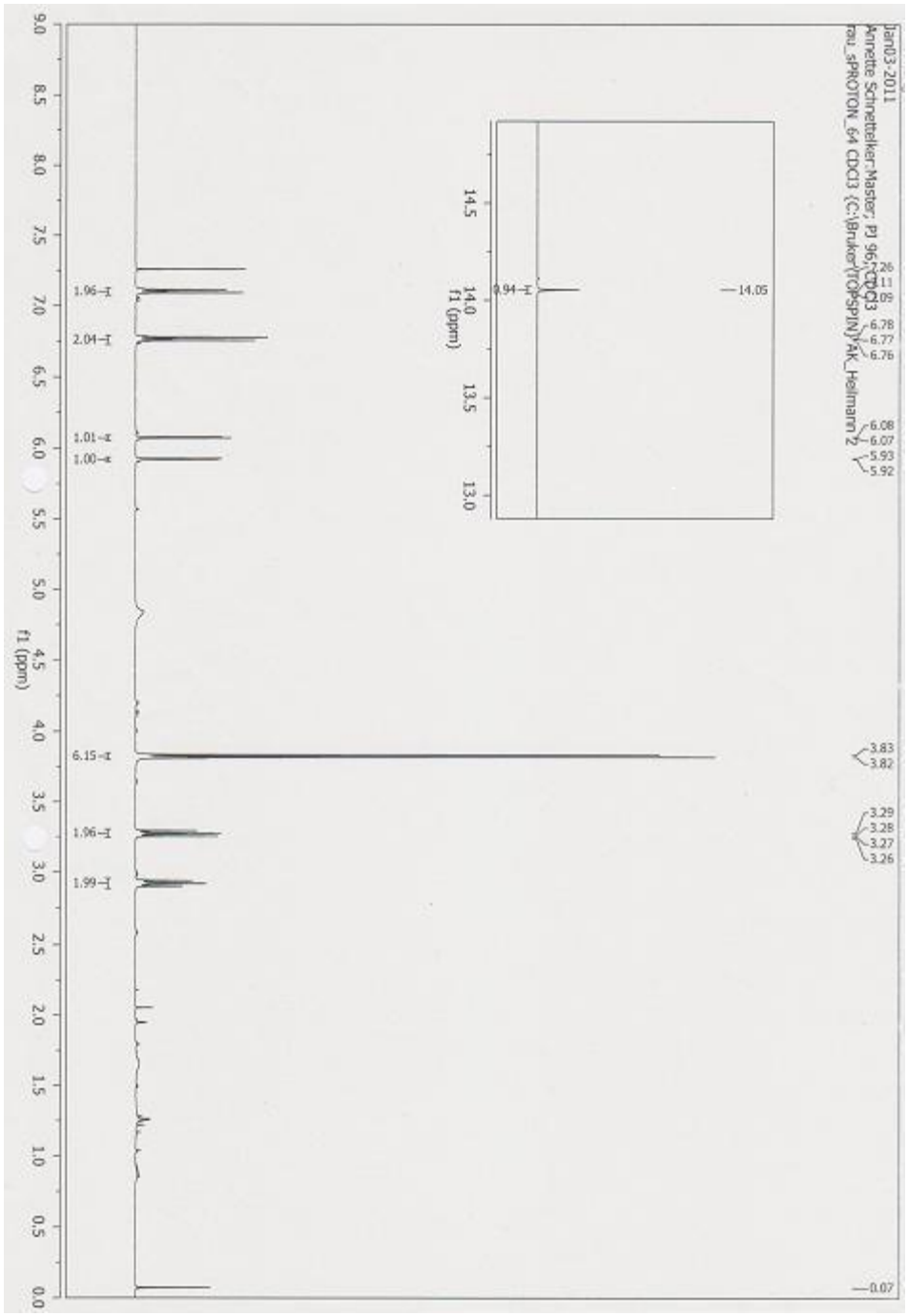

**C** Compound **11**

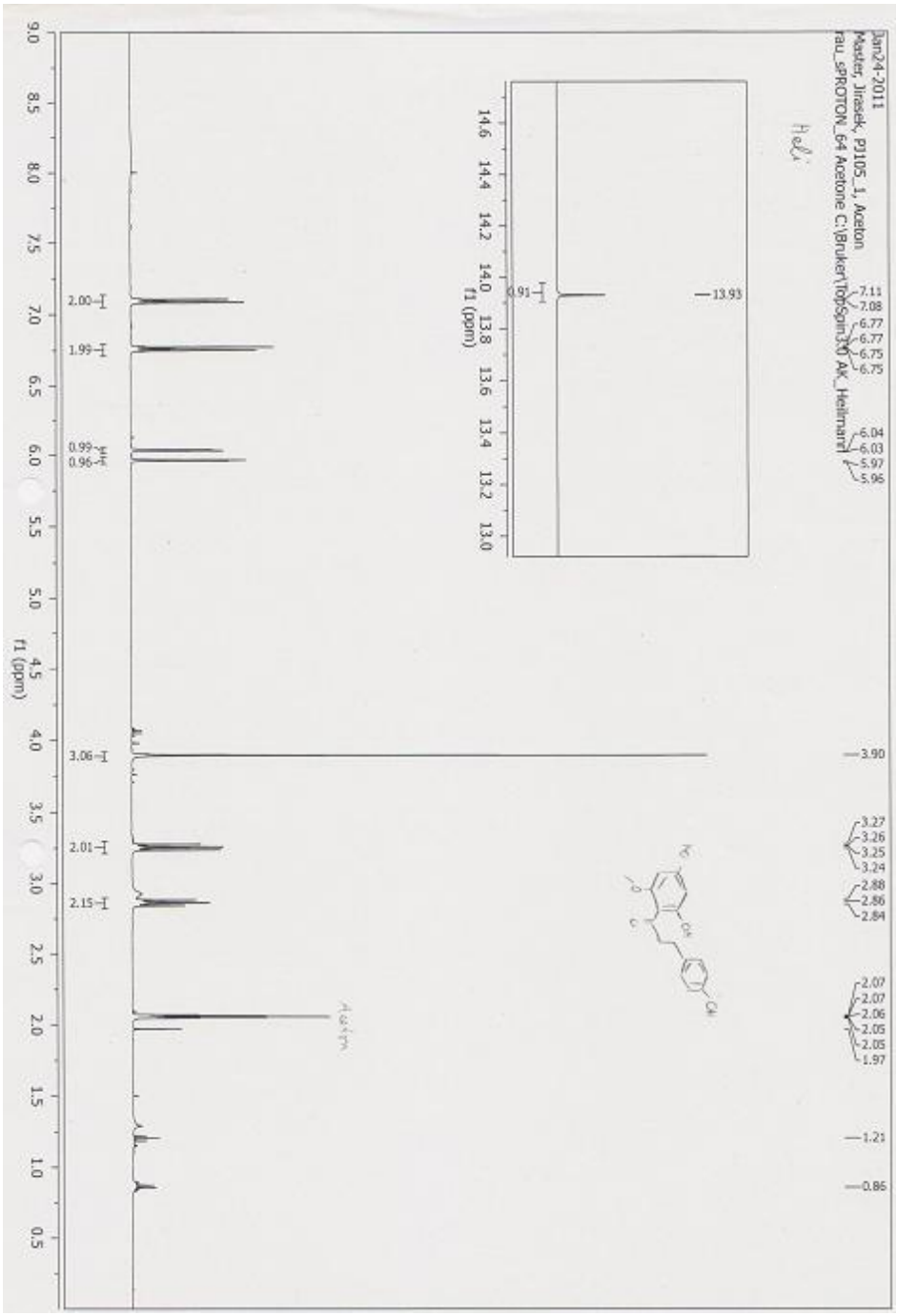


**Figure 9-1: The $^{1}$H NMR spectra of 10 (A), 12 (B) and 11 (C). The molecular structures were confirmed by NMR using a Bruker Avance spectrometer (400 MHz). $^{1}$H NMR spectra were recorded at ambient temperature. For this purpose, 10 and 12 were dissolved in $CDCl_3$ Compound 11 was dissolved in deuterated acetone.**

## 9.3 List of publications

**Prior of submission of this thesis, results were published in part or presented as posters.**

Publications

C. Dorn, B. Kraus, **M. Motyl**, T. S. Weiss, M. Gehring, J. Schölmerich, J. Heilmann, C. Hellerbrand, Xanthohumol, a chalcon derived from hops, inhibits hepatic inflammation and fibrosis, Mol. Nutr. Food Res. 54 (2) (2012) S205-S213.

**M. Motyl**, B. Kraus, J. Heilmann, Pitfalls in cell culture work with xanthohumol, Pharmazie 67 (2012) 91–94.

**M. Motyl**, C. Dorn, B. Kraus, M. Gehring, C. Hellerbrand, and J. Heilmann, Influence of dose and phenolic congeners on absorption and distribution of the hop chalcone xanthohumol after oral application in mice, Manuscript in preparation.

H. Wolff, **M. Motyl**, C. Hellerbrand, J. Heilmann, and B. Kraus: Xanthohumol uptake and intracellular kinetics in hepatocytes, hepatioc stellate cells and intestinal cells. J. Agr. Food Chem. 59, (2011) 12893-12901.

Conference abstracts

**M. Motyl**, C. Dorn, C. Hellerbrand, J. Heilmann, B. Kraus, Uptake of xanthohumol in human liver and intestinal cells, Congress Society for Medicinal Plant and Natural Product Research, Geneva (Switzerland) (2009).

L. Lacikova, E. M. Pferschy-Wenzig, **M. Motyl**, I. Mašterová, D. Grančai, R. Bauer, J. Heilmann, Antioxidant activity of water infusions from selected plants of TCM and their qualitative analysis, Congress of the Austrian Pharmaceutical Society, Vienna (Austria) (2009).

## 9.4 Curriculum Vitae

PERSONAL DETAILS

| | |
|---|---|
| Name: | Magdalena Dorothea Motyl |
| Date of birth: | February 6th 1985 |
| Place of birth: | Danzig, Polen |
| Nationality: | German |

PROFESSIONAL TRAINING

| | |
|---|---|
| 09.2012 - | Deputy head of laboratory, section method development and validation ,Phytos Labor für Analytikvon Arzneimitteln GmbH & Co. KG, Neu-Ulm |
| 01.2012 – 08.2012 | Elaboration of the Ph. D. thesis |
| 01.2009 - 12.2011 | Ph. D. student, University of Regensburg, Institute of Pharmacy |
| 03.2008 - 12.2008 | Graduate Assistant, University of Regensburg, Institute of Pharmacy |
| 09.2007 - 02.2008 | Diploma student, University of Regensburg, Institute of Pharmacy |
| 03.2007 - 04.2007 | Student research project, Fraunhofer Institute for Interfacial Engineering and Biotechnology, Stuttgart |
| 08.2006 - 02.2007 | Internship, Fraunhofer Institute for Interfacial Engineering and Biotechnology, Stuttgart |

EDUCATION

| | |
|---|---|
| 09.2004 - 04.2008 | Graduate engineer (FH) in environmental and process engineering (course specialization biotechnology) and Bachelor of engineering in biotechnology, University of Furtwangen |
| 09.2001 - 07.2003 | Technician in chemistry,Institute Dr. Flad in Stuttgart |

## 9.5 Eidesstattliche Erklärung

Ich erkläre hiermit an Eides statt, dass ich die vorliegende Arbeit ohne unzulässige Hilfe Dritter und ohne Benutzung anderer als der angegebenen Hilfsmittel angefertigt habe. Die aus anderen Quellen direkt oder indirekt übernommenen Daten und Konzepte sind unter Angabe des Literaturzitats gekennzeichnet.
Weitere Personen waren an der inhaltlichen-materiellen Herstellung der vorliegenden Arbeit nicht beteiligt. Insbesondere habe ich nicht die entgeltliche Hilfe eines Promotionsberaters oder anderer Personen in Anspruch genommen. Niemand hat vor mir weder unmittelbar noch mittelbar geldwerte Leistungen für die Arbeit erhalten, die im Zusammenhang mit dem Inhalt der vorgelegten Dissertation stehen.
Die Arbeit wurde bisher weder im Inland noch im Ausland in gleicher oder ähnlicher Form einer anderen Prüfungsbehörde vorgelegt.

Regensburg, den _____ _____

Magdalena Motyl